NTNU – Trondheim
Norwegian University of
Science and Technology

Surface Seismic While Drilling

A new method for relief well drilling

Kristoffer Evensen

Petroleum Geoscience and Engineering
Submission date: June 2013
Supervisor: Sigbjørn Sangesland, IPT
Co-supervisor: Ståle Emil Johansen , IPT

Norwegian University of Science and Technology
Department of Petroleum Engineering and Applied Geophysics

NTNU
Norges teknisk-naturvitenskapelige universitet | **Fakultet for ingeniørvitenskap og teknologi**
Faculty of Engineering and Technology
Studieprogram i Geofag og petroleumsteknologi
Study Programme in Earth Sciences and Petroleum Engineering

Institutt for petroleumsteknologi og anvendt geofysikk
Department of Petroleum Engineering and Applied Geophysics

HOVEDOPPGAVE/DIPLOMA THESIS/MASTER OF SCIENCE THESIS

Kandidatens navn/The candidate's name:	Kristoffer Evensen
Oppgavens tittel, norsk/Title of Thesis, Norwegian:	Overflateseismikk under boring – En ny metode for boring av avlastingsbrønner
Oppgavens tittel, engelsk/Title of Thesis, English	Surface Seismic While Drilling – A new method for relief well drilling

Utfyllende tekst/Extended text:

Background:

A blowout is the most severe consequence of loss in well integrity. If efforts to stop the blowing well using top kill techniques do not succeed, a relief well might be the only solution to permanently stop the flow of oil and gas to the surface. Modern relief wells use direct intersection by homing in on steel tubular in the blowing well. Because of this, the openhole section might not be utilized during the killing operation. Surface Seismic While Drilling (SSWD) may allow direct intersection at the bottom of the blowing. This approach will reduce the flow rates and pressures needed to kill the well, and reduce the static kill mud density.

Task:

1) Describe critical aspects of well integrity and relief well drilling.
2) Evaluate wellbore-positioning uncertainty when using conventional survey tools.
3) Perform state of the art analysis for homing-in/ranging tools.
4) Create a computer model and simulate the flow rate and pressure required for killing a blowing well based on intersection at casing shoe and at the bottom of hole.
5) Evaluate the benefits of using SSWD and bottomhole intersection for well killing.

Supervisor	*Sigbjørn Sangesland*
Co-supervisor	*Ståle Emil Johansen*
Studieretning/Area of specialization:	*Petroleum Engineering, Drilling Technology*
Fagområde/Combination of subject:	*Drilling*
Tidsrom/Time interval:	*January 14 – June 10, 2013*

…… ……..

Sigbjørn Sangesland *Ståle Emil Johansen*

Summary

The first relief wells emerged out of necessity, and have since been shaped by several disastrous events throughout the 20th and 21th century. The modern relief well shows little resemblance to the first relief wells that were drilled in the early 20th century. Today's relief wells are drilled to directly intersect a blowing wellbore at depths of several thousand meters, and often with a diameter of less than one foot. At these depths, conventional positioning surveying tools can yield horizontal errors approaching 100 meters, and therefore cannot offer the accuracy required to facilitate direct intersection between the two wells. Because of this, special survey tools have been developed to home in on the steel tubular in the blowing wellbore.

Ranging Tools

Two types of tools generally exist. Passive magnetostatic tools use conventional magnetic survey tools integrated into the bottomhole assembly to measure the remanent magnetism present in steel, and have a range of 15 meters. Active electromagnetic tools apply an alternating (AC) current to the blowing tubular to inducing a magnetic field around the blowing wellbore. This current can either be applied directly to the casing of the blowing well at the surface, or be injected into the subsurface formations through an injector electrode integrated into the tool. Under ideal conditions, a downhole sensor package can detect the magnetic field at a distance of 60 meters. This survey method traditionally requires a specialized electromagnetic survey string to be run into the hole.

Wellbore Positioning Surveys

To be able to utilize magnetic ranging instruments to home in on the casing of the blowing well, conventional surveys must be able to safely position the relief well within the maximum ranging distance from the blowing well. Considering uncertainty in wellbore position of both wells, this can be a challenge. Typical relief well strategies involves drilling towards the blowing well, using conventional magnetic positioning surveys integrated into the measurements while drilling (MWD) package. Before the large uncertainty makes premature interception possible, a gyro-survey is performed to reduce the positioning uncertainty. Once the wells are within the ranging distance from each other, the homing in process can start.

Trajectory Requirements

Generally it is desired to intersect the blowing well at a relatively narrow angle of between 3 and 15º. Because of the surface conditions at the blowing well site, the relief well is often spudded more than one kilometer away. Because of these two conditions,

the relief well is drilled at a high angle to approach the blowing well, and is dropped down to near parallel before intersection is made. To increase the accuracy of the homing-in tools, a triangulation approach is often utilized. This is performed by drilling the relief well past the blowing well, at a relative distance of around 10 meters, before it drops down and is drilled parallel to the target well. This technique can reduces the uncertainty of the homing-in measurements to below one meter. Once the wells are at this distance from each other, the pressure drawdown will most likely cause the formation between the wells to collapse, creating a direct hydraulic communication between the wells.

Depth of Intersection

Because of the inherent nature of the surveying techniques utilized to home in on the target, steel must be present in the blowing wellbore. Most often this means that the last set casing shoe will be the deepest point possible to intersect. This means that if an openhole section exists below the casing shoe, this cannot be utilized during the bottom kill operation.

Surface Seismic While Drilling

Johansen et al. (2013) suggested using repeated Surface Seismic While Drilling (SSWD) to measure the relative distance between the two wells in real time, as the relief well is being drilled. This is performed by acquiring seismic reference data before drilling is initiated, then the seismic survey is repeated continuously as the bit propagates down into the earth. If the reference seismic data is subtracted from the newly acquired seismic data, this will yield only the changes in the subsurface. Hence, the true wellpath can be found. This method has the potential of facilitating a direct intersection, regardless of the presence of steel in the blowing wellbore.

Simulation Results

Simulations were performed to evaluate the benefits of a deeper intersection point. The results showed that a casing shoe intersection would require an injection rate of 290 l/s to dynamically kill the blowing well with seawater. If the well were intersected at the bottom, the dynamic killing rate was reduced to 151 l/s, or a reduction of 48%. The pump power requirements are dependent on the injection method, but the minimum pump power was 19759 and 4942hp, for casing shoe- and bottomhole intersection, respectively. This is a total reduction of 75%. The casing shoe pressure during killing was reduced by 21%. When circulating from the bottom, calculations showed that the well could be killed using a high-capacity drilling rig utilizing the mud circulation system and the cement pumps. A casing shoe intersection required several additional pumps. Depending on deck capacity, pumping vessels or an additional rig would have to be mobilized, increasing the cost of the operation and mobilization time.

Oppsummering

De første avlastingsbrønnene ble boret for å stoppe utblåsninger tidlig på 1900-tallet, etter at alle andre metoder hadde feilet. Avlastningsbrønnen har siden den gang utviklet seg, og de moderne avlastningsbrønnene har lite til felles med de primitive brønnene som ble boret tidligere. Dagens avlastningsbrønner blir boret for å treffe de blåsende brønnene direkte, på flere tusen meters dyp, og diameteren på målet er ofte ikke større enn en tallerken. På disse dybdene kan konvensjonell brønnposisjoneringsutstyr ha en horisontal usikkerhet opp mot hundre meter, det er derfor helt umulig å benytte seg av disse metodene for å treffe målet. Grunnet dette har det blitt utviklet spesialverktøy som søker inn mot stålrør i den blåsende brønnen.

Søkingsverktøy

Det eksisterer i dag to typer kommersielle søkningsverktøy. Magnetostatiske verktøy bruker magnetiske søkere integrert i den nederste delen av borestrengen. Disse vil søke etter gjenværende magnetisme som er tilstede i stål, og har en rekkevidde på omlag 15 meter. Aktive elektromagnetiske verktøy injiserer spenning gjennom foringsrør i den blåsende brønnen, og vil dermed generere et magnetisk felt rundt disse. Dette kan enten gjennomføres ved direkte å tilføre strøm til foringsrørene ved overflaten, eller føre strømmen gjennom formasjonene ved hjelp av en elektrode integrert i boreverktøyet. En nedihulls sensorpakke vil søke etter det genererte magnetiske feltet, og dette er brukt til å søke inn den blåsende brønnen. Denne metoden har en rekkevidde på om lag 60 meter, og en spesialisert elektromagnetisk streng må brukes.

Brønnposisjoneringsverktøy

Siden søkingsverktøy har en begrenset rekkevidde så må konvensjonelle brønnposisjoneringsverktøy benyttes for å få avlastingsbrønnen innenfor den maksimale rekkevidden til de magnetiske søkingsverktøyene. Hvis man tar i betrakting usikkerheten knyttet til disse målingene så kan dette være en utfordring. Strategien for en avlastningsbrønn er å bruke magnetiske målingsutstyr integrert i borestrengen til å nærme seg den blåsende brønnen. Hvis det er for stor usikkerhet knyttet til disse målingene, så kan gyroposisjoneringsverktøy bli senket ned i brønnen for å redusere usikkerheten. Når brønnen er nærme nok for å benytte magnetiske søkeverktøy, starter søkingsprosessen. Den relative retningen og avstanden mellom brønnene vil være viktig i denne fasen, i motsetning til den absolutte posisjonen til avlastingsbrønnen.

Brønnbanekrav

Generelt er det foretrukket å treffe den blåsende brønnen med en relativ liten vinkel på mellom 3 og 15º. På grunn av forholdene ved utblåsningsbrønnen, og krav til avlastningsbrønnens bane, så vil avlastningsbrønnen ofte starte mer enn en kilometer borte fra utblåsningsbrønnen. Dermed vil avlastningsbrønnen ha en lang seksjon med høy vinkel for å nærme seg målet, for så å bøyes ned for å bores nær parallelt med den blåsende brønnen. Det vil ofte være gunstig å utføre triangulering for å redusere usikkerheten til søkeverktøy. Dette gjøres ved å bore forbi den blåsende brønnen med en relativ avstand på bare et par meter, for så å bøye av brønnen og bore parallelt med målet. Denne teknikken kan redusere usikkerheten til søkeverktøy til under en meter.

Treffpunkt

Tradisjonelle søkeverktøy er avhengig av å søke etter stål. Dette betyr at treffpunktet må være i en seksjon som er beskyttet av foringsrør, rett under foringsrørskoen eller i en seksjon der det er borestreng tilstede. Vanligvis vil foringsrørskoen være det dypeste treffpunktet som er tilgjengelig tilgjengelig når tradisjonelle metoder blir benyttet.

Seismikk Under Boring

Johansen et al. (2013) foreslår å bruke gjentatt overflateseismikk under boring (SSWD) for å måle den relative avstanden mellom de to brønnene mens avlastingsbrønnen blir boret. Dette muliggjøres ved å anskaffe seismisk referansedata før boring starter. Seismiske målinger blir repetert under boring. Referansedataen blir trukket fra den nye dataen, og vil dermed bare vise endringene som har blitt utført av borekronen. Dette kan brukes til å finne brønnbanen etter hvert som det bores nedover. Denne metoden har potensialet til å muliggjør direkte boring inn i den blåsende brønnen, uavhengig av om det er stål tilstede i brønnen.

Resultat fra Simuleringer

Med utgangspunkt i typiske brønndata ble det utført simuleringer for å evaluere fordelene med et dypere treffpunkt. Resultatene viste at dynamisk dreping med sjøvann fra foringsrørskoen krevde en pumperate på 290 l/s for å balansere trykket ved reservoaret. Dersom brønnen ble truffet i bunnen, vil raten reduseres til 151 l/s. Den nødvendige pumpekapasiteten på riggen er avhengig av injeksjonsmetoden. Den minste nødvendige effekten ble redusert fra 19759 til 4942hk, eller en reduksjon på 75%. Foringsrørtrykket ble redusert med 21% når sirkulasjon ble gjort fra bunnen av brønnen, i forhold til ved foringsrørskoen. Simuleringer viste at brønnen kunne drepes dynamisk fra bunnen med en standard høykapasitets bore rigg hvor man benytter både slamsirkulasjonssystemet og sementpumpene. Hvis brønnen skulle drepes fra foringsrørskoen, så måtte det brukes flere pumper. Dette vil være avhengig av dekkapasitet, og kan føre til at skip eller en ekstra rig må mobiliseres før drepeoperasjonen starter.

Preface

This master thesis was prepared in connection with the course TPG4910 Drilling Technology, at the department of Petroleum Engineering & Applied Geophysics, at the Norwegian University of Science and Technology. The thesis is written during the spring of 2013, as the final requirement for a Master of Science degree, with specialization in drilling engineering.

The method described in this thesis was suggested by Professor Sigbjørn Sangesland and Professor Ståle Emil Johansen in the beginning of 2013. This thesis has been shaped by several meetings and continuous guidance, together with individual research, simulations and ideas.

I would like to thank my supervisor, Professor Sigbjørn Sangesland, for excellent guidance and support during the entire project. He has provided technical knowledge, background material, new ideas and feedback continuously throughout my work. I would also like to thank my co-supervisor, Professor Ståle Emil Johansen. He has provided essential technical knowledge on all aspects of geophysics, as well as feedback and ideas on the entire thesis.

I hereby declare that this thesis, together with all simulation scripts, is solely my original work, and that the work is written in accordance with regulations declared by NTNU. Whenever contributions from other authors is used, this will be clearly indicated in the text, with due reference to the literature. The full reference is included in the bibliography.

_____

Kristoffer Evensen
10.06.2013 NTNU, Trondheim

Table of Contents

Summary ..... **iii**

Oppsummering ..... **v**

Preface ..... **vii**

Table of Contents ..... **ix**

List of Figures ..... **xi**

List of Abbreviations ..... **xiii**

1. Introduction **1**

2. Background **3**

2.1 Well Integrity **3**

2.1.1 Detecting and Verifying Inflow 4

2.2 Circulating Out Kicks **6**

2.2.1 Driller's Method 7

2.2.2 Wait and Weight Method 7

2.2.3 Volumetric Method 8

2.2 Causes of Blowouts **9**

2.2.1 Exploratory- versus Development Wells 9

2.2.2 Shallow Blowouts 10

2.2.4 Deep Blowouts 15

2.2.5 Blowouts during Completion and Workovers 17

2.3 Blowout Control **18**

2.3.1 Killing Technique Selection 18

2.3.2 Top Kill 19

2.3.3 Bottom Kill 20

2.4 Relief Wells **21**

2.4.1 Relief Well Killing Methods 21

2.4.2 Relief Well Planning 23

2.4.3 Relief Well Intersection Point 25

2.4.4 Static versus Dynamic Kill 27

2.5 State of the Art: Homing-in devices **28**

2.5.1 Passive Electrostatic Tools 28

2.5.2 Active Electromagnetic Tools 29

2.5.3 Novel Approaches to Direct Intersection 30

2.6 Relief Well Trajectory and homing-in procedure **32**

2.7 Survey Uncertainty **35**

2.7.1 Wellhead Position 35

2.7.2 Wellbore Positioning 35

2.7.3 Ellipse of Uncertainty 38

3. Surface Seismic While Drilling 49
3.1 Description of Method 49
3.2 Benefits 50

4. Simulation Model 53
4.1 Base Case 53
4.2 Description of Model 56
4.2.1 Reservoir Fluid 56
4.2.2 Temperature Profile 61
4.2.3 Pressure drop calculations 77
4.2.4 Flow Regime 91
4.2.5 Simulating Seawater Injection through Relief Well 94
4.3 Blowout Simulation Results 98
4.3.1 Investigation of Critical Aspects of Blowout Simulation 99
4.3.2 Sensitivity Analysis 108
4.4 Dynamic Kill Simulation Results 113
4.4.1 Investigation of Critical Aspects of Dynamic Kill Simulation 115
4.4.2 Casing Shoe Pressure 122
4.4.3 Depth of Intersection Point 123
4.4.4 Density of Static Kill Mud 124
4.5 Discussion 125

5. Pumping Capacities 131
5.1 Pump Pressure 131
5.1.1 Bottomhole Pressure 131
5.1.2 Hydrostatic Pressure in Relief Well 132
5.1.3 Frictional Pressure 132
5.2 Number of Pumps Needed 143
5.3 Discussion 147

6. Main Discussion 149
6.1 Results 149
6.2 Time from Relief Well Initiation to Static Kill 150
6.3 Accuracy of Ranging Methods 154
6.4 Further Work 155

7. Conclusion 157

Bibliography 159

Appendix A 167

Appendix B 179

Appendix C 183

List of Figures

TABLE 2.1 – CAUSES OF KICKS FOR DIFFERENT PARTS OF THE DRILLING OPERATION (GRACE, 2003; SKALLE & PODIO, 1998; ADAMS & KUHLMAN, 1994) 5
FIGURE 2.1 – RELIEF WELL INTERSECTION POINT 25
FIGURE 2.2 – INTERSECTION STRATEGY UTILIZING ELECTROMAGNETIC RANGING TOOLS 31
FIGURE 2.3 – TRIANGULATION APPROACH TO REDUCE RANGING TOOL UNCERTAINTY (JWCO, 2009B) 34
FIGURE 2.4 – ELLIPSE OF UNCERTAINTY (WOLFF & DE WARDT, 1981) 39
TABLE 2.2 – COMMON SURVEY ERRORS (WOLFF & DE WARDT, 1981) 39
GRAPH 2.1 - ELLIPSE OF UNCERTAINTY FOR 5000 METERS MEASURED DEPTH AND 30º INCLINATION 41
GRAPH 2.2 - HORIZONTAL UNCERTAINTY FOR GOOD GYRO SURVEY 42
GRAPH 2.3 - HORIZONTAL UNCERTAINTY FOR POOR GYRO SURVEY 43
GRAPH 2.4 – EFFECT OF CHANGE IN INCLINATION ON WELLBORE POSITION UNCERTAINTY 44
GRAPH 2.5 - HORIZONTAL UNCERTAINTY FOR GOOD MAGNETIC SURVEY 45
GRAPH 2.6 - HORIZONTAL UNCERTAINTY FOR POOR MAGNETIC SURVEY 46
GRAPH 2.7 - EFFECT OF CHANGE IN INCLINATION ON WELLBORE POSITION UNCERTAINTY 47
FIGURE 3.1 – BOTTOM INTERSECTION USING SSWD 51
FIGURE 4.1 - OVERVIEW OF BASE CASE PROPERTIES 54
FIGURE 4.2 – SCHEMATICS OF CASING SHOE- AND BOTTOMHOLE INTERSECTING RELIEF WELLS 55
TABLE 4.1 - BLACK OIL MOLAR COMPOSITION FROM PEDERSEN ET AL. (1989) 57
GRAPH 4.1 - PHASE ENVELOPE OF RESERVOIR FLUID 58
GRAPH 4.2 - FRACTIONS OF FLOWING PHASES FOR DIFFERENT PRESSURES 59
GRAPH 4.3 - LIQUID PHASE COMPOSITION 60
GRAPH 4.4 - GAS PHASE COMPOSITION 60
GRAPH 4.5 - IN-SITU HEAT CAPACITIES 65
GRAPH 4.6 – EFFECT OF PRESSURE ON INJECTION WATER 66
TABLE 4.2 –PARAMETERS USED IN TEMPERATURE CALCULATIONS 67
GRAPH 4.7 – TEMPERATURE PROFILE IN BLOWING WELL 68
GRAPH 4.8 - EFFECT OF WELLBORE DIMENSIONS 69
GRAPH 4.9 – EFFECT OF HEAT TRANSFER COEFFICIENT 70
GRAPH 4.10 - EFFECT OF CHANGE IN RESERVOIR FLUID SPECIFIC HEAT CAPACITY 71
GRAPH 4.11 – TEMPERATURE PROFILE IN RELIEF WELL WHEN INTERSECTING AT THE BOTTOM 75
GRAPH 4.12 – TEMPERATURE PROFILE IN RELIEF WELL WHEN INTERCEPTING AT CASING SHOE 75
GRAPH 4.13 – EQUATIONS FOR RELIEF WELL BOTTOMHOLE TEMPERATURE 76
GRAPH 4.14 – MOLAR MAS OF GAS PHASE 78
GRAPH 4.15 – LIQUID FRACTION VERSUS PRESSURE 80
GRAPH 4.16 – MOLAR MASS OF LIQUID PHASE 81
GRAPH 4.17 – DENSITY OF LIQUID PHASE 82
GRAPH 4.18 – VISCOSITY OF LIQUID PHASE 83
GRAPH 4.19 – COMPARISON BETWEEN CORRELATION AND SIMULATION 85
GRAPH 4.20 – SURFACE TENSION BETWEEN PHASES 86
TABLE 4.3 – FLOW REGIME DETERMINATION AND RELATED EQUATIONS (BEGGS & BRILL, 1973) 88
FIGURE 4.3 - FLOW PATTERN MAP (BEGGS & BRILL, 1973) 91
FIGURE 4.4 – DEVELOPMENT OF FLOW PATTERN 93
GRAPH 4.21 – EFFECTIVE LIQUID MIXTURE VISCOSITY 95
GRAPH 4.22 – EFFECT OF PRESSURE CHANGE ON WATER DENSITY 97

Graph 4.23 – Wellbore pressure during blowout 98
Graph 4.24 – Wellbore velocity during blowout 99
Graph 4.25 – Friction factor during blowout 100
Graph 4.26 – In-situ densities during blowout 102
Graph 4.27 – Viscosity during blowout 103
Graph 4.28 – Frictional pressure drop during blowout 105
Graph 4.29 – Hydrostatic pressure loss during blowout 106
Graph 4.30 – Wellbore pressure against total pressure loss 107
Graph 4.31 – Effect of wellbore dimensions on blowout rate 108
Graph 4.32 – Effect of openhole roughness on blowout rate 109
Graph 4.33 – Effect of casing roughness on blowout rate 110
Graph 4.34 – Influence of reservoir pressure on blowout rate 111
Graph 4.35 – Influence of water depth on blowout rate 112
Graph 4.36 – Blowout rate for different relief well injection rates 113
Graph 4.37 – Frictional and hydrostatic pressure loss, bottom intersect 114
Graph 4.38 – Frictional and hydrostatic pressure loss, casing shoe intersect 115
Graph 4.39 – Wellbore velocity 116
Graph 4.40 – Frictional pressure during dynamic killing operation 117
Graph 4.41 – Hydrostatic pressure during dynamic killing operation 119
Graph 4.42 – Wellbore pressure during dynamic killing operation with bottomhole intersect 120
Graph 4.43 – Wellbore pressure during dynamic killing operation with casing shoe intersect 121
Graph 4.44 – Casing shoe pressure during dynamic killing operation 122
Graph 4.45 – Effect of intersection depth on dynamic kill rate 123
Graph 4.46 – Effect of intersection depth on static kill density 124
Graph 5.1 – Frictional pressure when circulating down drill string, casing shoe intersect 133
Graph 5.2 - Frictional pressure when circulating down drill string, bottomhole intersect 134
Graph 5.3 – Kill line pressure loss 135
Graph 5.4 – Annular friction loss, casing shoe intersect 136
Graph 5.5 - Annular friction loss, bottomhole intersection 136
Graph 5.6 – Combined injection, standard kill line dimensions, casing shoe intersect 138
Graph 5.7 – Combined injection, standard kill line dimensions, bottomhole intersection 138
Graph 5.8 – Combined injection, large dimension kill/choke line, bottomhole intersection 140
Graph 5.9 – Combined injection, large dimension kill/choke line, casing shoe intersect 140
Graph 5.10 – Adaptive solution, bottomhole intersection 141
Graph 5.11 – Adaptive solution, casing shoe intersect 142
Table 5.1 – Pump pressure needed for different situations 143
Table 5.2 – Description of cases 143
Table 5.3 - HT-400 Specifications (Halliburton, 2013) 144
Table 5.4 – Number of HT-400 cement pumps needed for different situations 145
Graph 6.1 – Depth versus Time for both intersection points 153

List of Abbreviations

B

BHA	Bottomhole Assembly
BOP	Blow Out Preventer

G

GOR	Gas Oil Ratio

M

MAASP	Maximum Allowable Annular Surface Pressure
MWD	Measurements While Drilling

P

POOH	Pull Out Off Hole

S

SSWD	Surface Seismic While Drilling

T

TVD	True Vertical Depth

1. Introduction

A blowout is by far the most severe consequence of loss in well control. Because of the tremendous powers at play, a blowout can rapidly become a disastrous event. Large volumes of hydrocarbons and toxic gasses can be released to the surface, potentially causing huge environmental damage and put human lives at jeopardy. Considering the resources required to stop the blowout, penalties imposed on the liable, reduction in share values, lost hydrocarbon resources, and destroyed reputation of companies involved, a blowout often becomes a dramatic and costly ordeal (CNN, 2010).

Extensive research, many years of experience and large resources has contributed to developing relief well technology to what it is today. Many blowing wells have been brought under control using this technique. Modern relief wells are drilled to directly intersect the blowing wellbore. This is accomplished by using ranging tools that home in on steel tubular of the blowing well. This often means that the last set casing shoe is the deepest point available for a relief well. If an extended openhole section exists below the casing shoe, this cannot be utilized during the killing operation.

During both dynamic- and static killing phases a deeper intersection point will be favorable because a lower flow rate and lighter fluid density is needed to balance the reservoir pressure. This will reduce the pump requirements on the kill rig, and reduce the pressures in the openhole section of the blowing well.

Johansen et al. 2013 proposed the use of repeated Surface Seismic While Drilling to facilitate a direct intersection of a blowing wellbore, regardless of the presence of steel. This thesis will evaluate the benefits of utilizing this method in relief well drilling. A model was prepared in MATLAB to simulate both casing shoe- and bottomhole intersection. The results have been evaluated in regards to kill rig requirements and wellbore pressures during the operation.

In addition to this, a thorough description of well integrity and well control is included, with emphasis on relief well planning and drilling.

2. Background

In this chapter well integrity will be defined, as well as a description on how an inflow of formation fluids can be taken during different parts of the drilling operation, and how different methods are used to regain control. In addition to this, it will be specified how complete loss of well control usually occurs. Different killing methods will be described, with special emphasis on relief well drilling, and critical aspects of this operation.

2.1 Well Integrity

According to the NORSOK Standard D-010 (2004: 12) well integrity is defined as "application of technical, operational and organizational solutions to reduce risk of uncontrolled release of formation fluids throughout the life cycle of a well". A number of different safe guards are implemented into the design and execution of a drilling operation, to prevent unintentional inflow of fluids into the well, and consequently possible loss of well control. However, several processes can take place during operation, leading to compromised well integrity.

Depending on operation, one or two independent physical well barriers must be in place during all well activity. The primary well barrier will provide protection against inflow during normal operation, while the secondary barrier will provide redundancy if the primary barrier is lost. The primary well barrier during drilling commonly comprises of the drilling fluid column, or some sort of mechanical seal that can contain the pressure from the formation that is being drilled (NORSOK Standard D-010, 2004). If the fluid column is to be used as a barrier, it must exert a hydrostatic pressure on the wellbore walls equal to, or higher than, the pore pressure at any given depth where the possibility of flow exists. This positive pressure differential between wellbore and the surrounding formation will prevent inflow of formation fluids into the wellbore. The secondary well barrier is a pressure-sealing envelope, and typically comprises of casing cement, casing, wellhead, and blow out preventer (BOP). If the BOP is located at the surface, a high-pressure riser will connect the BOP to the wellhead, and be part of the pressure-sealing envelope. The blow out preventer can be activated to seal the wellbore if the primary barrier fails (Adams & Kuhlman, 1994).

2.1.1 Detecting and Verifying Inflow

Definition

A kick is defined as an unintentional inflow of formation fluids into the wellbore, and will occur when the positive pressure differential between the wellbore and a permeable formation, with the potential to flow, is lost (Skalle, 2012a). The rate of inflow is governed by the permeability and porosity of the formation in question, as well as the pressure differential between wellbore and formation. Sandstone formations with high permeability will cause more severe kicks than shale formations with relatively low permeability (Adams & Kuhlman, 1994). The total influx volume of a kick will depend on how fast the drilling crew can react to the situation, and how fast the bottomhole pressure can be increased to regain overbalance. Table 2.1 summarizes the most common causes of kicks during different parts of the drilling operation.

Operation	Major causes of kicks	Description
Drilling	Insufficient mud weight	Drilling into zones with higher pressure than anticipated
	Lost circulation	The formation is fractured and drilling fluid is lost to the formation. This might result in reduced hydrostatic head and reduced bottomhole pressure
	Gas cut mud	The mud might be diluted with trip gas, or gas from the formation being drilled, causing lowered mud density
Tripping	Swabbing	Bottomhole pressure reduction when pulling out of the hole can cause the well to go underbalanced
	Insufficient hole filling	Insufficient filling of mud into the well when pulling out of the hole causes reduced bottomhole pressure
Running casing	Surge/lost circulation	Surge if casing/liner is run to fast can fracture the formation and cause lost circulation
	Swabbing/pressure drop	Swabbing if casing/liner is to be repositioned can reduce bottomhole pressure
Circulating	Fracturing formation	Circulating out kicks can cause excessive pressure at casing shoe and,

		causing fractures to the formation and possible mud loss
Other operations	Surge and swab	Surge and swab during fishing, freeing stuck pipe and other operations can cause increased or lowered bottomhole pressure

Table 2.1 – Causes of kicks for different parts of the drilling operation (Grace, 2003; Skalle & Podio, 1998; Adams & Kuhlman, 1994)

Identifying Inflow

It is crucial to identify kicks as fast as possible, and take action to stop the inflow. A large kick will be more difficult to handle, and the possibility of loss of complete well integrity will increase. There are several methods to identify inflow into the wellbore, and some are more reliable than others. When an unintentional inflow of formation fluids is encountered, some of the mud inside the annulus of the well will be displaced. This will cause the return flow from the well to increase. If the pumping rate is kept constant, the kick can be observed by an increase in the return flow rate. Another indication of a kick is an increase in mud pit volume, as this volume should remain constant when the outflow equals the inflow (Skalle, 2012b).

More subtle signs of inflow can be change in drill string weight, or fluctuations in pump rate and pressure. The drilling fluid in the well provides a buoyancy effect on the drill string, lowering its effective weight. If a kick is taken, the properties of the fluid occupying the annulus of the wellbore are changed. When a formation fluid of lower density is diluting the mud in the wellbore, this can be observed as an increase in drill string weight on the surface. A sudden increase in pump pressure can be observed as influx of formation fluids often causes temporary flocculation of the drilling mud. This will cause a local increase in mud viscosity, and hence increase the pump pressure required to circulate the mud (Skalle, 2012b). Inflow can also cause a slight U-tubing effect in the mud circulation system, causing increased pumping rates and decreased pumping pressure. As the mud column in the annulus is diluted with formation fluid, lowering the density, the heavier mud inside the drill string may start to fall. This will cause a higher flow velocity inside the drill string, and therefore the pump rate will increase. Since a positive pressure differential exists between the drill string and annulus, a lower pump pressure is required to circulate the mud.

Verifying Inflow and Retaining Overbalance

If the drilling crew suspects that the well is kicking, circulation can be stopped to verify if the well is actually flowing. If it is, the secondary barrier must be activated to stop the inflow, and prevent fluid emission to the environment. First, the drill string is hoisted up a couple of feet to hinder pack-off around the bottomhole assembly (BHA) from settling of cuttings and barite. Then the annular preventer is closed to seal off the wellbore. Once the wellbore is sealed, the shut in- and hydrostatic pressure will prevent further inflow.

The annular preventer barrier element has the capability to seal around collars, drill pipe and tool joints. The drill string is sealed by the pressure applied by the mud pumps, or by a float valve preventing flow up the drill string (Adams & Kuhlman, 1994). Once the well is sealed, the surface pressure inside the drill string and annulus can be observed, and kick volume, kick density and pore pressure can be calculated. When the position of tool joints is known, the pipe rams can be closed and the drill string hung off inside the BOP (Skalle, 2012a).

2.2 Circulating Out Kicks

Once overbalance is obtained, the inflow volume must be circulated out of the wellbore, before drilling can be initiated. There are several different methods that are used to circulate out the kick from the wellbore. Different methods have different benefits and downsides, and in certain situations conventional methods cannot be utilized. The method that will be used will be evaluated based on time required to kill the well, maximum allowable annular surface pressure (MAASP), down hole stresses applied to casing and weak formations, position of the drill string, complexity of operation, and kick fluid (Adams & Kuhlman, 1994).

The kick fluid depends on the pore fluid of the kicking formation, and can consist of water, oil, gas, or a mixture of different fluids. Gas kicks are considered the most difficult to handle, since it will expand greatly as it rises to the surface. Oil kicks can yield gas if the pressure is reduced below the bubble point as well. Water kicks are less complicated to handle, since water is near incompressible (Skalle, 2012a).

Equal for all killing methods is that the kick volume is allowed to expand as they rise to the surface, by bleeding off the pressure through the choke (Adams & Kuhlman, 1994). If a gas kick were not allowed to expand during rising, it would carry the bottomhole pressure up to the surface, causing extreme pressures in the annulus. This would potentially fracture the formation, leading to complete loss of well integrity.

2.2.1 Driller's Method

The driller's method utilizes two circulation phases. During the first phase the kick is circulated out of the wellbore, without increasing the mud weight. When the kick is out of the well, kill mud is circulated down the drill string, and the entire annulus is displaced with a kill mud of higher density than the original mud. The kill mud will balance the bottomhole pressure, without having to apply a surface pressure. A slow circulation rate is used throughout the killing procedure to prevent pressure fluctuations, and high frictional pressure in the annulus. The slow circulation rate is normally one half of that of normal operation, causing most of the pump pressure to be lost in the drill string and over the bit (Adams & Kuhlman, 1994).

The advantage of the Driller's method is that it is fairly simple to conduct. The method does not require the weight and volume of kill mud to be calculated and kill mud mixed, before the operation starts. If the drill string is tapered, and the wellbore trajectory is complex, this can become a rather time-consuming operation. This allows the kill operation to start as soon as possible, minimizing the time the well is left without circulation, and hence minimizes the potential for pack-off around the BHA, or rising of the kick (Skalle, 2012a).

2.2.2 Wait and Weight Method

The Wait and Weight Method uses only one circulation phase, where the kill mud is circulated down the drill string as soon as the killing procedure is initiated. The name of this method comes from the fact that there is a certain waiting time while the kill mud is weighted up. Another name for the method is the Engineer's method, referring to the fact that the wellbore pressure can be reduced during the killing operation, if it is carried out correctly.

When circulation is initiated, kill mud is immediately pumped down the drill string. As the kill mud front propagates down towards the bottom of the drill string, the original mud is displaced and pushed out into the annulus. The circulation will cause the kick to rise in the annulus, together with the drilling fluid. When the kill mud has reached past the bit, and the bottom of the well is being filled with kill mud, the hydrostatic pressure in the lower part of the well is increased. Because of this, the surface pressure can be reduced corresponding to the additional hydrostatic pressure, causing a lower wellbore pressure (Roy et al., 2009). This can be critical if the formation integrity in the open-hole section is low.

The open-hole section is the weakest part of the wellbore, since it is not protected by a casing. The fracture pressure of the formation is dependent on the formation strength and the horizontal pressure. If the open-hole section consists of formation of equal strength, the weakest part of the open-hole section will be the formation just below the casing shoe, where the horizontal pressure is lowest. This however, is not true if some part of the open-hole section has been damaged, or consists of a weaker formation.

During a killing operation, the highest pressure at the casing shoe is experienced when the top of the kick reaches it. Beyond this point, the pressure will be reduced. Because of this, the advantages of the wait and weight method is lost if the kick volume enters the cased section before the kill mud reaches the annulus. This can happen if the kick rises to far before the killing operation is initiated, or if the mud volume inside the drill string is larger than the annular volume beneath the casing shoe. If this is the case, there will be no benefits of performing the wait and weight method (Skalle, 2012a).

2.2.3 Volumetric Method

A kick taken when the pipe for some reason is out of the hole must be handled differently than when the pipe is at the bottom of the well. There are several situations where a well integrity problem could occur when the pipe is partially, or completely, out of the hole. Some of the most common is during tripping, logging, running casing, cementing, or installing the wellhead. During these situations, the kicks are most often caused by swabbing, mud loss or inadequate hole fill up (Adams & Kuhlman, 1994). If a kick occurs at this point, the wellbore must be sealed off by the BOP. Conventional killing methods require circulation from the bottom of the well, and efforts will often be made to snub the drill string back down.

If it is not possible to get the drill string to the bottom of the well, or circulation is lost, the volumetric method can be used to bring a kick to the surface in a controlled manner, and without imposing extreme pressures to the wellbore. The volumetric method is carried out by repeatedly bleeding off a certain volume of liquid at the top of the well, letting the gas expand as it rises in the wellbore. The volume that is bled off is adjusted so that the bottomhole pressure always stays above the calculated bottomhole pore pressure (Skalle 2012a). When the kick reaches the choke, heavy mud can be pumped into the well through the kill line, as the casing pressure is bled off through the choke. At this point the drill string should be run down to the bottom of the well, and the well killed by using conventional methods (Skalle, 2012a).

2.2 Causes of Blowouts

A blowout can only occur if several barriers are broken, and is not a result of a single isolated event. Kicks are relatively common during a drilling operation, and can in most cases be controlled and circulated out in a controlled fashion, according to procedures presented earlier in this chapter. Skalle and Podio (1998) investigated reported kicks and blowouts for the Gulf Coast area from 1960 to 1996. It was reported roughly 110 kicks per blowout, and 1.5 blowouts per 1000 well drilled. The trend showed some annual variation, but the frequency of blowouts did not seem to decrease over the years.

Per Holand (1997) investigated the causes of offshore blowouts from the Norwegian and UK sector of the North Sea, and from the US Gulf of Mexico. Blowouts can be categorized after the operation being performed, and is a result of failure in both the primary and secondary barrier. An exception to this is shallow blowouts, caused by shallow charged formations (Holand, 1997). When drilling the top section of a well, the BOP and riser system is often not in place, and a secondary barrier may not exist (Adams & Kuhlman, 1994).

2.2.1 Exploratory- versus Development Wells

A well can often be categorized as either an exploratory well, or a development well. The inherent differences of these wells make the causes of blowouts during drilling rather different.

Exploratory Wells

An exploration well can either be a wildcat- or an appraisal well. Wildcat wells will be drilled into formations that have been explored by a seismic survey, but have not been drilled into before. The seismic survey, together with measurements while drilling, logging while drilling, and wireline surveys, can give a good indication of what lies ahead of the bit. Logging efforts will depend on many factors, but generally wildcat wells are drilled with the least information on the formations ahead. Because of this, unexpected pressurized zones have the highest probability of being encountered for these wells (Holand, 1997). If a wildcat well yields hydrocarbons, appraisal wells might be drilled to evaluate the findings. At this point, more information about the underground is available, but it is still considered an exploratory well (NORSOK standard D-010, 2004).

When an exploratory well has reached the terminal depth, it can be logged and flow tested, before it is either plugged and abandoned, or completed with downhole and surface equipment to become a producer or injector (Sangesland, 2008). Most wildcat- and appraisal wells are not used for production purposes, and are plugged after they

have been tested. Since these wells are not going to be used beyond this point, they do not have the same requirements to wellbore dimensions, well trajectory or casing strength. This can make exploratory wells easier and faster to drill than development wells. According to the SINTEF offshore blowout database, blowouts have occurred 60% more frequently (19 versus 12 cases) during drilling of exploratory wells (Holand, 1997).

Development Wells

Development wells are drilled in areas that have already been investigated by appraisal wells, therefore a lot of information about the underground is known before the drilling operation starts. Development wells can also be drilled in producing fields that already have many producer- and injector wells in place. The extensive knowledge about the formations ahead of the bit makes hitting unexpected high-pressure zones less likely. However, these wells are going to be produced, and requirements with regards to well placement, well trajectory and wellbore dimensions must be fulfilled. This can make the drilling operation complex. After the well has been drilled, it has to be completed with downhole equipment. This extra operation can also lead to well control issues. Because of the possibility of producing wells in very close proximity to the well being drilled, the chance of drilling into these producing wells does exist (Holand, 1997).

2.2.2 Shallow Blowouts

According to the depth of influx, blowouts are often categorized as either a shallow- or a deep blowout. Shallow pressurized permeable formations can present a big challenge for drilling operations. A shallow blowout can occur if the pressure in the top formations is higher than anticipated, or if the bottomhole pressure for some reason unintentionally falls beneath the pore pressure. Gas is the most difficult formation fluid to handle, as it expands greatly when rising towards lower pressure. Because of this, shallow gas is the second biggest cause of offshore blowouts (Grepinet & Flak, 1997).

The upper most formations below the ocean are often poorly consolidated, and the pressure required to fracture them are low. This results in a very narrow pressure window, and the section is often drilled with mud weight very close to the pore pressure. If a kick is taken during drilling, and the wellbore is sealed, the increasing pressure can easily fracture the formations that are unprotected by casing (Holand, 1997). After fracturing, formation fluids can migrate up to the seafloor, or into other formations. To prevent this, it has become common to drill the top section without a BOP installed, hence the section is drilled with only primary well barrier in place.

Since little well control equipment is installed at this stage of the drilling operation, a kick will often lead to complete loss of well control (Adams & Kuhlman, 1991). Shallow gas blowouts often develop very fast. This is contributed to highly permeable formations, small hydrostatic overbalance and large diameter holes.

Because of the weak formations and high flow rates associated with shallow high-pressurized zones, kicks can quickly escalate to complete loss of well control, leading to severe cratering around the wellhead and possibly loss of both well and equipment (Grepinet & Flak, 1997).

Buoyancy Reduction and Surface Conditions

If shallow gas is allowed to escape from the wellhead, and start to rise to the surface, the decreasing pressure will cause the gas to expand and displace the water. Even though the gas will cause a density reduction of the water column, it has become evident in later years that the buoyancy reduction at the surface is small, and that this will not present a danger with regards to sinking floating vessels. Actually, the upward force of the water being displaced has been shown to exceed the effect of reduced buoyancy (Adams & Kuhlman, 1991).

The buoyancy reduction caused by gas flow will increase for increasing water depth, and for ultra-deepwater operations, this effect might be more critical. However, the rising gas will cause the surface of the water to rise locally, and create radial flow of water out from the plume. This can cause floating drilling rigs to capsize and sink. Cratering around the wellhead can cause problems for bottom-supported rigs. Shallow gas blowouts have caused more lost rigs than any other well control issue (Adams & Kuhlman, 1991). To save equipment, the gas must be diverted using ether surface or subsea diverter systems, the rig has to be moved, or a rig capable of handling the gas plume must be used.

Preventing Shallow Blowouts

The safest method for avoiding a shallow gas blowout, is to avoid zones with shallow gas present all together. Special seismic surveys are often carried out to identify shallow gas hazards. Prediction of shallow gas using seismic surveys have been shown to yield unreliable results in the past, and the value of them was considered limited. However, development of 3D seismic surveys to identify shallow gas has improved greatly after the West Vanguard blowout in 1985 (Holand, 1997).

Drilling into a shallow gas zone will not lead to a blowout if the pressure in the well is kept above the pore pressure of the formation in question. Because of the low formation fracture pressure the mud weight window is often fairly narrow in the top formations, and small pressure reductions may cause the well to start flowing.

When drilling exploratory wells, shallow gas blowouts are predominantly experienced during drilling, and can be credited mostly to unexpected high pressure, or to low bottomhole pressure. This can happen for a number of reasons. Since exploratory wells are drilled in areas where limited information on the geological properties of the formations are available, the pore pressure might be underestimated, and the hydrostatic pressure of the mud might be too low to control the formation pressure. If the formations drilled contain high-pressurized gas, it is often of relatively high porosity. The gas inside the formation being drilled will be dissolved into the drilling mud, causing a gas cut mud. If the volume of gas is high, the mud can become so diluted that it is not heavy enough to apply the adequate bottomhole pressure. On the other hand, the low fracture pressure of the shallow formations might cause fractures and mud loss if the wellbore pressure becomes too high. This can lead to annular losses, which again can reduce the bottomhole pressure (Holand, 1997).

When drilling development wells, more information on the formation being drilled is available, and the probability of drilling into zones with unexpected high pressure is small. Because of this, fewer blowouts are experienced during development drilling. The blowouts most often starts when pulling out of the hole, and is caused by a reduced bottomhole pressure because of swabbing (Holand, 1997).

According to Holand (1997) swabbing caused 20 and 40% of shallow gas blowouts in exploratory- and development wells, respectively. The Norwegian Petroleum Directorate recommends drilling a pilot hole if a formation is suspected to contain shallow gas. A pilot hole is simply a hole with a small diameter, used to examine the formation. The hole is increased to the final wellbore diameter at a later stage. The pilot hole is drilled slowly, and circulation is high to reduce the effect of gas cut mud. Pilot holes make dynamically killing the well easier, because of the smaller flow area (Adams & Kuhlman, 1991).

However, drilling pilot holes also has some downsides. When tripping out of small diameter holes, the effect of swabbing is increased. This can cause kicks that would not happen if the hole were drilled with a larger bit diameter. The smaller borehole volume will also be more vulnerable to kicks, as a given influx of gas will displace a higher column of mud. The possibility to dynamically kill the well is also questionable, since the loosely consolidated top formation can be washed out easily at high circulation rates (Holand, 1997).

Handling Shallow Blowouts

The handling of shallow blowouts differs somewhat from conventional blowout control. A BOP is often not in place, the upper formations are normally poorly consolidated and the high wellbore dimensions cause extremely high flow rates.

Diversion

Diverting the gas might not be considered a killing technique, but many shallow gas blowouts only flow for a limited time, before the zone is depleted or the well is bridged. Bridging means that the wellbore collapses in on itself, and the well is plugged naturally. For the shallow gas blowouts recorded in the SINTEF blowout database, 34 of 52 shallow blowouts were brought under control this way (Holand, 1997). Diverting the gas flow away from the drill site will make other well control operations easier since the gas plume is not interfering with surface operations, and flammable gas is handled, or diverted away from the rig.

If a surface diverter system is used, the gas is brought to the surface through the riser. As the gas rises inside the riser, it expands and reaches high flow velocity. This could cause severe sandblasting of surface equipment and overloading of riser slip joints. Shallow gas blowouts often carry with them a lot of debris, and this can block the diverter system, causing increasing pressures down hole. The added friction through the diverter system will also cause additional backpressure in the wellbore (Adams & Kuhlman, 1991). Failure to contain the gas at the rig makes ignition a possibility (Skalle, 2012a).

According to Adams and Kuhlman (1994) studies have shown failure rates from 50 to 70% for diverting the gas flow. The diverter system used on the West Vanguard blowout could only handle the flow for two minutes, before it failed. Attention was put on this equipment in the years following the blowout, resulting in more reliable systems (Holand, 1997).

A subsea diverter system will divert the gas flow from the rig site, but has some of the same downsides as a surface diverter system. The diverted unit is connected directly to the wellhead, and does not need a BOP to operate. The system consists of vent lines with hydraulically operated ball valves, connector, spool adapter, and an annular preventer. The system will apply a backpressure to the well according to the friction created by the fluid that is flowing through it. However, the system is prone to mechanical failure because of erosion, high pressure and flow rates, or debris. The added backpressure could also potentially fracture the shallow formations (Adams & Kuhlman, 1994).

Dynamic kill

It will be difficult to raise the mud weight in the annulus to statically kill the well. When the blowout has escalated, the annulus will most probably be completely filled with gas. If the pipe is still in the hole, efforts can be made to kill the well dynamically. Because of the high flow rate, any mud that is pumped into the well will be diluted by formation gas, and it will be difficult to achieve the proper mud weight. However, if seawater is pumped through the annulus at a high velocity, the frictional pressure loss can raise the bottomhole pressure enough to kill the well. At this point the well can be displaced to a heavier mud, to statically kill the well (Adams & Kuhlman, 1991).

This method can only be applied to small pilot holes. According to Adams and Kuhlman (1994), wellbores with a diameter of 12 ¼-inches and above, and a moderate blowout rate, will be impossible to kill dynamically. Even if it is possible to kill the well using this method, it is still a possibility of severe washouts and fracturing because of the weak top formations.

Vertical Intervention

A shallow blowout can also be killed using vertical intervention. This requires a rig to enter into the blowing well from directly above it. If the gas has been diverted, and the rig is still in place, it can perform the killing operation. If the rig has been moved off location, a semi-submersible rig has to be mobilized. The rig will have limitations with respect to operating draught. Tools are lowered into the wellbore, and down to the bottom of the well. At this point the well can be killed dynamically if the situation allows it, or methods to promote bridging can be utilized. Underwater explosives have been investigated for this use in particular (Adams & Kuhlman, 1991).

Bottom Kill through Relief Wells

Killing by using relief wells will be addressed in chapter 2.4. Special considerations apply when killing shallow gas blowouts. If a dynamic kill is planned, the diameter of the wellbore must be small. Highly angled holes, with high build rates, must be used to intersect the blowing well. Potential for washouts must be evaluated before the pumping rate is decided. If a reservoir flooding technique is to be applied, the relief well should intersect the reservoir horizontally, and at some distance from the blowing well. High pump rates and pressures may be needed to flood the reservoir, and stop the blowout (Adams & Kuhlman, 1991).

2.2.4 Deep Blowouts

When drilling beyond the surface casing, kicks and blowouts can be handled differently because the formations are generally much stronger, and can contain a certain pressure without fracturing. At this stage a BOP is installed on top of the wellhead, and the wellbore can be sealed, if a kick is taken. Compared to shallow gas kicks, which often lead to a blowout, kicks taken when drilling beyond the surface casing can usually be brought under control (Holand, 1997). The NORSOK standard D-010 (2004) states that a drilling BOP shall be installed before drilling out of the surface casing. For a blowout to occur when a BOP is in place, both the primary and the secondary barrier must fail.

Failure of Primary Well Barrier

The most common causes of loss of primary barrier when drilling exploratory wells, is unexpected high formation pressure and too low mud weight. Too low mud weight could be caused by underestimated pore pressure, annular losses or gas cut mud. These problems are inherent to the exploratory wells, considering that less information is known about the pressure and fracture strength of the formations ahead of the bit. Swabbing has also been recorded to cause blowouts during exploratory drilling. This can be credited to both unexpected pressure and bad drilling practice (Holand, 1997).

For development wells, primary barrier were most frequently lost because of swabbing and reduced hydrostatic pressure while cement was setting (Holand, 1997). The reason why swabbing is the most frequent cause for failure of primary barrier, can be credited to the fact that the mud pressure is often kept as close as possible to the pore pressure, to achieve higher drilling rates. When drilling with mud pressure close to the estimated pore pressure, a relative small, unexpected pore pressure increase can cause formation fluids to flow into the well. Swabbing occurs when pulling the pipe out of the hole. A suction effect is created, reducing the bottomhole pressure slightly. The mud weight is often increased according to a trip margin to account for this, but if the pipe is pulled at excessive tripping speeds, the bottomhole pressure can be reduced below the pore pressure, and the well can start to flow (Adams & Kuhlman, 1994). While the cement is setting in the annular space between casing and formation, the cement might shrink, or cement fluid might be forced into the surrounding formation. This can cause a reduction in hydrostatic pressure, leading to influx (Adams & Kuhlman, 1994). It is worth noting that some blowouts had other causes, and some even had unknown causes.

Failure of Secondary Well Barrier

Once a kick has been taken, the methods of controlling, and circulating the influx volume out of the wellbore, is fairly equal for development- and exploratory wells. Methods for detecting a kick have been described in chapter 2.2. The most frequent reason for failure of the secondary barrier was, according to the SINTEF blowout database, failure to operate the BOP, or mechanical failure of the BOP. For development wells, failure to operate the BOP contributed to 25% of secondary barrier failures, while mechanical failure contributed to 16.7%. For exploratory wells, 10% of secondary barrier failures were caused by failure to operate the BOP, while 15% were caused by mechanical failure. In some instances, the BOP was not in place when the well control issue arises. Usually, this was because the BOP had been nippled down to be able to run casing into the hole (Holand, 1997).

Another reason for loosing well control was failure to seal the drill string. If the drill string is left open during a kick, the kick can migrate up the drill string and cause a blowout. During drilling and tripping the drill string can be closed by a kelly valve, above or below the kelly, or a valve inside the top drive (Adams & Kuhlman, 1991). During connections the valves needs to be stabbed against the flowing well, to close the drill string. A one-way flowing valve may be located just above the bit, this will close if the flow inside the drill string reverses. If the drilling crew is not able to shut in the drill string once a well integrity issue arises, it can be cut and sealed by the blind ram inside the BOP (Holand, 1997).

Even though the BOP and drill string is able to contain the pressure from a kick, the secondary barrier also comprises of the formation, casing and cement. Blowouts have been caused by either of these components failing. If a kick is shut in, the increasing pressure can cause the weakest formation in the openhole section to fail. If this formation is permeable, and has lower pore pressure than the pressure in the wellbore, the well can start to flow into this formation. This is categorized as an underground blowout, and is the most common well control problem (Tarr & Flak, 2006). If the formation is of lower permeability, a fracture can propagate into nearby wells causing a cross flow between the wells.

If the cement surrounding the casing is not sufficiently tight and impermeable, the formation fluid might migrate up in the annulus between casing and formation, and reach the surface. Another possibility is that the casing might be subjected to excessively high pressure, causing it to rupture (Holand, 1997).

2.2.5 Blowouts during Completion and Workovers

Completion

The process of completing a well includes several operations where a kick can be induced, and well control can be lost. Depending on completion strategy, a casing is run down to a predetermined depth and cemented into place. The well is displaced to a completion fluid and a production tubing, fitted with various equipment, is installed. The BOP is replaced with a X-mas tree, to control the production of fluids from the well. During equipment installation, the barriers are the same as during drilling. When the well has been completed and production has started, the barriers are the X-mas tree and a downhole safety valve (Sangesland, 2011).

Substantially fewer completion blowouts have occurred compared to drilling blowouts (Holand, 1997). Surge and swab can occur during completion as well, but enough knowledge should exist on the pore pressure and fracture limit of the formations to prevent the pressure in the well to reach critical values. At this point in the operation, casing will protect a substantial part of the hole as well. Most of the blowouts occurred as a combination of too low hydrostatic pressure and failure of safety valves and BOP. The reduced pressure was generally caused by swabbing or inadequate mud weight. In some cases annular losses led to reduced height of the mud column, and subsequently an unexpected inflow. The losses were induced by increased pressure caused by high circulation rates, or surge (Holand, 1997).

Workovers

A workover is the process of maintenance or treatment on a well to restore, improve, or prolong production- or injection capabilities of the well. The process involves placing a rig over the wellhead, killing the well, and often partial- or complete pulling of tubing and equipment (Schlumberger, 2013). In later years, through-tubing workovers, utilizing coiled tubing or snubbing, have become more common. This has made workovers safer and more efficient (Holand, 1997).

When the packer is pulled from the well, the producing zone is exposed, and the possibility of flow exists. Workovers will often expose the well to productive formation for longer periods of time than during drilling. However, several casing strings protect parts of the wellbore, and in many cases the productive formation is also cased and perforated. Because of this, the wellbore can withstand higher pressure. Subsequently, many workover blowouts have been killed by bullheading (Holand, 1997).

Most workover blowouts were caused by a combination of too low hydrostatic pressure, together with failure of BOP or safety valves. The reduction of hydrostatic pressure was mostly caused by swabbing, or trapped gas (Holand, 1997).

2.3 Blowout Control

There are three stages associated with controlling a blowout. These are detection and response, containment, and control. First the rig and all equipment must be shut down, rigs in danger must be moved, wellbore sealed and personnel evacuated. Secondly the oil spill must be contained. Thirdly the blowout must be killed (Adams & Kuhlman, 1994).

2.3.1 Killing Technique Selection

When planning a well, a contingency plan with regards to killing of a potential blowout should be developed. The content of the contingency plan will be dependent on the location of the well, and will be governed by legislations and operator's internal requirements. The NORSOK standard D-010 (2004) states that a blowout contingency plan should contain the kill methods that are going to be used in case of a blowout, a mobilization plan for equipment, services and personnel, location for potential relief wells, and measures for reducing emissions and damage on the surface.

The kill technique chosen will depend on the properties of the blowout. It is difficult to choose a single kill technique for all applications. A kill technique should be chosen based on its success factor, the time and cost of implementation, and safety of operation. It should also minimize the emissions to the environment. It can often become necessary to deploy several methods to secure the fastest and safest termination of the blowout (Adams & Kuhlman, 1994).

If the primary kill method takes a long time to implement, is very complex, or has a high risk of failing, a secondary method should be implemented as well. The time factor is especially important if the blowout fluid is oil or sour gas, as this is especially damaging to the environment, and has high cleanup costs. A blowout will often be given high media attention, and public pressure to stop the blowout can become very high. This can make the operators choose several kill methods, to secure the success of the killing operation (Adams & Kuhlman, 1994).

2.3.2 Top Kill

An offshore top kill operation is carried out by means of vertical intervention, or by an offset kill. A vertical intervention is carried out by a semi-submersible, directly above the blowing well. During this operation, the semi-submersible will be affected by the rising formation fluids. Care should be taken when choosing the correct vessel, since it must be able to withstand the forces from the gas plume, and subsequent water flow, created by the rising and expanding gas. If the water depth is very deep, the buoyancy reduction might have to be considered (Adams & Kuhlman, 1994).

An offset kill is carried out by semi-submersibles, barges, drillships, or potentially jack-up rigs. During this operation the rig is at a small horizontal offset from the wellhead. Cranes are used to get the equipment directly above the blowing wellhead. This method can be utilized if the blowout has been ignited, or if the surface conditions are too bad (Adams & Kuhlman, 1994).

Capping

Capping refers to putting a surface cap on the well, and hence stopping the flow. To perform a capping operation, access to a casing string, with integrity to handle the shut in pressure is required. The depth of this casing is also important, since the formation below the casing shoe must withstand the shut in pressure. To cap the well, the old wellhead equipment is removed, and a new wellhead and BOP stack is installed. At this point the BOP can be shut to stop the flow. The pressure in the annulus should be monitored, and the flow diverted if the MAASP is exceeded (Adams & Kuhlman, 1994).

When the blowout is contained, operations can be started to kill it. Bullheading is the most common killing technique for capped blowouts. Bullheading is performed by injecting a heavy fluid through the kill lines of the BOP, and applying a surface pressure to force it down into the well. When the kill mud has been bullheaded down to the blowing formation, the well should be in static overbalance. Bullheading subjects the wellbore to high stresses. If the wellbore has weak spots, that will not withstand the pressure from the operation, for example eroded wellhead or ruptured casing, a packer can be stung into the well, and the bullheading performed below the packer (Adams & Kuhlman, 1994). Bullheading cannot be performed if the formation below the casing is in danger of fracturing because of the increased pressure from the operation. If this happens, the blowout can escalate to an underground blowout.

Surface Stinger

A quick method to try to control a blowout is by the use of a stinger. The stinger operation is performed by forcing a packer into the flowing pipe, and set it hydraulically. When the well is shut, killing fluid is pumped through the stinger and into the wellbore. This method can be used on blowouts where the flow rates and pressure are low (Adams & Kuhlman, 1994). This operation is performed faster than a capping operation, since the BOP and wellhead does not need to be replaced.

2.3.3 Bottom Kill

A bottom kill is executed by injecting fluid into the lower parts of the well. If the drill string is off bottom, and snubbing is not possible, the only option to get access to the lower parts of the well is to drill a new well, called a relief well. Once hydraulic communication has been obtained between the relief well and the blowing well, the process of killing the blowing well can be initiated. Killing a well from the bottom up can be less complicated than performing a top kill. When kill fluid is injected into the blowing well at a certain depth, the pressure and flow in the well will push the fluid up towards the surface, distributing it along the wellpath. When performing a top kill, the kill fluid is forced down into the well, against the direction of the flow, by applying a large surface pressure (Adams & Kuhlman, 1994). Chapter 2.4 will go into detail about all aspects of performing a killing operation through a relief well.

2.4 Relief Wells

Relief wells can be used to kill a blowing well in a number of different ways. The name originates from the fact that the early relief wells were used to relieve the pressure from the blowing formation. This was simply performed by drilling a vertical relief well straight into the reservoir, and producing them at extremely high rates, trying to kill the blowing well by means of pressure draw down (Adams & Kuhlman, 1994).

As drilling techniques have evolved, relief well drilling has become more sophisticated. The early relief wells were drilled vertically with no surveying instruments. As deviated wells, with increased positioning accuracy, became possible, relief wells developed. With advanced surveying methods, MWD-capabilities, steerable systems, and powerful surface equipment the relief wells have become what they are today (Wright & Flak, 2006).

2.4.1 Relief Well Killing Methods

Pressure Draw Down

The first use of relief wells was fairly simple. Methods to intersect a blowing well were nonexistent. Because of this, the only option was to drill vertical wells to intersect the blowing reservoir. The relief well was produced at as high rates as possible. The goal of the relief well was to reduce the pressure as fast as possible, to kill the blowing well through pressure drawdown. This often required several relief wells. When the reservoir pressure had dropped to a sufficient level, the hydrostatic- and frictional pressure drop throughout the blowing well would overcome the reservoir pressure, and the well would seize to flow (Wright & Flak, 2006).

Reservoir Flooding

Development of surveying instruments, deviated wells and whipstock-tools made directional wells, with some degree of accuracy, possible. This led to advancements in relief well drilling. A 1933 blowout in Texas, were killed with the first directional relief well. The relief well intersected the formation below the blowing well, and was killed by pumping water down the relief well (Wright & Flak, 2006).

This method is called reservoir flooding, or the saturation method. It kills the blowout by pumping water into the reservoir, and flooding the vicinity of the blowing well. If successfully performed, the water from the relief well will replace the reservoir fluid in the blowing well. Once the hydrostatic pressure of the flooded part of the reservoir equals the reservoir pressure, the blowout will seize to flow. This method is dependent on relatively close proximity of the relief well compared, to the blowing well. The water

volume needed to control the well increases greatly when the distance between the wells is increased (Adams & Kuhlman, 1994).

Communication through Hydraulic Fracturing

Direct communication between the relief well and the blowing well will drastically reduce the amount of fluid needed to perform the killing operation. Up until the 1970s, communication was often obtained through hydraulic fracturing. First, the relief well was drilled as close to the blowing well as possible. Secondly, the bottomhole pressure was increased, and the formation around the relief well fractured. For the method to be successful, the fractures would have to propagate, and intersect the blowing well. If this were not possible, acid squeezes could be performed (Wright & Flak, 2006).

The fractures induced around the relief well will propagate perpendicular to the lowest horizontal stress. Because of the high degree of uncertainty with regards to position of the wells, and downhole stress regime, several wells often had to be drilled. This would increase the probability that hydraulic communication would be established. Water was pumped down the relief wells to verify that communication was obtained. At this point the blowout could be killed by water flooding the reservoir, or by pumping fluid directly into the blowing well (Wright & Flak, 2006).

Since the fractures must also be able to support a flow rate high enough, and injection pressure low enough, to kill the well. The technique has been most successful at controlling blowouts of relatively low flow rates (Adams & Kuhlman, 1994).

Direct Intersect

Previously used kill methods utilizing relief wells were difficult to implement for high-pressure gas reservoirs, deep reservoirs or low permeability reservoirs. In the 1970s a deep exploration well, operated by Shell Oil in Mississippi, blew out. This prompted the development of new technology. Wireline surveys were used to detect proximity of the steel casing of the blowing well, relative to the relief well. The well was directly intersected at approximately half of total depth, and communication was established through perforating the steel casing. When communication was established, the well was killed through pumping heavy mud directly into the blowing well (Wright & Flak, 2006). This represented a big leap forward for relief well drilling.

2.4.2 Relief Well Planning

Surface Position

Several considerations must be taken when deciding the surface position of a relief well. According to the Norwegian legislation, plans should be present for a relief well for every well, or cluster of wells, that is being drilled. This plan should contain two surface locations suitable for drilling a relief well. Further, the plan should contain shallow seismic interpretations, accurate water depth, seabed and sub-surface drilling hazards, seabed topography, identification of anchor holding capacities, boulders, pipelines, and other obstructions. Shallow gas hazards must be within an acceptable limit for the drilling location (NORSOK standard D-010, 2004). Depending on blowout scenario, other considerations have to be taken into account as well.

Intersection Angle

Generally, an intersection angle between 3 and 15º is considered the optimum angle to intersect the target casing (Adams & Kuhlman, 1994). This is considered the optimum range because a lower intersection angle would result in the need for milling or perforating of the target casing. A larger angle would make the relief well move in on the target at a faster pace, and trajectory adjustments would be difficult. Since the two wells are positioned near parallel to each other, this also increases the accuracy of the ranging tools. In addition to this, if a relief well was drilled to intersect the target perpendicularly, and missed, the drill string would have to be pulled back, a whipstock deployed, and a sidetrack started (JWCO, 2009a).

Horizontal Offset with Regards to Relief Well Trajectory

The consideration in regards to intersection angle might influence the choice in spud location of the relief well. If the blowout is shallow, a large horizontal displacement means that the well must be drilled highly deviated to reach the target, before it is adjusted to intercept at the appropriate angle. This trajectory might require build angles that are too aggressive, and might make the well difficult to drill. If the blowout is deeper, this leads to more flexibility with regards to spud location, as large build angles are not needed (Adams & Kuhlman, 1994).

Wind and Current Considerations

The rig that is going to drill a relief well must be safe from dangers posed by the blowout. If the blowout fluid consists of gas, the relief well drilling site should not be located downwind from the blowout. Flammable and toxic gases can be carried with the winds, and present dangers to the drilling crew and equipment. If the blowout fluid consists of oil, currents can carry flammable oil over to the relief well site. This must also be considered (Leraand et al., 1992).

Knowledge of Downhole Formations

If some locations around the blowing well have been investigated by seismic surveys to a higher degree than other, it will be favorable to drill from this location. When the relief well to kill the 2/4-14 blowout was in planning, it was decided to put the relief well spud at the intersection between two seismic lines. This gave good information about the formations below the relief well rig site (Leraand et al, 1992).

Minimum Water Depth

Semi-submersible drilling rigs are often used to drill relief wells. These rigs will have a certain operating draft requirement. If the water depth is too shallow, some rigs might not be able to operate (Adams & Kuhlman, 1994). If a jack-up rig is going to be used, this rig will have a maximum operating water depth.

Safe Distance from Gas Plume

A high rate gas blowout can create a plume on the ocean surface exceeding one hundred meters in diameter. This plume creates stability issues for floating rigs, and should be avoided if the rig is not strong enough to handle it. If the possibility of a large gas plume is present, this must be considered when choosing the relief well drill site (Warriner & Cassity, 1988).

Casing Considerations

The casing program used on the relief well must be specialized to the task that is going to be performed. If fluids are going to be pumped down the relief well at high rates, the casing diameters must be large enough to handle the flow rates without causing intolerable surface pressures. The burst rating of the casings must also be able to withstand the forces they will be subjected to during the killing operation. There should be planned for one contingency casing in case of unforeseen trouble during the drilling operation. Depending on relief well trajectory, aggressive doglegs might be required, and this might set limitations on the casing design (JWCO, 2009a).

2.4.3 Relief Well Intersection Point

Even though a relief well is classified as a bottom kill technique, the intersection point is not always at the bottom of the well. The position of the kill point will influence the entire planning of the relief well. Generally it is desired to intersect the blowing well as deep as possible. However, when using conventional ranging tools to locate the blowing well relative to the relief well, steel have to be present in the borehole of the blowing well (Leraand et al., 1992). Figure 2.1 compares casing shoe- and bottomhole intersection.

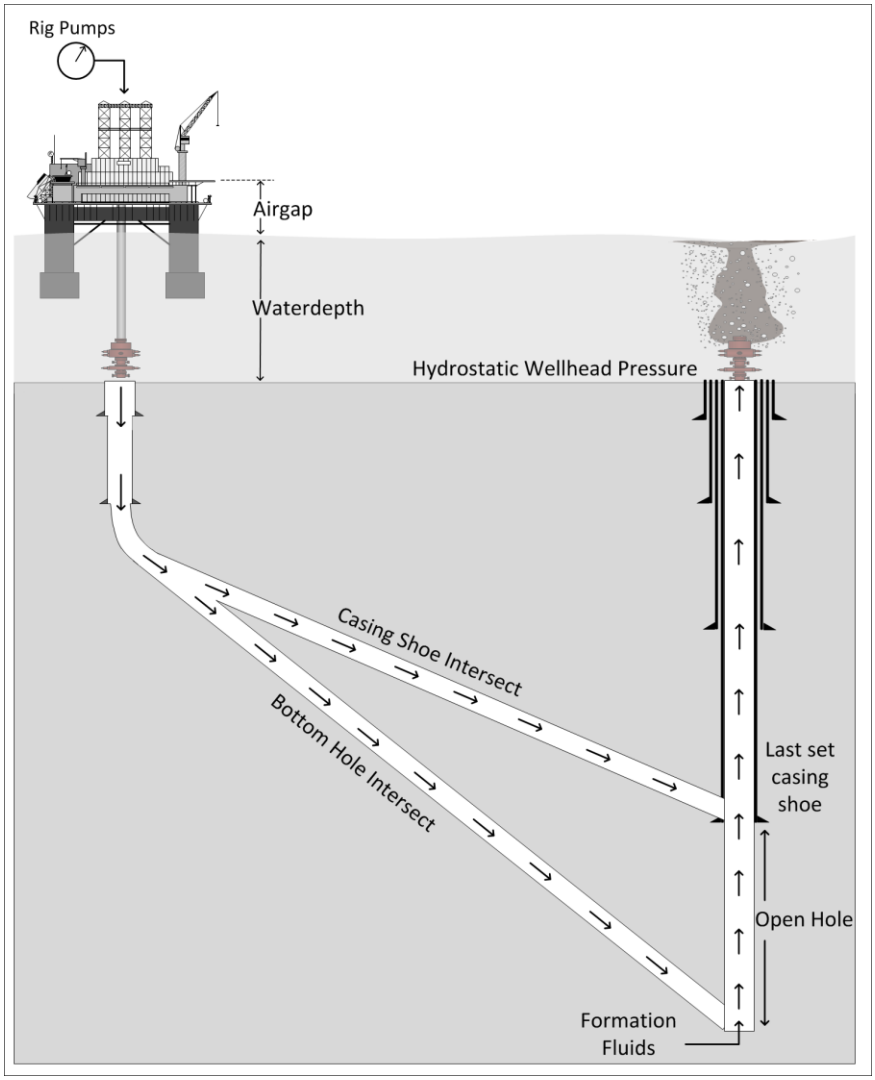

Figure 2.1 – Relief well intersection point

Both casing and drill pipe can be used to home in on the blowing wellbore. However, the position of the drill pipe might be unknown. If the blowout took place when the drill string was off bottom, the entire openhole section will not contain steel. If the drill string were on bottom, the forces in the wellbore during a blowout can cause the drill string to be pushed further up in the well.

The flow path must also be considered before choosing the intersection point. Depending on the position of the drill string, and what top kill methods have been carried out at a earlier stage, certain parts of the wellbore might be sealed by cement, settled barite or hydraulic plugs. The flow path might be through the annulus, drill pipe, outside of casing strings, through underground formations, or a combination of any of these (Leraand et al., 1992).

A bottom intersection will be favorable in a number of different ways. Since a higher column of kill mud can be obtained through a bottom intersect, the increase in hydrostatic pressure on the blowing formation will be higher. If a dynamic killing method is utilized, the increased length of the wellbore will also result in a higher frictional backpressure for a given pump rate. In addition, since the pressure in the wellbore increase with depth, the wellbore pressure at the bottom will be higher. Hence, the influx fluid will be under higher pressure at this point, and also of smaller volume. This is especially true for a gas blowout. When the volume is at its smallest, the flow rate, and velocity, will be at its minimum. The kill mud will not be diluted to the same extent as higher up in the wellbore. This leads to a quicker pressure build up (Adams & Kuhlman, 1994).

There are some advantages to intersecting the blowing well off bottom. The intersection point is shallower, and hence the drilling length is shorter. The relief well will be drilled faster. Since the survey errors ad up with depth, the position of the wellbore can be determined with a higher accuracy for the upper sections of the well. Since the relief well must come within a certain distance from the blowing well before ranging tools can be utilized, the increased accuracy can make drilling the relief well easier. If an extra casing string must be used for a deeper intersection, the wellbore dimensions will be smaller. This will increase the frictional pressure drop throughout the relief well, and hence the pump capacity needed to successfully kill the blowout (Adams & Kuhlman, 1994).

Tools that are used to accurately position the blowing well has, up until today, been dependent on some steel in the well. If no pipe is left in the hole beyond the last set casing shoe, this will be the deepest point a relief well can intersect the blowing well (Adams & Kuhlman, 1994).

2.4.4 Static versus Dynamic Kill

Once hydraulic communication is obtained, the blowing well is killed by increasing the pressure in the wellbore, to obtain overbalance. This can be done by increasing the hydrostatic pressure, the frictional pressure, or a combination of both. The pressure in the blowing well is determined by the hydrostatic- and frictional pressure applied by the flowing fluid (Wright & Flak, 2006). Once the killing operation is initiated, a heavier fluid is injected into the blowing well. This will cause the hydrostatic pressure to increase. When performing a static killing operation, a kill fluid with sufficient density to balance the reservoir pressure by the hydrostatic pressure alone, is used. Once the entire blowing well is displaced to this fluid, it will be statically dead.

By circulating kill fluid at a high rate through the blowing wellbore, high frictional pressure is created. This will enable killing the blowout with a lighter fluid than during a static killing operation. This is referred to as a dynamic kill. It is dependent on good communication between the two wells, to ensure minimum pressure loss as the liquid flows into the blowing wellbore. During a dynamic kill, the bottomhole pressure is sufficiently high as long as the fluids in the blowing wellbore flows at a velocity high enough to create the frictional backpressure required (Adams & Kuhlman, 1994).

A dynamic killing operation is usually performed in two stages. First a lightweight fluid, like seawater, is pumped into the relief well at a calculated dynamic kill rate. The high flow rate in the blowing well will create a frictional backpressure that supplements the hydrostatic pressure, and allows for killing the blowout with a lighter fluid. Once inflow is stopped, a lower rate is maintained for an extended period to ensure that all hydrocarbons are circulated out of the well. At this point, mud with sufficient density to provide static overbalance, is circulated into the well to kill it statically (Leraand et al., 1992).

This method has both advantages and disadvantages. First of all it is less complicated to calculate the kill rate, since once the flow consists of seawater only, the frictional pressure loss is dependent on flow conduit dimensions, fluid properties and wellbore friction factors only. Since the flow is stopped before kill mud is injected, the pressures in the wellbore is not dependent on reservoir production index or reservoir fluid properties. Seawater is readily available, and does not present any dangers if released to the environment. Since the injection of kill mud takes place when the well is dynamically killed, the mud losses are greatly reduced. By building the pressure in stages, the bottomhole pressure can be measured, and the risk of fracturing the formation is reduced (Leraand et al., 1992).

The disadvantages associated with dynamic killing are the high rates often required to produce the required frictional pressure drop in the blowing well. It might require multiple powerful pumps, putting limitations on the deck capacity of the kill rig. It also has limitations with regards to well dimensions. The relief well must have large enough dimensions so that the frictional pressure loss in the relief well tubular does not become too high. The blowing well must have dimensions that can facilitate the high frictional pressure losses required during the dynamic killing operation (Leraand et al., 1992)

2.5 State of the Art: Homing-in devices

Borehole positioning surveys are performed repeatedly as the bit propagates down into the earth. However, systematic errors inherent in the survey tools used, and errors related to the borehole environment, cause borehole position uncertainty. This will be addressed in subchapter 2.7. The maximum error is dependent on the borehole conditions, presence of steel, tool alignment, type of survey tool utilized, and wellbore inclination. As the bottomhole assembly moves deeper into the underground, the errors multiply and can range from under one meter, up to above 100 meters (de Lange & Darling, 1990). These uncertainties will exist both for the blowing well, and the relief well being drilled. Consequently it becomes impossible for a relief well to directly intersect the blowing well, using conventional survey techniques alone. Because of this, homing-in devices is used to detect the steel present in the blowing well, once the two wells are within a certain distance of each other. Commercially there are generally two types of tools available for this task, passive magnetostatic tools, and active electromagnetic tools.

2.5.1 Passive Electrostatic Tools

The passive homing-in tools used today was developed in 1975, during a blowout in the Gulf of Mexico (Wright & Flak, 2006). The earth's magnetic field can be measured by using a DC magnetometer. The steel tubular inside the blowing well will have a certain degree of remanent magnetization, and this will affect the magnetic field measured in the formations surrounding the wellbore of the blowing well. The tool would be lowered into the relief well, and measure the earth's magnetic field along the wellpath. Once the measurements started to become skewed by the influence of the remanent magnetization of the steel tubular in the blowing well, the drilling crew could calculate the relative position between the wells (de Lange & Darling, 1990).

The magnetization of steel casing is week and unpredictable, and generally the detection range of electrostatic tools is estimated at 15 meters under ideal conditions (de Lange & Darling, 1990). This means that traditional surveying techniques must get the relief well within this distance, and the magnetostatic downhole tool is used to guide the relief well

the last distance before intersecting the well. De Lange & Darling (1990) discussed the possibility of artificially magnetizing the casing to saturation, before it is run into the well. Field tests were performed at Rogaland Research Institute, Stavanger, and showed that doing this doubled the detection range of passive ranging tools.

Today, magnetostatic tools are offered through GE Energy's MagRange III, Schlumberger's GPIT and Vector Magnetics PMR. A big advantage with using this passive method is that the tools can be integrated into the MWD-package, and hence it is not necessary to pull out of the hole, and perform a wireline survey, to establish the relative position between the wells. It is also not affected by the formation type surrounding the borehole (de Lange & Darling, 1990).

2.5.2 Active Electromagnetic Tools

The first active homing-in tool was developed during another Gulf of Mexico blow out in 1980. This wireline tool relied on an electromagnetic survey to find the distance and position of the blowing well, relative to the relief well. A surface AC current was applied to the deepest set casing of the blowing well. Hence, a magnetic field would be induced. Magnetic sensors were lowered into the relief well, and the relative position of the two wells was calculated based on the strength and direction of the induced magnetic field. During a 1982 blowout, this technique was used to great success. The casing of the blowing well could be detected over 200 feet (61 meters) away, and the blowing well was directly intersected by the relief well (Wright & Flak, 2006).

In the years following these events, the active electromagnetic tools were developed further. Today, active ranging tools send out a low-frequency AC current from electrodes integrated into the tool itself. The survey builds on the fact that the steel casing of the relief well impose a much lower resistance to the current, than the surrounding formations. The current will flow radially out from the electrode until it hits the casing of the blowing well. At this point the current will choose the path of least resistance, and flow up and down the casing. This will create a magnetic field around the casing that can be measured by a sensor package in the relief well (de Lange & Darling, 1990).

Since the tool emits a current into the formations surrounding the relief well, this method is dependent on the properties of these formations. The method has shown poor results in the presence of salt formations. In addition to this, limitations are put on the drilling fluid used during the survey. A highly conductive mud will cause much of the injected current to flow along the mud column. Because of this, oil based mud are generally used in combination with electromagnetic surveys (de Lange & Darling, 1990).

Active electromagnetic tools are offered by Vector Magnetics, through the Wellspot tools, and through the Elrec logging method (de Lange & Darling, 1990). Traditionally, electromagnetic tools were run into the hole using a dedicated survey string, and this is still the standard today. This means that the entire drill string has to be pulled out of the hole, making the survey procedure very time-consuming. Recently, Vector Magnetics released the WellSpot at Bit tool. This tool can be integrated into the BHA, and does not require the drill string to be pulled to perform a survey (Vector Magnetics, 2011).

2.5.3 Novel Approaches to Direct Intersection

In addition to the standard techniques used to facilitate direct intersection during relief well drilling, several more novel solutions exist.

Trajectory Relative to Subsurface Formations

Patent number US4480701A describes the process of using subsurface formations to find the trajectory of the relief well, relative to the blowing well. Good logging data should be available from the blowing well. By evaluating these logs, the depths of different subsurface formations can be obtained. Once the relief well has been drilled to a predetermined position, based on conventional surveying techniques, the wellbore is traversed with an accurate acoustic logging tool. By doing this, the depths at which the relief well intersects the same subsurface formations can be recorded. The results will be compared to data from the blowing well, and based on this the relative position of the two wells can be established (Baldwin, 1984).

By running a dipmeter log into the relief well, the dip angle of a subsurface formation can be determined. Together with the intersection depths of the two wells, this can be used to calculate the absolute distance between the two wells (Baldwin, 1984).

Acoustic Sensor Tool

Patent application number US 20130118809 A1 describes a method where the fluid flow of the blowing well is used for homing-in purposes. An acoustic sensing tool is included in the BHA, and connected to a surface processing system via wired drill pipe. Once the relief well is within a certain distance of the blowing well, circulation is stopped and the acoustic sensor is used to acquire acoustic signals generated from the flowing fluids in the blowing well. The results are transmitted to the surface, where they are interpreted to yield the direction and distance to the target (Veeningen, 2013).

Figure 2.2 shows how a blowing well is intersected via standard survey methods, and electromagnetic ranging tools.

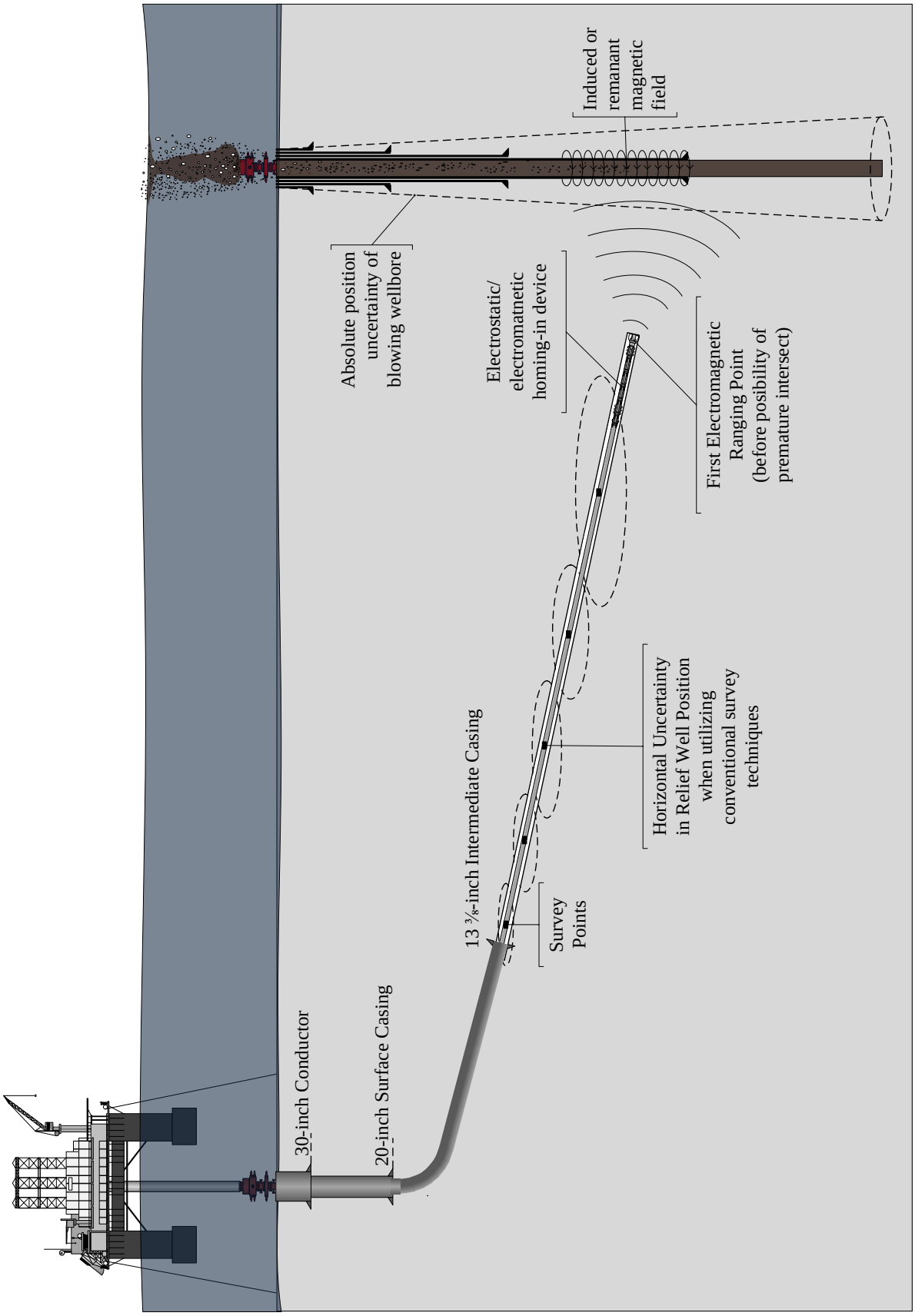

Figure 2.2 – Intersection strategy utilizing electromagnetic ranging tools

2.6 Relief Well Trajectory and homing-in procedure

The relief well killing strategy will dictate the trajectory of the relief well. Reservoir flooding only requires that the well hits the reservoir, but will be more effective if the distance between the blowing well and the relief well is shorter. Communication through hydraulic fracturing requires that the relief well is closer to the blowing well. It is also beneficial if the relief well is located in such a manner that the fractures propagate towards the blowing well. If communication is not obtained, the pressure can be increased to just below the pressure rating of the casing shoe formation, or acid squeeze can be considered (Leraand et al., 1992).

Direct intersection requires more of the relief well trajectory. First of all, as mentioned previously, the intersection angle should be between 3 and 15º. Depending on the blowing well, this will most likely mean that the lower section of the relief well must be near vertical. Because of the horizontal displacement between relief- and blowing well, this means that the relief well will have a vertical section in the loosely consolidated top formations, then kick off to a deviated section, before it drops back to vertical (Adams & Kuhlman, 1994). To accurately intersect the blowing wellbore, the relative position between the wells must be known with a high accuracy. Depending on ranging procedures, this might require a triangulation approach. To be able to triangulate the ranging survey tools, the wellpath of the relief well must cross the blowing wellbore as close as possible, before it drops off to parallel to the blowing wellbore (Leraand et al., 1992).

Ranging Procedure

Once standard survey tools have positioned the relief well as close as possible to the blowing well, without the danger of drilling into it, the homing-in process can start. It is important that the maximum uncertainty between the two wells does not exceed the maximum ranging distance for the ranging tools. Beyond this point the relative distance between the wells is important, as opposed to the absolute position of the wells.

Magnetostatic tools have a shorter detection distance, but can be integrated into the BHA, and do not require the drill string to be pulled out of the borehole to perform a survey (de Lange & Darling, 1990).

If electromagnetic ranging tools are used, the drill string is pulled out of the hole, and a specialized tool containing a magnetic field sensor and a current injector electrode is run into the hole. A uniform alternating current is injected into the formation. If the current hits a steel casing, the alternating current will short circuit and create an electromagnetic field. Sensors in the ranging tool pick up the magnetic field, and the distance and direction to the casing of the blowing wellbore is calculated (Add Energy, 2013).

It is generally recommended that the first ranging point is located at least 300 meters true vertical depth (TVD) above the planned kill point. This allows the relief well to be dropped off and drilled parallel to the blowing wellbore, and course corrections can be made before the target is reached (JWCO, 2009a). The parallel section of the well also allows for triangulation ranging to be performed, and this greatly reduces the accuracy of the ranging tools (Add Energy, 2013). Vector Magnetics also recommends that a bypass of the blowing wellbore is performed. This means that the relief well is drilled past the blowing well as it is dropped off. This method ensures that the target casing is located, and it reduces the relative positioning uncertainties between the wells further (JWCO, 2009a).

Electromagnetic survey tools have an uncertainty of 10% when a bypass is performed. This means that if the blowing casing is bypassed at a distance below 10 meters, the uncertainty is reduced to below one meter. By using the bypass section to calibrate the ranging tools, and continuously performing surveys in the parallel section, a direct intersection can be accomplished. Once the wells are within one meter of each other, the pressure drawdown will cause the formation to cave in under the pressure, and direct hydraulic communication will be obtained (Leraand et al., 1992).

Figure 2.3 shows how the triangulation bypass reduces the uncertainty.

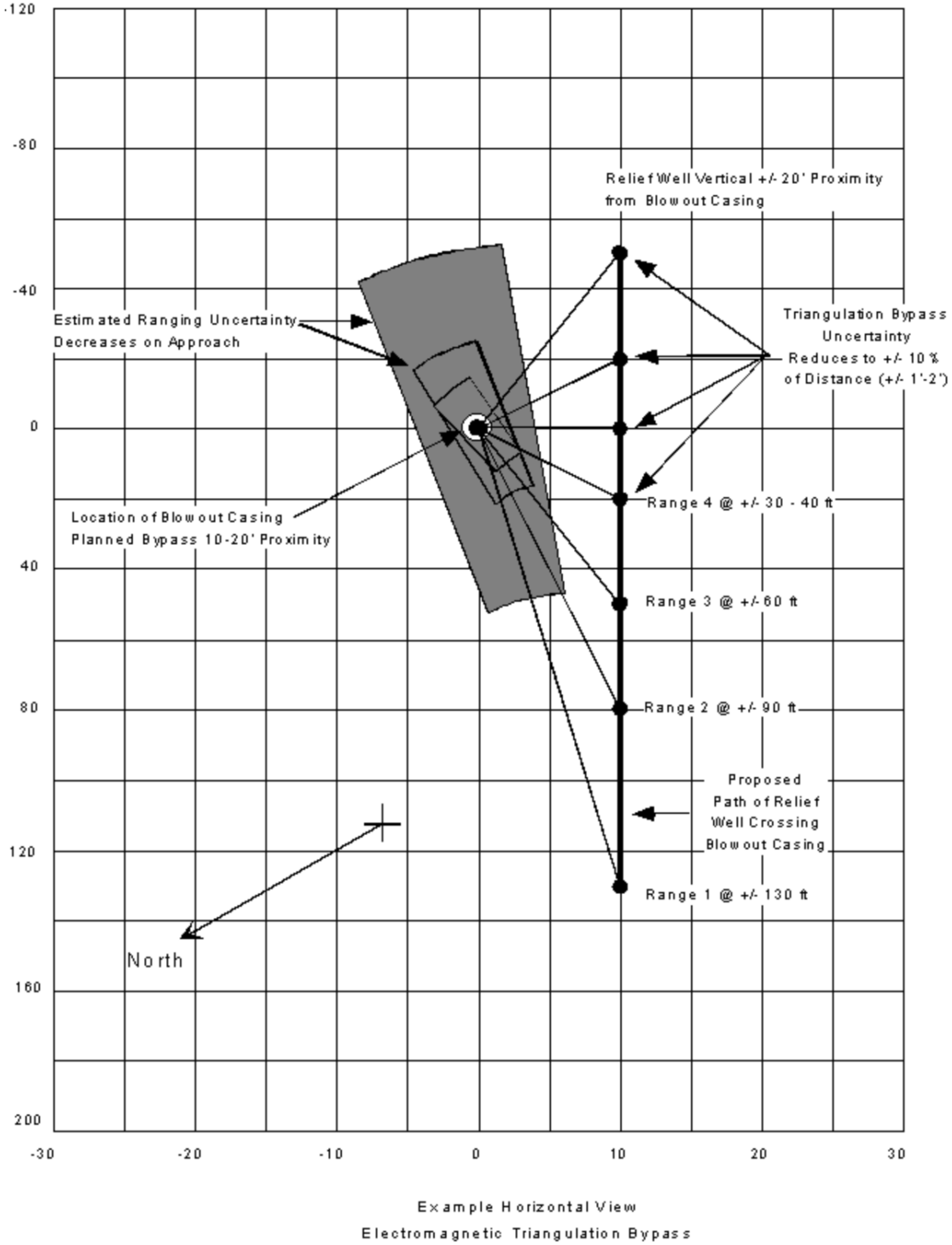

Figure 2.3 – Triangulation approach to reduce ranging tool uncertainty (JWCO, 2009b)

2.7 Survey Uncertainty

2.7.1 Wellhead Position

It is very important to have an accurate position of the wellhead before drilling is initiated. Together with drill floor coordinates, this will be the reference point for the well. The NORSOK standard D-010 (2004) states that a wellbore center must be determined by the use of differential global positioning system. The position of individual wellheads can be established by measurements from fixed reference points. Because of this, the geographic position of the blowing wellhead should be very accurate. As the drill bit propagates down into the earth, efforts are made to keep the inclination and azimuth of the wellbore according to the well plan. However, many processes take place during drilling that can push the bit out of course, leading to a deviation in wellbore trajectory, compared to the well plan. Because of this, surveys are performed at certain intervals to reduce this uncertainty.

2.7.2 Wellbore Positioning

A survey is performed with a downhole tool that measures the inclination and azimuth of the borehole relative to the earth's gravity, magnetic field or some other reference. The tool can be lowered down the drill string by the use of a wireline survey, dropped inside the drill string, or be integrated into the bottomhole assembly as MWD-packages (Samuel & Liu, 2009). Norwegian legislations require that a survey measuring inclination and azimuth must be performed every 100 meters drilled (NORSOK standard D-010, 2004). Once the position of the well has been established at a given depth, different calculation methods are used to determine the well path between the survey points.

Downhole surveying tools may be categorized as either magnetic-, or gyroscopic surveying instruments. They can be further categorized as single shot, multi shot, or MWD-surveys. Single shot instruments perform only one reading at a given depth, while the multi shot instrument have capabilities of performing several surveys. MWD-surveys utilize tools integrated into the BHA, and transmit the results up to the surface through mud telemetry (Samuel & Lui, 2009).

Magnetic Surveying Tools

Magnetic surveying tools measure the earth's magnetic- and gravitational field, at the given position in the wellbore. Once information about the magnetic conditions at the drill site is known, this can be used to calculate the inclination and azimuth of the wellbore. Magnetic surveying tools can either be mechanical, or electrical.

A mechanical surveying tool builds on the same principles as a compass, and will reference to the magnetic north. Electronic magnetic surveying tools contain magnetometers and accelerometers, which measure the local magnetic field and gravitational components. These measurements can be used to calculate the inclination, azimuth and toolface of the instrument (Samuel & Lui, 2009).

Mechanical magnetic surveys are performed either as singleshot-, or multishot surveys. The device is lowered into openhole on a wireline, or dropped down inside the drill string. A timer, or motion sensor, will be used to take a reading once the tool is at rest. Singleshot surveys are used to perform a single positioning survey, at a given depth. Multishot surveys are most often used to take a large number of surveys as the drill string is pulled out of the hole. This is done to increase the density of the surveys, and get a more accurate wellbore trajectory (Samuel & Lui, 2009).

Electrical magnetic surveying tools are integrated into the BHA, and do not require any additional instruments to be lowered into the hole to perform a survey. Mud telemetry is used to transmit the results up to the surface. This makes it possible to perform a survey that corresponds with the make-up of a new pipe segment at the surface. At this point the pipe is at rest, and the survey can be performed without disturbance (Samuel & Lui, 2009).

Errors in Magnetic Surveys

The most common error in magnetic surveying tools is mechanical defect within the tool itself. Wolff & de Wardt (1981) performed surveys with 16 singleshot units, and found a systematic deviation of 2º. Inspections showed that this was caused by bearing damage within the tool. This emphasizes the necessity of routinely maintenance on these kinds of tools.

Since magnetic survey tools measure the local magnetic field, they are susceptible to environmental disturbance. Any steel present, from casing, drill pipe, drill collars or nearby wells, can lead to large errors in the survey (Samuel & Lui, 2009). Generally, nonmagnetic drill collars are used near the magnetic survey tools, but some magnetization may still be present (Wolff & Wardt, 1981). If a casing string of another well is in close proximity to the wellbore, or hotspots are present in the drill string, this can result in a 10º error (Samuel & Lui, 2009).

Magnetic tools also show poor results when used in near vertical boreholes. This is because the horizontal component of the earth's magnetic field becomes small, and difficult to measure. When drilling in east-west direction, the accuracy of magnetic tools is also reduced (Samuel & Lui, 2009).

Gyro Surveying Tools

Surveys using gyro tools are often performed when the accuracy of magnetic surveying tools has been impaired by the close proximity of magnetized steel, or when the accuracy of the survey is especially crucial. The gyro consists of a highly balanced spinning wheel, mounted on a gimbal. Because of the high spinning rate applied to the wheel, at 40,000 rpm, a moment of inertia is created. This will keep the wheel at a given position, regardless of the position of the surveying tool itself (Samuel & Lui, 2009). The direction of the gyro wheel is set at the surface, and this will act as the reference point when the survey is performed downhole. Once the gyro is back at the surface, the direction is measured to account for any gyro drift (Wolff & de Wardt, 1981).

Gyro tools are used in single- and multi shot configurations. Single shot surveys are most commonly used when accuracy is especially critical, or when magnetic surveys cannot be performed. This can be when orienting deflection tools, before drilling into the reservoir, or when magnetic interference is suspected. Multi shot surveys are most commonly performed to survey extended cased sections of the well or openhole sections where magnetic interference is present (Samuel & Lui, 2009). In recent years gyro tools have been developed that can be integrated into the MWD-package (Bashaar et al., 2010).

Errors in Gyro Surveys

The gyro is a high precision instrument, and the gimbals are mounted on jewel bearings to reduce the friction to a minimum (Samuel & Lui, 2009). However, since the tool is not frictionless, some drift will be experienced during running of the tool. This is dependent on the borehole direction, dogleg severity, running procedures, time required to perform the survey, temperature, gyro construction, gimbal balance, and the earth's rotation. This will cause the gyro to drift during the survey. If this drift is constant, it can be accounted for easily, and the results corrected. However, the drift is observed to be nonlinear, and this might cause errors in the survey results (Wolff & de Wardt, 1981). The gyro tools also have to be aligned at the surface, and the alignment must be measured when the gyro is returned, if this is performed wrongfully, errors will arise (Samuel & Lui, 2009).

Gyros have also been shown to yield large errors for near horizontal boreholes (Wolff & de Wardt, 1981).

Environmental Errors

In addition to errors related to the surveying instruments alone, environmental errors can cause the wrong direction and azimuth to be measured as well. First of all, to measure the direction of the wellbore, the tool has to be correctly aligned with the borehole. Misalignment can be caused by bad centralization within the collars, or bending of the BHA itself. The downhole pressure and temperature may pose limitations on the tools being used. If the downhole conditions exceed the specifications of the surveying tools, errors can arise (Samuel & Lui, 2009).

2.7.3 Ellipse of Uncertainty

Because of the errors related to both survey instrument and wellbore environment, conventional surveying methods can never find the true position of the borehole. When a survey is performed at a certain depth, possible errors in measured depth, inclination and azimuth creates an uncertainty in regards to the results of the survey. Because of this, an ellipse of uncertainty can be drawn around the reported wellbore position. The survey tool used, together with the properties of the wellbore, decides the dimensions of this ellipse. The true position of the wellbore can be anywhere within this body. The probability of the wellbore actually being at a certain offset from the initially reported position becomes smaller as the offset becomes larger, but it is still not possible to rule out that the wellbore in reality is located at the very edges of the ellipse.

Wolff & de Wardt Borehole Position Error Model

The borehole position uncertainty is crucial when a relief well is being drilled to directly intersect the blowing wellbore. Since magnetic ranging tools have a maximum detection range, conventional surveying techniques must get the two wells within a certain relative position of each other. In this chapter, an error model will be presented, and the uncertainty will be calculated for different cases.

The systematic error model presented by Wolff & de Wardt (1981) has been used to give an overview of the total uncertainty expected when performing surveys with both magnetic- and gyro surveying tools. The uncertainty can be expressed as the along hole uncertainty, the lateral uncertainty and the upward uncertainty. This will create the ellipse of uncertainty. The true position of the wellbore can be anywhere within this ellipse. Figure 2.4 shows the ellipse of uncertainty for a well with a constant inclination and azimuth.

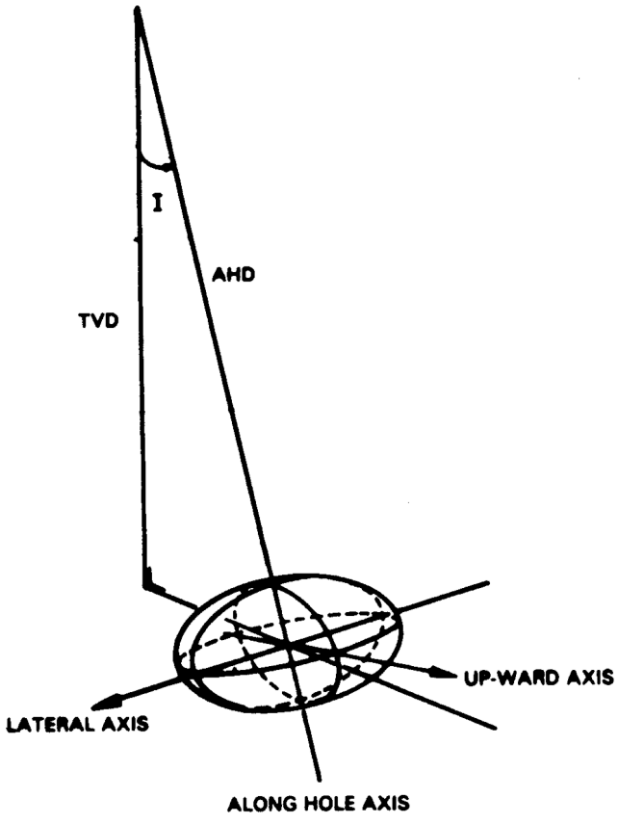

Figure 2.4 – Ellipse of uncertainty (Wolff & de Wardt, 1981)

Table 2.2 summarizes the typical values for expected errors using different surveying tools.

Survey Tool	Relative Depth, ε (10^{-3} m)	Misalignment, ΔI_m (Degrees)	True Inclination, ΔI_{t0} (Degrees)	Reference Error ΔC_{10} (Degrees)	DS magnetization ΔC_{20} (Degrees)	Gyro compass ΔC_{30} (Degrees)
Good Gyro	0.5	0.03	0.2	0.1	-	0.5
Poor Gyro	2.0	0.2	0.5	1.0	-	2.5
Good Magnetic	1.0	0.1	0.5	1.5	0.25	-
Poor Magnetic	2.0	0.3	1.0	1.5	5.0 + 5.0	-
Weight	1	1	Sin I	Sin I	SinI SinA	$(\text{Cos I})^{-1}$

Table 2.2 – Common survey errors (Wolff & de Wardt, 1981)

Wolff and de Wardt (1981) define a good survey as a survey where good equipment and procedures are used. And hence the smallest uncertainty is reflected. When running a gyro survey, good procedures involve standard running procedures, good maintained equipment and close supervision during operation. During magnetic surveying, good procedures involve proper spacing of calibrated compasses, and adequate lengths of truly nonmagnetic collars. A poor survey, on the other hand, refers to the errors obtained under "worst case" conditions. These errors have been observed in practice, but should be avoided if attention is given to the quality of the survey.

The measured depth will affect the horizontal positioning uncertainty for inclined wells. Wolff & de Wardt (1981) reported an uncertainty of 0.2×10^{-3} times total measured depth (MD) for a well-performed wire line survey, and 1.5×10^{-3} times MD for a poorly performed wire line survey. Because of the fact that drill pipe and casing most often is measured with a one-centimeter accuracy, and because of temperature effects, the measured depth of the drill string has an uncertainty of 1×10^{-3} times MD.

Equation 2.1 through 2.3 describes the maximum uncertainty along hole, and in lateral and upward direction.

$$Along\ Hole\ Uncertainty = D_{MD} \times \varepsilon \tag{2.1}$$

$$Lateral\ Uncertainty = D_{MD} \times \sqrt{\Delta I_m{}^2 + (\Delta C \sin I)^2} \tag{2.2}$$

$$Upward\ Uncertainty = D_{MD} \times \sqrt{\Delta I_m{}^2 + \Delta I_t{}^2} \tag{2.3}$$

Where D_{MD} is the measured depth of the well, ΔI_m is the tool misalignment error, ΔI_t is the true inclination error, and ΔC is the general compass error.

The true inclination error is dependent on the inclination of the borehole, and the reference inclination value, ΔI_{t0}.

$$\Delta I_t = \sin I \ \ \Delta I_{t0} \tag{2.4}$$

The reference error of the different survey tools is independent on the inclination, while the drill string magnetization error is dependent on both inclination and azimuth. The gyro compass error is dependent on inclination as well.

$$\Delta C_1 = \Delta C_{10} \tag{2.5}$$

$$\Delta C_2 = \Delta C_{20} \sin I \sin A \tag{2.6}$$

$$\Delta C_3 = \frac{\Delta C_{30}}{\cos I} \tag{2.7}$$

Further, the general compass error is:

$$\Delta C = \left(\sum_i \Delta C_i{}^2 \right)^{1/2} \tag{2.8}$$

Results

Graph 2.1 shows the ellipse of uncertainty for a survey performed at a measured depth of 5000 meters, with an inclination of 30º, and an azimuth of 90º. The smallest ellipse is generated when a good gyro survey is performed, while the largest one represents the uncertainty for a good magnetic survey.

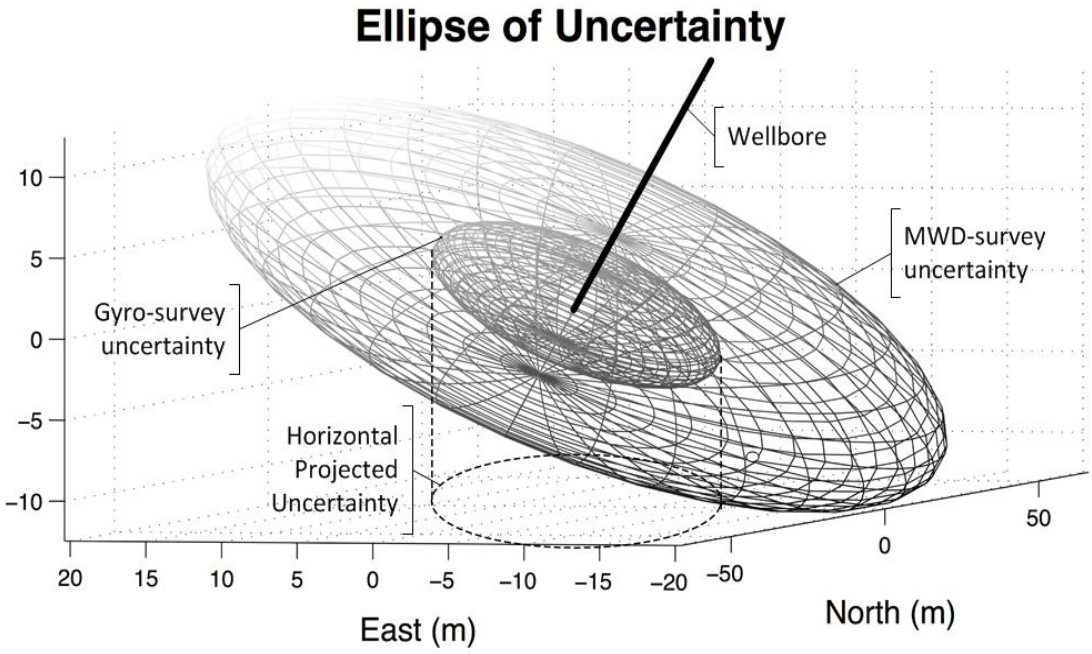

Graph 2.1 - Ellipse of uncertainty for 5000 meters measured depth and 30º inclination

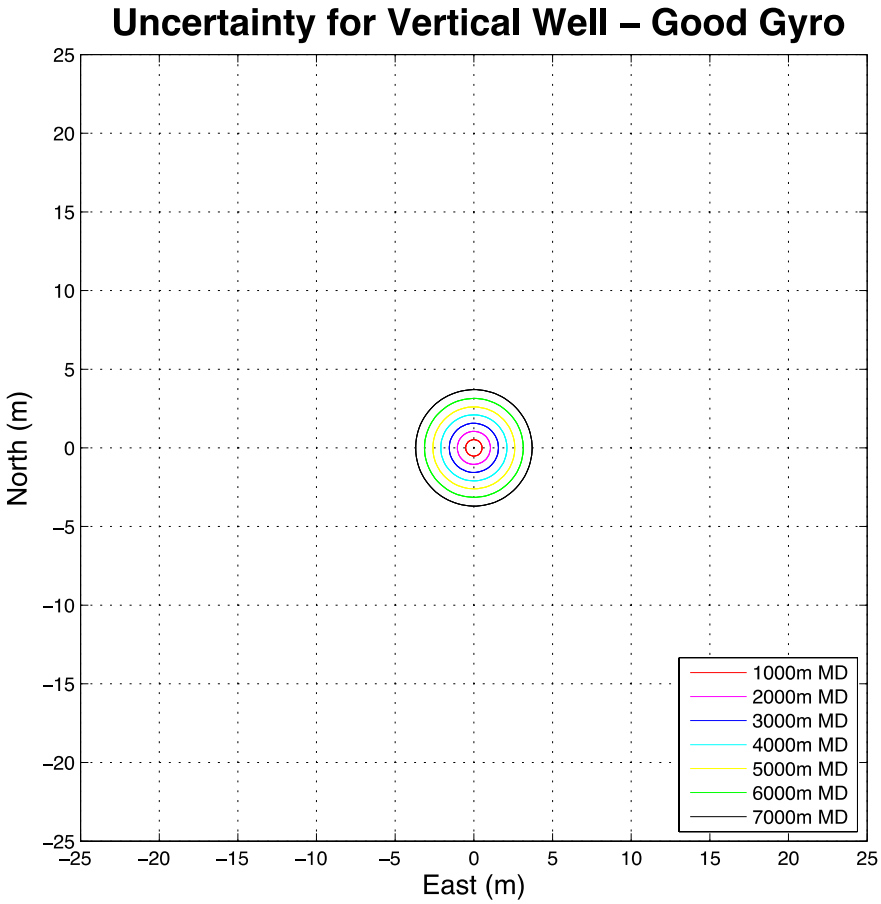

Graph 2.2 - Horizontal uncertainty for good gyro survey

Graph 2.2 displays the horizontal component of the ellipse of uncertainty when a good gyro survey is performed. This represents the minimum uncertainty that can be expected from a gyro survey. The vertical component was removed, to make the graphs easier to read. For a measured depth of 7000 meters, the horizontal uncertainty was 3.7 meters. For a vertical well, the ellipse of uncertainty is shaped like a circle, because the lateral- and upward uncertainty is equal. The measured depth uncertainty is 3.5 meters.

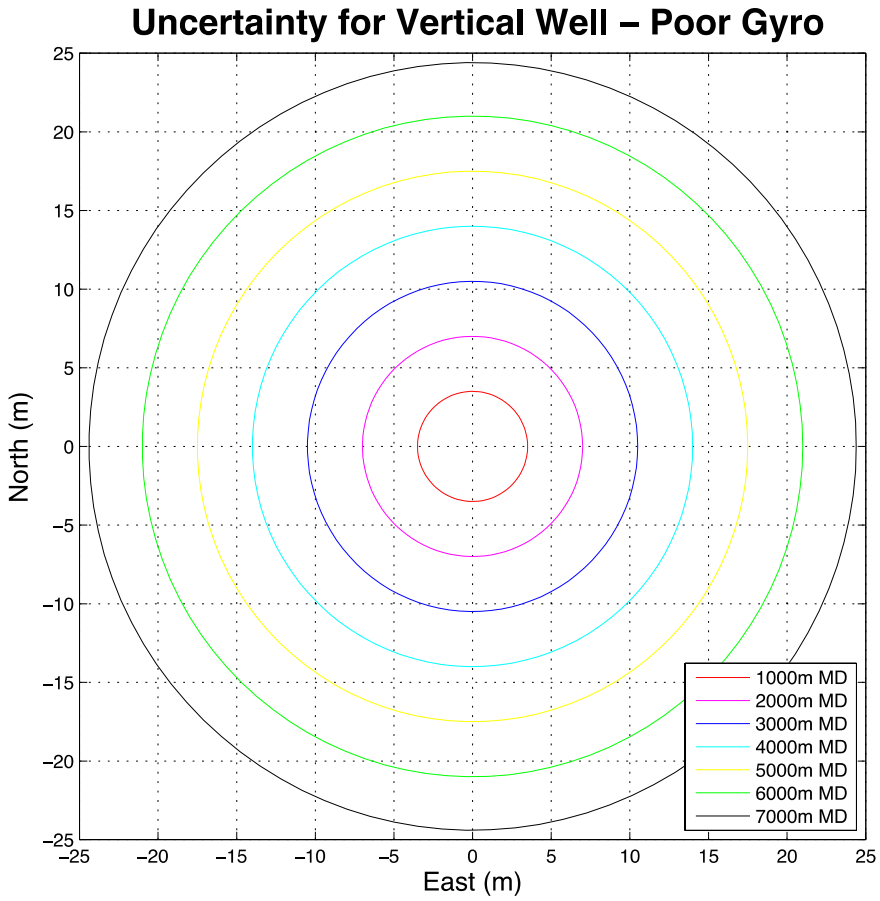

Graph 2.3 - Horizontal uncertainty for poor gyro survey

Graph 2.3 displays the calculated uncertainty for a low quality gyro survey. It can be observed that the uncertainty is increased to 24.4 meters for a measured depth of 7000 meters. The measured depth uncertainty is increased as well, for a measured depth of 7000 meters the uncertainty has increased to 14 meters.

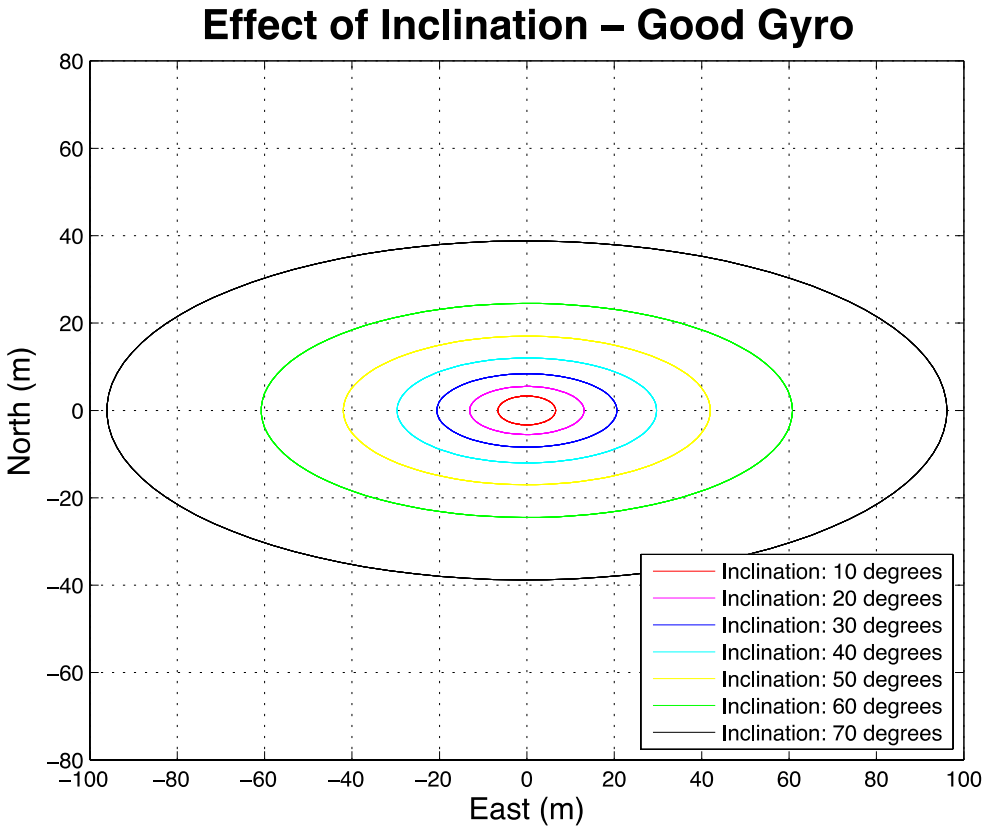

Graph 2.4 – Effect of change in inclination on wellbore position uncertainty

It can be seen that the horizontal positioning uncertainty for a good gyro survey increases dramatically when the wellbore inclination is increased. The measured depth is constant, at 4000 meters. When the wellbore inclination is above 70º, the gyro survey has a larger uncertainty than the magnetic survey (Wolff & de Wardt, 1981). The uncertainty with regards to measured depth of the well is not dependent on the inclination, and stays constant at 2 meters for a measured depth of 4000 meters.

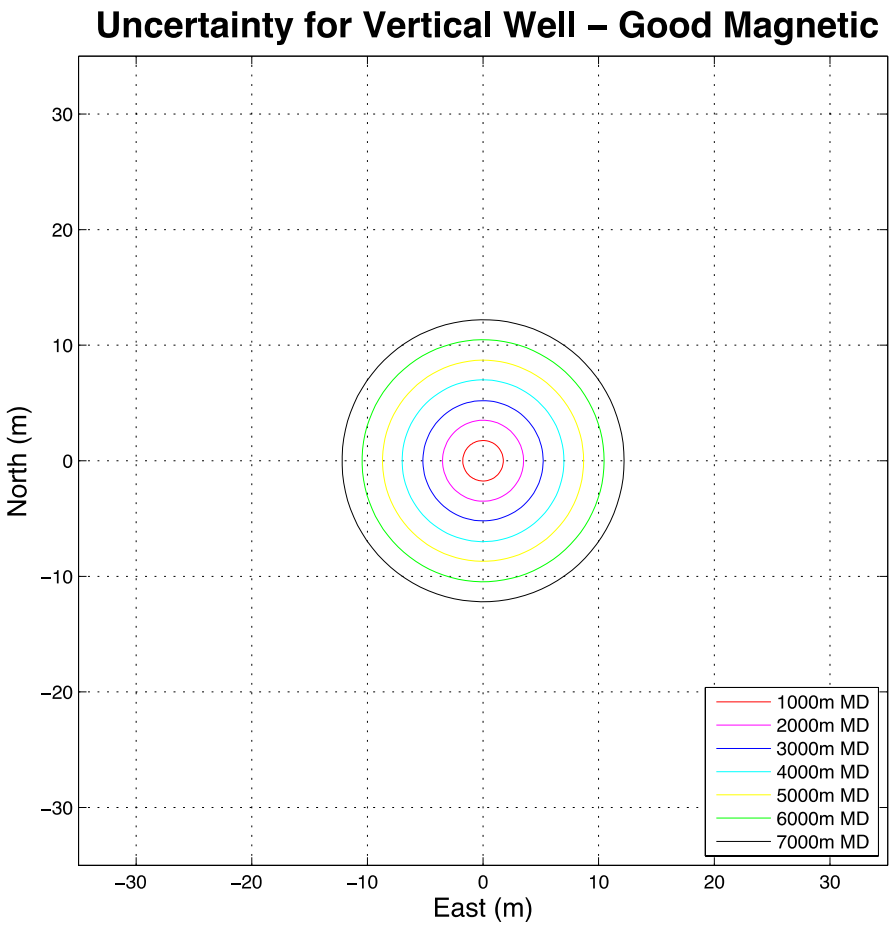

Graph 2.5 - Horizontal uncertainty for good magnetic survey

Graph 2.5 displays the minimum uncertainty when performing a magnetic positioning survey. It can be observed that the uncertainty is approximately 3.3 times higher than for a gyro survey. At 5000 meters depth, the uncertainty is ± 8.72 meters. These results correspond well with the calculated uncertainty of the 2/4-14 Saga well. This well was near vertical, and Saga Petroleum reported an uncertainty of ± 8.6 meters at the 9 ⅝-inch casing shoe, located at 4733m TVD (Leraand et al., 1992). The measured depth uncertainty when performing a good magnetic survey was calculated at 7 meters, for a measured depth of 7000 meters.

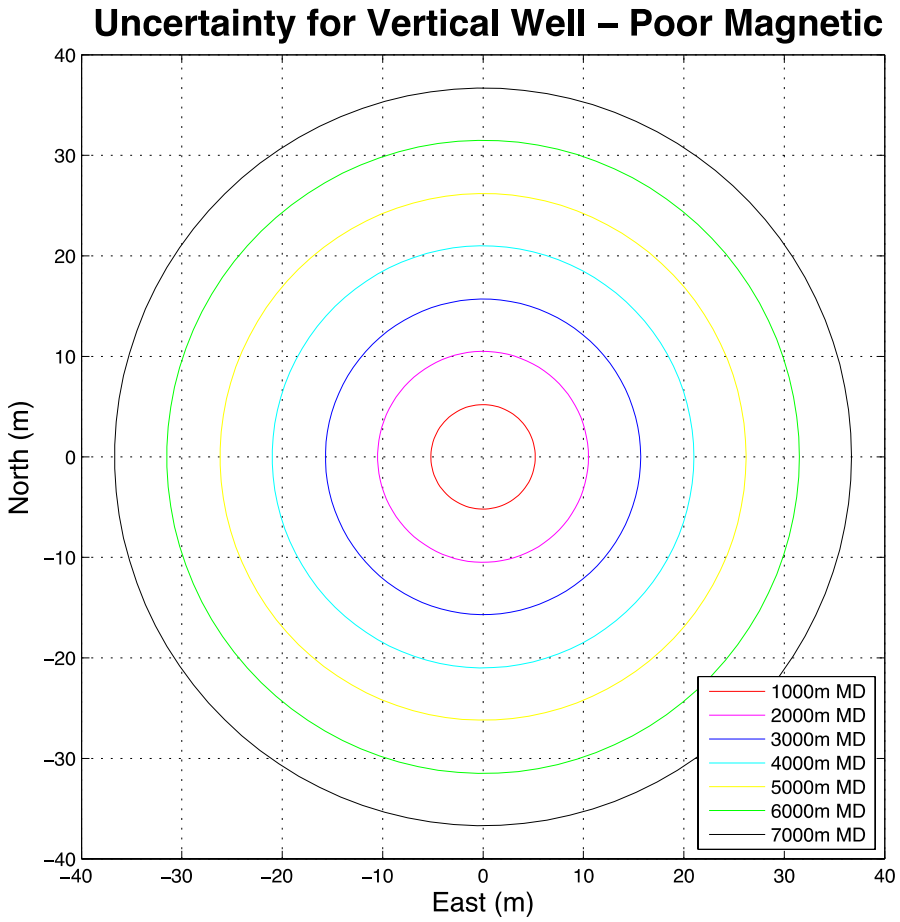

Graph 2.6 - Horizontal uncertainty for poor magnetic survey

If a poor magnetic survey is performed, the uncertainty increases. At a measured depth of 5000 meter, the horizontal uncertainty is 26.2 meter. Hence, the uncertainty becomes three times larger when good practices are not followed when performing a magnetic survey.

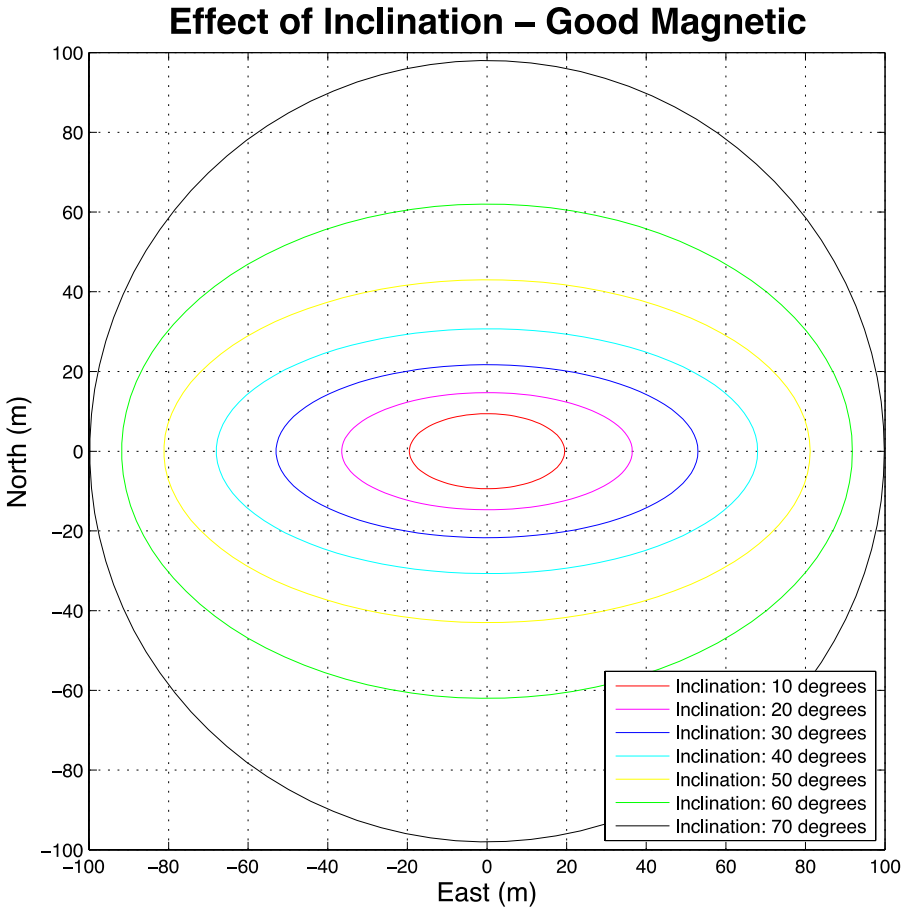

Graph 2.7 - Effect of change in inclination on wellbore position uncertainty

Graph 2.7 shows the effect of wellbore inclination on a good quality magnetic survey. The measured depth is constant, at 4000 meters. It can be observed that the inclination affect the magnetic survey in a similar manner as the gyro survey, however since the gyro compass error is divided by the cosine value of the inclination, the gyro error increase rapidly as the wellbore inclination approaches 90º. The magnetic survey does not show this exponential error increase, and at an inclination of above 70º, the magnetic survey yields better results than the gyro survey.

Effect of Azimuth

The azimuth of the wellbore does not affect a gyro survey, but has a small impact on magnetic surveys. As can be seen from table 2.2, the effect of azimuth is small for a good quality magnetic survey. This means that as little magnetized steel as possible is present, and hence the azimuth has a limited effect on the uncertainty of the survey. At 4000 meters MD the horizontal uncertainty is increased from 52.8 to 53.0 meters by going from a 0 to a 60º azimuth. The effect of azimuth is much greater when magnetized steel is in close proximity of the surveying equipment. For a poor quality magnetic survey the uncertainty rises from 56.4 to 161.3 meters when the azimuth is changed from 0 to 60º. This emphasizes the importance of using un-magnetized collars, and performing a gyro survey when cased wells are nearby.

Discussion

Conventional surveying tools do not offer the accuracy to facilitate direct intersection of a blowing wellbore. Therefore, electromagnetic- or magnetostatic ranging tools are used to home in on steel tubular in the blowing wellbore. Because of the maximum detection distance associated with ranging tools, conventional surveying techniques must get the relief well within a certain relative distance from the steel tubular in the blowing well, without posing any risk of premature intersection.

By observing the graphs presented in this chapter, it becomes evident that the uncertainty can become a challenge for long measured depth wells, or high inclination wells. Uncertainty calculations also emphasize the importance of performing surveys according to good practices, and that magnetic surveying tools are not in close proximity of magnetized steel. This should be accounted for in the planning phase of the relief well. If the uncertainty approaches the maximum detection range of the ranging tool, a gyro survey should be performed to reduce the uncertainty.

The Wolff and de Wardt systematic error model has been modified extensively since its publication date. It can be considered the industry standard because of its simplicity and relatively accurate results. However, it does have some shortcomings, and in recent years more advanced methods using error propagation mathematics has been developed (Williamson, 1999). However, the investigation of these methods was outside the scope of this thesis, and the Wolff and de Wardt method was deemed accurate enough for this analysis.

3. Surface Seismic While Drilling

Before the drilling of a well is initiated, surface seismic surveys have been performed both to investigate the possibility of presence of hydrocarbon deposits, and to map the subsurface formations. These surveys provide vital information for the operator when planning a well. Repeated surface seismic surveys are currently being performed on many oil fields to continuously monitor the changes in the reservoir, as it is being produced. Johansen and Sangesland (2013) suggested using repeated surface seismic methods to continuously monitor the propagation of the bit into the subsurface. This new method is called surface seismic while drilling.

3.1 Description of Method

When the bit drills away the rock beneath it, it is changing the subsurface formations. If seismic data with a high enough resolution is obtained, it should be possible to see this change, and hence find the true path of the well being drilled.

First, a reference seismic image of the subsurface is obtained, before drilling is initiated. This can be the original seismic data obtained before the decision to drill was taken, a simulated dataset from an earth model, or simply the first set of seismic data obtained through the SSWD method. As the bit propagates down into the subsurface, the seismic survey is repeated. This is accomplished by installing fixed seismic receivers and sources at the surface. For an onshore location, 2D or 3D arrays can be placed on the ground around the drill site. For an offshore location, ocean bottom seismic- or traditional marine seismic equipment can be used.

Once another seismic data set is obtained, the data from the reference seismic image is subtracted from the newly obtained data. Hence, only the changes in the subsurface should be visible. Seismic simulations indicate that using this method should make it possible to find the true wellpath, as the well is being drilled (Johansen & Sangesland, 2013). If this technology can be utilized as anticipated, it can revolutionize several aspects within drilling technology.

3.2 Benefits

With regards to well integrity, SSWD will offer accurate and continuous wellbore positioning that can be used together with existing technology, or as a standalone survey method. It can be used to determine the absolute position of the wellbore, as well as relative position with regards to subsurface structures outlined on seismic images, or other nearby wells. The method can also aid in increasing the productivity of producing wells by enabling accurate placement of wells in the most productive parts of the reservoir.

In case of a blowout, SSWD may provide an accurate and effective method of intersecting the blowing wellbore. The model relies on seismic surveys that are accurate enough to detect that a certain volume of rock has been drilled out by the bit, and replaced by a column of mud. This means that the blowing wellbore can be intersected by a relief well, regardless of the presence of steel. If a long open-hole section exists between the last set casing shoe, and the point of inflow, the blowing well can be intersected at a deeper depth than with conventional techniques.

There are many advantages associated with intersecting the relief well at a deeper depth. First of all, a higher column of kill mud can be obtained, reducing the required density of the kill mud, and hence the pressure on the casing shoe. If a dynamic killing operation is planned, the extended well length will provide a higher frictional pressure drop, for a given injection rate. The pressure at the kill point will be higher, if the blowing reservoir contains a fluid with a high gas oil ratio (GOR), less gas have boiled out of the reservoir fluid, and hence the volumetric flow rate will be smaller. This will make the killing operation less complicated, since the injected kill mud, or seawater, is not diluted to the same extent.

The method also eliminates the need to drill past the blowing well in order to perform triangulation. In addition to this, there is no need to pull the drill string out of the hole to perform ranging surveys. It might also be possible to hit the blowing well at a higher intersection angle. This will eliminate the need for a drop section, and a section parallel to the blowing wellbore. This will make the well trajectory much less complex, and enable a more effective drilling operation.

Figure 3.1 shows how bottomhole intersection can be achieved using SSWD.

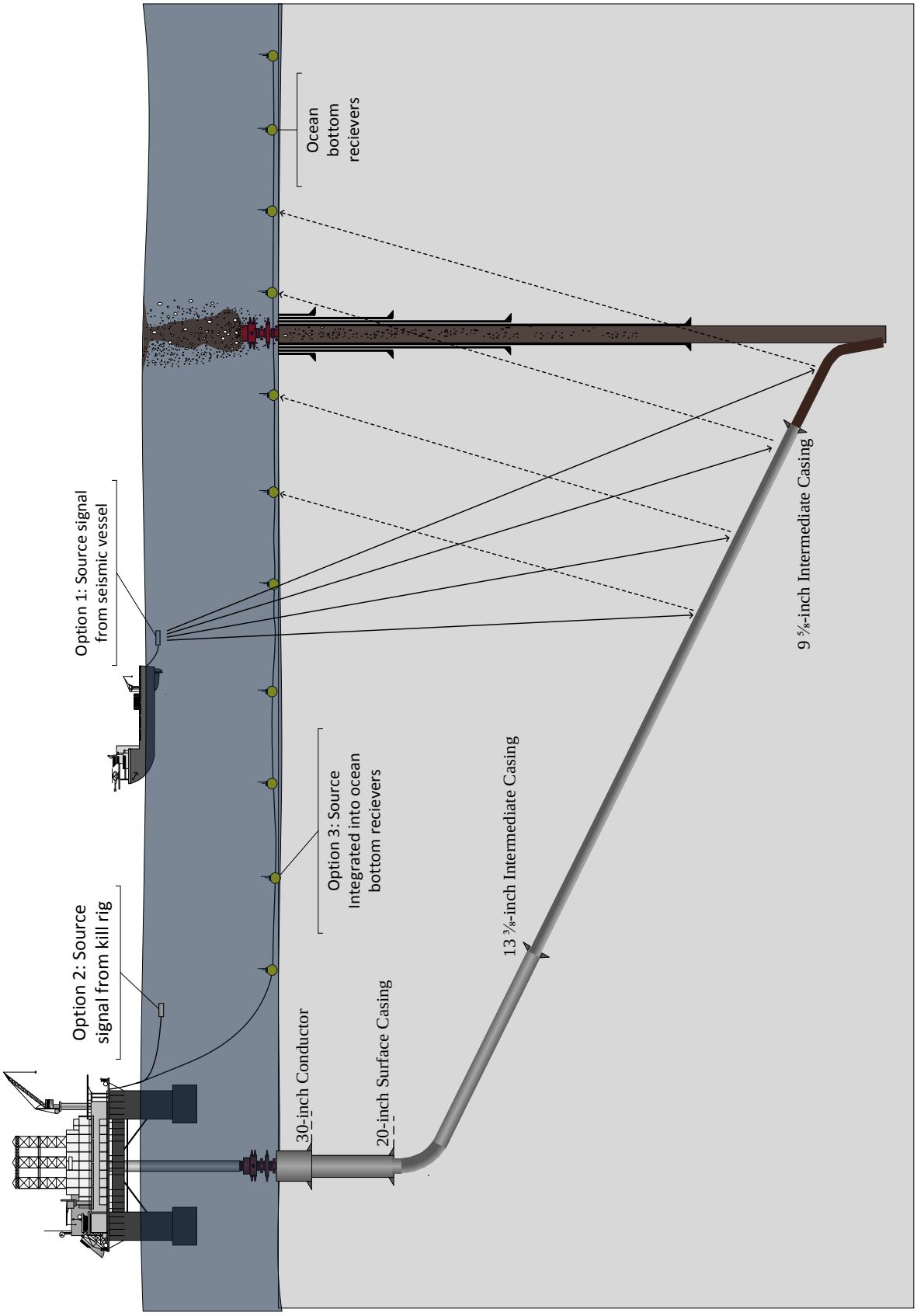

Figure 3.1 – Bottom intersection using SSWD

4. Simulation Model

To be able to accurately evaluate the benefits of intersecting a blowing well at the deepest point possible, regardless of the presence of steel in the wellbore, a simulation model was created in MATLAB. An idealized well profile was used, and for a given flowing temperature and reservoir fluid composition, all other parameters could be changed. The MATLAB model will calculate the stabilized blowout rate that will develop under the given conditions, and the subsequent dynamic kill rate required to kill the well. Aspen HYSYS simulation software, or correlations, was used to find the properties of the fluids for the pressure and temperature at a given point in the well.

4.1 Base Case

A simple vertical well was chosen for proof of concept. However, the model can be adjusted for more complex well trajectories. The water depth decides the wellhead pressure, and is set to 150 meters. A 9 ⅝-inch casing spans from the wellhead, down to 2000 meters below the ocean floor. Beyond the casing there is a 1000-meter long openhole section, drilled out with a 8 ½-inch bit. The point of inflow is set at 3000 meters below the wellhead, and the reservoir pressure and temperature is 400 bar and 100ºC, respectively. The reservoir fluid is black oil, with a composition as suggested by Pedersen et al. (1989).

Figure 4.1 summarizes the properties of the well. Figure 4.2 shows the two relief wells considered in this thesis. In addition to these, a sensitivity analysis will be performed for all intersection depths.

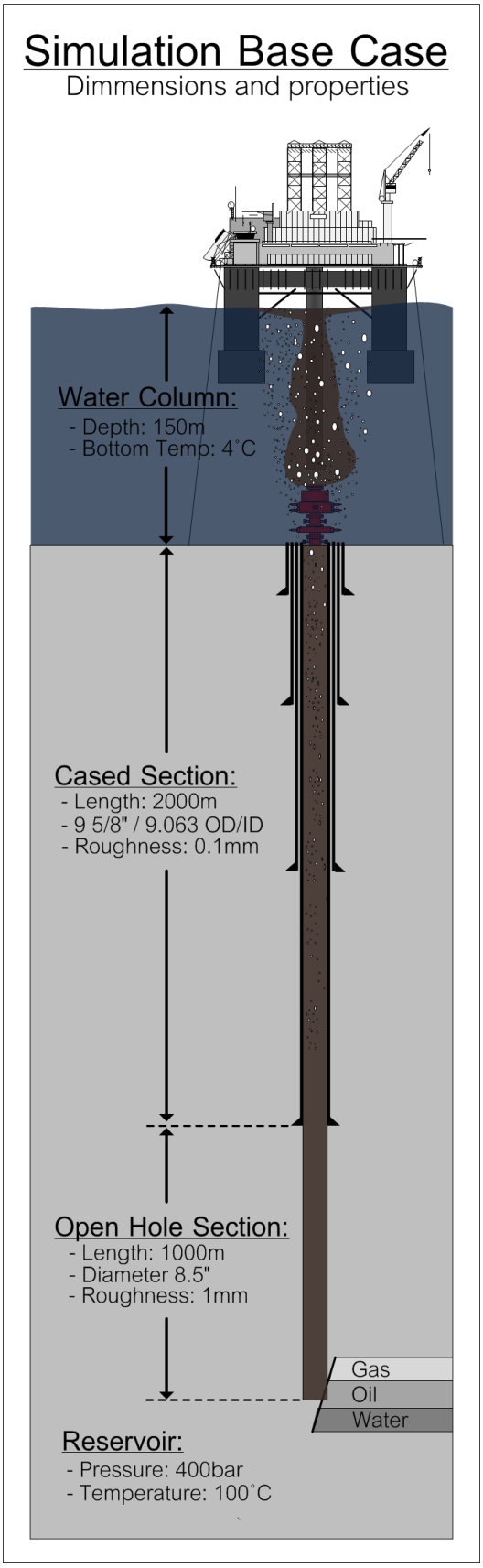

Figure 4.1 - Overview of base case properties

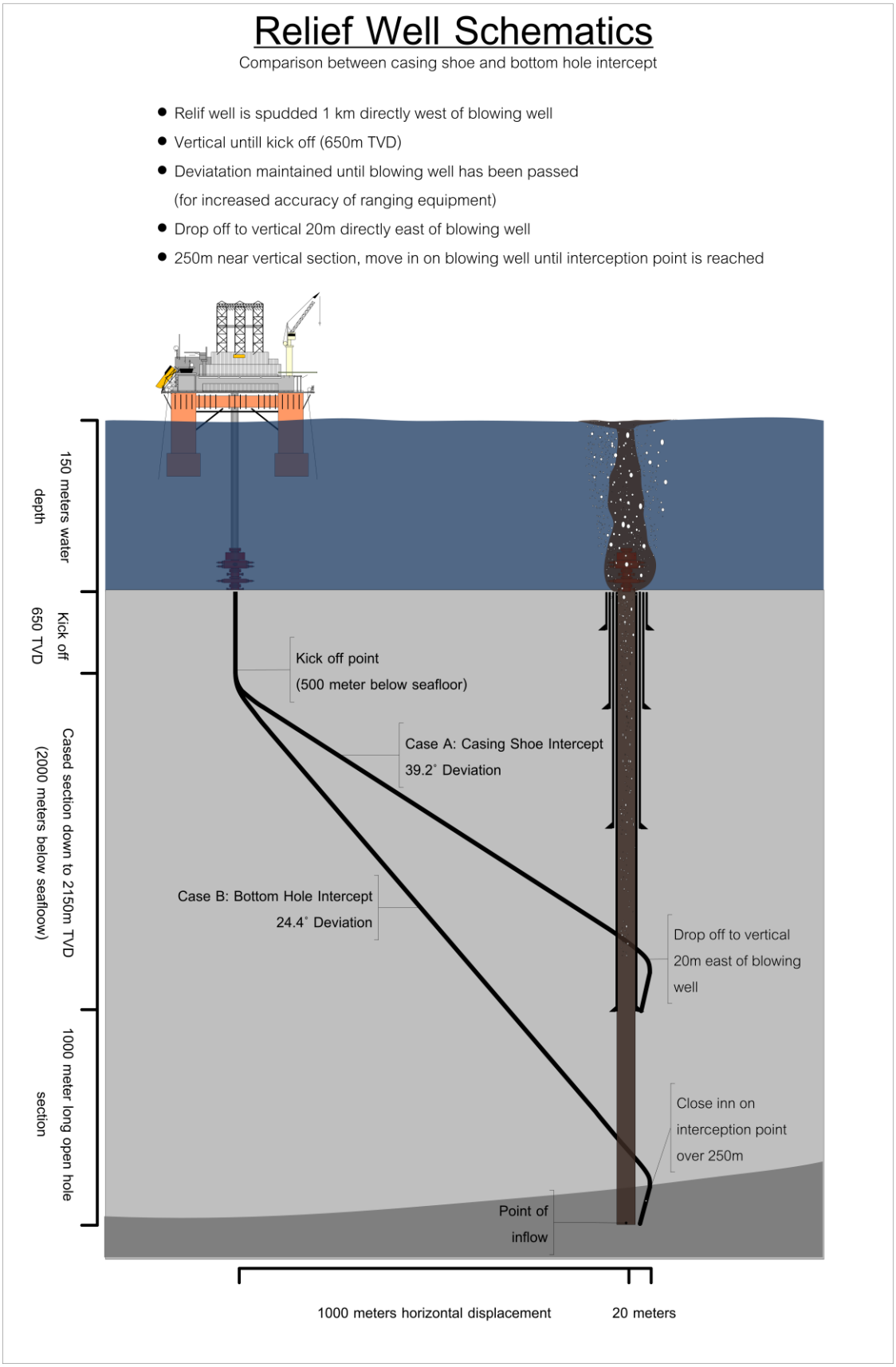

Figure 4.2 – Schematics of casing shoe- and bottomhole intersecting relief wells

4.2 Description of Model

4.2.1 Reservoir Fluid

This subchapter describes the reservoir- and injection fluid used in the simulation model. These compositions are fixed in the MATLAB-model. However, by performing new simulations in Aspen HYSYS, and using regression analysis to find new equations for the different properties, these fluids can be changed.

The injection fluid during the dynamic killing phase is water, with a certain predetermined percentage of salt dissolved. This concentration of salt is set as an input parameter, and can be changed before the simulation is started. Once the well is dynamically killed, kill mud can be circulated into the blowing wellbore. At this point the effect of pressure and temperature will be less important, since the well is statically killed through the hydrostatic pressure contribution from the column of kill mud.

Reservoir Fluid Composition

A typical black oil composition based on Pedersen et al. (1989) was used in the simulation. It was chosen to use an oil mixture with a relatively high gas content, as this would require the most complex simulation model, and require both two- and three- phase flow calculations. At a later time the model could easily be modified to feature a dry gas, or an oil mixture with a lower GOR.

At reservoir conditions the fluid is in liquid form, and has a gravity of 175°API, corresponding to a density of 460 kg/m^3. The fluid has a GOR of 162.2 Sm^3/Sm^3, or 910.4 scf/stb. At standard conditions the liquid phase has a density of 743 kg/m^3, and a viscosity of 1.360 cP. The gas phase has a density of 1.1 kg/m^3, and a viscosity of 0.011 cP. The formation fluid composition can be seen in table 4.1.

Components	Percentage, (%)
N_2	0.67
CO_2	2.11
C_1	34.93
C_2	7.00
C_3	7.82
C_4 (i+n)	5.48
C_5 (i+n)	3.80
C_6 (i+n)	3.04
C_7	4.39
C_8	4.71
C_9	3.21
C_{10}	1.79
C_{11}	1.72
C_{12}	1.74
C_{13}	1.74
C_{14}	1.35
C_{15}	1.34
C_{16}	1.06
C_{17}	1.02
C_{18}	1.00
C_{19}	0.90
$C_{20}+$	9.18

Table 4.1 - Black Oil molar composition from Pedersen et al. (1989)

Phase Envelope

Graph 4.1 displays the phase envelope for the reservoir fluid. The solid blue line represents the bubble point line. For pressures and temperatures above this line, the fluid consists of liquid only. The solid red line is the dew point line. For conditions to the right of this line, the fluid is gas only. The solid black line represents the conditions where the fluid consists of a mixture of 50% liquid, and 50% gas, at equilibrium. The dotted lines above the solid black line represents a mixture of 90% liquid for the green line, 80% liquid for the purple line, 70% liquid for the green line, and 60% liquid for the orange line. Below the black line the same lines represents a mixture of 90, 80, 70 and 60% gas, respectively.

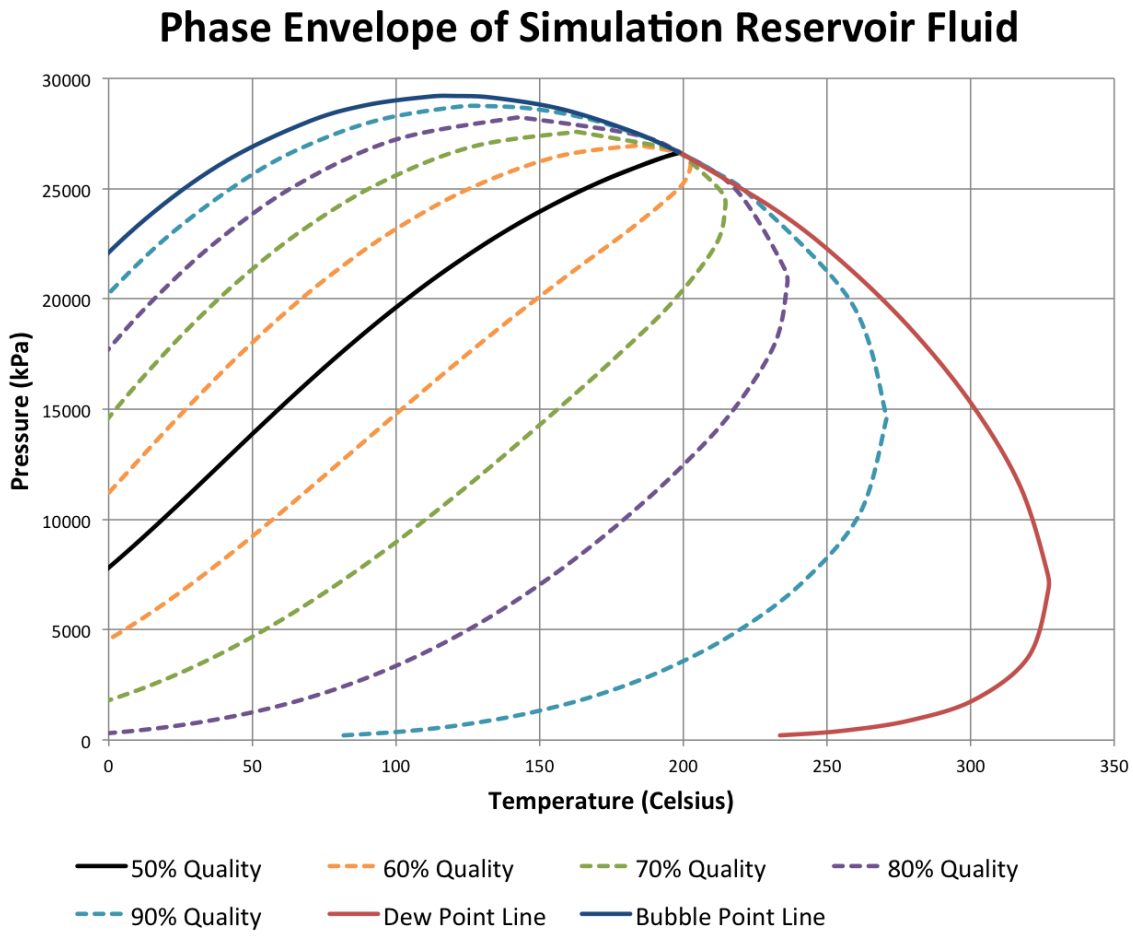

Graph 4.1 - Phase envelope of reservoir fluid

Gas will start to boil out of the reservoir fluid at a certain temperature and pressure. This causes a change in the composition of the oil phase, as well as an introduction of multiphase flow. This will make the simulation more complex than if the blowout fluid was assumed dry gas, or a liquid containing no gas at all. Assuming a constant flowing temperature of 100ºC, it can be seen that the flow enters the two-phase region when the wellbore pressure has been reduced below 290 bar. When the wellbore pressure has been reduced just below 200 bar, the flow consists of equal molar parts of liquid and gas.

Flowing Fractions and Phase Composition

Temperature calculations showed a very small temperature drop between the reservoir and the surface. This is investigated in detail in chapter 4.2.2. Even at moderate blow out rates, calculations showed a temperature drop of only a couple of degrees Celsius. Because of this, it is valid to assume that the pressure drop governs the majority of the gas boil out Using Aspen HYSYS simulation software, the in-situ flowing fraction for a constant temperature and different pressures could be simulated. Graph 4.2 shows the result of this simulation.

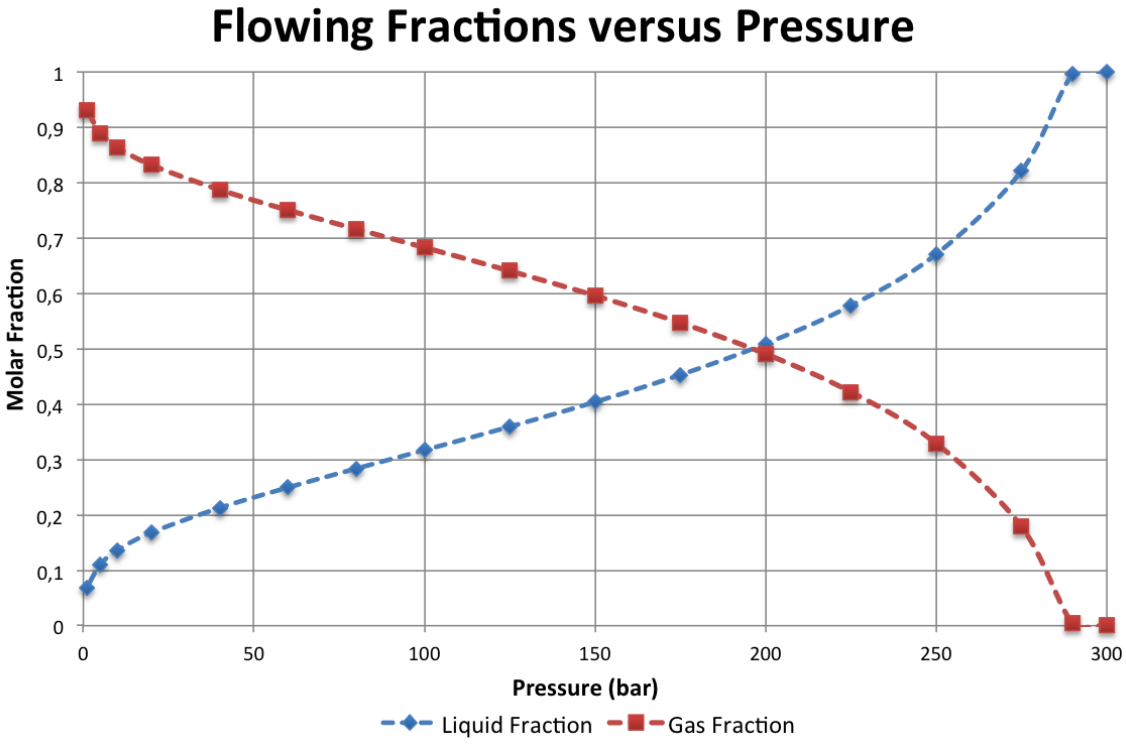

Graph 4.2 - Fractions of flowing phases for different pressures

Graph 4.3 and 4.4 shows the composition of the oil and gas phase as the pressure is reduced. It can be observed that the lighter components boil out of the oil phase first. The graphs also show how the viscosity of the different phases change, as the composition and pressure is changed. It can be observed that the viscosity of the oil phase increases as the lighter components boil out. The composition of the gas phase is more constant, and because of the large effect of pressure, the viscosity is decreased as the pressure is reduced.

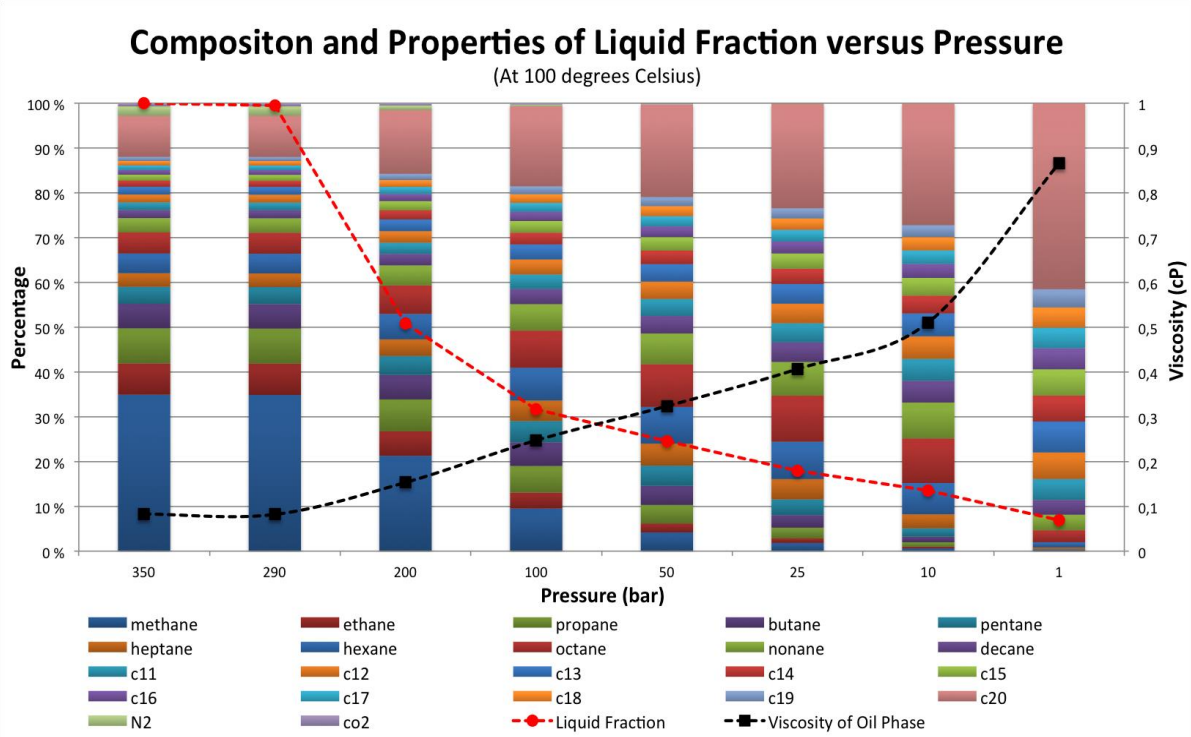

Graph 4.3 - Liquid Phase Composition

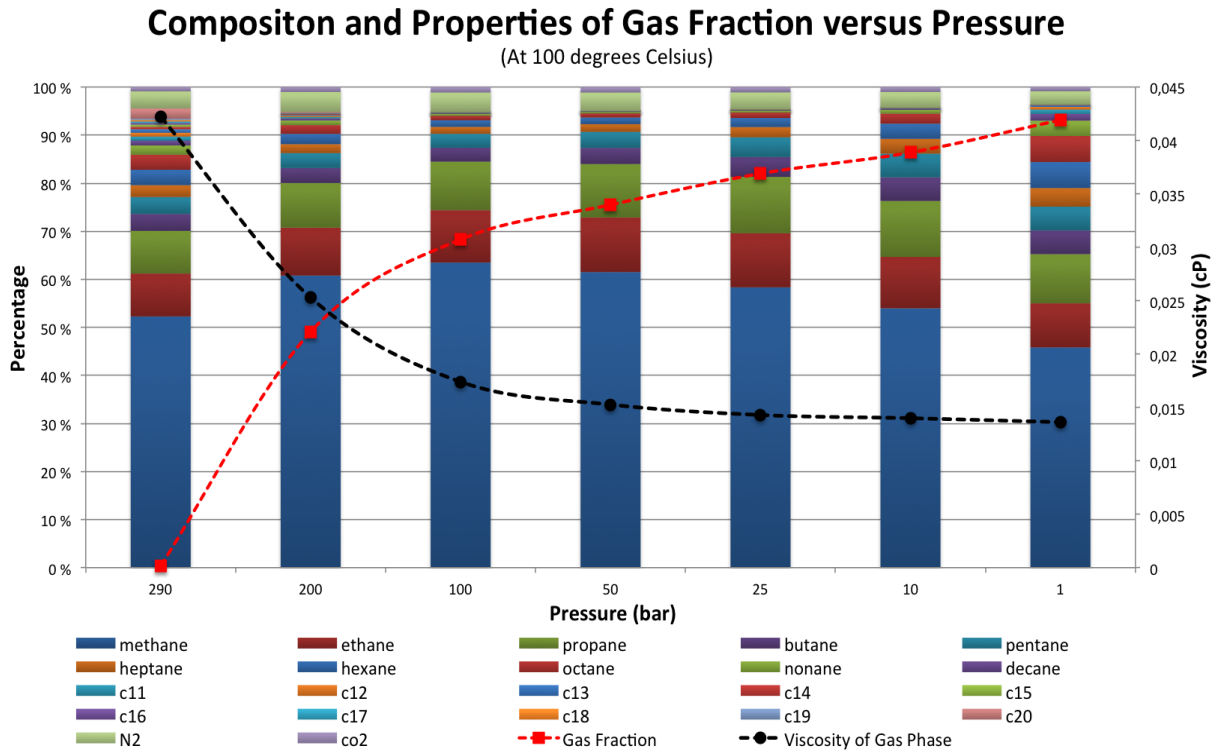

Graph 4.4 - Gas phase composition

4.2.2 Temperature Profile

The flowing temperature of a blowout has a large effect on both the hydrostatic- and frictional pressure loss experienced along the annulus of the blowing well. The temperature profile is important to establish, as this will, together with pressure, govern the amount of dissolved gas at any given point in the annulus. This will have a large impact on the flow regime, and the overall density of the flowing liquid. The temperature will also have a large impact on the in-situ viscosity of the phases.

There are several factors that will govern the flowing temperature of a blowout. As the fluids leave the blowing formation and flows up the annulus, the surrounding rock will start to cool it down. The temperature differential will depend on the geothermal gradient of the formations surrounding the wellbore. The amount of heat that can be removed from the flowing fluids will depend on the thermal conductivity of the rock in the openhole section. In the cased section the thermal conductivity of the casing, cement and surrounding formation will govern the heat transfer. The mass flow from the blowout will also impact the flowing temperature, as a higher mass flow requires more energy to be removed to lower the heat by a certain amount (Holmes & Swift, 1970).

Model for Blowout Flowing Temperature

Holmes & Swift's (1970) equations for circulating temperatures in both pipe and annulus have been used, and are modified to fit the situation at hand. Equation 4.1 and 4.2 describes the flowing temperature in drill pipe and annulus, respectively:

$$T_p = K_1 e^{C_1 x} + K_2 e^{C_2 x} + Gx + T_s \tag{4.1}$$

$$T_a = K_1 C_3 e^{C_1 x} + K_2 C_4 e^{C_2 x} + Gx + T_s \tag{4.2}$$

For a uniform layer of rock, x represents the depth from the reference temperature T_s. G is the geothermal gradient and is assumed to be linear. The equations for the constants C_1, C_2, C_3, C_4, A and B are as follows:

$$C_1 = \frac{B}{2A}\left[1 + \left(1 + \frac{4}{B}\right)^{\frac{1}{2}}\right], \quad C_2 = \frac{B}{2A}\left[1 - \left(1 + \frac{4}{B}\right)^{\frac{1}{2}}\right]$$

$$C_3 = 1 + \frac{B}{2}\left[1 + \left(1 + \frac{4}{B}\right)^{\frac{1}{2}}\right], C_4 = 1 + \frac{B}{2}\left[1 - \left(1 + \frac{4}{B}\right)^{\frac{1}{2}}\right]$$

$$A = \frac{mC_p}{2\pi\, r_p\, h_p}, \qquad B = \frac{r\, U}{r_p\, h_p}$$

C_p is the flowing fluid heat capacity, m is the mass flow rate, r_p is the radius of the pipe, h_p is the heat transfer coefficient across the drill pipe, r is the radius of the well and U is the heat transfer coefficient across the wellbore face.

In a blowout situation there will probably not be circulation from the rig and down the drill string. There might also not be any drill pipe in the well. To account for this, the radius of the pipe, and hence the surface area between the drill pipe and the flowing fluid, is set to be infinitely small. The heat transfer coefficient across the drill pipe is also set to be infinitely small. This will effectively eliminate the cooling/warming effect the drill pipe will have on the flowing annular fluid.

The constants K_1 and K_2 is calculated using boundary conditions with input- and surface temperature, and the equations are as follows:

$$K_1 = T_{pi} - K_2 - T_s + GA \tag{4.3}$$

$$K_2 = \frac{GA - \left[T_{pi} - T_s + GA\right]e^{C_1 H}(1 - C_3)}{e^{C_2 H}(1 - C_4) - e^{C_1 H}(1 - C_3)} \tag{4.4}$$

The input temperature is set to be the reservoir temperature. Since the surface area and the heat transfer coefficient of the pipe are infinitely small, the flowing temperature in the pipe will be constant. This will effectively set the inflow point at the bottom of the well, and will correspond to fluid flowing from the blowing formation, and into the well. Assuming that the blowout is occurring offshore, the surface temperature will be the ocean bottom temperature, and is set to be 4°C.

These equations does not account for a changing heat transfer coefficient of the surrounding formations, or a change in wellbore diameter. In a blowout situation there will most probably be one section that is cased, and one section that is openhole. Because of this, the equations had to be modified to allow the use of different wellbore diameter and heat transfer coefficient for the cased- and openhole section.

The heat transfer coefficient of sandstone has been showed to range from 1.3 to 2.3 W/m°C, depending on porosity and pore content (C-Therm, 2012). The heat transfer coefficient of Portland cement is lower, at 0.6 W/m°C. Iron shows good thermal conductivity, and the heat transfer coefficient is 80 W/m°C (Ceratechinc 2013). For this

model, the heat transfer coefficient of sandstone is used for the openhole section, while the heat transfer coefficient of Portland cement is used for the cased section. This was done because it is assumed that it is the Portland cement that will limit the thermal conduction between the formation and the flowing fluid, since both casing and formation shows higher heat transfer coefficients than that of Portland cement.

The temperature profile is found by first by calculating the values of the constants for both cased- and openhole section. The flowing temperature inside the cased section is calculating according to the original method. When performing the calculations for the bottomhole section, the surface is set to be at the casing shoe. Depths are changed corresponding to this, and the surface temperature is set to be the formation temperature at the casing shoe. The new equations for annular flowing temperature become:

$$T_{a,cased\ section} = K_{1,1}C_{3,1}e^{C_{1,1}x} + K_{2,1}\,C_{4,1}e^{C_{2,1}x} + Gx + T_{ob} \tag{4.5}$$

$$T_{a,open\ hole} = K_{1,2}C_{3,2}e^{C_{1,2}(x-H_{cs})} + K_{2,2}\,C_{4,2}e^{C_{2,2}(x-H_{cs})} + G(x-H_{cs}) + T_{cs} \tag{4.6}$$

The constants are calculated using the properties of the given section. H_{cs} is the depth of the casing shoe, T_{ob} is the ocean bottom temperature and T_{cs} is the formation temperature at the casing shoe.

The constants become:

$$C_{1,1} = \frac{B_1}{2A_1}\left[1 + \left(1 + \frac{4}{B_1}\right)^{\frac{1}{2}}\right], \quad C_{2,1} = \frac{B_1}{2A_1}\left[1 - \left(1 + \frac{4}{B_1}\right)^{\frac{1}{2}}\right]$$

$$C_{3,1} = 1 + \frac{B_1}{2}\left[1 + \left(1 + \frac{4}{B_1}\right)^{\frac{1}{2}}\right], C_{4,1} = 1 + \frac{B_1}{2}\left[1 - \left(1 + \frac{4}{B_1}\right)^{\frac{1}{2}}\right]$$

$$A = \frac{mC_p}{2\pi\, r_p\, h_p}, \quad B = \frac{r_{cased\ hole}\, U_{portland\ cement}}{r_p\, h_p}$$

$$C_{1,2} = \frac{B_2}{2A_2}\left[1 + \left(1 + \frac{4}{B_2}\right)^{\frac{1}{2}}\right], \quad C_{2,1} = \frac{B_2}{2A_2}\left[1 - \left(1 + \frac{4}{B_2}\right)^{\frac{1}{2}}\right]$$

$$C_{3,2} = 1 + \frac{B_2}{2}\left[1 + \left(1 + \frac{4}{B_2}\right)^{\frac{1}{2}}\right], C_{4,1} = 1 + \frac{B_2}{2}\left[1 - \left(1 + \frac{4}{B_2}\right)^{\frac{1}{2}}\right]$$

$$A = \frac{mC_p}{2\pi\, r_p\, h_p}, \quad B = \frac{r_{open\ hole}\, U_{sandstone}}{r_p\, h_p}$$

$$K_{1,1} = T_{res} - K_{2,1} - T_{ob} + GA$$

$$K_{2,1} = \frac{GA - [T_{res} - T_{ob} + GA]e^{C_{1,1}H}(1 - C_{3,1})}{e^{C_{2,1}H}(1 - C_{4,1}) - \mathrm{e}^{C_{1,1}H}(1 - C_{3,1})}$$

$$K_{1,2} = T_{res} - K_{2,2} - T_{cs} + GA$$

$$K_{2,2} = \frac{GA - [T_{res} - T_{cs} + GA]e^{C_{1,2}(x - H_{cs})}(1 - C_{3,2})}{e^{C_{2,2}(x - H_{cs})}(1 - C_{4,2}) - e^{C_{1,2}(x - H_{cs})}(1 - 2)}$$

Heat Capacity of Blowing Liquid

In these equations the heat capacity of the flowing fluid is assumed constant. This is not necessarily true for a blowout event. If the reservoir fluid is assumed to be oil, both temperature and pressure will affect the overall heat capacity of the flowing liquid to a small extent. At a certain point in the wellbore annulus, gas might start to boil out of solution because of reduced temperature and pressure. The lighter components of the oil phase will boil of first, and this will change the heat capacity of the remaining oil phase to a larger extent. When a killing operation is initiated, and mud or seawater is circulated into the blowing annulus at a certain depth, this will also affect the heat capacity.

In this work, it is assumed that the heat capacity of the flowing fluid at a certain depth in the annulus is expressed as an arithmetic mean of the individual heat capacities. Equation 4.7 expresses this relationship.

$$\mathrm{C_{p,mixture}} = \sum_{\mathrm{i}} \mathrm{C_{p,i}} \frac{\mathrm{V_i}}{\mathrm{V_{mixture}}} = \mathrm{C_{p,oil}} \frac{\mathrm{V_{oil}}}{\mathrm{V_{mixture}}} + \mathrm{C_{p,water}} \frac{\mathrm{V_{water}}}{\mathrm{V_{mixture}}} + \mathrm{C_{p,gas}} \frac{\mathrm{V_{gas}}}{\mathrm{V_{mixture}}} \quad (4.7)$$

The heat capacity of the oil and associated gas was simulated in Aspen HYSYS for a flowing temperature of 100°C. The pressure was reduced from 350 bar down to atmospheric pressure.

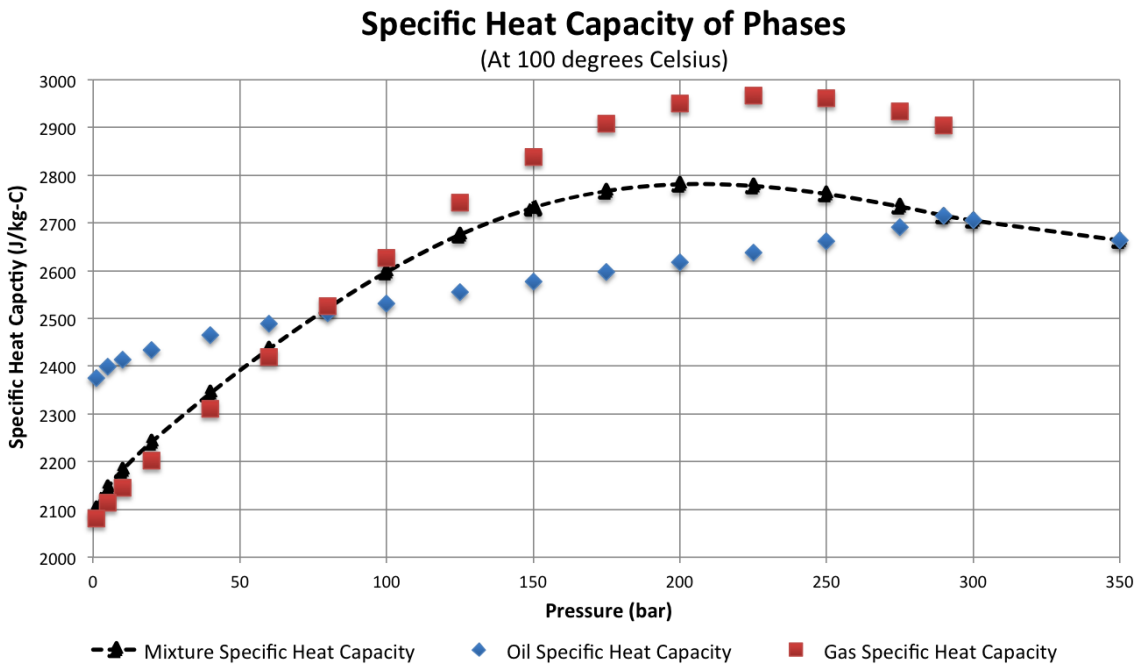

Graph 4.5 - In-Situ Heat Capacities

The specific heat capacity of the liquid before gas boil out occurs stays fairly constant at approximately 2700 J/kg-C. Once gas starts to boil out, the composition of the liquid phase is changed. Because of decrease in pressure, and change in composition, the heat capacity starts to sink. The gas specific heat capacity changes more dramatically, because the boil out gas has a fairly constant molecular weight, and is affected by the pressure decrease. The Holmes & Swift (1970) equations to calculate the flowing temperature uses a constant specific heat capacity, and hence an average mixture specific heat capacity of 2500 J/kg-C was used for the hydrocarbon mixture in the calculations.

Heat Capacity of Injection Water

The heat capacity of water was found using the same method as above. Regression analysis was used to find an equation for the dependence on pressure. Graph 4.6 shows the results:

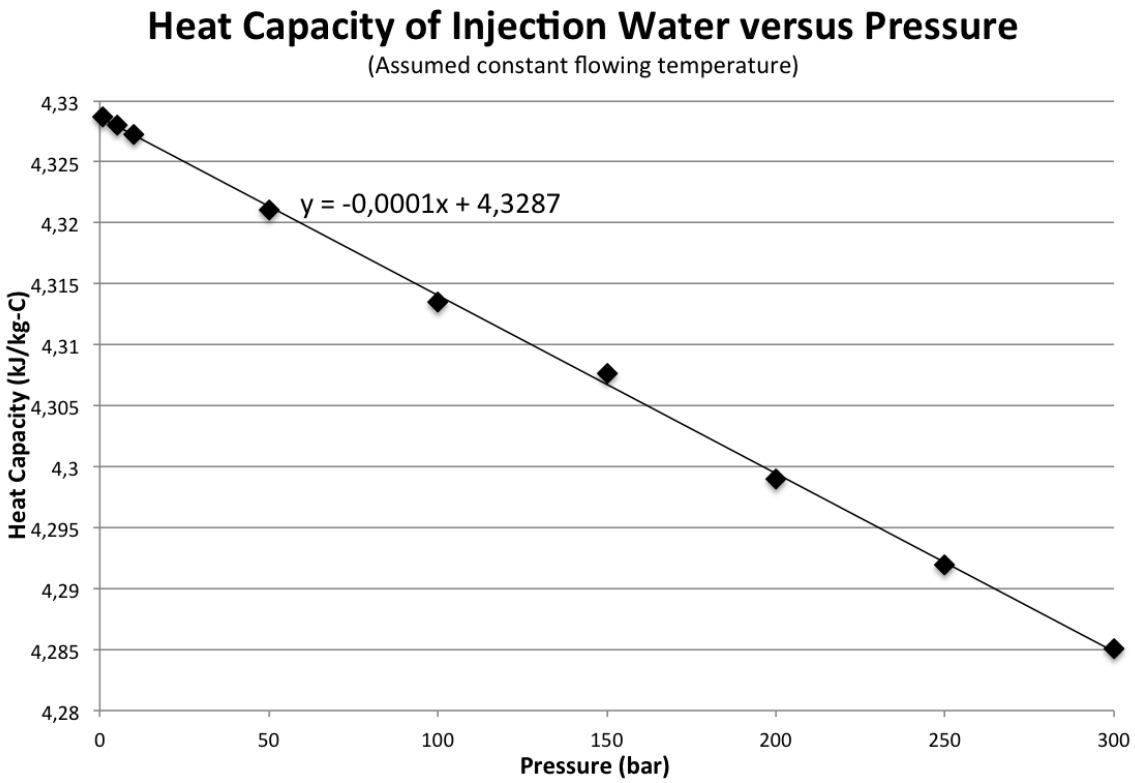

Graph 4.6 – Effect of pressure on injection water

The relationship between heat capacity and pressure is shown to be close to linear. It can also be observed that the heat capacity does not change very much. For an increase in pressure of 100 bar, the heat capacity is reduced by 10 J/kg-C. However, the heat capacity of water averages at 72% higher than the heat capacity of oil. When the relief well intersects the blowing well, and water is injected, the overall heat capacity of the flowing mixture will change.

Because of the relatively constant heat capacity of both reservoir and injection fluid, it was assumed that the heat capacity would be constant for the entire length of the blowing well. However, the injection of seawater at a certain depth in the wellbore would change both the temperature and the heat capacity of the flowing liquid.

Temperature Profile of Blowing Well

A base case for calculating the temperature profile of the blowing well was established. Table 4.2 summarizes the parameters used in calculating the flowing temperature.

Section	Parameters	Value	Source
Cased Section (0-2000m TVD)	Casing Inside Diameter	9,063" (9-5/8" outside)	Halliburton, 2012
	Specific heat capacity of reservoir fluid, Cp	2500 J/kg-C, "Worst Case"	Aspen HYSYS
	Formation heat transfer coefficient, U (Portland Cement)	0,58 W/m°C	Ceratechinc, 2013
	Surface temperature	4°C (Ocean bottom temperature)	Typical value
Openhole Section (2000-3000m)	Openhole diameter	8,5" (Bit diameter)	Halliburton, 2012
	Specific heat capacity of reservoir fluid, Cp	2500 J/kg-C, "Worst Case"	Aspen HYSYS
	Formation heat transfer coefficient, U (Sandstone)	2,37 W/mK	C-Therm, 2012
	Surface temperature	68°C (Casing shoe formation temperature)	From geothermal gradient

Table 4.2 –Parameters used in temperature calculations

Results of Flowing Temperature Calculations

Graph 4.7 shows the temperature profile of the blowing well for seven different blowout rates, using the base case parameters. It can be observed that the profile converges on a constant flowing temperature of 100°C, for higher blowout rates. Even for a relatively low blowout rate of 100 liters per second, the temperature of the blowout liquid is only reduced by 5°C, along the entire distance of the well. The higher temperature reduction rate in the openhole section is caused by the higher thermal conductivity of the sandface, compared to the cased section.

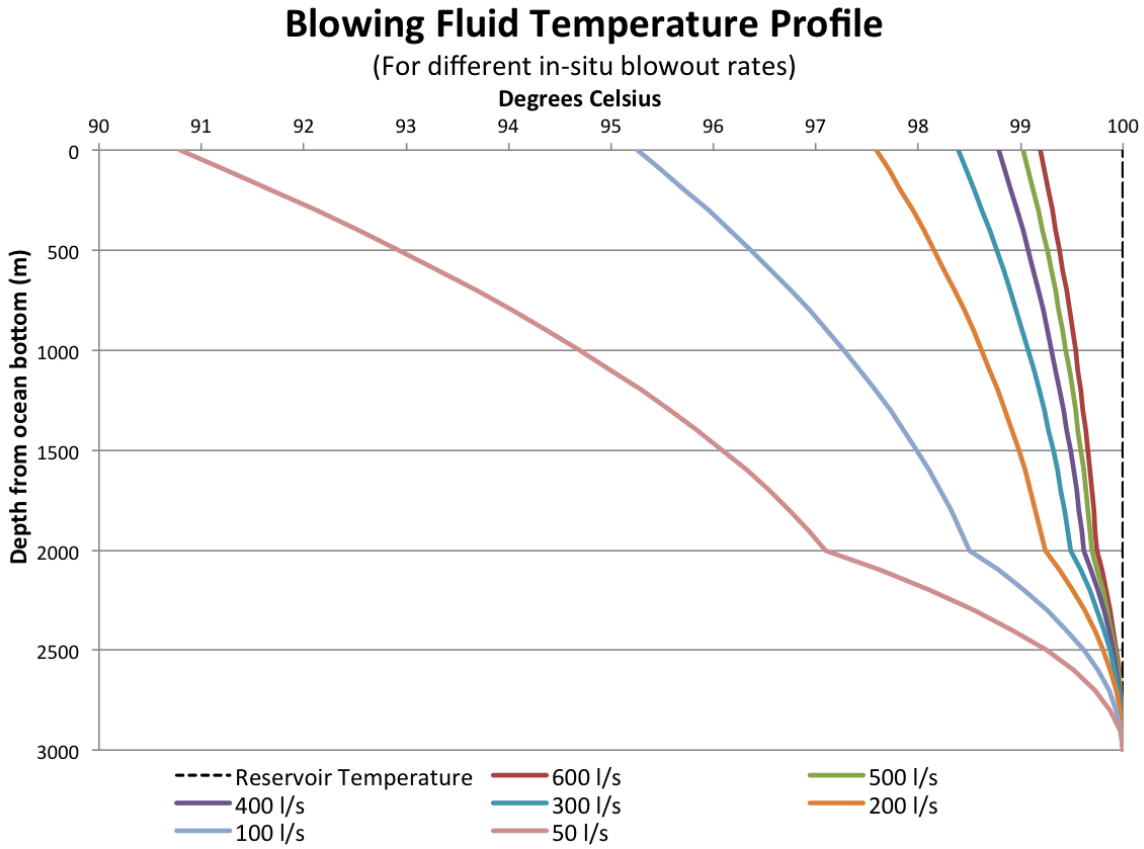

Graph 4.7 – Temperature profile in blowing well

Sensitivity Analysis

A sensitivity analysis was performed to investigate the effect of varying some of the important parameters in the temperature model. During these cases, a blowout rate of 400 l/s was chosen, while other parameters were subsequently changed.

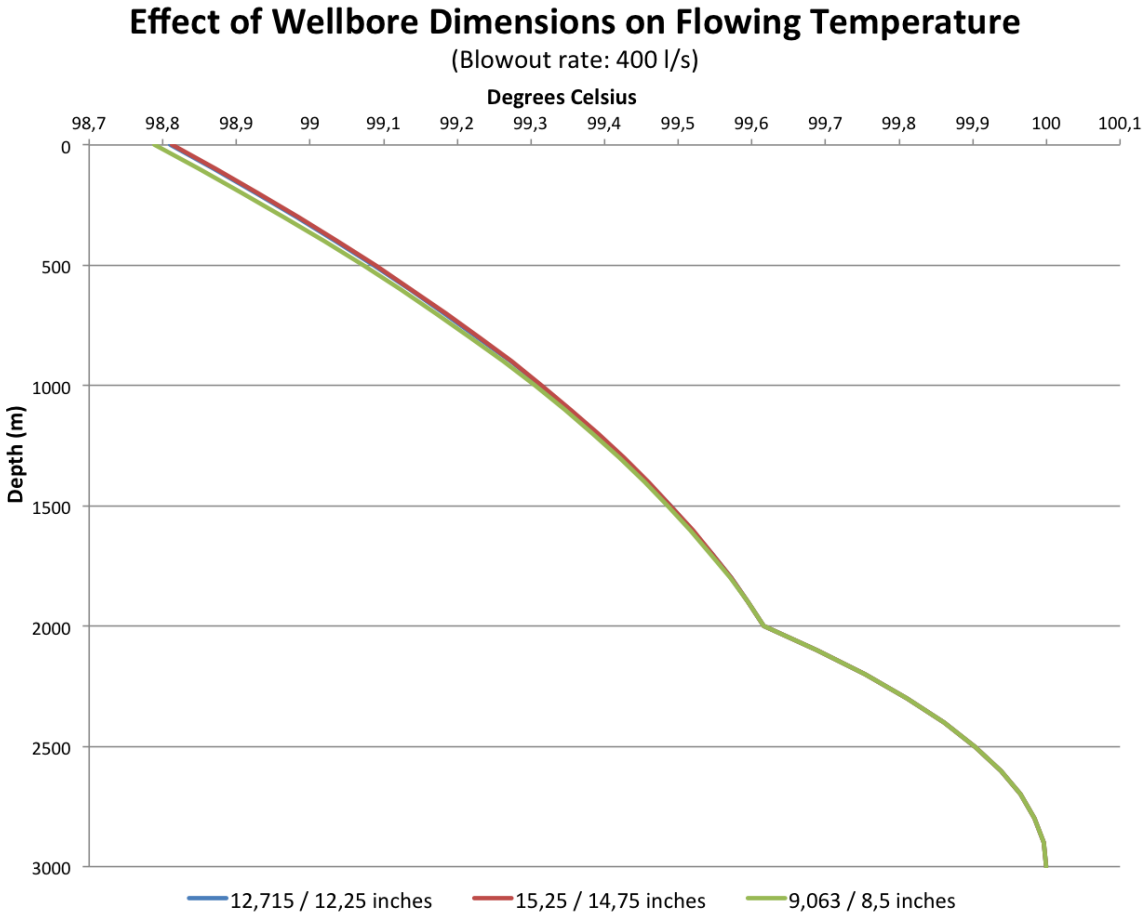

Graph 4.8 - Effect of wellbore dimensions

Graph 4.8 shows that the dimensions of the wellbore have little effect on the temperature profile of the well. Increased dimensions will make the flow velocity smaller, and also the surface area of the wellbore larger. However, the volumetric flow rates are the same, and the volume of formation fluid that must be cooled down is the equal for all cases. Hence this parameter changes the temperature profile very little.

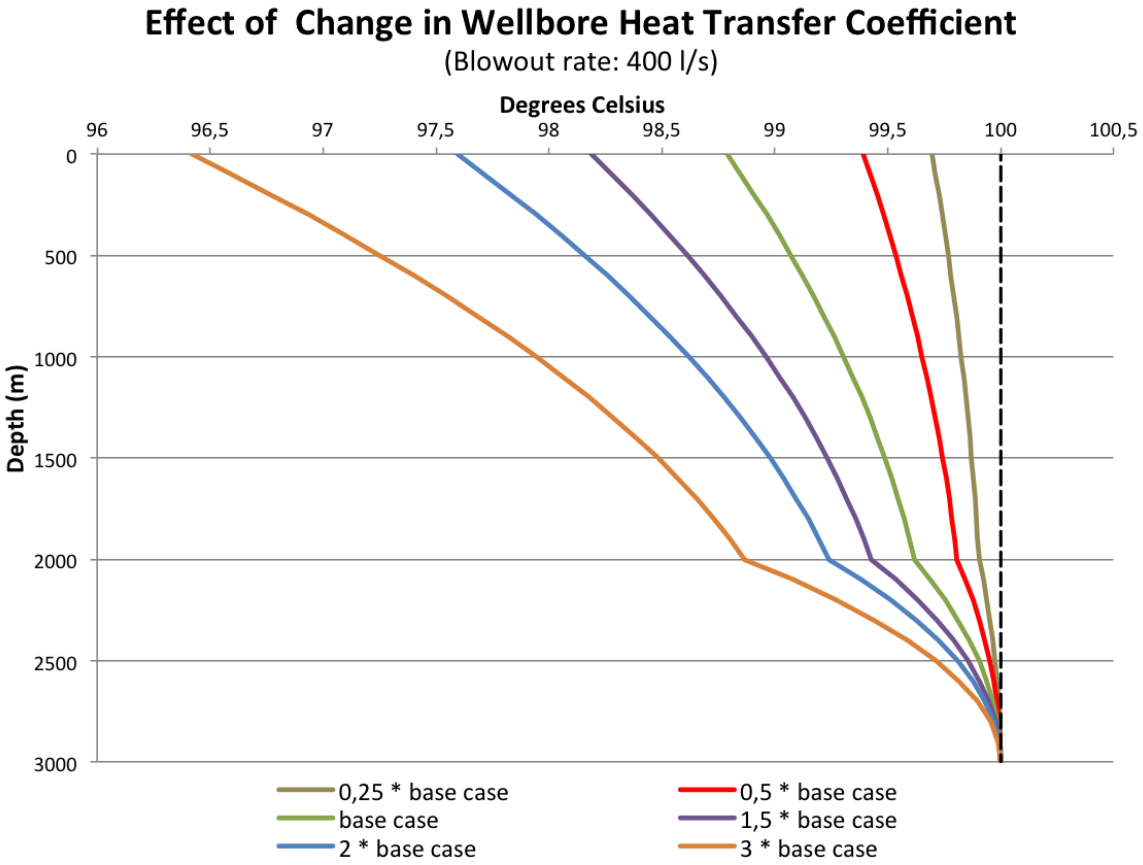

Graph 4.9 – Effect of heat transfer coefficient

The heat transfer coefficient of the material surrounding the wellbore determines the rate at which energy can be added or removed from the flowing fluid. The total heat transfer between the phases is dependent on this parameter, along with temperature difference and surface area between liquid and solid. Naturally, by increasing the ability to transfer heat, more energy will be removed from the hot stream of reservoir fluid. By multiplying the base case heat transfer coefficient of both openhole and cased section by three, the surface temperature of the stream is reduced to 96.4°C, compared to 98.8°C, for the base case. By multiplying the base case heat transfer coefficients with 0.25, the surface temperature of the stream is reduced only to 99.7°C.

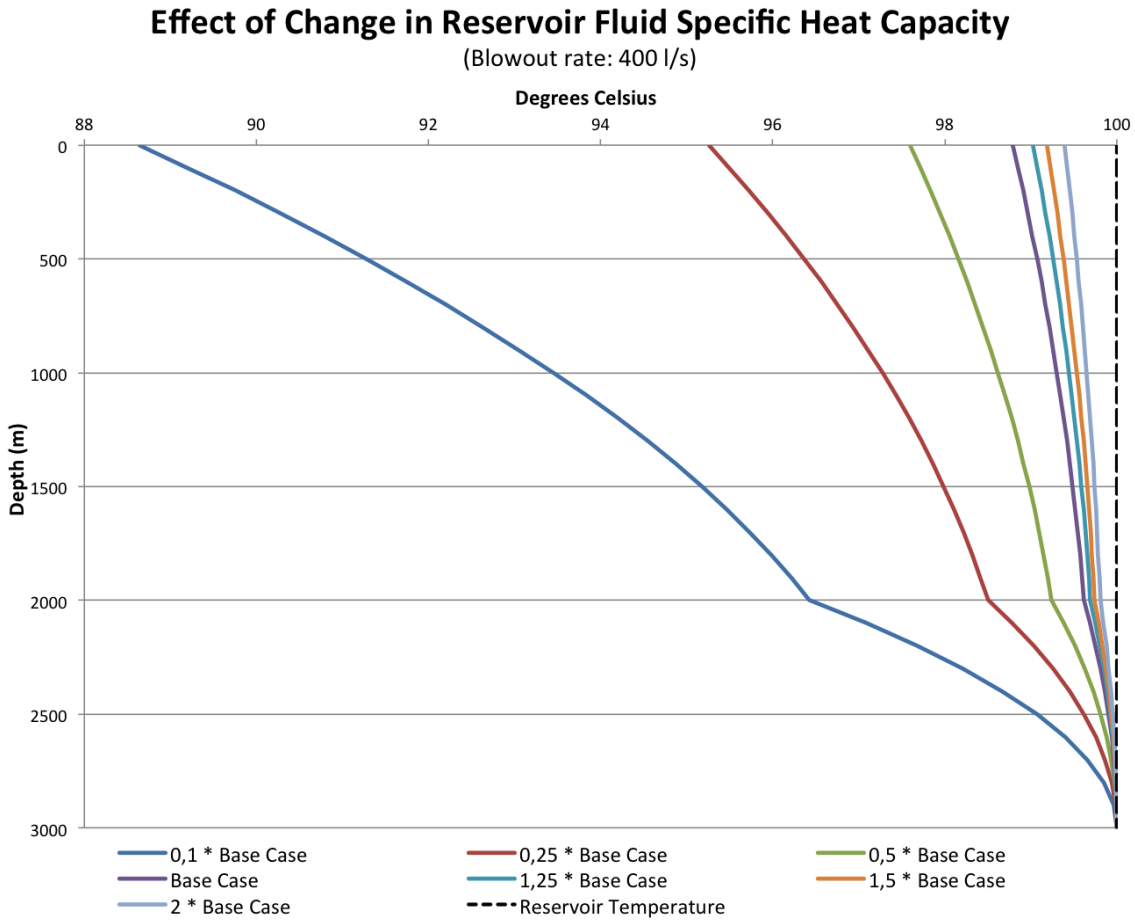

Graph 4.10 - Effect of Change in Reservoir Fluid Specific Heat Capacity

The specific heat capacity determines the amount of energy that must be added, or removed, to change a certain amount of liquid by a certain amount of degrees (Weisstein, 2007). This parameter will have a large impact on the temperature profile of the well. Graph 4.10 shows the temperature profile of the blowing well, for different values of specific heat capacity of the reservoir fluid.

Change in Wellbore Temperature Profile by Relief Well

The previous calculations established the temperature of the blowing well alone. When the relief well intersects the blowing well, the temperature profile will be changed dramatically. First of all, the liquid that will be injected into the blowing well will be of a lower temperature than the liquid blowing out of the reservoir. It is assumed that these liquids mix instantly, and that the temperature follows the relationship in equation 4.8.

$$T_{injection\ point} = T_{rf}\frac{V_{rf}}{V_m} + T_{if}\frac{V_{if}}{V_m} \tag{4.8}$$

Where T_{rf} is the temperature of the reservoir fluid, T_{if} is the temperature of the injection fluid, V_{rf} is the volumetric flow of reservoir fluid, V_{if} is the volumetric flow of injection fluid and V_m is the mixture flow rate. All values are taken at the injection point depth.

Further the heat capacity of the mixture will change. A constant heat capacity of 2500 and 4300 J/kg-C is assumed for reservoir- and injection fluid, respectively. The heat capacity is assumed to follow the relationship expressed by equation 4.7.

Bottomhole Temperature of Injection Fluid

A model was made to estimate the bottomhole temperature of the relief well. This will decide the temperature of the injection liquid just before it is mixed with the reservoir fluids. According to Leraand et al. (1992) a casing string is set just before drilling into the blowing well. Because of this, the heat transfer coefficient of the wellbore walls of the injection well is assumed constant, and equal to Portland cement. A casing inside diameter of 9.063 inches (9 ⅝-inch outside diameter) was used, according to the 2/4-15S Saga Petroleum relief well (Leraand et al., 1992).

When these parameters have been established, the situation can be described by a large number of pipe segments, where the ambient temperature is the average temperature over the short pipe segment. The ambient temperature is governed by the depth of the pipe segment, and the geothermal gradient.

Equation 4.9 expresses for the heat transfer coefficient between a fluid and a solid (Gudmundsson, 2009).

$$U = \frac{q}{A\Delta T_{LMTD}} \tag{4.9}$$

Where q is the heat flow in watt, A is the area of the pipe in square meters and ΔT_{LMTD} is the logarithmic mean temperature difference between the input and output of the pipe segment, and the ambient temperature. The energy required to change the temperature of a

fluid by a certain amount of degrees can be expressed according to the specific heat capacity of the fluid:

$$C_p = \frac{\Delta q}{m\Delta T} \tag{4.10}$$

Where Δq is the energy required to change the temperature of a fluid by a certain number of degrees, ΔT, and m is the mass of the fluid being heated or cooled. The logarithmic mean temperature difference is defined as:

$$\Delta T_{LMTD} = \frac{T_1 - T_2}{\ln \frac{T_1 - T_a}{T_2 - T_a}} \tag{4.11}$$

Where T_1 is the temperature at the start of the pipe segment, T_2 is the temperature at the end of the pipe segment, and T_a is the ambient temperature surrounding the pipe segment. Since the temperature of the formations surrounding the relief well is increasing with depth, the average temperature over the pipe segment is chosen as the ambient temperature. Since the model divides the relief well into small pipe segments, this error will be small. Combining equation 4.10 with 4.11, and inserting the formula for area of a cylinder yields the following equation:

$$C_p m\Delta T = U\ 2\pi rL\ \frac{T_1 - T_2}{\ln \frac{T_1 - T_a}{T_2 - T_a}} \tag{4.12}$$

Rewriting yields:

$$\ln \frac{T_1 - T_a}{T_2 - T_a} = (T_1 - T_2) \frac{U\ 2\pi rL}{C_p m(T_1 - T_2)} \tag{4.13}$$

Rewriting and taking the exponential function on both sides:

$$\ln \frac{T_1 - T_a}{T_2 - T_a} = \frac{U2\pi rL}{C_p m} \tag{4.14}$$

$$\ln \frac{T_2 - T_a}{T_1 - T_a} = -\frac{U2\pi rL}{C_p m} \tag{4.15}$$

$$T_2 = T_u + (T_1 - T_u)\, e^{-\frac{U2\pi rL}{C_p m}} \quad (4.16)$$

In most circumstances, a relief well will not have a vertical profile. The wellpath used in these calculations were based on the 2/4-15S Relief well. The simulation well has a vertical section of 650 meters, directly west of the blowing well. After the kick off point the well inclination is built to 39.2 and 24.4º when intercepting at casing shoe or bottom of the well, respectively. The inclination is maintained until the well is 20 meters directly east of the blowing well. At this point the well is kicked back to vertical for 250 meters before the well is intercepted.

The model was created in Excel by dividing the well into 300 pipe segments, each spanning over 10 meters true vertical depth. In the inclined section of the well, the measured length of the pipe would be higher, subsequently causing a higher temperature drop. The surface temperature was set to be 15°C, and the geothermal gradient is assumed linear and equal to the MATLAB model. Graph 4.11 and 4.12 shows the temperature gradient when intersecting the bottom of the blowing well, and the casing shoe, respectively.

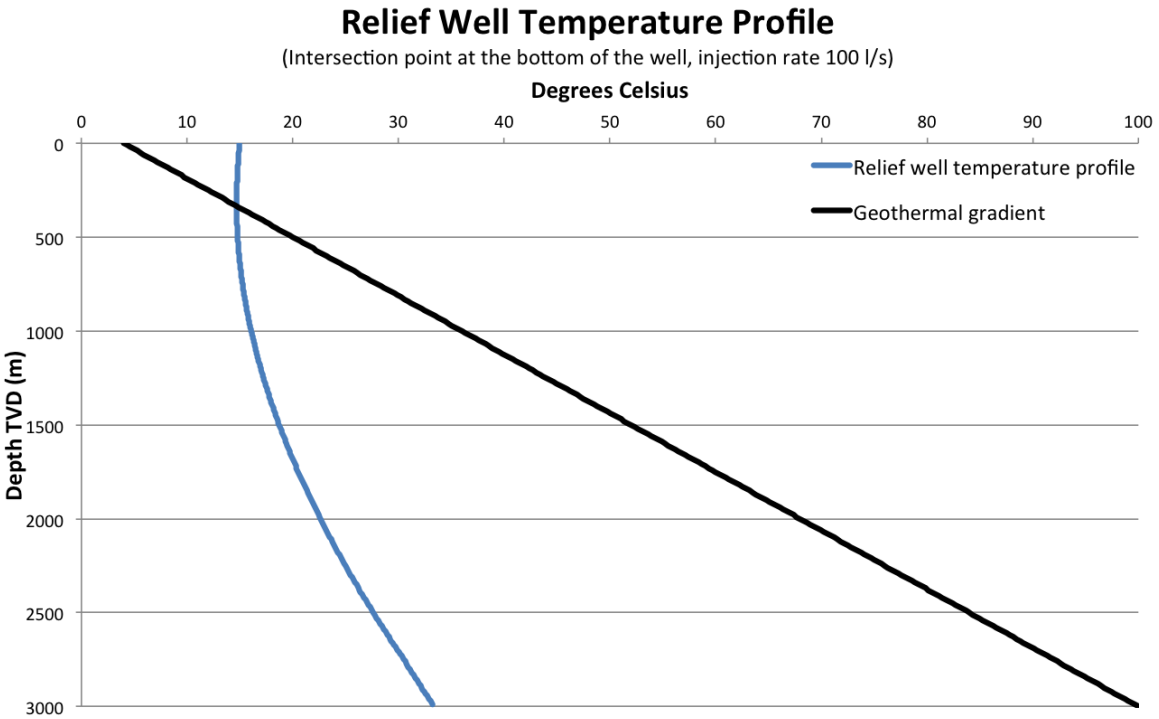

Graph 4.11 – Temperature profile in Relief well when intersecting at the bottom

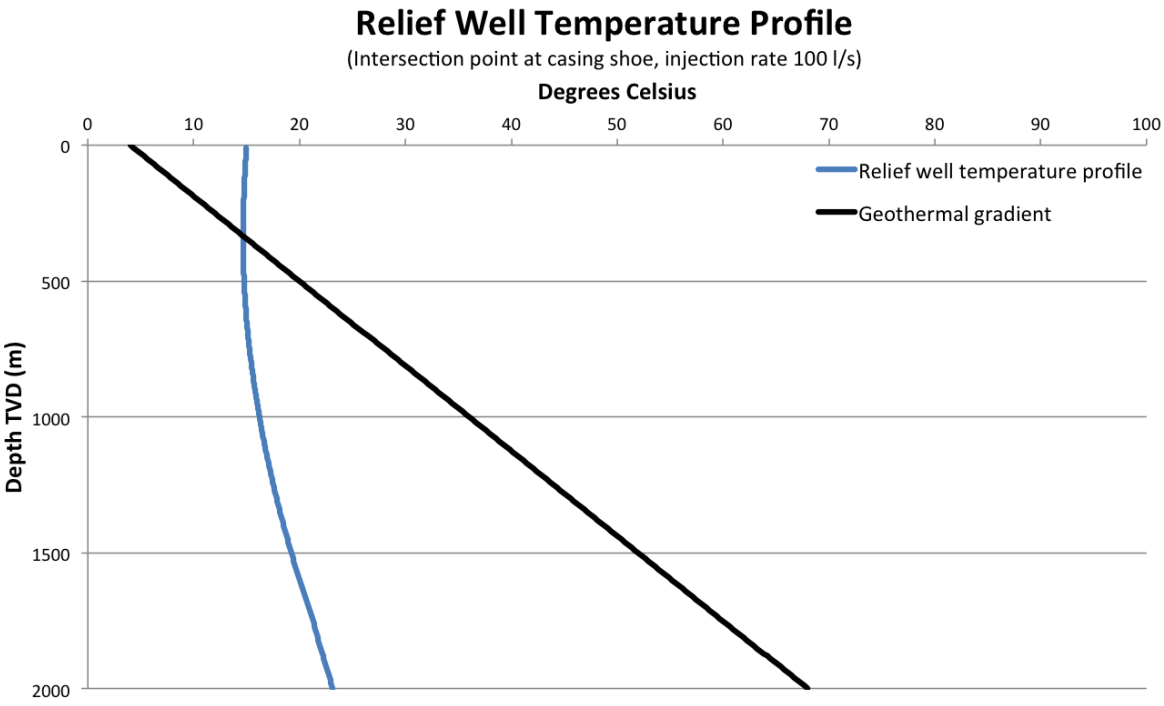

Graph 4.12 – Temperature Profile in Relief well when intercepting at casing shoe

Equation for Relief Well Bottomhole Temperature

By plotting the bottomhole and casing shoe injection fluid temperature against flow rate in Excel, equations can be established through regression analysis. This is used in the MATLAB model to correct the flowing temperature when water is injected to kill the well. Graph 4.13 shows the results.

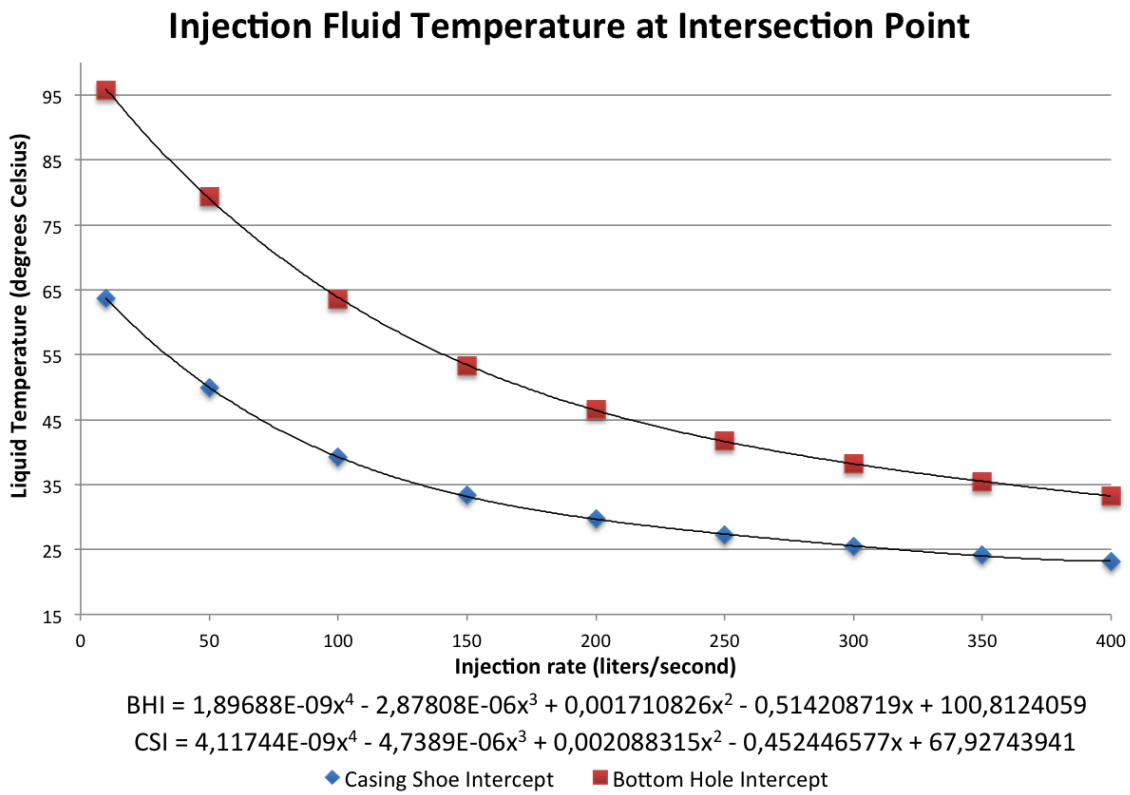

Graph 4.13 – Equations for relief well bottomhole temperature

4.2.3 Pressure drop calculations

A blowout has several similarities to a producing well, where the well is produced at the maximum rate possible. The flow rate will be dependent on the inflow performance at the sandface of the point of influx, and the vertical lift capacity of the well (Oudeman et al., 2010). According to Hasan et al. (2000) the blowout rate will increase until the hydrostatic-, frictional-, and acceleration pressure drop in the blowing well is high enough to balance the pressure at the wellhead. This statement is valid as long as the flowing capacity of the formation sandface is not the limiting factor on the flow rate, nor that sonic velocities is reached somewhere along the annulus of the flowing well.

The MATLAB-program will assume a low blowout rate for the first simulation, and the pressure drop for the entire wellbore will be calculated. If equation 4.17 is not balanced when the first iteration is performed, the blowout rate will be increased, and the simulation will be performed until the equation is balanced.

$$p_{wf} = p_{wellhead} + \Delta p_{hydrostatic} + \Delta p_{friction} + \Delta \mathrm{p}_{acceleration} \qquad (4.17)$$

According to Kouba et al. (1993) the pressure drop caused by acceleration can be neglected for the given circumstances. Further, the flowing reservoir pressure is assumed equal to the reservoir pressure immediately after influx.

The MATLAB-program will generate a matrix consisting of one row per wellbore meter. Important values are entered into this matrix as the simulation is being performed. First the temperature profile of the well is calculated according to the procedure described in subchapter 4.2.2. After this, the pressure in row number 3000 is set equal to the reservoir pressure.

The pressure drop is calculated over one meter segments in the well. The reservoir pressure represents the input pressure of the first segment. Once the pressure drop is calculated, the output pressure can be calculated as well. This output pressure is entered into the row above in the matrix, and represents the input pressure for the next segment. Because of this, the properties at the beginning of the interval are used, rather than the average properties. However, it is deemed accurate enough to do this, since the intervals are relatively small. When this operation is performed for all 3000 segments of the matrix, the first iteration is completed.

To be able to calculate the hydrostatic- and frictional pressure drop, a number of different properties must be established for the flowing temperature and pressure at a given depth in the well.

Compressibility Factor of Associated Gas

When the pressure and temperature at a certain depth in the well is known, the compressibility factor of the associated gas can be calculated. The molar mass of the gas phase for different pressures was simulated in Aspen HYSYS. By plotting in excel, and using regression analysis, an equation for the molar mas was obtained. Graph 4.14 shows the results. The molar mass of the associated gas changes as different components boils out of the solution, and because of this it shows a quite complex behavior. It must be described by a sixth order polynomial equation.

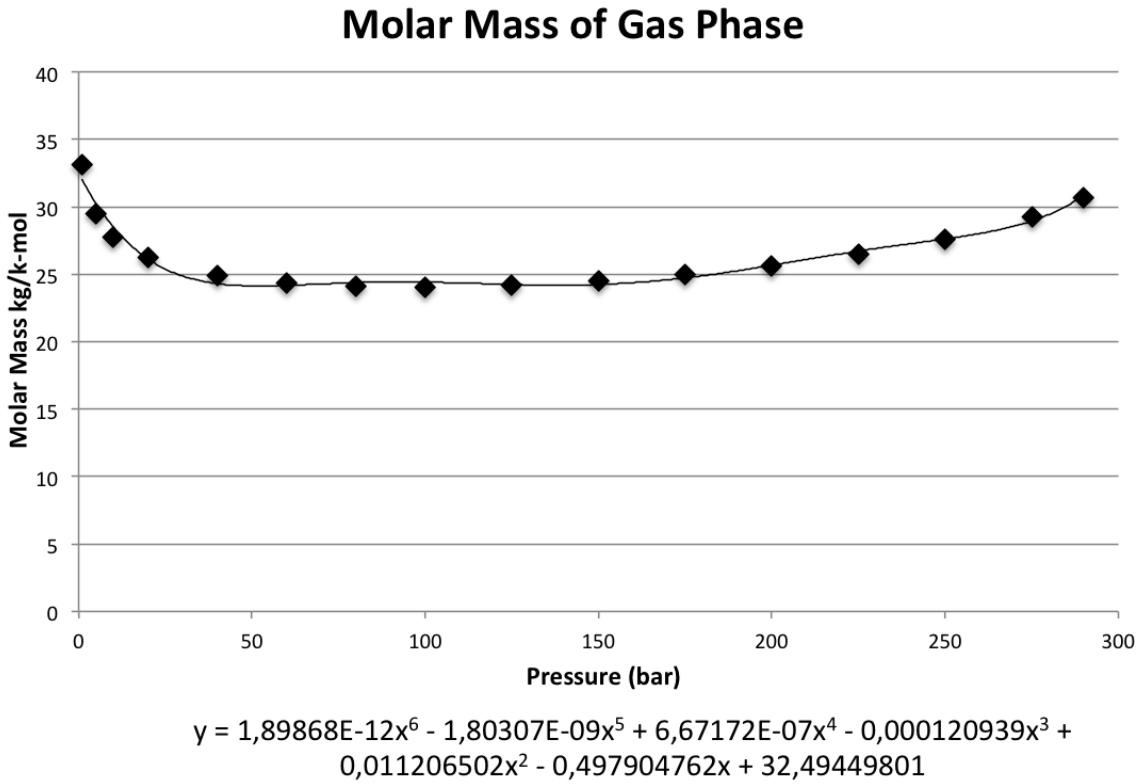

Graph 4.14 – Molar mas of gas phase

Equation 4.18 expresses the specific gravity of the associated gas:

$$\gamma_{gas} = \frac{M_{gas}}{M_{air}} \tag{4.18}$$

Standing's correlation for pseudo-reduced properties is used (Whitson & Brulé, 2000):

$$T_{pc} = 168 + 325\gamma_{gas} - 12.5{\gamma_{gas}}^2 \qquad \{\text{For } \gamma < 0.75\} \tag{4.19}$$

$$P_{pc} = 667 + 15\gamma_{gas} - 37.5{\gamma_{gas}}^2 \quad \{\text{For } \gamma < 0.75\} \quad (4.20)$$

$$T_{pc} = 187 + 330\gamma_{gas} - 71.5{\gamma_{gas}}^2 \quad \{\text{For } \gamma \geq 0.75\} \quad (4.21)$$

$$P_{pc} = 706 + 51.7\gamma_{gas} - 1.11{\gamma_{gas}}^2 \quad \{\text{For } \gamma \geq 0.75\} \quad (4.22)$$

$$T_{pr} = \frac{T}{T_{pc}} \quad (4.23)$$

$$P_{pr} = \frac{P}{P_{pc}} \quad (4.24)$$

Hall & Yarborogh's (1973) equation of state is used to calculate the z-factor:

$$z = \frac{0.06125t\ p_{pr}\ e^{[-1.2(1-t)^2]}}{y} \quad (4.25)$$

$$t = \frac{1}{T_{pr}} \quad (4.26)$$

$$\begin{aligned} F(y) = 0 = &-0.06125t\ p_r\ e^{[-1.2(1-t)^2]} \\ &+ \frac{y + y^2 + y^3 + y^4}{(1-y)^3} \\ &-(14.76t - 0.76t^2 + 4.58t^3)y^2 \\ &+(90.7t - 242.2t^2 + 42.4t^3)y^{2.18+2.82t} \end{aligned} \quad (4.27)$$

To solve the equation for y, the Newton-Raphson method is applied. A while loop in the program is utilized, where the initial value of y is set low, and the calculations are performed until $(y_i\text{-}y_{i+1})^2$ is smaller than 10^{-5}. Using this method the value of y will converge against the correct value.

$$\begin{aligned} \frac{dF}{dy} = &\frac{1 + 4y + 4y^2 - 4y^3 + y^4}{(1-y)^4} \\ &- (20.25t - 19.52t^2 + 9.16t^3)y \\ &+(2.18 + 2.82t)(90.7t - 242.2t^2 + 42.4t^3)y^{(1.18+2.82t)} \end{aligned} \quad (4.28)$$

$$y_{i+1} = y_i - \frac{F(y)}{F'(y)} \quad (4.29)$$

Determining Flowing Phase Fractions

Because of the relatively stable flowing temperature of the blow out, Aspen HYSYS were used to determine the in-situ flowing phase fractions for a constant flowing temperature. With a constant temperature of 100°C, the fractions were simulated for different wellbore pressures. These numbers were plotted into Excel, and regression analysis was used to find an equation for the flowing fraction of oil. Graph 4.15 shows the flowing oil fraction versus pressure.

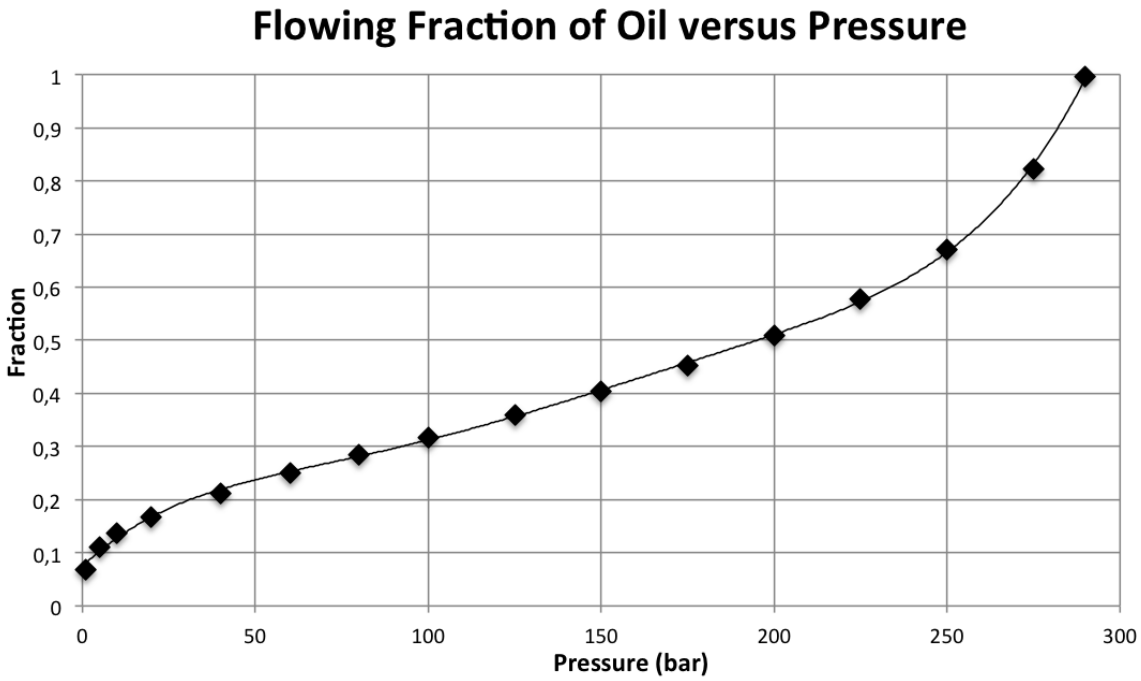

Graph 4.15 – Liquid fraction versus pressure

Determining Molar Mass of Liquid Phase

The molar mass of the oil phase will stay constant above the bubble point pressure. In the MATLAB-program, the molar mass is set to the initial value until the pressure falls below the bubble point pressure of the particular flowing temperature. Once gas starts to boil out, the lighter components will boil out first. This will make the molar mass of the oil phase progressively heavier.

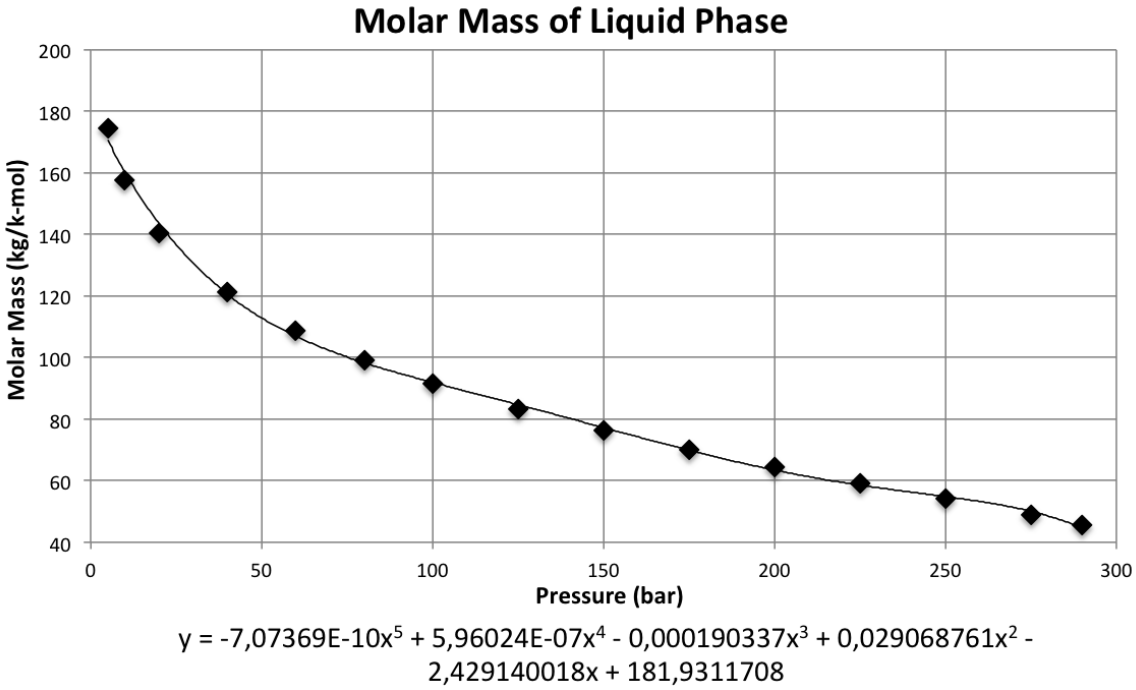

Graph 4.16 – Molar mass of liquid phase

Oil and Gas Densities

The density of the gas phase is calculated using the ideal gas law, and adjusted by multiplying with the compressibility factor, according to equation 4.30.

$$\rho_{gas,in-situ} = z \cdot \frac{pM_{gas}}{R\,T} \tag{4.30}$$

Where z is the compressibility factor, M is the molar mass of the gas phase, R is the gas constant, p is the pressure and T is the temperature.

The oil density is calculated through simulation and regression analysis. Above the bubble point the density is only dependent on the compressibility of the liquid, and can be described by a linear equation. Below the bubble point, lighter components start to boil off, changing the initial composition of the oil mixture. This has a large effect on the properties of the oil phase. Because of this, two separate equations had to be developed for the density of the oil, one for pressures above the bubble point, and one for pressures below. Graph 4.17 shows the in-situ density versus pressure, together with the equations for density.

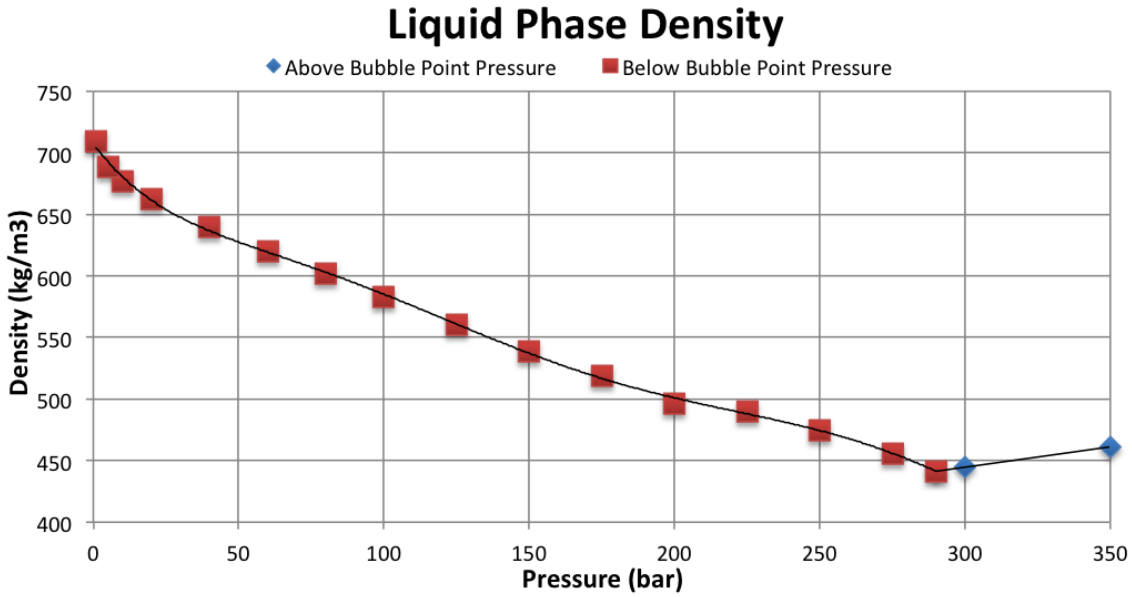

Above Bubble Point Pressure = 0,330750716x + 345,4400112

Below Bubble Point Pressure = $6{,}50336E\text{-}12x^6 - 6{,}98355E\text{-}09x^5 + 2{,}8333E\text{-}06x^4 - 0{,}000543422x^3 + 0{,}051180284x^2 - 3{,}103346739x + 707{,}0146945$

Graph 4.17 – Density of liquid phase

Viscosity of Oil Phase

It is important to get an accurate estimation of the viscosity of the flowing phases in the well, as this will have a large impact on the frictional pressure drop throughout the system. Viscosity of the flowing fluids is dependent on several parameters, where temperature, pressure and composition are the most important.

Above the bubble point pressure the viscosity of the oil phase is only affected by the change in pressure and temperature. Once gas starts to boil out, the composition of the liquid fraction is changed. Generally, lighter components boils out first, leaving the oil phase with a higher percentage of long chained alkanes, and hence a higher viscosity.

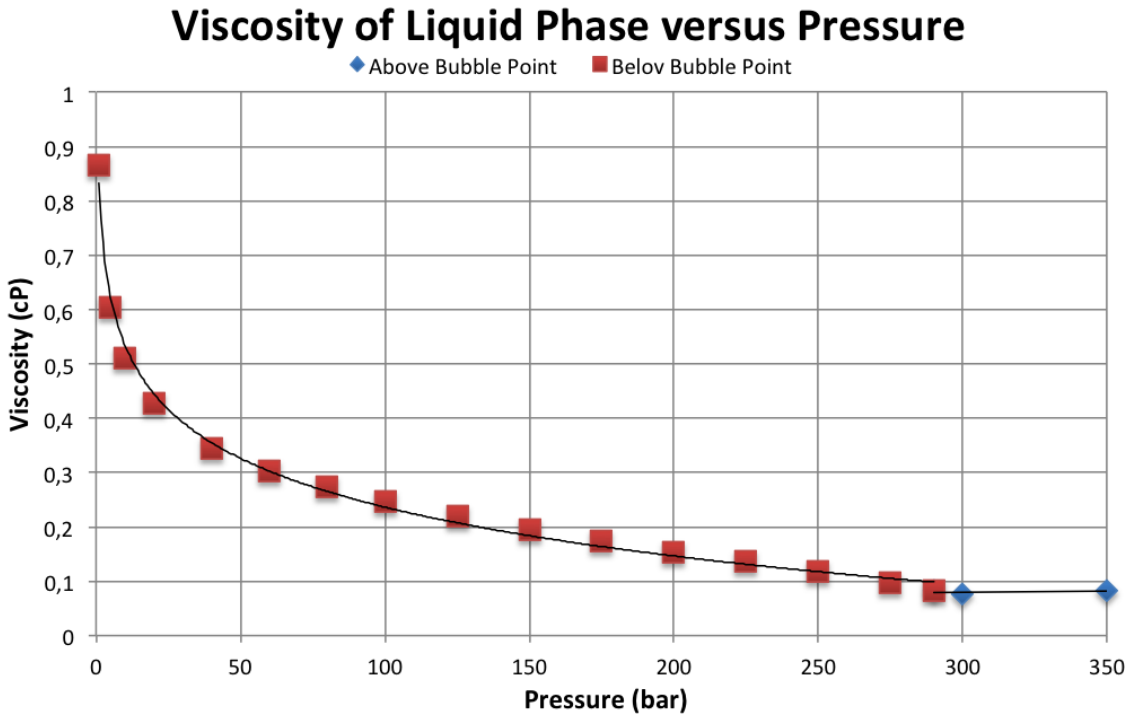

Graph 4.18 – Viscosity of liquid phase

Graph 4.18 shows how the viscosity of the oil phase develops as the pressure is reduced. The temperature is kept constant, at 100°C. The equations were obtained through simulation in Aspen HYSYS, and regression analysis in Excel. Together with the density, this parameter is calculated with one equation above the bubble point pressure, and another equation below. The viscosity above the bubble point can be described by a linear equation. Below the bubble point the viscosity increases exponentially.

Viscosity of Gas Phase

The in-situ gas viscosity was calculated by using the correlation suggested by Ohirhian and Abu (2008). This correlation is accurate from 10- to 283 bar, and 54- to 106°C. Because of this, it fits well with the blowout situation. Comparison with simulated values in Aspen HYSYS showed good results. Equations 4.31 through 4.34 are used to obtain the viscosity. Values for the compressibility factor have already been calculated in the MATLAB-program.

$$Rg = \frac{0.001031PT}{P - 0.061T} \tag{4.31}$$

$$Bg = \frac{0.0283zT}{P} \tag{4.32}$$

$$x = \frac{Rg}{100Bg} \tag{4.33}$$

$$\mu_g = \frac{0.0109388 - 0.0088234x - 0.0075720x^2}{1 - 1.3633077x + 0.0461989x^2} \tag{4.34}$$

In these equations, pressure and temperature are in pounds per square inch (psi) and Rankine, respectively. Rg is the relative density of the natural gas compared to dry air. Bg is the dimensionless gas volume factor. The viscosity is in centipoise (cP). Z is the compressibility factor of the gas.

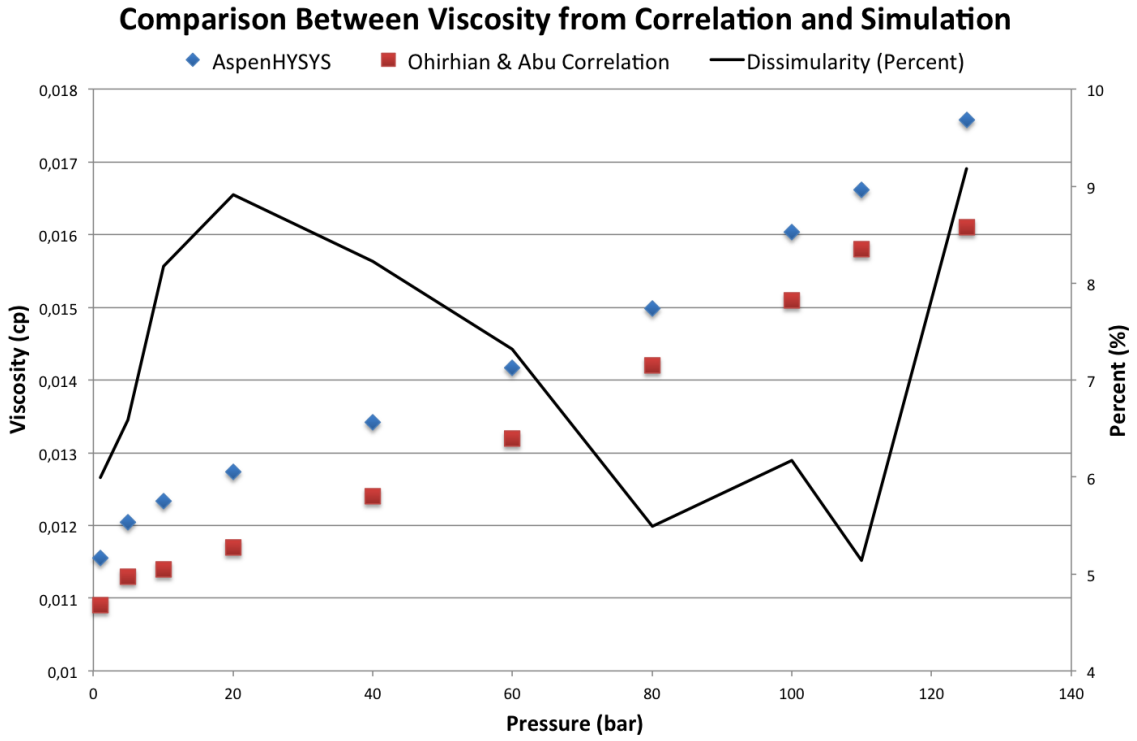

Graph 4.19 – Comparison between correlation and simulation

Comparison between viscosity values obtained from correlation and simulation results shows a similar trend. The maximum dissimilarity was 9.2%, while the average dissimilarity was 7%. It was chosen to use the correlation method to find viscosity of the natural gas in the MATLAB-program. These equations takes the small temperature drop into consideration, and is also the lowest viscosity values, and hence the "worst case" viscosity.

The mixing viscosity of the flowing hydrocarbon phases is assumed follow a weighted arithmetic mean, as suggested by Nickens (1987).

$$\mu_{mixture} = \sum_i \frac{Q_i}{Q_{tot}} \mu_i = \frac{Q_{gas}}{Q_{mixture}} \mu_{gas} + \frac{Q_{oil}}{Q_{mixture}} \mu_{oil} \tag{4.35}$$

Surface Tension between Liquid- and Gas Phase

Once two-phase flow has developed, surface tension between the phases will contribute to increasing the frictional pressure drop. Simulation in Aspen HYSYS and regression analysis were used to obtain a pressure dependent equation for this parameter. Graph 4.20 shows the results.

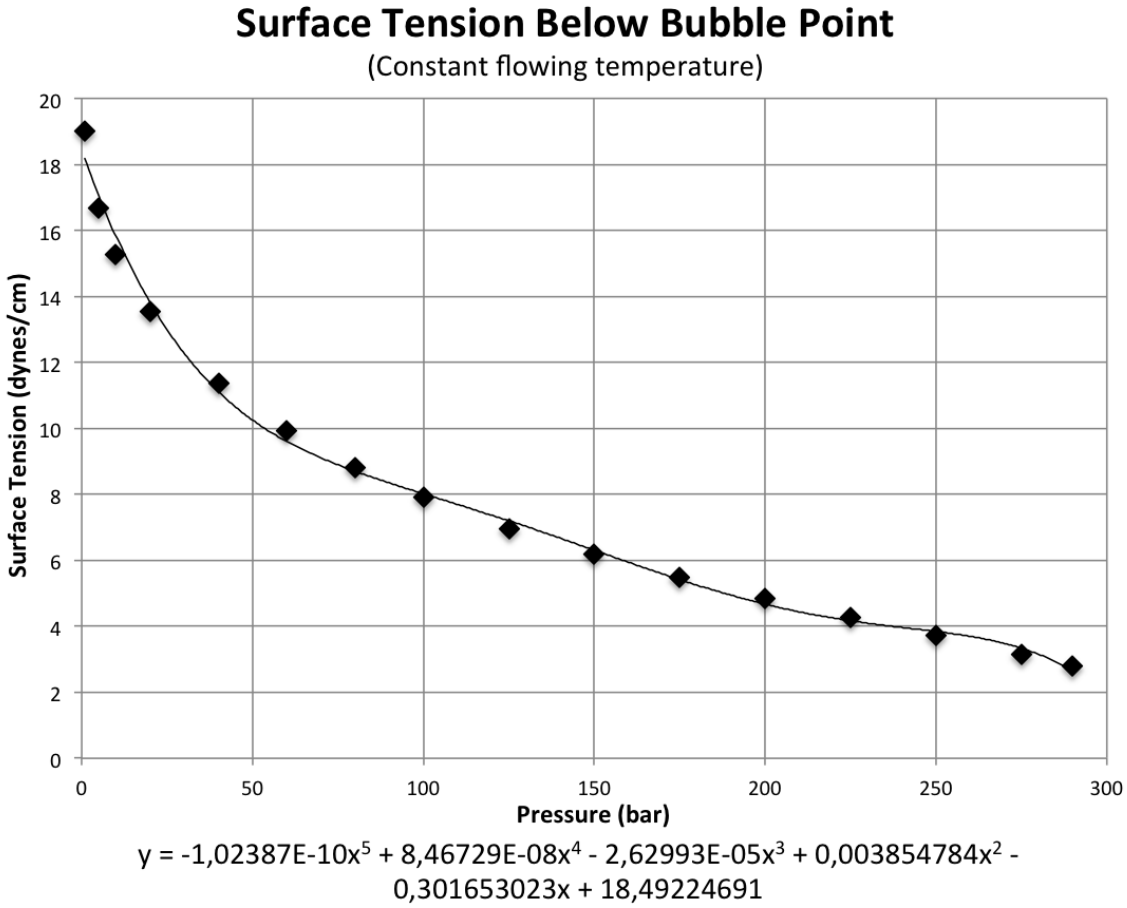

Graph 4.20 – Surface tension between phases

Calculating Hydrostatic- and Frictional Pressure Drop

At this point, enough information about the local flowing properties is known to calculate both hydrostatic- and frictional pressure drop. The Beggs and Brill Method (1973) were used for this purpose. All equations and theory in this subchapter have been found in their work. The method is valid for horizontal, vertical and inclined flow. The equations take into account the flow regime, flow pattern, liquid hold up and casing/openhole roughness (Beggs & Brill, 1973). Equations 4.36 through 4.41 are calculated first, to establish the flow regime at the current position in the well.

$$N_{FR} = \frac{{u_m}^2}{gD} \tag{4.36}$$

$$\lambda_l = \frac{q_l}{(q_l + q_g)} \tag{4.37}$$

Where N_{fr} is the mixture Froude number, λ_l is the input liquid content, u_m is the flow velocity of the mixture, defined as the volumetric flow of oil and gas divided by flow area, g is the gravitational constant, D is the diameter of the flow area, q_l and q_g is the volumetric flow of liquid and gas, respectively. Further four constants are calculated using the input liquid content.

$$L_1 = 316{\lambda_l}^{0.302}, \qquad L_2 = 0.0009252{\lambda_l}^{-2.4684} \tag{4.38; 4.39}$$

$$L_3 = 0.10{\lambda_l}^{-1.4516}, \quad L_4 = 0.50{\lambda_l}^{-6.738} \tag{4.40; 4.41}$$

The flow regime is determined using the input liquid content, together with the constants L_1, L_2, L_3 and L_4. During two-phase flow, and depending on flow regime, the gas phase will have a tendency to flow at a velocity greater than the liquid phase. Slippage between the phases will occur, causing liquid holdup. This is taken into account in these equations by first finding the liquid holdup for a horizontal pipe, and then adjusting for the inclination of the pipe. Table 4.3 gives the boundaries for the different flow regimes, as well as equations for calculating the liquid holdup in a horizontal pipe, $H_L(0)$, and the coefficient of flow and inclination, C.

Flow regime	Boundaries	$H_L(0)$	C (Coefficient)
Segregated	$\lambda_l < 0{,}01$, $N_{fr}<L_1$ $\lambda_l >= 0{,}01$, $N_{fr}<L_2$	$H_L(0)_s = \frac{0.98\lambda_l^{0.4846}}{N_{fr}^{0.0868}}$	$(1-\lambda_l)\ln\left[\frac{0.011N_{lv}^{3.539}}{\lambda_l^{3.768}N_{fr}^{1.614}}\right]$
Transition	$\lambda_l >= 0{,}01$, $L_2< N_{fr}<=L_3$	$H_L(0)_t = AH_L(0)_s - BH_L(0)_i$ $A = \frac{L_3-N_{fr}}{L_3-L_2}$, B=1-A	
Intermittent	$.01 <= \lambda_l < 0{,}4$, $L_3< N_{fr}<=L_1$ $\lambda_l >= 0{,}4$, $L_3< N_{fr}<=L_4$	$H_L(0)_i = \frac{0.845\lambda_l^{0.5351}}{N_{fr}^{0.0173}}$	$(1-\lambda_l)\ln\left[\frac{2.96\lambda_l^{0.305}N_{fr}^{0.0978}}{N_{lv}^{3.768}}\right]$
Distributed	$\lambda_l < 0{,}4$, $N_{fr}>=L_1$ $\lambda_l >= 0{,}4$, $N_{fr}>L_4$	$H_L(0)_d = \frac{1.065\lambda_l^{0.5824}}{N_{fr}^{0.0609}}$	C=0

Table 4.3 – Flow regime determination and related equations (Beggs & Brill, 1973)

N_{lv} is the liquid velocity number and is calculated according to equation 4.42.

$$N_{lv} = v_{sl}\left(\frac{\rho_l}{g\sigma}\right)^{0.25} \tag{4.42}$$

Where v_{sl} is the superficial liquid flow velocity, defined as the volumetric flow rate of liquid divided by the pipe cross-section, and σ is the liquid surface tension between the gas- and liquid phase.

Once the flow regime has been established, the horizontal liquid holdup is calculated for the specific position in the blowing well. The liquid holdup is adjusted according to inclination, by multiplying with the inclination correction factor, ψ, according to equations 4.43 and 4.44.

$$\psi(\theta) = 1 + C\left[\sin(1.8\theta) - \frac{1}{3}sin^3(1.8\theta)\right] \tag{4.43}$$

$$H_L(\theta) = H_L(0)\cdot\psi(\theta) \tag{4.44}$$

When the liquid holdup for the inclination in question is known, the hydrostatic pressure change can be calculated according to equation 4.46, where equation 4.45 describes the effective mixture density when taking the liquid holdup into account.

$$\rho_{mixture} = H_L(\theta)\rho_{liquid} + \big(1 - H_L(\theta)\big)\rho_{gas} \tag{4.45}$$

$$\Delta p_{hyd} = \rho_{mixture} g \Delta h \tag{4.46}$$

The effect of liquid holdup on frictional pressure drop is accounted for by using a two-phase friction factor, f_{tp}, together with the no slip mixture density. The two-phase friction factor and the no slip friction factor are proportional to the exponential value of an empirical constant, S. This relationship is expressed in equation 4.47.

$$\frac{f_{tp}}{f_{ns}} = e^{S} \tag{4.47}$$

$$S = \frac{\ln(y)}{-0.0523 + 3.182\ln(y) - 0.8725\ln(y)^2 + 0.01853\ln(y)^4} \tag{4.48}$$

$$y = \frac{\lambda_l}{[H_L(\theta)]^2} \tag{4.49}$$

As the flow approaches all liquid, or all gas, equation 4.48 becomes unbounded, and cannot be solved. This takes place in the interval when the constant y is higher than 1 and lower than 1.2. In this interval Beggs and Brill (1973) suggested that the empirical constant S should be calculated using equation 4.50. In the simulation model, this happens as the liquid goes from all liquid and into the two-phase region.

$$S = \ln(2.2y - 1.2) \tag{4.50}$$

Equation 4.47 is solved with regards to f_{tp}. The no slip friction factor is expressed by equation 4.51 for turbulent flow, as suggested by Chen (1979). This equation is valid for rough conduits where relative roughness (ε/D) ranges from 5×10^{-7} to 0.05, and Reynolds number ranges from 4000 to 4×10^{8}. This equation has shown similar accuracy as the more known Colebrook equation, but is explicit and does not require iteration to be solved (Ghanbari et al., 2011). Considering the number of times this equation had to be calculated during simulation, the Chen equation was chosen to make the program run faster. The small deviations that might result from this will be many orders of magnitude smaller than the uncertainty in regards to in-situ roughness of both formation and piping.

$$\frac{1}{\sqrt{f_F}} = -2\log_{10}\left(\frac{\frac{\varepsilon}{D}}{3.7065} - \frac{5.0452}{Re}\log_{10}\left(\frac{\left(\frac{\varepsilon}{D}\right)^{1.1098}}{2.8257} + \left(\frac{7.149}{Re}\right)^{2}\right)\right) \tag{4.51}$$

For laminar flow the Darcy friction factor is used:

$$f_D = \frac{64}{Re} \tag{4.52}$$

The Reynolds number is defined as:

$$Re = \frac{\rho_{mixture} {u_{mixture}}^2 D}{\mu_{mixture}} \tag{4.53}$$

Where the no-slip mixture density, velocity and viscosity is used. D is the hydraulic diameter of the cross sectional flow area, which is equal to the pipe- and open-hole diameter as long as there are no obstructers in the blowing well.

The Chen equation was used in the transient region as well. This might cause an underestimated friction factor during these flow conditions. The inconsistency of the flow pattern in this region, causing the flow to show tendencies of both laminar- and turbulent flow, makes prediction of the friction factor difficult (Dobrnjac, 2012). However, simulation showed that the flow always stayed in the turbulent flow area.

It is worth noting that the Chen equation gives the Fanning friction factor, while the Darcy friction factor is found using the equation for friction factor during laminar flow. The Fanning friction factor is four times smaller than the Darcy friction factor, and this has to be taken into account when calculating the pressure drop.

Pressure drop is calculated using the Darcy-Weisbach equation, adjusted for liquid holdup.

$$f_{tp,D} = f_{NS,D} e^S = 4 f_{NS,F} e^S \tag{4.54}$$

$$\Delta p_{friction} = f_{tp,D} \frac{\rho_{NS} {u_m}^2 \Delta L}{2D} \tag{4.55}$$

4.2.4 Flow Regime

The flow regime of a particular section of the well is important because the liquid holdup is largely dependent on this factor. In the method described by Beggs and Brill (1973) different holdup correlations are used for three different flow patterns. Figure 4.3 shows the flow pattern map, and displays the flow regime for different Froude number and liquid input content.

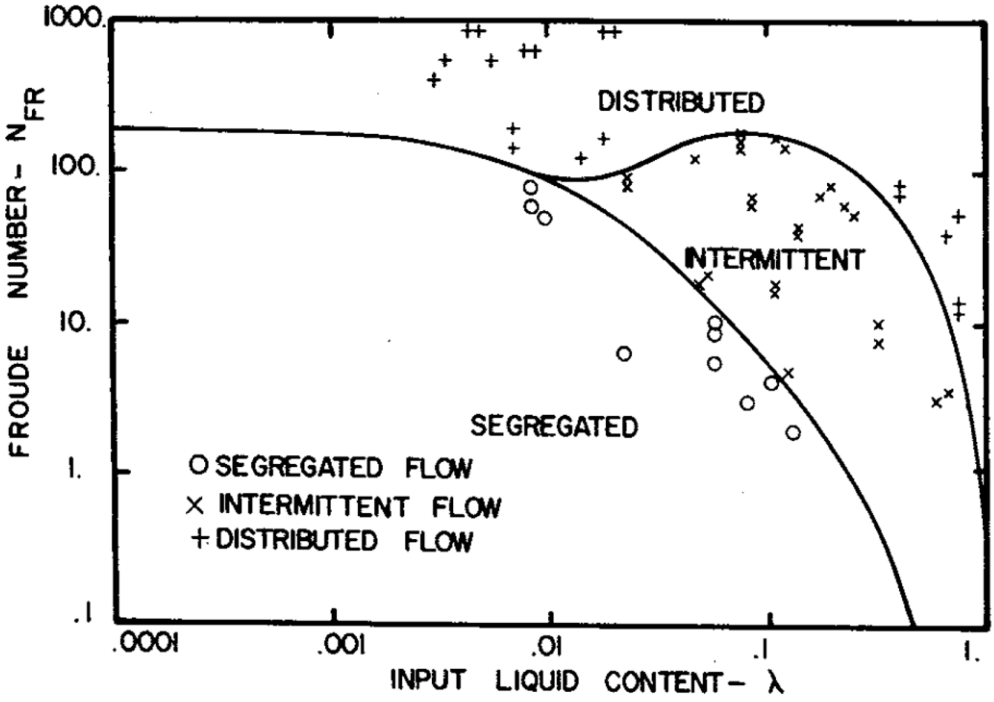

Figure 4.3 - Flow Pattern Map (Beggs & Brill, 1973)

Distributed Flow

In the two-phase flow regime, a distributed flow is described by dispersed, discrete and nearly spherical bubbles of varying size, but much smaller than the diameter of the flow conduit itself (Thome, 2007). Depending on the gas/liquid ratio, the dispersed fluid or continuous phase may consist of either gas or oil. It can be observed on figure 4.2 that for a flow where the liquid input content is close to one, the flow will be distributed, even for very small Froude numbers. For very high Froude numbers the flow will be distributed as well, independent on the liquid input content.

For the particular situation described in this work, the liquid input content will be one until the pressure is reduced to below the bubble point pressure. At this point the liquid input will be high, and the associated gas will be distributed in the oil fraction. In the upper parts of the well the pressure is low, flow velocity high, and the flow consists mainly of gas. Under these conditions the flow may be distributed as well, but then the gas will make up

the continuous phase, and tiny droplets of oil will be distributed in the gas phase. This flow is referred to as mist flow (Thome, 2007).

Intermittent Flow

As the pressure is reduced, the gas void fraction will increase. The proximity of the gas bubbles will increase as well, and the bubbles will start to collide and coalesce. This will form larger bubbles, with diameters approaching the diameter of the flow conduit. These bubbles of gas have a similar shape as a bullet, and are referred to as Taylor bubbles. The Taylor bubbles are typically separated by slugs of liquid, which again contain smaller distributed gas bubbles (Thome, 2007).

Segregated Flow

In a vertical pipe, segregated flow does not develop as easily as in a horizontal pipe. Segregated flow can be described as stratified flow, wavy flow or annular flow. All of which can develop in a horizontal pipe. The latter is the only segregated flow pattern that develops in a vertical pipe (Beggs and Brill, 1973).

Annular flow develops if the gas velocity becomes so high that the interfacial shear forces between the two phases overcomes the forces from gravity, and the liquid is expelled from the center of the pipe. Gas flow will occur in the center of the pipe, while the liquid flows as a film on the pipe walls and as distributed droplets in the gas phase (Thome, 2007).

Figure 4.4 shows how the flow regime would develop in a vertical pipe, for a hydrocarbon mixture that is liquid at reservoir conditions, and gas at surface conditions.

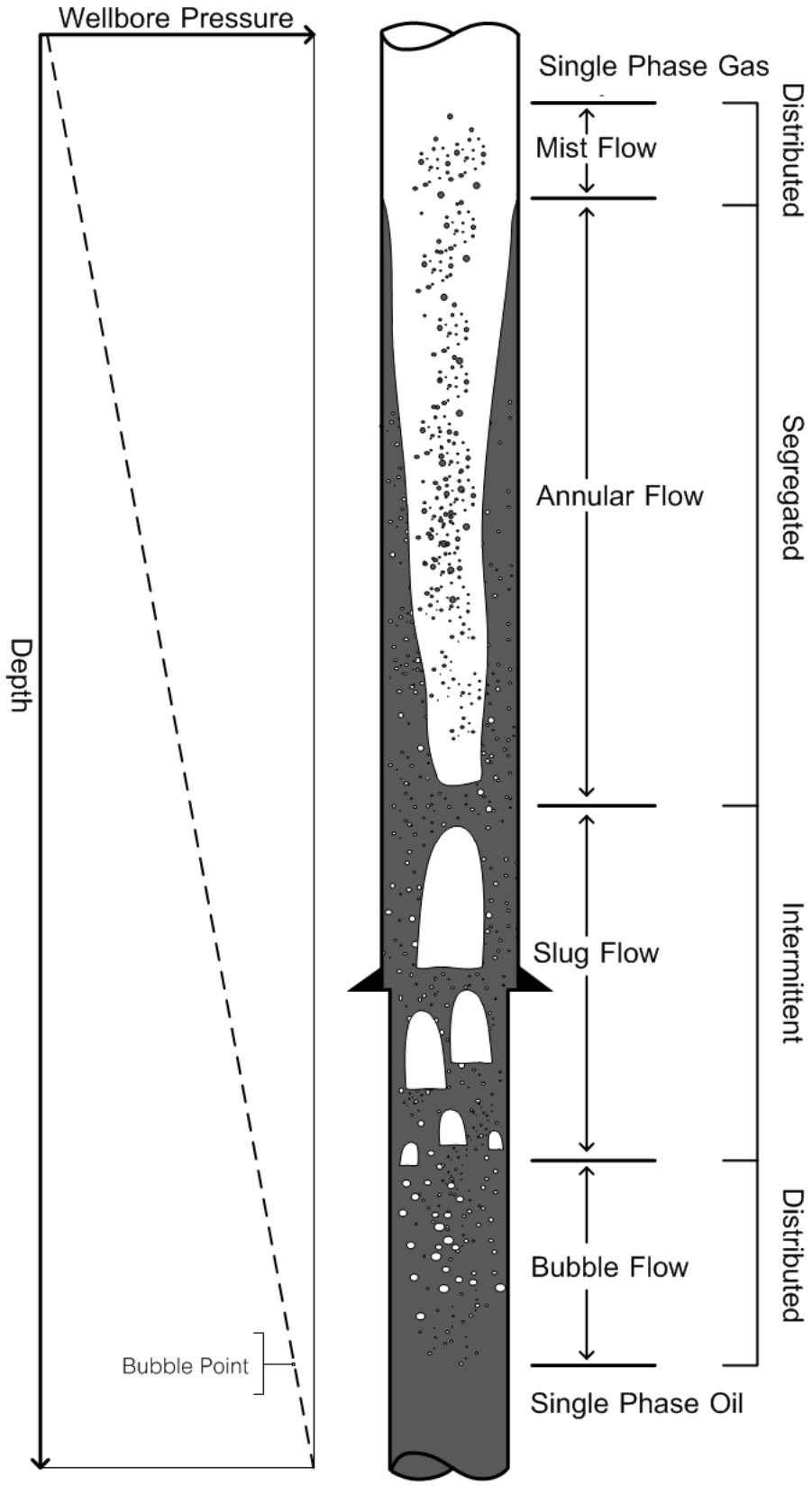

Figure 4.4 – Development of flow pattern

4.2.5 Simulating Seawater Injection through Relief Well

The purpose of the relief well is to introduce a high enough frictional- and hydrostatic pressure in the wellbore, to balance the pressure at the point of inflow. When a positive pressure differential exists between the wellbore and the blowing formation, the potential for inflow will not exists.

The introduction of another fluid, in this context seawater, will change several parameters in the blowing wellbore. First of all, the injected seawater will have a cooler temperature than the fluids originating from the reservoir. Hence, the well stream is cooled down from the injection point and upwards. This will change the viscosity, position of first boil out of gas and density of the reservoir fluids. Further, the mixture properties will change, since the seawater has different properties than the reservoir fluids.

The largest change during the killing operation is however the change in hydrostatic- and frictional pressure drop caused by the change in wellbore fluid density and volumetric flow rate.

Three Phase Flow

Oil and water can be considered immiscible fluids, and will not readily mix together. The effective liquid viscosity will depend on what phase is continuous in the particular section of the well. The continuous phase is determined by predicting an inversion point, where the continuous liquid changes from oil to water. This is dependent on the interfacial chemistry of the immiscible fluid mixture, and is best predicted through experimental measurements (Hall, 2010).

Because of the lack of methods to determine the inversion point theoretically, it was chosen to set this as an input parameter (Hall, 2010). This will have an effect on the blowout rates as the injection rate is increased, but not on the final injection rate required to dynamically kill the well. In this situation, the flow consists of seawater only, and is therefore a one-phase flow regime. The inversion point of water/light-oil mixtures generally happens between 40 and 60% water liquid ratio (Falcone et al., 2009). In the base case conditions the inversion point were set to a flowing fraction of 0.5.

A volume fraction average cannot be used to calculate the viscosity of the mixture of two immiscible fluids. This is because the effective viscosity of one fluid dispersed in another, will in practice be considerably higher than the viscosity of the pure liquids. Rather the equation suggested by Brinkman (1952) can be used. This equation shows accurate results for a dispersed water/oil-system, as well as a slug flow system (Hall, 2010).

$$\mu_{mixture,Brinkman} = \mu_c \frac{1}{(1-\varphi)^{2.5}} \tag{4.56}$$

Where μ_c is the viscosity of the continuous phase, and φ is the fraction of the non-continuous phase.

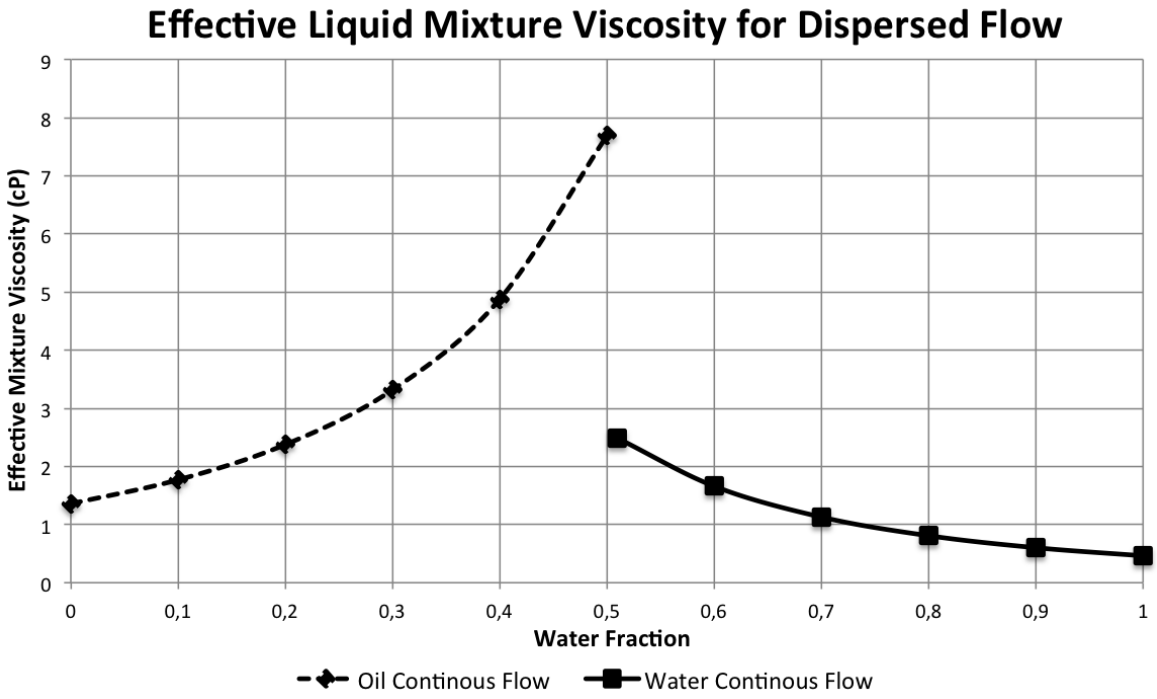

Graph 4.21 – Effective liquid mixture viscosity

Graph 4.21 shows how the mixture viscosity changes for different liquid fractions, for an inversion point of 0.5. At a water fraction of zero, the mixture viscosity is equal to the viscosity of the pure oil. As the concentration of water bubbles in the oil phase increase, the effective mixture viscosity increase as well. As the inversion point is reached, the dispersed water bubbles coalesce and water forms the continuous phase. As the concentration of dispersed oil bubbles decrease, the mixture viscosity is decreased towards the viscosity of pure water.

Change in Temperature Profile

In the MATLAB-model, the temperature profile of the blowing well is changed to account for the injection of a cooler fluid, with a different specific heat transfer coefficient. Depending on the injection depth, the temperature from that point and upwards will be affected.

The temperature at the kill point is calculated by a weighted average based on the temperature and rate of the injected seawater and reservoir fluids, at the point of intersection, according to equation 4.57.

$$T_{kill\ point} = T_i \frac{m_i}{m_i + m_r} + T_r \frac{m_r}{m_i + m_r} \tag{4.57}$$

Where T_i and T_r is the in-situ temperature of the fluid from the relief well, and reservoir, respectively. While m_i is the mass rate of injected seawater, and m_r the mass rate of reservoir fluid.

The new specific heat capacity of the mixture is calculated in the same manner, according to equation 4.58.

$$C_{p,mixture} = C_{p,i} \frac{m_i}{m_i + m_r} + C_{p,r} \frac{m_r}{m_i + m_r} \tag{4.58}$$

Density of Dynamic Killing Fluid

The injected seawater is never heated close to boiling point for the elevated pressures in the wellbore system, and hence behaves like an inert liquid with respect to density calculations. Water is highly incompressible, but the density of the relief well injection fluid is dependent on temperature, pressure and salt concentration. Graph 4.22 describes the density of pure water for different pressure, assuming a constant flowing temperature according to the mixing of reservoir and injection water.

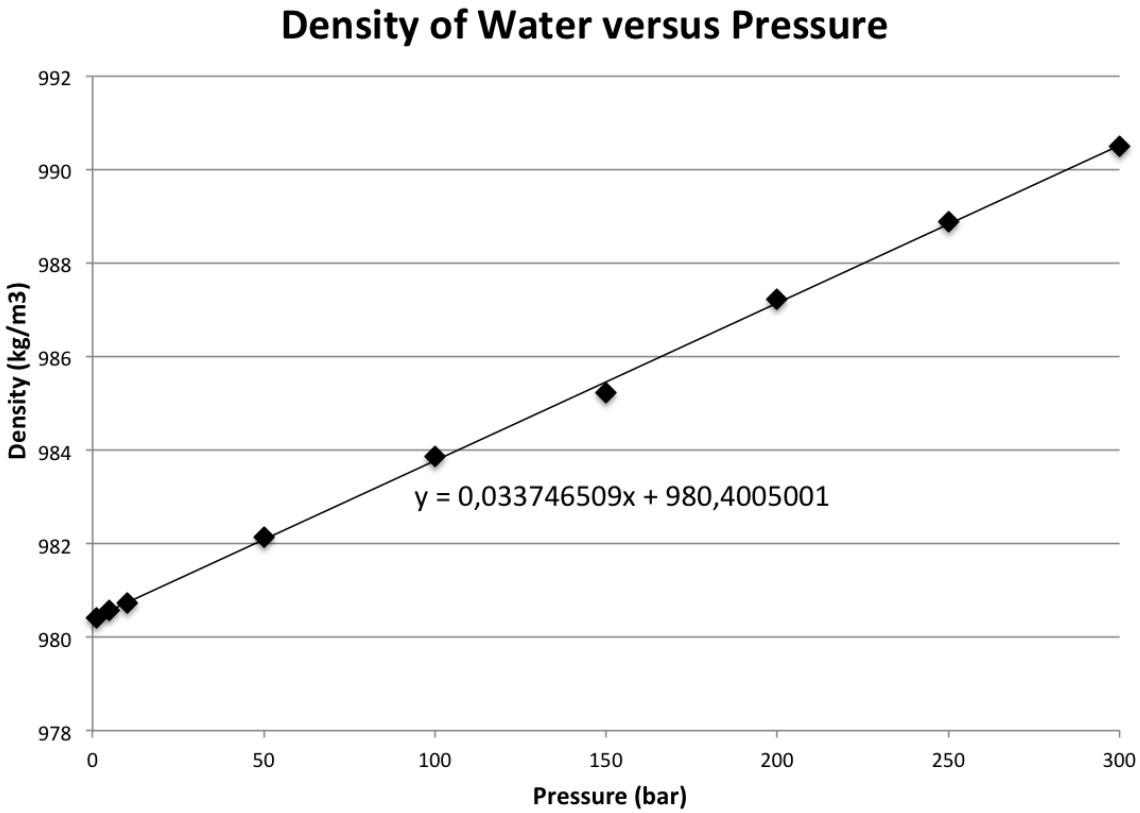

Graph 4.22 – Effect of pressure change on water density

To account for the dissolved salt the density of water is adjusted according to equation 4.59.

$$\rho_{kill\ fluid} = \rho_{water}(p) + M_{salt} \tag{4.59}$$

The injected water will change the density of the liquid phase according to equation 4.60, and is independent on flow regime (Hall, 2010).

$$\rho_{mixture} = \rho_{oil}\frac{V_{oil}}{V_{tot}} + \rho_{kill\ fluid}\frac{V_{kill\ fluid}}{V_{tot}} \tag{4.60}$$

4.3 Blowout Simulation Results

Under the given base case parameters, a blowout rate of 524 l/s at reservoir conditions was calculated. At standard conditions this corresponds to a blowout rate of 0.71 MSm^3/d of gas and 4377 Sm^3/d of crude oil. As a reference, the Macondo blowout in the Gulf of Mexico had an estimated blowout rate of 5500 to 9500 Sm^3/d of crude oil, according to the Flow Rate Technical Group (CNN, 2010).

Under these conditions the fluids in the wellbore exerts a hydrostatic pressure of 99 bar on the blowing formation. The high flow rate causes a frictional pressure loss, from the reservoir and up to the wellhead, of 286 bar. Hence, the pressure at the wellhead is 15 bar, and because of the particular water depth, the pressure at the wellhead is balanced. Graph 4.23 shows the wellbore pressure. The depth is from the wellhead. In the next section critical parameters that govern the blowout rate will be investigated further.

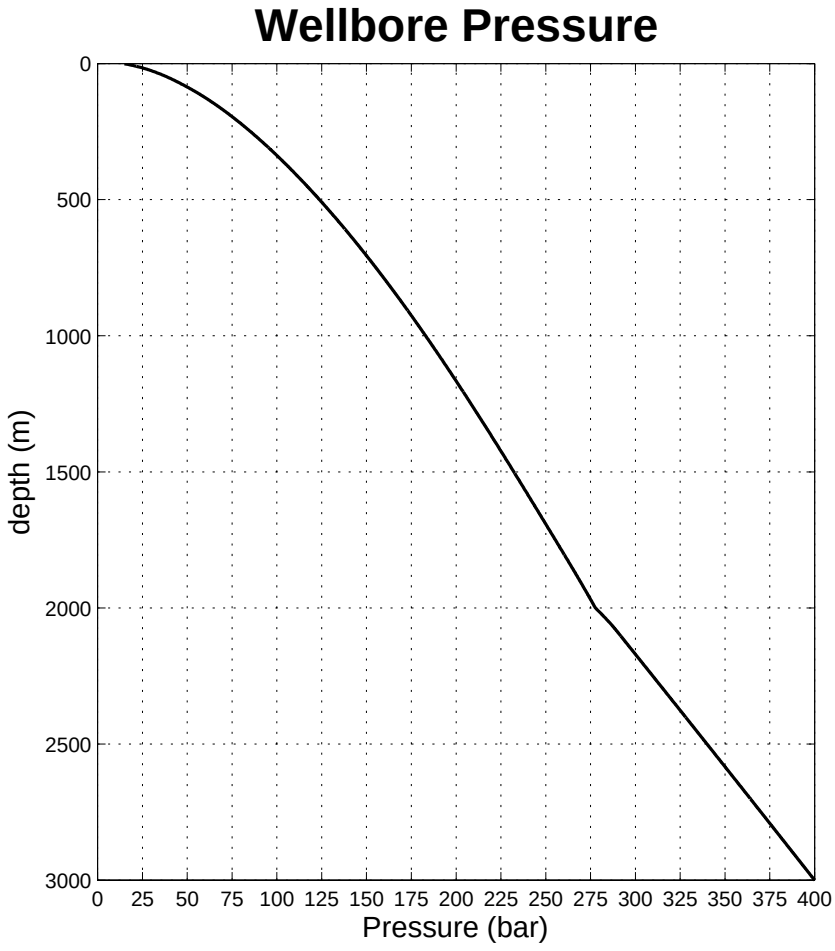

Graph 4.23 – Wellbore pressure during blowout

4.3.1 Investigation of Critical Aspects of Blowout Simulation

Flow Velocity

The velocity affects both the frictional- and the hydrostatic pressure loss in the well. Firstly, the frictional pressure loss is proportional to the square of velocity. Secondly, the flow velocity will also govern the flow regime, and hence the liquid hold-up. Since the liquid hold-up can change the effective density of the fluid, the flow velocity will also affect hydrostatic pressure loss. Graph 4.24 shows the velocity profile for the entire well, under the base case conditions.

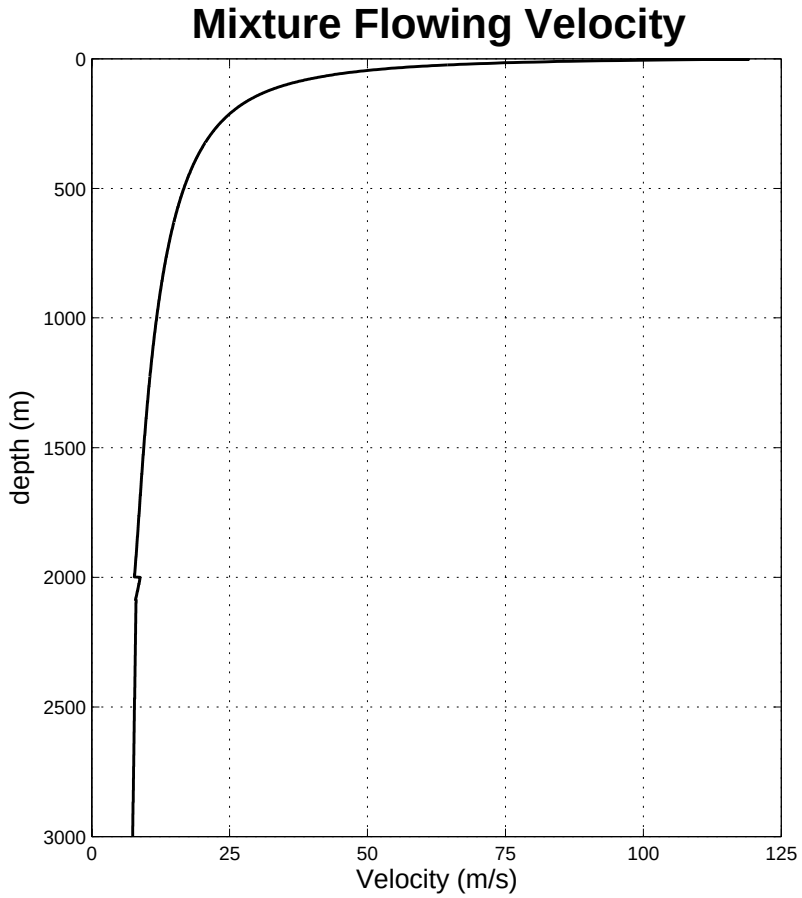

Graph 4.24 – Wellbore velocity during blowout

The fluid enters the two-phase region at a depth of 2087 meters. Below this point the flow is of one phase, and the velocity only increases slightly because of the compressibility of the liquid. Beyond the point of first gas boil out, the velocity rises faster because of the increased volumetric flow. At 2000 meters a small drop in the velocity can be observed, this is caused by the flow moving into the cased interval, where the flow area is slightly larger. The low pressures at the upper parts of the well cause an exponential increase in fluid velocity. At the wellhead the flow velocity is 119 m/s.

Friction Factor

Graph 4.25 shows the friction factor for the blowing well. The no-slip friction factor is calculated with the Chen equation (1979), and does not account for the gas slippage in the well. The two-phase friction factor is calculated according to the Beggs and Brill method (1973), and accounts for the gas slippage by calculating the liquid hold-up. The two-phase friction factor is used throughout the simulation.

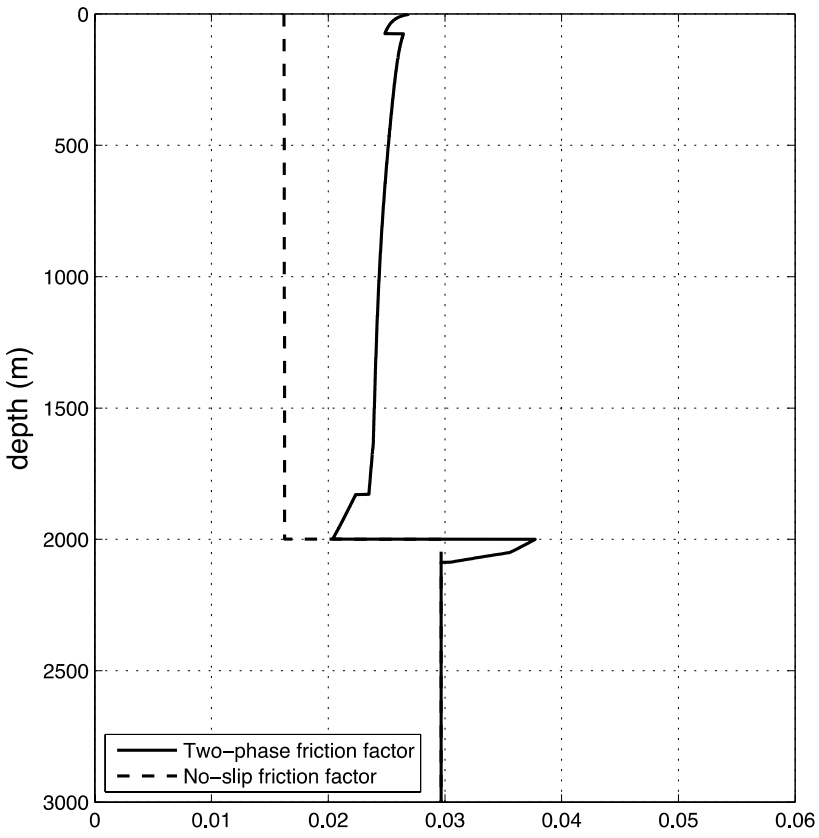

Graph 4.25 – Friction factor during blowout

In the one-phase flow region, the no-slip- and two-phase friction factor is identical. The first boil out of gas starts at a depth of 2087 meters TVD. Initially the gas will be dispersed as tiny bubbles in the oil phase, causing the two-phase friction factor to increase dramatically. At 2000 meters depth, the flow moves into the cased section, where the roughness is ten times smaller, causing the friction factor to be reduced to almost half of the value in the openhole section. Beyond this point the no-slip friction factor remains fairly constant, at the upper parts of the well the large increase in flow velocity and Reynolds number, causes the no-slip friction factor to be reduced slightly.

The two-phase friction factor behaves very differently compared to the no-slip friction factor, when gas is present in the wellbore. At a depth of 1829 meters TVD, the two-phase flow moves into an intermittent flow pattern. The initial large increase in the two-phase friction factor, as the liquid flowing fraction was reduced, is subdued. However, the two-phase friction factor increases steadily for the middle part of the well. At the upper parts of the well, the gas fraction and flow velocity causes an exponential growth in the two-phase friction factor. At a depth of 75 meters the flow pattern changes back to a dispersed flow, where tiny droplets of oil is distributed as a mist in the continuous gas phase, and the friction factor drops slightly.

The abrupt change in friction factor as the flow approaches all liquid, or all gas, is caused by equation 4.48 going into an unbounded area. According to Beggs and Brill (1973) another equation is used to describe the relationship between the no-slip and two-phase friction factor under these conditions.

Mixture Density

According to Beggs and Brill (1973), the liquid hold-up is accounted for in the hydrostatic pressure equation by adjusting the mixture density. When calculating friction pressure drop, the no-slip density is used, together with the adjusted two-phase friction factor.

Graph 4.26 shows the density adjusted for liquid holdup, the no-slip mixture density, the gas density, and the liquid density. In the one-phase region of the blowout, the density is reduced according to the compressibility of the oil mixture. As gas boils out the mixture density is reduced more dramatically. It can be observed that the liquid holdup is larger for a distributed flow regime, than for an intermittent flow regime. As the fraction of gas increases, the liquid holdup has a pronounce effect on the mixture density in the intermittent flow regime as well.

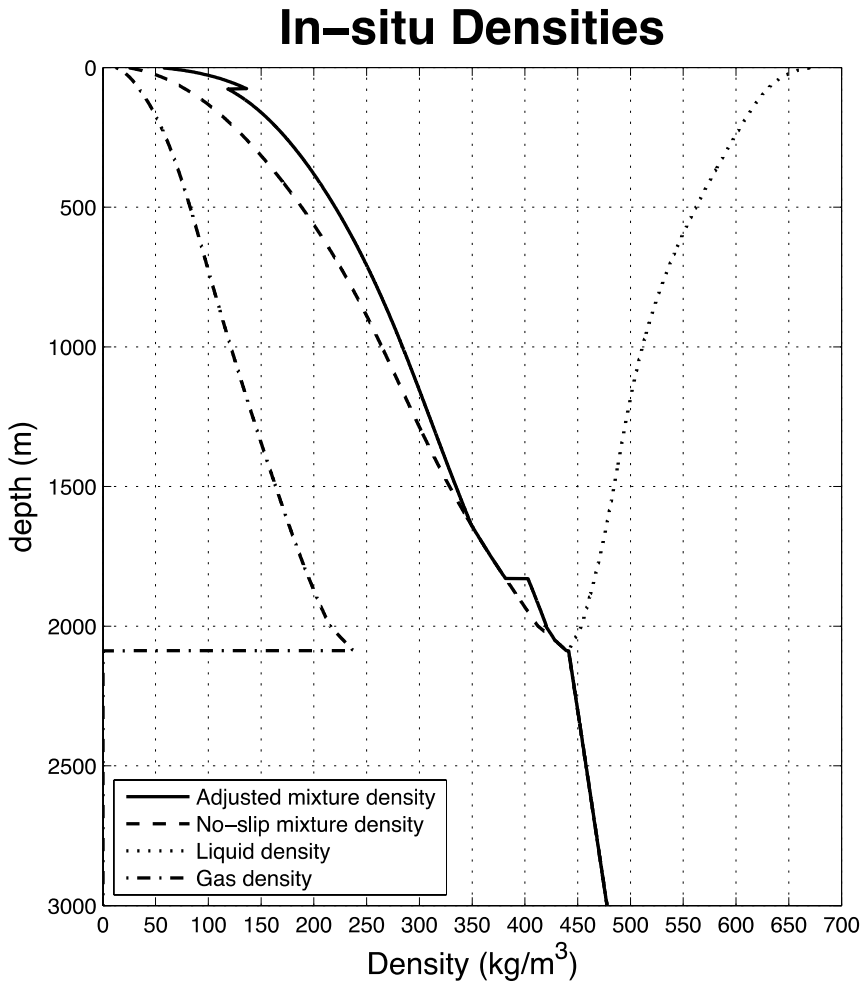

Graph 4.26 – In-situ densities during blowout

Viscosity

The viscosity has a large effect on the frictional pressure drop. Increased viscosity will reduce the Reynolds number, causing the frictional factor to increase. Since the hydrostatic pressure is adjusted for liquid hold-up, the viscosity might have an indirect effect on the hydrostatic pressure as well, since the viscosity will affect the frictional pressure drop, and hence the pressure regime in the well.

Graph 4.27 shows the effective viscosity of the two-phase mixture, as well as the viscosity of the gas- and liquid phase. It has a similar appearance to mixture density in that it is only affected by the compressibility of the oil in the one-phase region. As gas boils out, the mixture viscosity is reduced, since the gas has a lower viscosity than oil, at the given temperature and pressure.

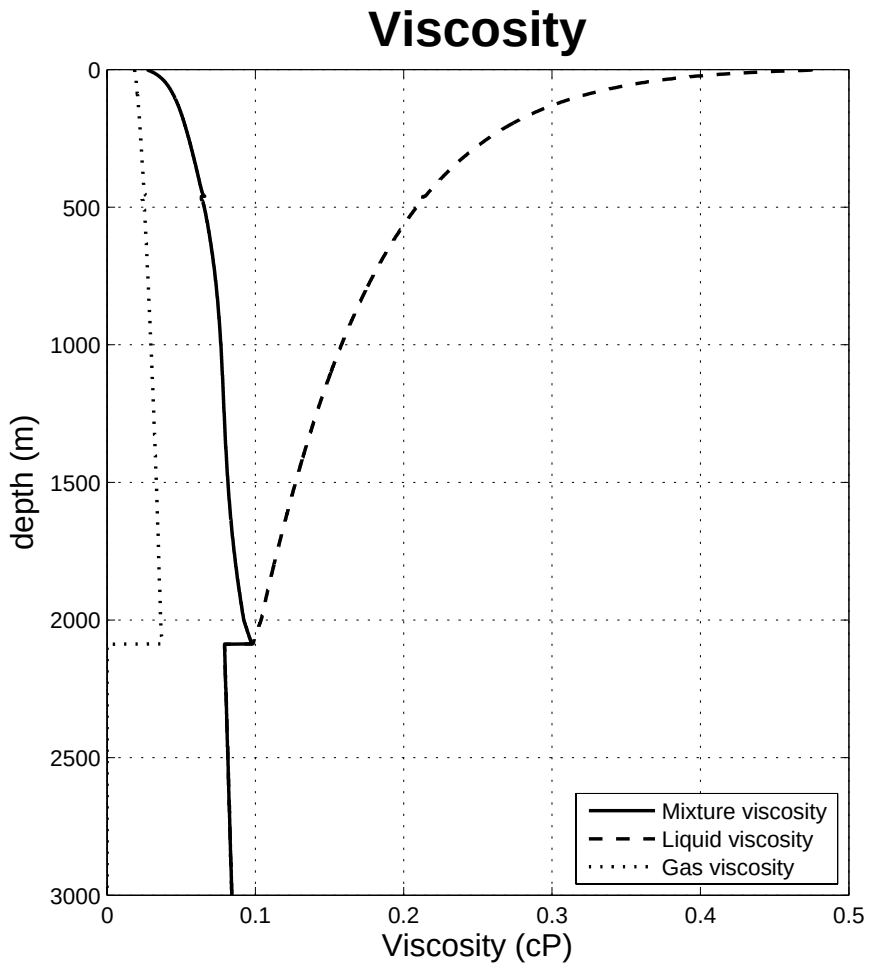

Graph 4.27 – Viscosity during blowout

Frictional Pressure Loss

The frictional pressure drop per unit length is, according to equation 4.55, dependent on the two-phase friction factor, no-slip mixture density, mixture velocity squared, and diameter of the flow area. The friction factor is dependent on flow regime, liquid holdup, viscosity, Reynolds number, surface tension, and relative roughness of the conduit walls.

Graph 4.28 shows the pressure drop per meter for the entire wellbore. The dotted line represents the pressure drop when liquid hold-up is not accounted for. By comparing the two graphs, the effect of flow regime and gas slippage becomes evident. It also underlines the importance of including liquid hold-up when performing calculations on two-phase flow.

For the one-phase region in the lower part of the well, the frictional pressure drop increases according to the compressibility of the oil. As the pressure is reduced, the volumetric flow rate is increased, and hence the velocity and frictional pressure drop increase as well. As gas starts to boil out, the interfacial shear forces between the two phases increases the frictional pressure drop.

The reduced roughness, and velocity, in the cased interval reduces the frictional pressure loss in this section. An exponential increase in the pressure drop caused by friction can be observed for the upper parts of the well. This is because of the increase in velocity and friction factor. It can be observed that the friction between the two flowing phases is less for a distributed flow pattern, and therefor the pressure drop is reduced as the flow moves in to mist flow in the top of the well.

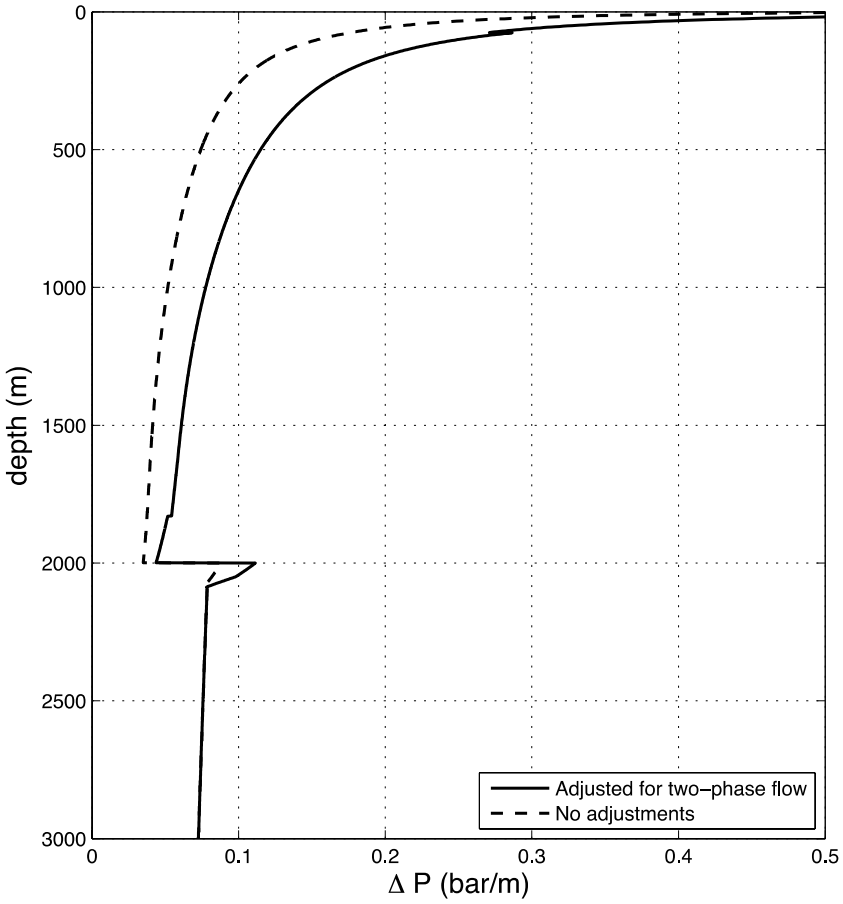

Graph 4.28 – Frictional pressure drop during blowout

Hydrostatic Pressure Loss

The hydrostatic pressure loss is dependent on the density of the fluid in the well, and will accordingly follow the mixture density. In addition to this, liquid hold-up will also affect the hydrostatic pressure loss, as it makes the effective density of the liquid higher. This can be observed as the flow moves into two-phase flow. The hydrostatic pressure loss that has been adjusted for liquid holdup increases, when compared to the pressure loss with no adjustments. When the gas bubbles is distributed in the liquid phase, the liquid holdup rises rapidly as more gas boils out. Once the flow moves into the intermittent flow pattern, liquid holdup is reduced. However, as more gas boils out, liquid holdup is experienced in the intermittent flow regime as well. At a depth of 75 meters from the wellhead, the high flow rates cause the liquid fraction to become distributed as a mist in the gas phase. This causes the liquid holdup to be increased further. Graph 4.29 shows the hydrostatic pressure loss throughout the blowing well.

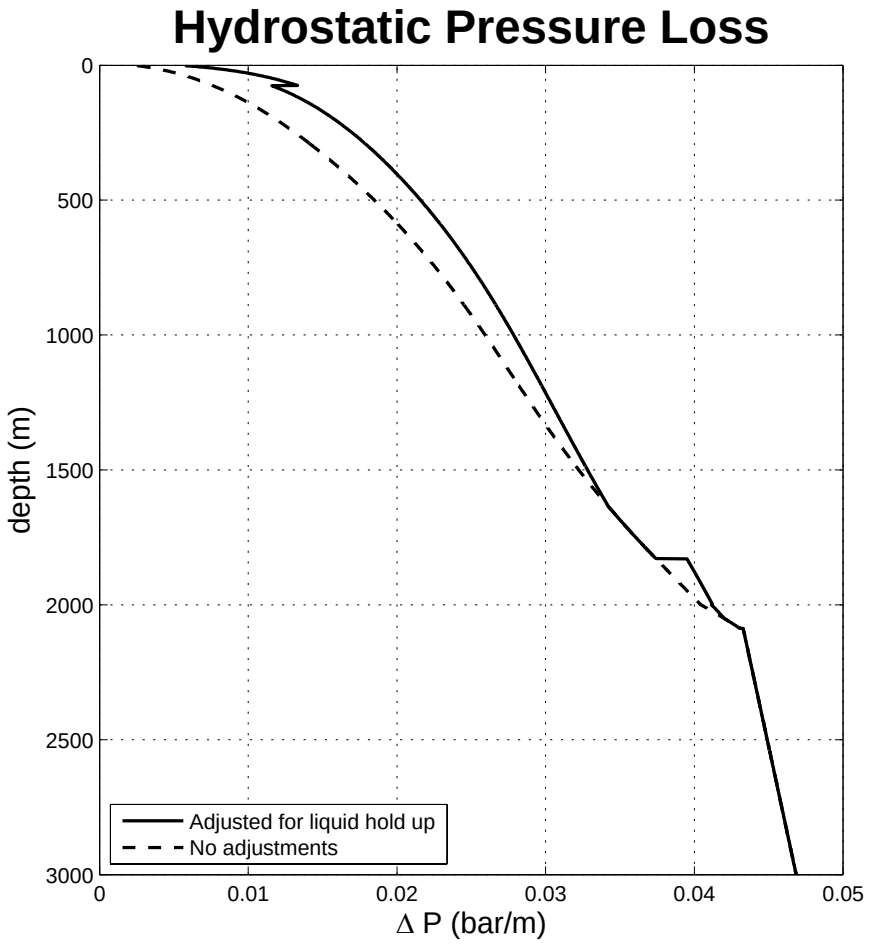

Graph 4.29 – Hydrostatic pressure loss during blowout

Wellbore Pressure against Pressure Loss

Graph 4.30 shows the wellbore pressure compared to pressure loss for the entire blowing well.

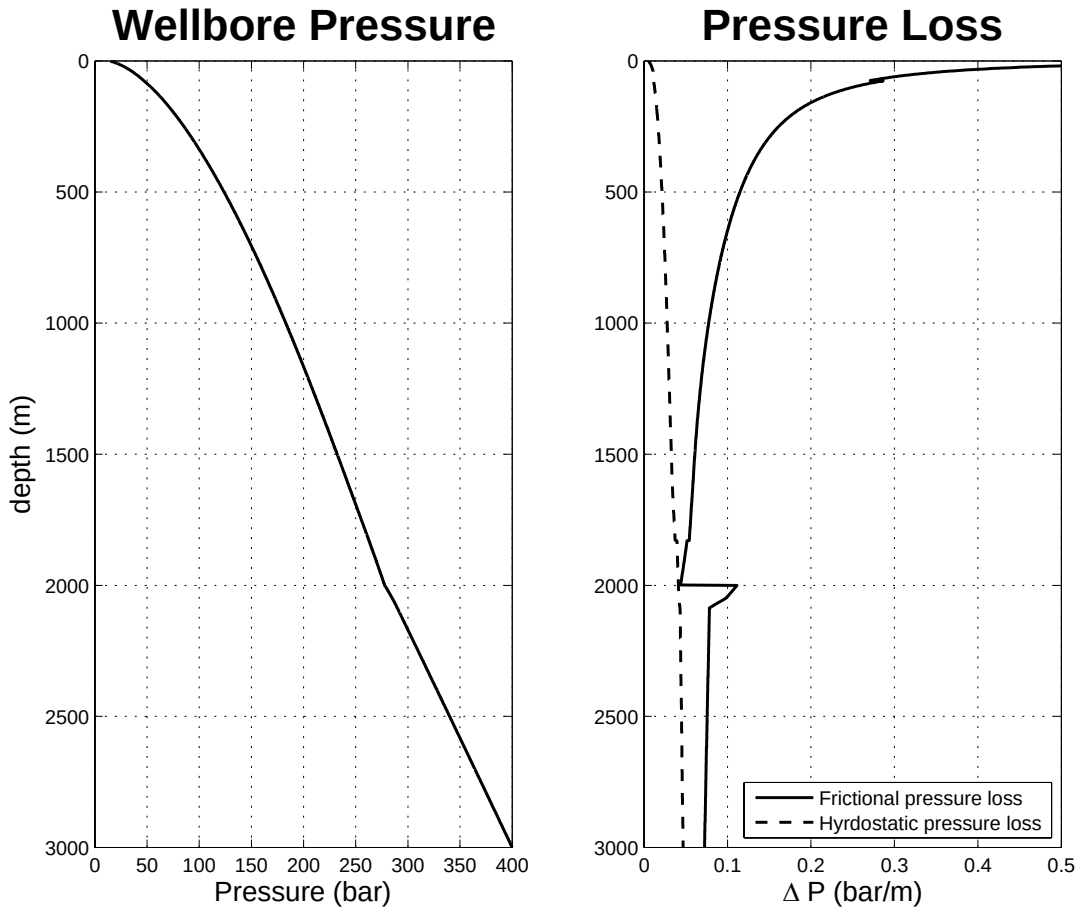

Graph 4.30 – Wellbore pressure against total pressure loss

The wellbore pressure can be divided into three distinct sections. First, the near linear pressure drop in the open-hole section, then the near linear pressure drop in the lower part of the cased section, and at last the exponential pressure drop in the upper parts of the cased section. By investigating graphs 4.24 through 4.29, it becomes evident why the pressure develops this way. The pressure drop in the open-hole section is higher than the pressure drop in the lower part of the cased section. This is caused by the smaller flow area, higher conduit wall roughness, and higher density of the flowing mixture. The frictional pressure loss starts to rise when more gas boils out of solution, but this increase is counteracted to some degree by a reduction in mixture density. Because of this, the pressure loss in the lower parts of the cased section is smaller than for the open-hole section. The exponential in pressure loss for the upper parts of the well, is caused by rapid gas boil out, creating high flow velocities and liquid holdup.

4.3.2 Sensitivity Analysis

The blowout rate will be highly dependent on the properties of the well. In this section different parameters will be changed to investigate how this affects the blowout-rate.

Wellbore Dimensions

The mixture velocity in the well is dependent on the volumetric flow rate and the cross sectional flow area. By changing the diameter of the casing or bit, the mixture velocity will change as well. This will have a large effect on the frictional pressure loss in the well. If the flow area of the well is reduced, while the volumetric flow rate is kept constant, the velocity will increase. This will cause the frictional pressure drop to increase as well, and the blowout rate will be reduced.

A well with larger dimensions will allow the blowout rate to increase to a greater magnitude before the frictional- and hydrostatic pressure will start to choke the inflow from the reservoir. These wells will also be more difficult to kill dynamically, as it requires a much greater volumetric flow rate of water to achieve the frictional pressure drop necessary to overbalance the reservoir pressure. Graph 4.31 shows the effect change in wellbore diameter has on the blowout-rate. Simulations were performed for 7-, 9 ⅝-, 13 ⅜- and 20-inch outer diameter casing. Halliburton's API Casing Chart (2012) was used to find the standard inside diameter of the casing, in addition to appropriate bit diameter for the openhole section.

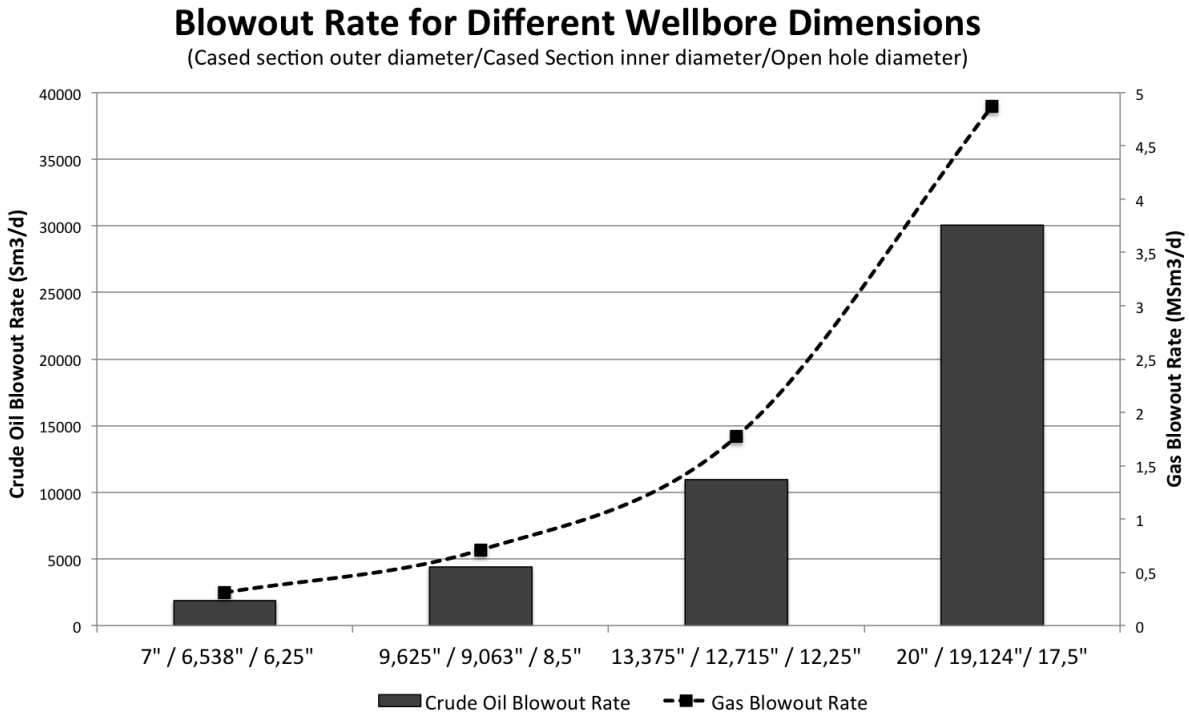

Graph 4.31 – Effect of wellbore dimensions on blowout rate

Wellbore Roughness

Particularly the openhole roughness can be difficult to estimate. It will be highly dependent on the particular formation being drilled, as well as the drilling parameters used. Wellbore washouts and formation breakouts can cause large local variations in roughness, and the formation of filter cake will change the roughness as well. By assuming that the formation being drilled can be compared to concrete, the absolute roughness would average at 0.5mm for smooth cement, and 0.8 to 3mm for rough cement (Pipeflow, 2013). Guo & Liu (2011) suggested, based on evaluation of core samples, that the absolute roughness of the wellbore walls could be compared to a coarse concrete road, with an absolute roughness of 0.06 to 0.12 inches (1.52 to 3.05mm). Extreme absolute roughness values of 0.3 inches (7.62mm) could be obtained as a result of extensive washouts when performing air drilling.

Because of the uncertainties in regards to openhole roughness, an absolute roughness of 1 mm was chosen for the base case simulation. This can be changed in the simulation model. Graph 4.32 shows how increased, or lowered, roughness values for the openhole section will affect the blowout rate.

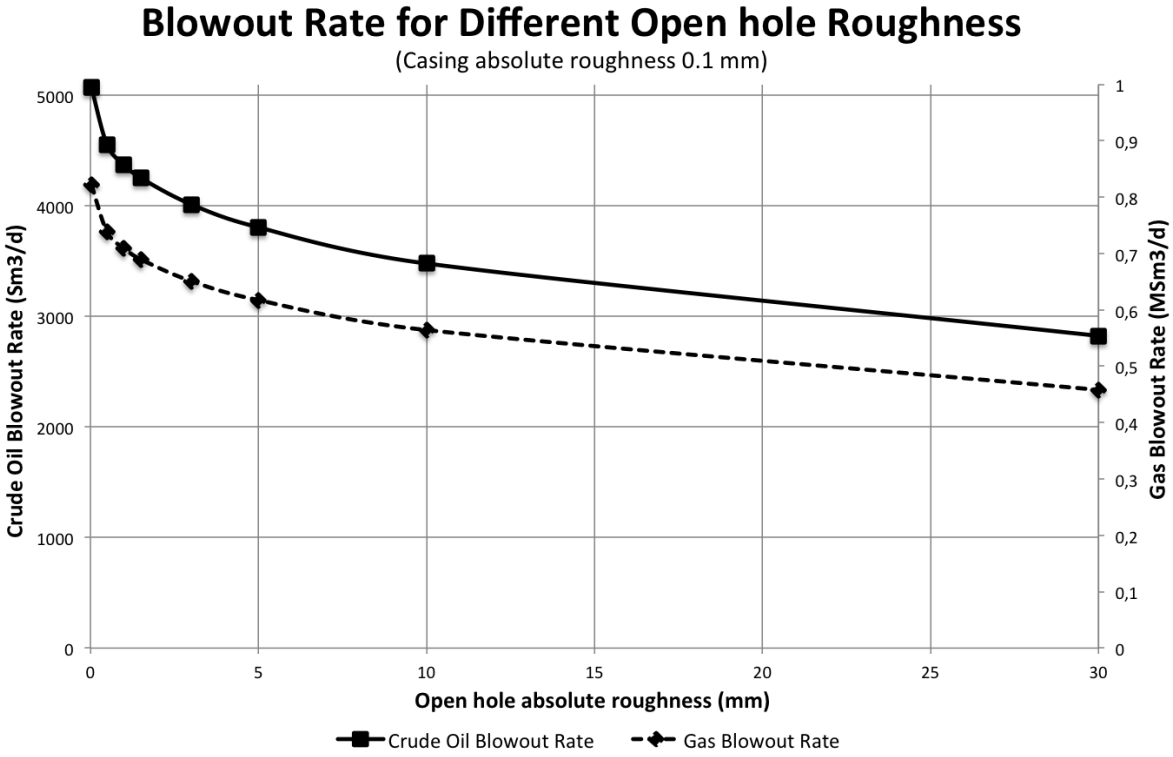

Graph 4.32 – Effect of openhole roughness on blowout rate

The roughness of the cased section is easier to determine, as it is made of a material with a relatively consistent roughness. Wrought iron shows an absolute roughness of 0.045 mm, while carbon steel has an absolute roughness of 0.02 to 0.05 mm. Corrosion and damage will increase this roughness. Moderately corroded carbon steel has an absolute roughness of 0.15 to 1 mm, while sandblasted cast iron has an absolute roughness of 1 mm. Badly corroded carbon steel can show an absolute roughness up to 3 mm (Pipeflow, 2013). The absolute roughness of drill pipe and casing, when tool joints and couplings are not considered, should be set to a minimal value of 0.05 mm (Guo & Liu, 2011).

Graph 4.33 shows the effect different roughness in the cased section has on the stabilized blowout rate.

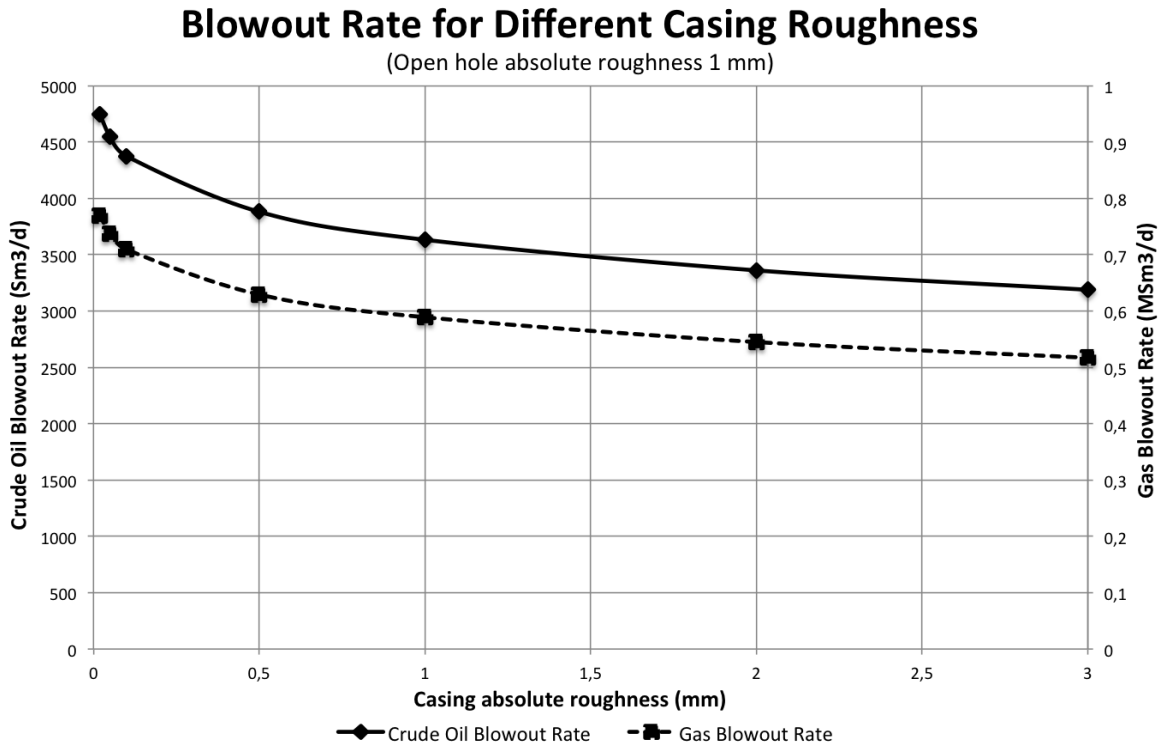

Graph 4.33 – Effect of casing roughness on blowout rate

Reservoir Pressure

The reservoir pressure is what gives energy to the blowout, and subsequently this parameter affects the blowout rate to a great extent. With the given base case conditions, a reservoir at normal pressure would contain 317 bar, assuming a water column consisting of incompressible salt water at 1025 kg/m^3. A reservoir with pressure below normal pressure would still have potential to flow, since the reservoir fluids often has a lower density than saltwater. However, a blowout would be improbable under these conditions. The reservoir pressure could certainly be of higher than normal pressure, and an unexpected high pressure could surely lead to a blowout.

Graph 4.34 displays the effect various reservoir pressures have on the blowout rate. The other parameters are kept according to the base case.

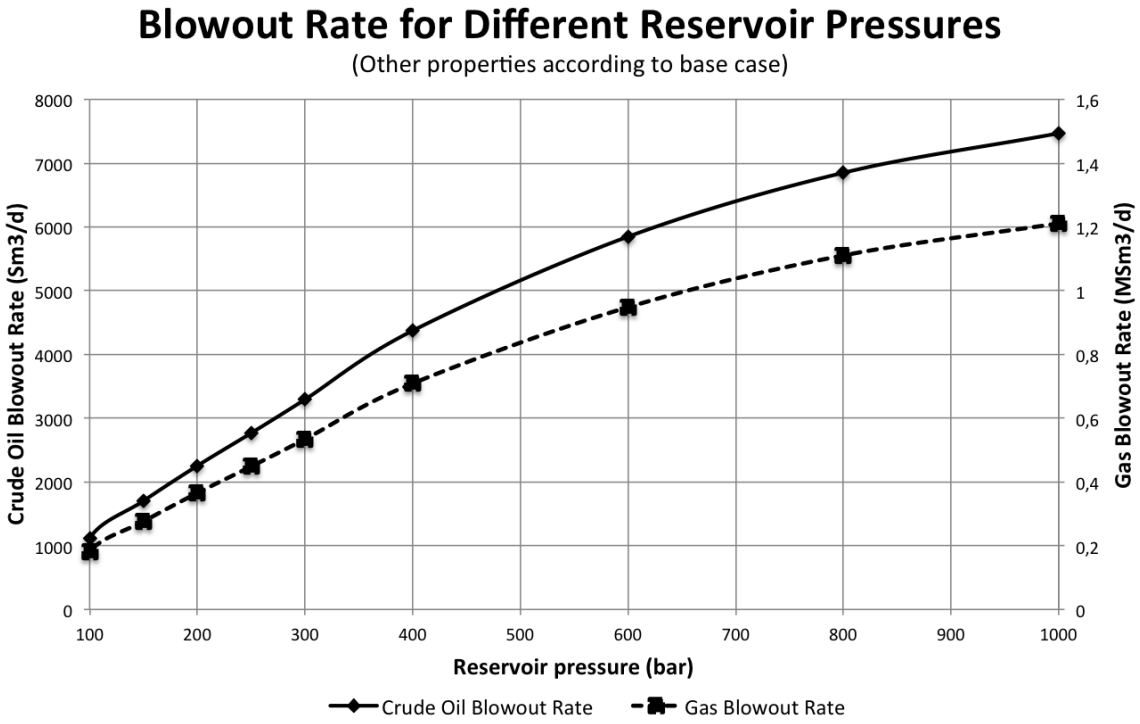

Graph 4.34 – Influence of reservoir pressure on blowout rate

As can be observed on graph 4.34, the reservoir pressure has a considerable effect on the blowout rate. By increasing the reservoir pressure, a larger pressure drop can be experienced in the blowing well to balance the pressure at the wellhead. It can be observed that the blowout has a potential to flow for very small reservoir pressures. This is because the reservoir fluid is relatively light, and applies a small hydrostatic pressure on the bottom of the well. The flow of gas also affects the hydrostatic pressure, and because of this the blowout simulation becomes unstable for very small reservoir pressures. This is because of the fact that at these low pressures, the gas that boils out immediately coalesce and form an

intermittent flow pattern in the MATLAB model. This intermittent flow creates a very high liquid hold-up. Because of the effect liquid hold-up has on hydrostatic pressure, the reservoir pressure is balanced by the hydrostatic pressure alone, and the flow dies down. Once the flow stops there is no liquid holdup, the bottomhole pressure is reduced, and the flow starts again.

Water Depth

Water depth will affect both hydrostatic- and frictional pressure drop. The water will effectively act as an additional pressure throughout the wellbore. This will suppress boil out of gas, causing the two-phase flow regime to start further up in the blowing well. In addition to this, the wellhead pressure will be increased. This means that the pressure drop along the well can be smaller for the pressure to be balanced at the wellhead.

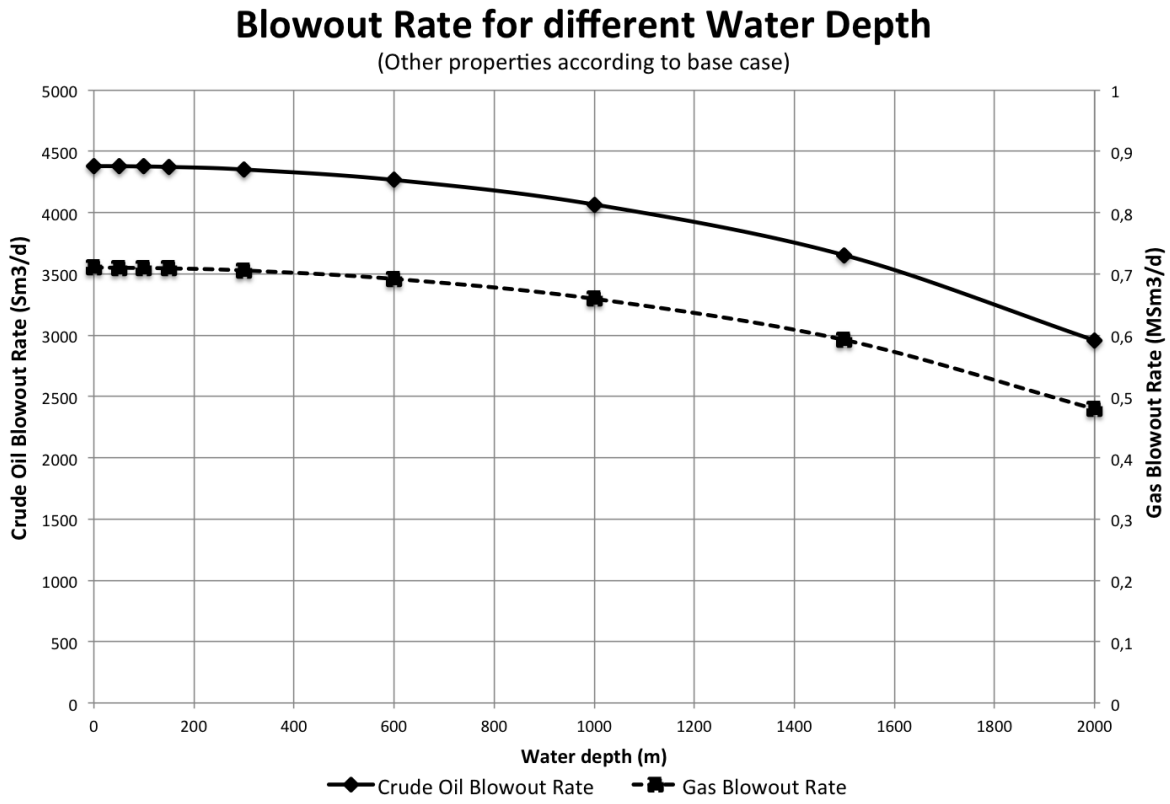

Graph 4.35 – Influence of water depth on blowout rate

Graph 4.35 shows how the blowout rate responds to change in water depth. In the MATLAB-model the water depth is adjusted by adjusting the wellhead pressure, according to the hydrostatic pressure that specific column of water would impose. The solid line represents the flow of crude oil, while the dotted line represents the gas flow, both at standard conditions.

4.4 Dynamic Kill Simulation Results

To investigate the benefits of a deeper intersection point when performing a dynamic killing operation, the blowout simulated in chapter 4.3 was dynamically killed by direct intersection at both the casing shoe and bottomhole, in the MATLAB program. Rates and pressures required will be compared to describe the benefits of this new method.

Graph 4.36 shows how the blowout rate will develop during the dynamic killing operation. To successfully kill the blowout, seawater must be injected at a rate of 151 l/s for bottomhole intersection, and 290 l/s for casing shoe intersection.

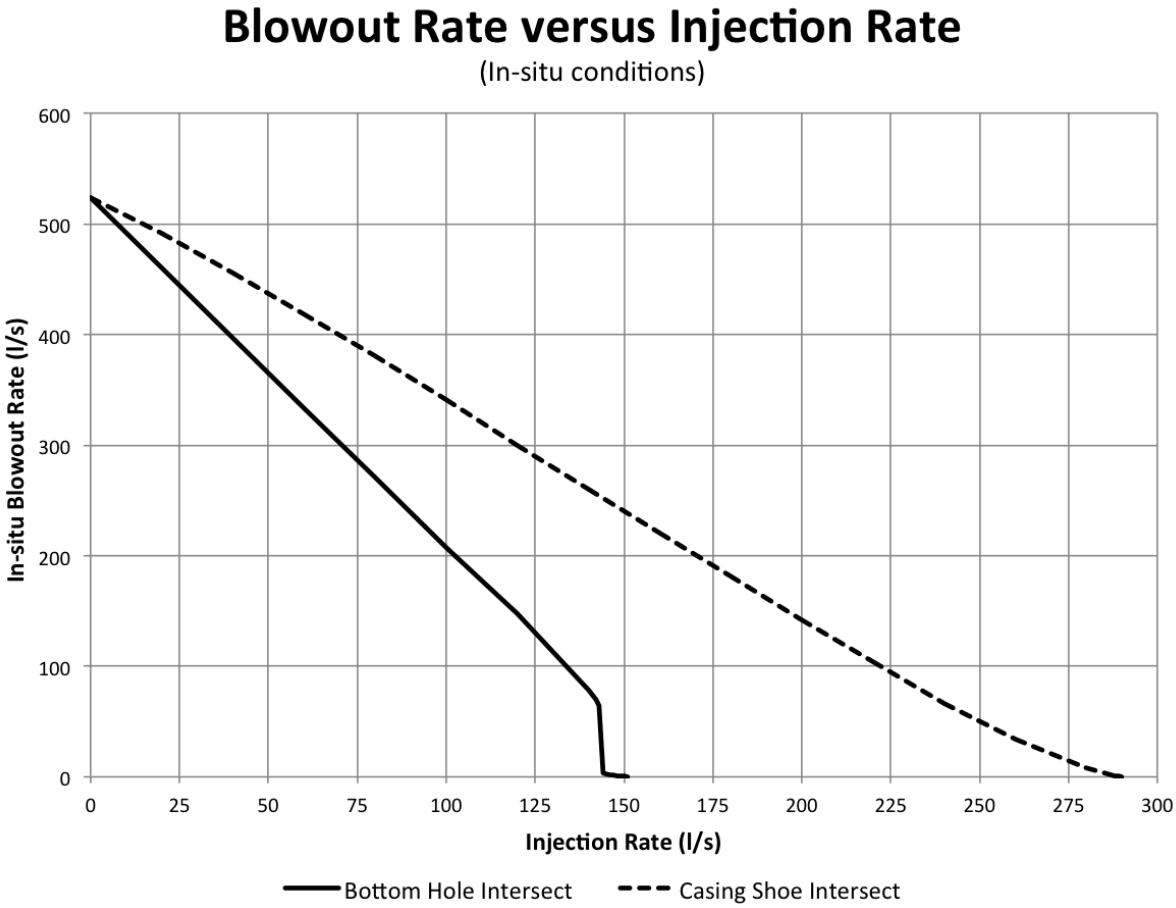

Graph 4.36 – Blowout rate for different relief well injection rates

At an injection rate of 143 l/s, the blowout rate during bottom intersection is suddenly reduced from 64.7 to 3.6 l/s. This is caused by a change in flow regime in the well. For higher blowout rates, the associated gas will first be distributed as tiny bubbles in the liquid phase, before the bubbles coalesce and form Taylor bubbles separated by liquid slugs. Once the blowout rate, mixture velocity and wellbore pressure reaches a certain value, the conditions to form Taylor bubbles does not exist, and the gas fraction remains distributed

for the entire length of the well. Liquid holdup is higher for a distributed flow pattern, and because of this, the hydrostatic pressure in the well is increased, increasing the bottomhole pressure as well. This causes a sudden drop in the blowout rate.

Frictional and Hydrostatic Pressure Loss

Graph 4.37 and 4.38 shows the frictional- and hydrostatic pressure loss for bottomhole- and casing shoe intersection, respectively. It can be observed that the hydrostatic pressure loss increases as a larger fraction of the flowing mixture consists of seawater. Once the blowout is killed, and the entire wellbore is displaced to seawater, the hydrostatic pressure remains constant, regardless of injection rate. As the hydrostatic pressure is increased, the flow from the reservoir is suppressed. This causes a decrease in mixture velocity, decreasing the frictional pressure loss as well.

The frictional pressure loss will increase if the injection rate is increased beyond the dynamic kill rate, as the seawater flowing velocity in the well is increased.

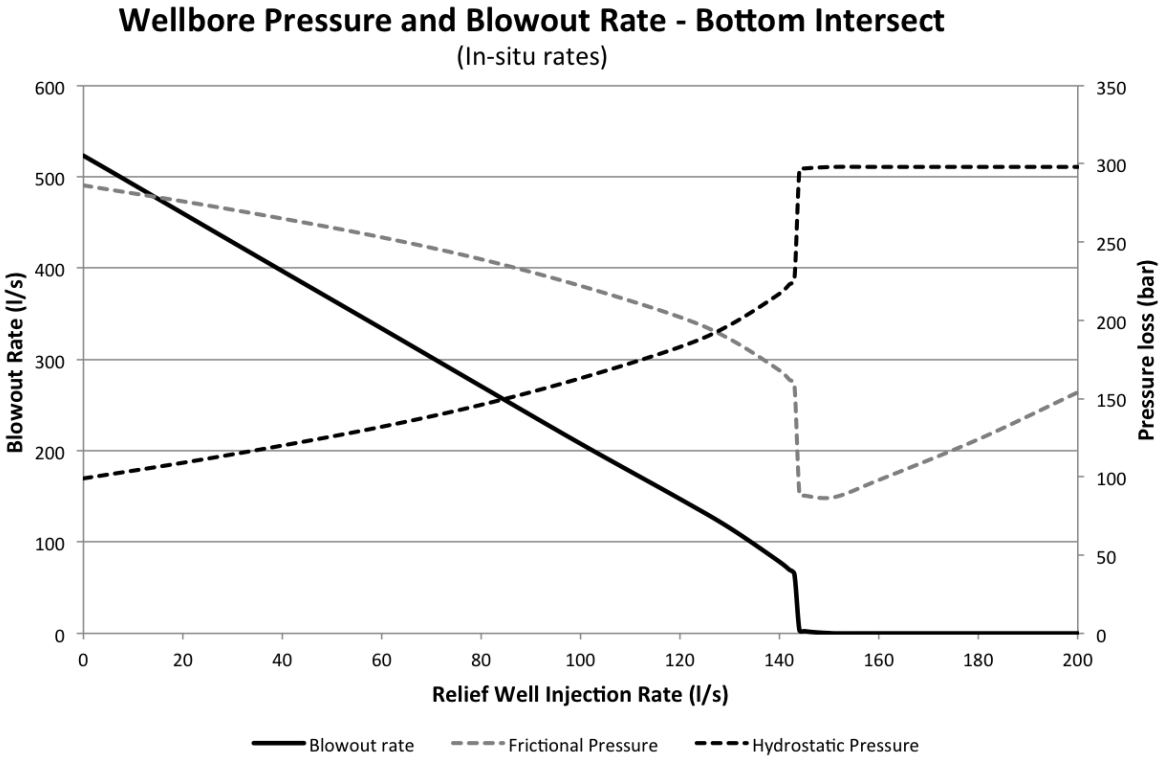

Graph 4.37 – Frictional and hydrostatic pressure loss, bottom intersect

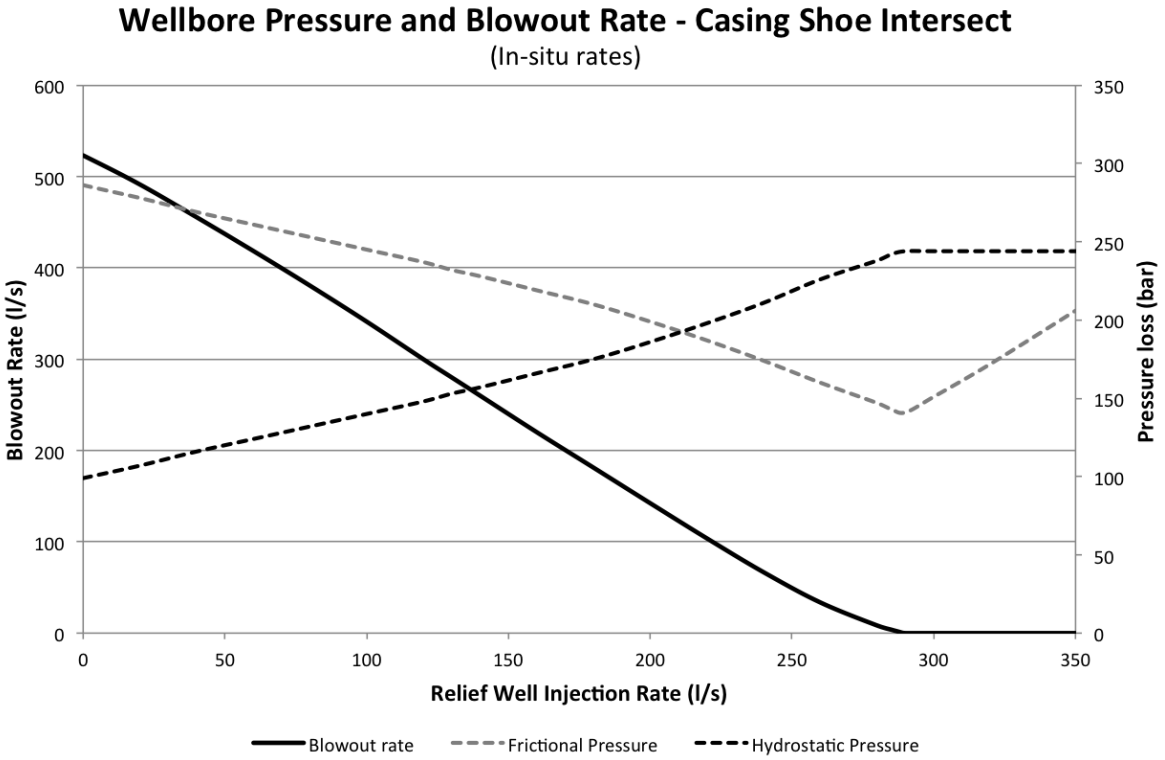

Graph 4.38 – Frictional and hydrostatic pressure loss, casing shoe intersect

4.4.1 Investigation of Critical Aspects of Dynamic Kill Simulation

In this section critical parameters will be investigated as the dynamic injection rate is increased.

Velocity

Graph 4.39 shows the mixture velocity versus depth, for different injection rates. Since seawater is heavier than the reservoir fluid used in this simulation, a lower wellbore velocity is needed to balance the bottomhole pressure once the water fraction increases. Hence, the overall velocity of the mixture is reduced, as the injection rate is increased. It can also be observed that the exponential increase in velocity for the upper parts of the well is subdued, as the flow from the reservoir is reduced. Once the well is killed dynamically, the fluid velocity is close to constant for the two sections of the well. For bottomhole intersection the final circulating velocity is approximately 4.1 m/s for the open-hole section, and 3.6 m/s for the cased section. A slight increase can be observed as the pressure is reduced, because of the small compressibility of water.

When intersecting the blowing well at the casing shoe, it can be observed that the flow beneath the casing shoe is reduced to zero when the blowout is killed. This means that there will be no frictional pressure loss in this section of the well. Final circulating velocity for casing shoe intersection is 0 m/s in the open-hole section, and 7 m/s in the cased section.

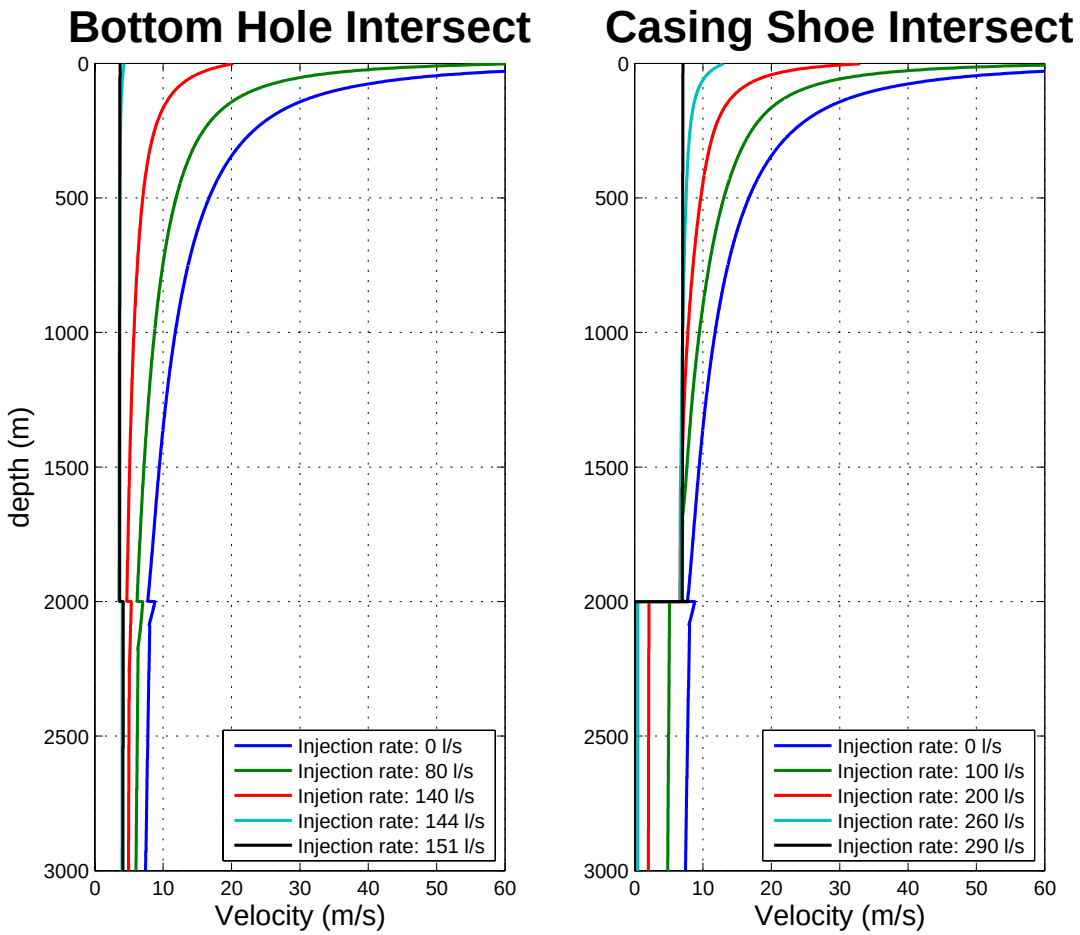

Graph 4.39 – Wellbore velocity

Frictional Pressure Loss

Graph 4.40 displays the frictional pressure loss throughout the well, for different injection rates. Generally, the friction pressure loss in the well is reduced as the injection rate is increased, because a lower frictional pressure is required when the well is filled with a denser fluid.

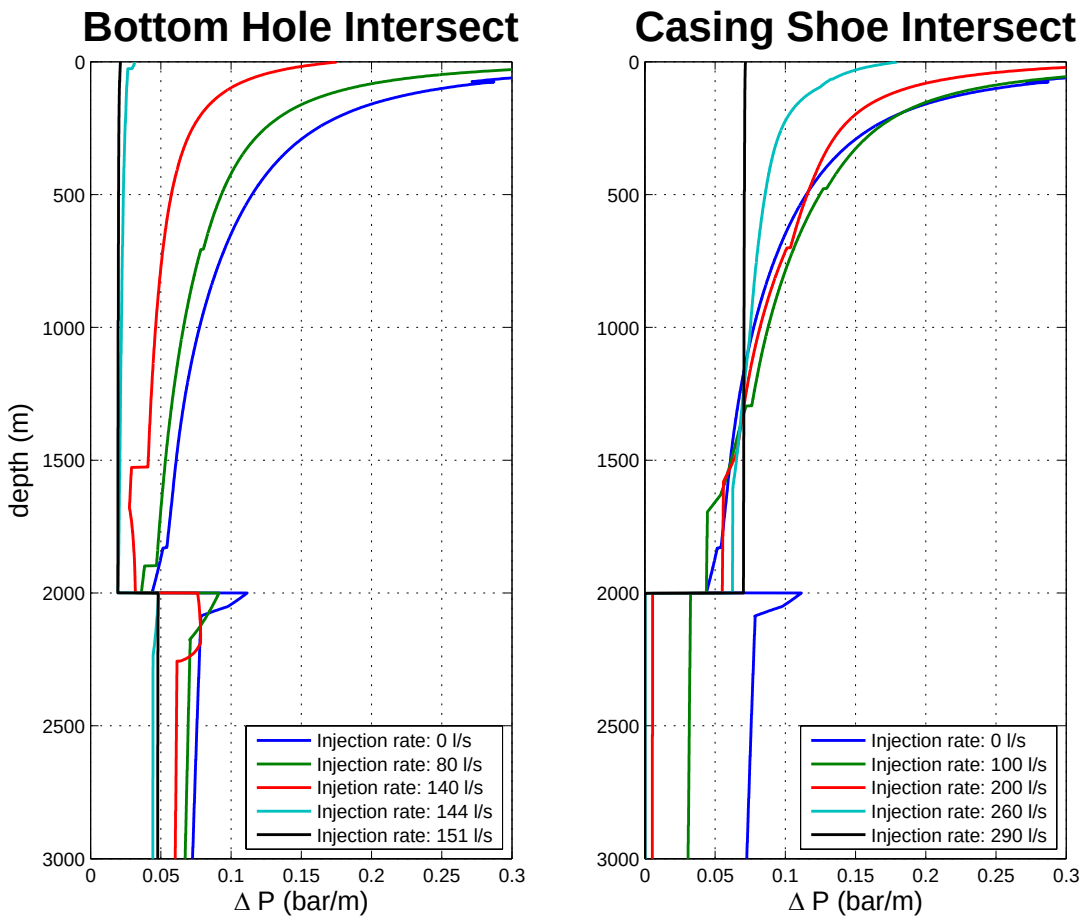

Graph 4.40 – Frictional pressure during dynamic killing operation

The frictional pressure loss follows the same shape for all injection rates, as long as gas is present in the well. The frictional pressure loss can be divided into four phases. In the first phase, the flow consists of liquid only. This is because the wellbore pressure is above the bubble point pressure. In this phase the frictional pressure drop only rises slightly because of the liquid expansion. The second phase starts when the first gas boils out. A sudden increase in frictional pressure drop can be seen. However, the frictional pressure drop smooth out as the fraction of gas is increased. The third phase starts when the gas bubbles, which once were distributed as tiny bubbles in the liquid phase, coalesce and form larger Taylor bubbles.

The friction pressure loss increases instantaneously as the flow enters into this flow pattern. In this phase the frictional pressure drop is more stable, and an exponential increase can be observed. The fourth phase only develops for certain conditions. The gas fraction has become so large, and the flow velocity so high, that the liquid will be distributed as small droplets in the continuous gas phase. This causes the frictional pressure loss to drop slightly.

During bottomhole intersection, the mixture density in the entire well is increased as the injection rate is increased. Hence the frictional pressure is reduced. When no water is injected into the bottom of the well, a large pressure drop is experienced in the upper parts of the well. When water is injected the pressure loss becomes more uniform, and the pressure loss in the lower parts of the well is increased. This causes the point of first boil out of gas to be progressively pushed further down in the well, as the injection rate is increased. Since the liquid input fraction is increased, the point where the flow transition into intermittent flow is pushed further up the well. When the well is dynamically killed the frictional pressure drop in the open-hole section is 0.048 bar/m, and 0.02 bar/m in the cased section.

Killing through intersection at the casing shoe behaves quite differently. As the relief well starts to circulate seawater from the casing shoe and up the blowing well, the flow beneath the casing shoe is gradually reduced. When the well is dynamically killed, there is no flow beneath the casing shoe. This causes the frictional pressure drop in the open-hole section to be reduced. The point of first boil out of gas is pushed further up the well, as is the point of transition into intermittent flow. Once the well has been killed dynamically, a frictional pressure drop of 0.07 bar/m is experienced in the cased section.

Hydrostatic Pressure Loss

Hydrostatic pressure loss is dependent on mixture density and liquid holdup. Graph 4.41 displays the hydrostatic pressure loss throughout the blowing well, for both bottomhole- and casing shoe intersection. In both cases it can be observed that the hydrostatic pressure loss is increased, as a larger fraction of the flowing liquid consists of seawater. Once the well is dynamically killed, the part of the wellbore that is occupied by seawater shows an almost constant hydrostatic pressure loss of 0.1 bar/m.

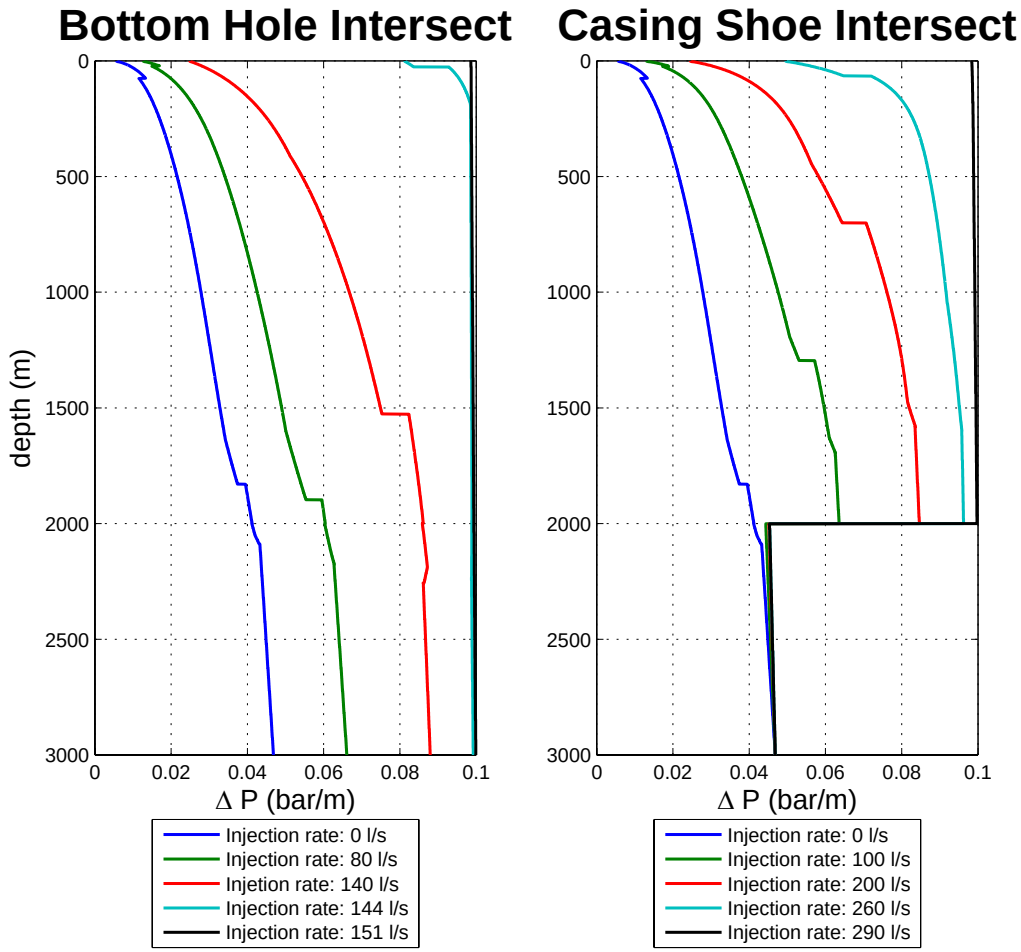

Graph 4.41 – Hydrostatic pressure during dynamic killing operation

Wellbore Pressure Profile

Bottomhole Intersection

Graph 4.42 shows the pressure profile for the blowing well, during injection of seawater through a relief well that intersects the blowing well at the bottom of the open-hole section.

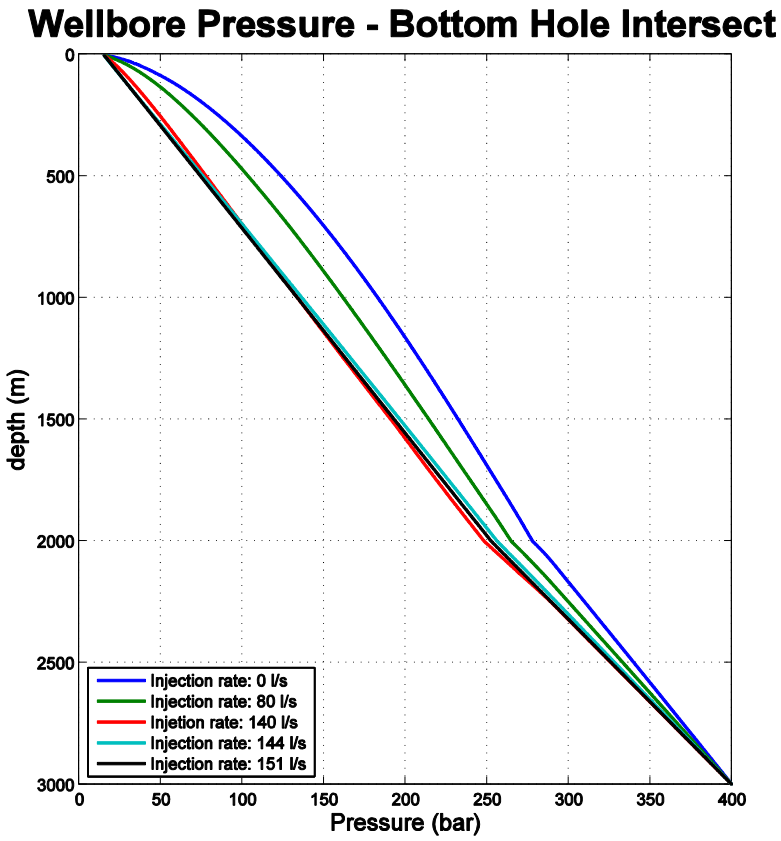

Graph 4.42 – Wellbore pressure during dynamic killing operation with bottomhole intersect

It can be observed that the pressure when the well is dynamically killed almost forms a straight line from the reservoir and up to the surface. The friction pressure loss will be slightly higher in the open-hole section, since the roughness is higher.

Casing Shoe Intersection

Graph 4.43 shows the pressure profile when the blowing well is intersected at the casing shoe. It is different compared to the case with bottom intersect, in that the pressure is reduced very little in the bottomhole section. To compensate, the pressure loss must be higher in the cased section.

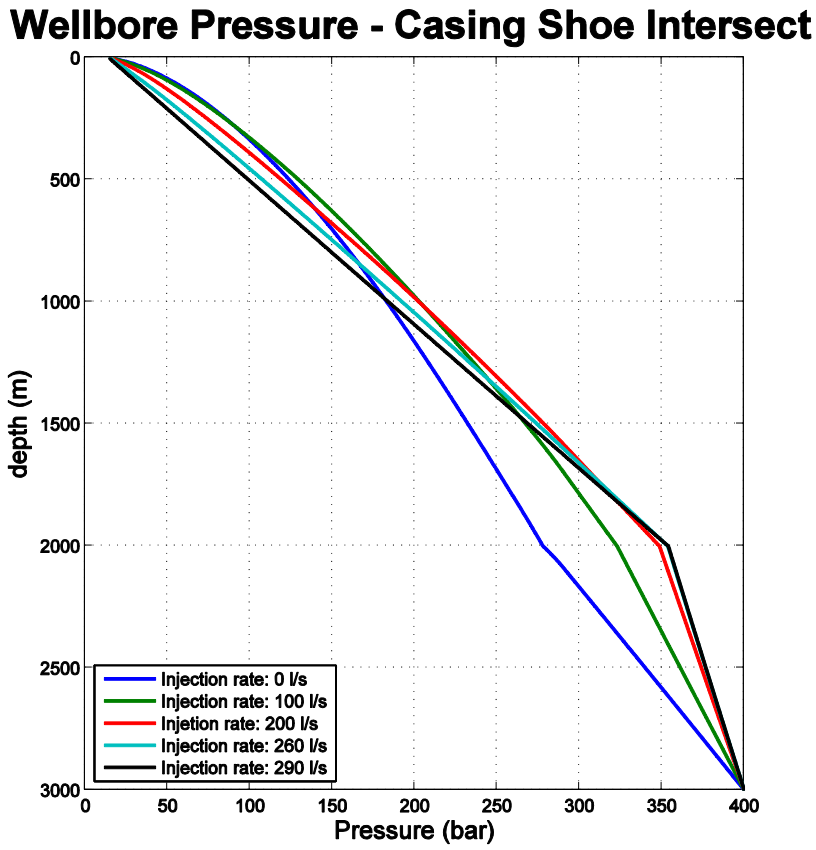

Graph 4.43 – Wellbore pressure during dynamic killing operation with casing shoe intersect

4.4.2 Casing Shoe Pressure

It is important that the killing operation does not expose the formations surrounding the open-hole section to pressures exceeding the fracturing pressure. This may lead to lost circulation, further complicating the killing operation, or even lead to an underground blowout. By observing the wellbore pressure in the open-hole section on graph 4.42 and 4.43, it can be seen that the pressure decrease as the injection rate is increased for a bottomhole intersection, for casing shoe intersection the casing shoe pressure increase, as the injection rate is increased.

Graph 4.44 shows how the pressure develops, as the injection rate is increased for both cases. When the dynamic kill rate is injected for the two cases, the casing show pressure is reduced by 29% when the kill point is at the bottom of the well, compared to at the casing shoe. Since the casing shoe pressure is at its highest during the beginning of a bottomhole dynamic killing operation, the overall reduction in casing shoe pressure becomes 21.4%.

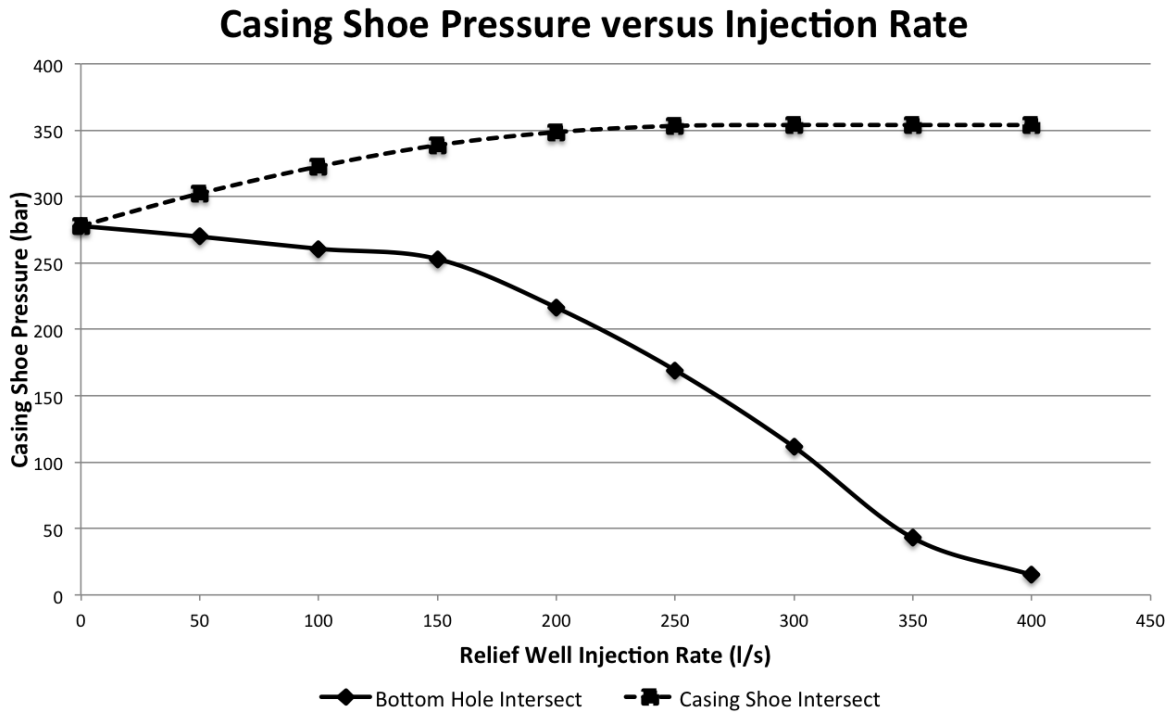

Graph 4.44 – Casing shoe pressure during dynamic killing operation

4.4.3 Depth of Intersection Point

Depending on the situation, the openhole section might be of a different length than that described in the base case. If a shorter openhole section exists, the benefits of a bottomhole kill point will me smaller. The MATLAB-model described earlier in this chapter can simulate a dynamic kill operation that intersects the blowing well at any depth. To investigate the dynamic killing operation further, simulations were performed to find the dynamic kill rate when intersecting anywhere along the open-hole section. Graph 4.45 shows the dynamic kill rate versus intersection depth. The dotted line shows the reduction in dynamic kill rate for the given intersection depth, compared to a casing shoe intersection.

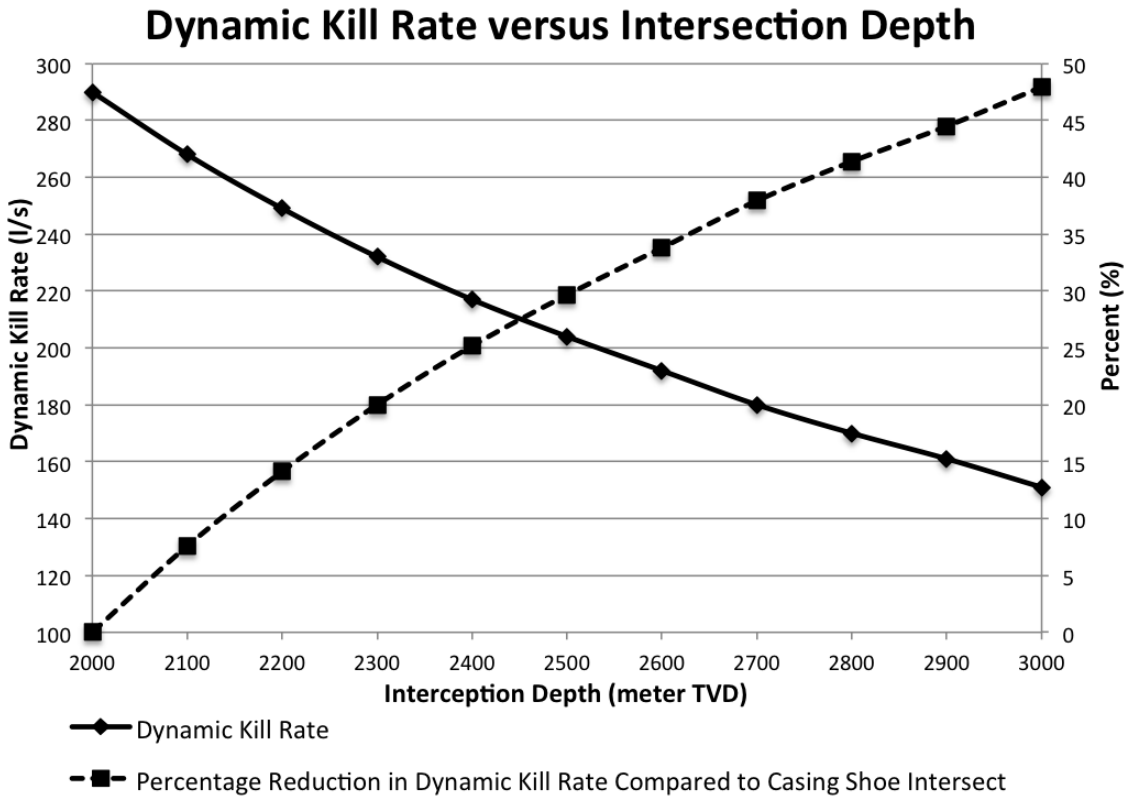

Graph 4.45 – Effect of intersection depth on dynamic kill rate

It can be observed that the relationship between dynamic kill rate and intersection depth is not linear. When the bottomhole of the blowing well is intersected, the dynamic kill rate is reduced by 48%, compared to casing shoe intersection. The effect of a deeper intersection is larger for the upper parts of the openhole section. If the relief well intersects 100 meters below the casing shoe, the dynamic kill rate is reduced by 8%. If the well can be intersected at a depth of 2400m TVD, the dynamic kill rate is reduced by 25%.

This shows that a deeper intersection point has a large effect on a dynamic killing operation, even though the openhole section is shorter.

4.4.4 Density of Static Kill Mud

When considering a water depth of 150 meters, the density of the static kill mud can be calculated. In this calculation, it is assumed that the hydrostatic pressure from the kill mud, and the water column, must balance the pore pressure in the reservoir. In reality there will be fluids of a certain density beneath the kill point as well, and these will contribute to the hydrostatic pressure. Graph 4.46 shows the static kill mud density required to kill the blowing well for different intersection points. The solid line shows the mud density when the fluids beneath the kill point is not considered, while the dotted line shows the static kill mud when the fluids beneath the kill point is considered. The pressures were simulated in the MATLAB-model.

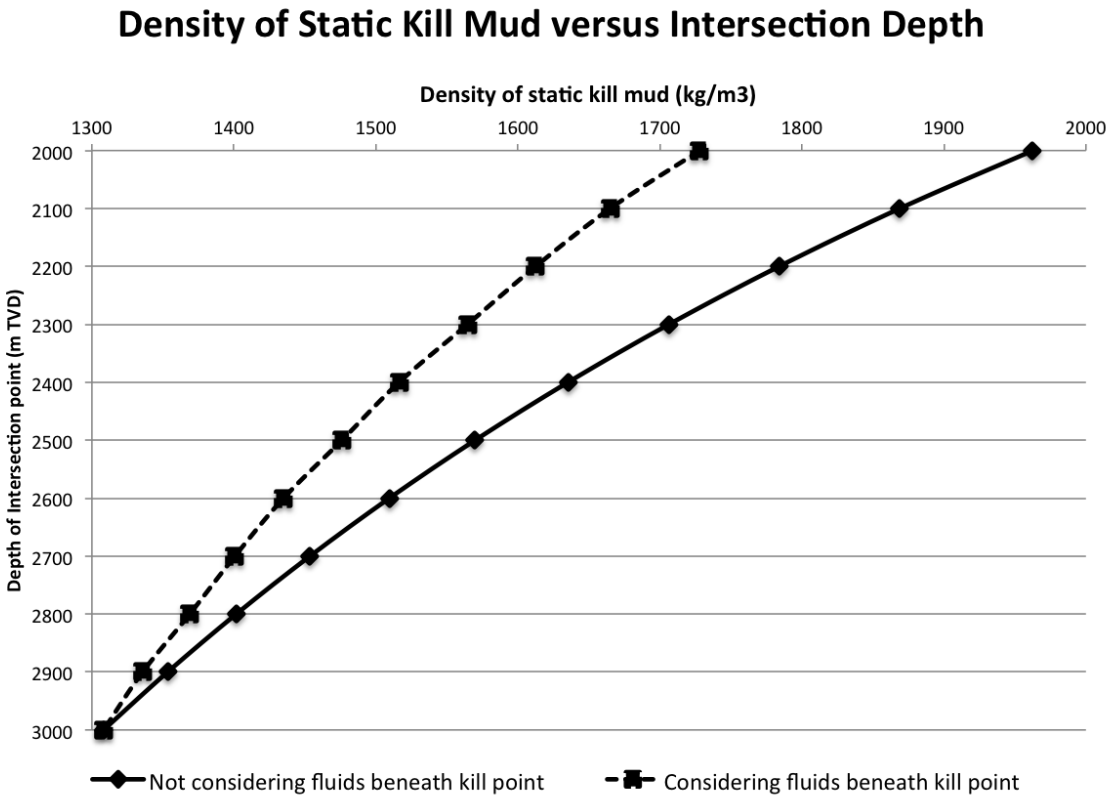

Graph 4.46 – Effect of intersection depth on static kill density

It is assumed that the pressure at the intersection point will cause all kill mud to flow up towards the surface. If an increased pressure is applied at the injection point, the kill mud can be bullheaded down into the openhole section as well. This can reduce the kill mud density required. However, the maximum casing shoe pressure has already been experienced during the dynamic killing operation, and the bullheading operation will subject the openhole section to even higher stresses.

It can be observed that bottom intersection reduces the density of the static kill mud required greatly, again reducing the wellbore pressure. This can be critical if the openhole section consists of formations with low fracture resistance. When considering the fluids below the casing shoe, the static kill mud density is 1728 kg/m^3 for casing shoe intersection. For bottomhole intersection the static kill mud density required is 1308 kg/m^3. The corresponding casing shoe pressure when the well is killed statically is 272 and 354 bar, for bottomhole and casing shoe intersection, respectively.

4.5 Discussion

Results

The model presented in this work calculates both blowout rates, and the subsequent dynamic killing rate required to balance the reservoir pressure. The determination of the blowout rate requires far more complex calculations, since the flow can be of one-, two-, or three phases. However, it was decided to perform these calculations as well, to investigate how the pressures and rates would develop as the injection rate was increased. Once a rate corresponding to the dynamic kill rate is injected into the blowing well, the wellbore pressure at the reservoir will be balanced, and inflow will seize. Hence, at this point the flow will be one-phase.

The simulations showed that a deeper intersection point offers many benefits to both a static- and a dynamic killing process. The base case assumed that conventional ranging tools would facilitate a casing shoe intersection at 2000 meters TVD, while SSWD made a bottom intersect at 3000 meters TVD possible. This increased the total length of the well with 34%. During one-phase flow, the frictional pressure loss is 2.5 times higher in the openhole section because of the increased roughness and smaller flow area. Therefore, the required dynamic killing rate was reduced by 48%.

Once a static kill mud is circulated into the blowing wellbore, the increased mud column height makes it possible to utilize a lighter kill mud. This will reduce the wellbore pressure in the well, and can be critical if the openhole section consists of weak formations. Considering the base case well, a bottomhole intersection would require a 24% lighter static kill mud, compared to casing shoe intersection.

Additional simulations showed that a bottomhole intersection would be beneficial for shorter openhole section as well. Compared to casing shoe intersection, a 300 meters deeper kill point would reduce the dynamic kill rate by 20%, and the static kill mud density with 9%. For a 100 meters deeper kill point, the dynamic kill rate was reduced by 8%, and the static kill density with 3.6%.

The calculations yielded results that were comparable to real world cases. The crude oil blowout rate was calculated at approximately half of the maximum estimate of the Macondo blowout rate (CNN, 2010). Further, Kouba et al. (1993) investigated the dynamic killing operation of the C-II-2 blowout in Arun, Indonesia. This near vertical well had a measured depth of 3112 meters, a reservoir pressure of 490 bar and a reservoir temperature of 110ºC. It was intersected off-bottom and dynamically killed with a rate of 304 l/s. This rate is 4.6% higher than the calculated off-bottom kill rate for the base case well.

Blowing Well Trajectory

The model was prepared to simulate a blowout in a vertical well. If simulations should be performed on a well with inclined sections, the model must be updated. The Beggs and Brill method works for all inclinations, and because of this the model can easily be updated to perform simulations on other well trajectories. The answer matrix should still refer to the true vertical depth, but each well segment must be adjusted to account for the increased measured length and inclination. By doing this, the well profile can simply be an input matrix that specifies the inclination at every point in the wellbore. If extended near horizontal sections exists, it might be more beneficial to divide the wellbore into sections corresponding to measured depth.

When simulation is performed on a well with changing inclination, this will affect the flow pattern and pressure profile of the well. The frictional pressure loss will be dependent on the measured depth of the well, while the hydrostatic pressure loss is dependent on the vertical depth of the well.

Flowing Temperature

Some simplifications had to be made to be able to simulate the blowout using MATLAB. Since the blowing fluid consists of a mixture of hydrocarbons, Aspen HYSYS had to be used to find the pressure and temperature dependent properties of the mixture. Temperature simulations showed a near constant flowing temperature for stabilized blowout rates. Hence, simulations could be performed, and regression analysis used to find pressure dependent equations for the mixture properties. Once the blowing well was intersected, and a cooler fluid is injected, the temperature profile is adjusted. Further work could be conducted to implement the small change in flowing temperature along the blowing well. However, these changes would not change the dynamic killing rate, as this is independent on the properties of the reservoir fluid.

Flowing Reservoir Pressure

Further, the assumption that the flowing reservoir pressure is equal to the average reservoir pressure might not be true if the blowout has flowed for an extended time, or if the well was drilled into an already producing reservoir. As the fluid is produced, or released uncontrollable, a pressure drawdown will develop, reducing the flowing reservoir pressure.

This will cause a lower rate to balance the pressure, and hence the blowout rate, and dynamic kill rate will be reduced. This can easily be adjusted for in the model by making a time dependent flowing reservoir pressure, dependent on the cumulative fluid production (Fekete, 2012). For this work, it was more important to establish the maximum rates, and show the difference between the two different kill points.

Reservoir Productivity Index

The blowout rate is also dependent on the productivity index of the reservoir. In this work it is assumed that the reservoir is able to deliver the calculated flow. This might not be true if the exposed reservoir sandface is small, or if the reservoir has poor producing capabilities. The productivity index is dependent on reservoir fluid viscosity and volume factor, the reservoir permeability and thickness, and the skin factor. (Romero et al., 2002). This can also be adjusted for in the MATLAB-model by finding an upper limit for the influx rate at in-situ conditions, based on productivity index and pressure drawdown. For the purpose of this work, it was most sensible to use a reservoir that were able to support the calculated blowout rate, as the productive capabilities of the reservoir was outside the scope of this thesis.

Sonic Velocity

The fluid mixture travelling up the blowing well cannot reach a flowing velocity higher than the sonic velocity of the fluids. At this point the critical velocity is reached, and the flow is naturally choked (Hasan et al., 2000). The sonic velocity of a natural gas is dependent on temperature and pressure, but is typically from 410 to 440 m/s. The sonic velocity of fluids is much higher (Smith & Clancy, 2010). Because of the water depth used in the base case simulation, the expansion of the gas is suppressed enough so that sonic velocities are never encountered. During the blowout, the mixture velocity is 122 m/s at the wellhead. Additional simulations performed with atmospheric pressure at the wellhead yielded a mixture velocity of 444 m/s at the wellhead. At this point sonic velocities must be considered, and the maximum velocity of the gas phase should be set to the sonic velocity in the MATLAB-program.

Choking Effect

In addition to this, there might be objects in the blowing well that will choke the flow. These might be objects used in the drilling operation, like tubular or plugs, or debris from the blowing reservoir. This will change the flow conditions of the blowout. During the 2/4-14 killing operation, the flow rates were lower than estimated. It was assumed that the old BHA and bit in the blowing well acted like a choke on the flow (Leraand et al., 1992). This can be accounted for in the MATLAB-program by changing the hydraulic diameter of certain sections of the blowing well.

Hydraulic Communication

This model assumes that full hydraulic communication is obtained, and that there is no fluid loss to the surrounding formations. Further it is assumed that there is no pressure loss over the interface between the relief well and the blowing well. This is true if the blowing wellbore is directly intersected so that there is no reduction in flow area as the fluid is pumped into the blowing well. To ensure that no fluid is lost during the dynamic killing phase, the formations at the kill point should be investigated. The blowing well should be intersected in a hard and impermeable formation where washouts and fracturing is less likely. This will minimize fluid loss during the dynamic killing operation (Leraand et al., 1992).

Change in Flow Pattern

The flow pattern is decided according to the procedure described by Beggs and Brill (1973). This will cause the flow pattern to change abruptly once the Froude number and liquid volume input moves into another region. This causes the sudden reduction in blowout rate that can be observed during the bottomhole dynamic kill. In reality the flow pattern might transition between the phases in a more gradual way.

Wellbore Properties and Dimensions

Environmental and wellbore properties must be specified in the MATLAB-program before simulation is performed. In the base case simulation, properties were obtained from the literature, or standard values were used. Wellbore dimensions were based on the dimensions of the 2/4-14 Saga well. It was assumed that the ambient temperature at the wellhead was 4ºC, and that the temperature of the surrounding formations increased linearly to 100ºC at the point of inflow.

This gave the basis for evaluating different kill point depths, and will show the how the kill requirements will change for that specific base case well. By changing the input properties of the well, the magnitude between the different strategies might change.

Counter Current Flow during Casing Shoe Intersection

In this model it is assumed that the pressure differential, and the flow of fluids, at the casing shoe will cause all injected seawater to flow up the blowing wellbore, and towards the surface. It is common when performing dynamic kill simulation to assume that no injected fluid will fall below the injection point, and flow in the opposite direction of the fluid flow from the reservoir. This might not be the case for gas- or high GOR blowouts. (Flores-Alvila et al., 2003).

Research completed by Flores-Alvila et al. (2003) showed that the effect of liquid fallback during an off-bottom dynamic kill should be considered, when the superficial gas velocity is below the critical gas velocity in the well. Depending on flow conditions and flow

medium, the injected seawater might start to fall into the flowing reservoir fluids, effectively increasing the hydrostatic pressure in the openhole section. If this were not considered under the specific situations, a potentially exaggerated off-bottom dynamic kill rate would be calculated.

However, the reservoir fluid used in this model does not have a high GOR, and during the blowout, the flow consists of 86% liquid at the casing shoe. Therefore, the conditions for counter current liquid flow during off-bottom dynamic killing are not present. This phenomenon should, on the other hand, be considered if the model were to be adapted to simulate a gas blowout.

Transient Effects

The temperature calculations in this chapter do not take in to account any transient effects in the surrounding formations. Since heat is exchanged between the flowing liquid and the neighboring rock, the temperature in the formations surrounding the wellbore will change. During the blowout, the formations surrounding the blowing well will be heated. In the temperature calculation model presented in this work, the formation temperature is assumed constant, and equal to the geothermal gradient.

Hence, the real temperature drop from reservoir to surface will become even smaller. This further strengthens the assumption that the flowing temperature can be assumed constant. The relief well will change the temperature of the surrounding formation as well, however this effect will be much smaller because of the limited time that circulation is performed, and because of the smaller flow rate.

Overall Accuracy of model

Because of the considerations taken in regards to multi-phase flow, the model should calculate accurate blowout rates for all dynamic injection rates, and for any kill point depth. It is important that the input parameters are as accurate as possible, and that the mixture flow path has been found, and the hydraulic diameter of the model is adjusted to account for any unconformities along the flow path.

To further increase the accuracy, work can be done to implement temperature change in the property equations described earlier in this chapter. Equations with two variables, or additional MATLAB programs, could be used. This will be more critical during multiphase flow, as temperature will change the gas boil out pressure. Once the well is dynamically killed, and the flow is one phase, the temperature will only change the density and viscosity of the seawater. The difference in density of water at 4 and 100ºC is only 4.1% (USGS, 2013). Considering the small temperature drop expected when circulating at these high rates, the error resulting from this assumption will be small.

Since the model was made in MATLAB, a given oil composition was used. Accordingly, equations used to calculate the different fluid properties must be changed if simulations are to be performed for a different reservoir fluid. The dynamic kill rate will be independent on the reservoir fluid composition, since the flow consists of seawater only once the reservoir pressure is balanced (Leerand et al., 1992).

5. Pumping Capacities

In the previous chapter, the injection rates required to dynamically kill the blowout with seawater was found. This, together with the total pump pressure needed, will decide how many pumps will be required to successfully kill the blowing well. In this chapter the pump pressure, and number of pumps required, for casing shoe- and bottomhole intersection will be investigated.

5.1 Pump Pressure

The maximum pump pressure required during the killing operation is experienced once the blowout is dynamically killed, and is expressed by equation 5.1, as suggested by Warriner & Cassity (1988).

$$p_{pump} = p_{bh} - p_{h,ann} + \sum_{i=1}^{n} p_{f,i} \tag{5.1}$$

Where p_{bh} is the bottomhole pressure in the relief well, $p_{h,ann}$ is the hydrostatic pressure in the relief well, and $p_{f,I}$ is the frictional pressure loss throughout the flow path of the injected fluid.

5.1.1 Bottomhole Pressure

The bottomhole pressure of the relief well must be equal to, or higher than, the pressure in the blowing well at the kill point. If this were not true, the reservoir fluids would start to flow up the relief well, once hydraulic communication was established. In addition to this, to be able to inject fluids into the blowing wellbore, a higher pressure must exist in the bottom of the relief well, than at the kill point of the blowing well. The bottomhole pressure in the relief well is composed of the hydrostatic pressure of the drilling fluid, and any pressure applied at the surface.

During the 2/4-14 killing operation, the drill string was pulled inside the 7” casing, once communication had been established. The annulus was filled with a heavy mud to balance the bottom pressure, and the annular preventer was closed. The riser booster pump was used to refill the annulus with heavy mud (Leraand et al., 1992). Once the dynamic killing operation is initiated, the pump must be able to deliver the pressure needed to obtain overbalance, in addition to the pressure needed to circulate the fluids.

According to calculations described in chapter 4, the pressure in the bottom of the relief well must be above 354 and 400 bar, for casing shoe- and bottomhole interception, respectively. If the hydrostatic pressure from the dynamic kill fluid is less than this, the pumps must deliver the additional pressure.

5.1.2 Hydrostatic Pressure in Relief Well

The hydrostatic pressure in the relief well is a function of the density of the dynamic kill fluid and the true vertical depth of the well. When the water depth according to base case parameters is used, together with an air gap of 40 meters, the true vertical depth of the casing shoe is 2190 meters, while the bottom of the well is located at 3190 meters TVD. Assuming incompressible seawater, with a density of 1025 kg/m^3, the hydrostatic pressure contribution is 220.2 bar for casing shoe intersection, and 320.8 bar for bottomhole intersection. This means that the pump must apply a pressure of 133.8 bar when kill point is at the casing shoe, and 79.2 bar when the kill point is at the bottom of the well.

5.1.3 Frictional Pressure

The frictional pressure loss is highly dependent on the dimensions of the fluid flow path. Because of the high flow rate required to dynamically kill the blowing well, special consideration must be taken in regards to the frictional pressure loss throughout the relief well system. Several different flow paths should be investigated so that the option that yields the lowest possible frictional pressure loss can be chosen. Equations 5.2 through 5.4 from Bourgoyne Jr. et al. (1986) were used to calculate the frictional pressure drop. Since the dynamic kill fluid is seawater, a Newtonian model was assumed.

$$\frac{dp_{f,pipe}}{dL} = \frac{f_f \rho \bar{v}^2}{25.8d} \tag{5.2}$$

$$\frac{dp_{f,annulus}}{dL} = \frac{f_f \rho \bar{v}^2}{21.1(d_2 - d_1)} \tag{5.3}$$

$$\bar{v} = \frac{q}{2{,}448d^2} \tag{5.4}$$

In these equations the pressure drop is in psi, friction factor is the fanning friction factor, ρ in lbm/gal, v is the average velocity in ft/sec, and d is the diameter of the flow conduit in inches.

Circulation through Drill pipe

The most obvious flow path is through the drill pipe. This however can yield very high frictional pressure losses, resulting from the low cross sectional area and high flow velocity. Graph 5.1 and 5.2 shows how the frictional pressure develops for different drill pipe inner diameter. Values for dimensions on pipe and steel roughness have been obtained from Bourgoyne Jr. et al. (1986). The viscosity of seawater was obtained from Schmelzer et al. (2005). The well profile is described in chapter 4.1, with an ocean depth of 150 meters, and an air gap of 40 meters between ocean surface and drill floor. Any pressure loss over the bit is not accounted for in these calculations.

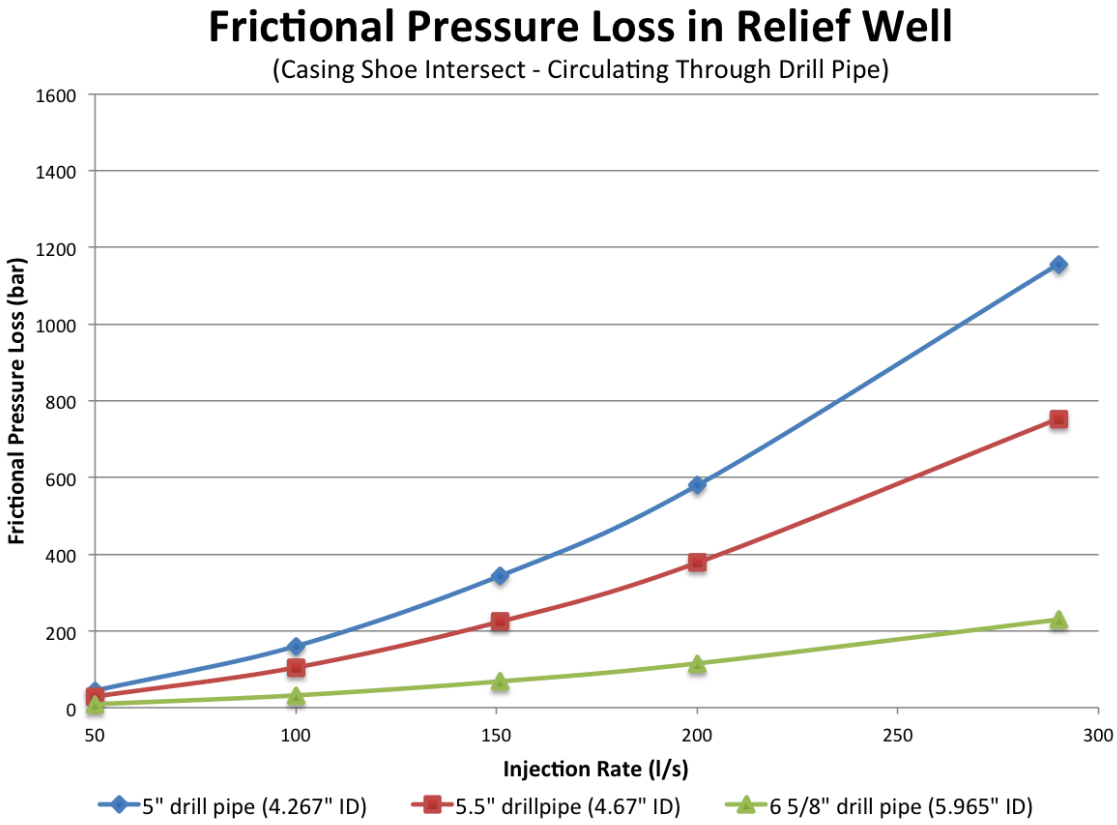

Graph 5.1 – Frictional pressure when circulating down drill string, casing shoe intersect

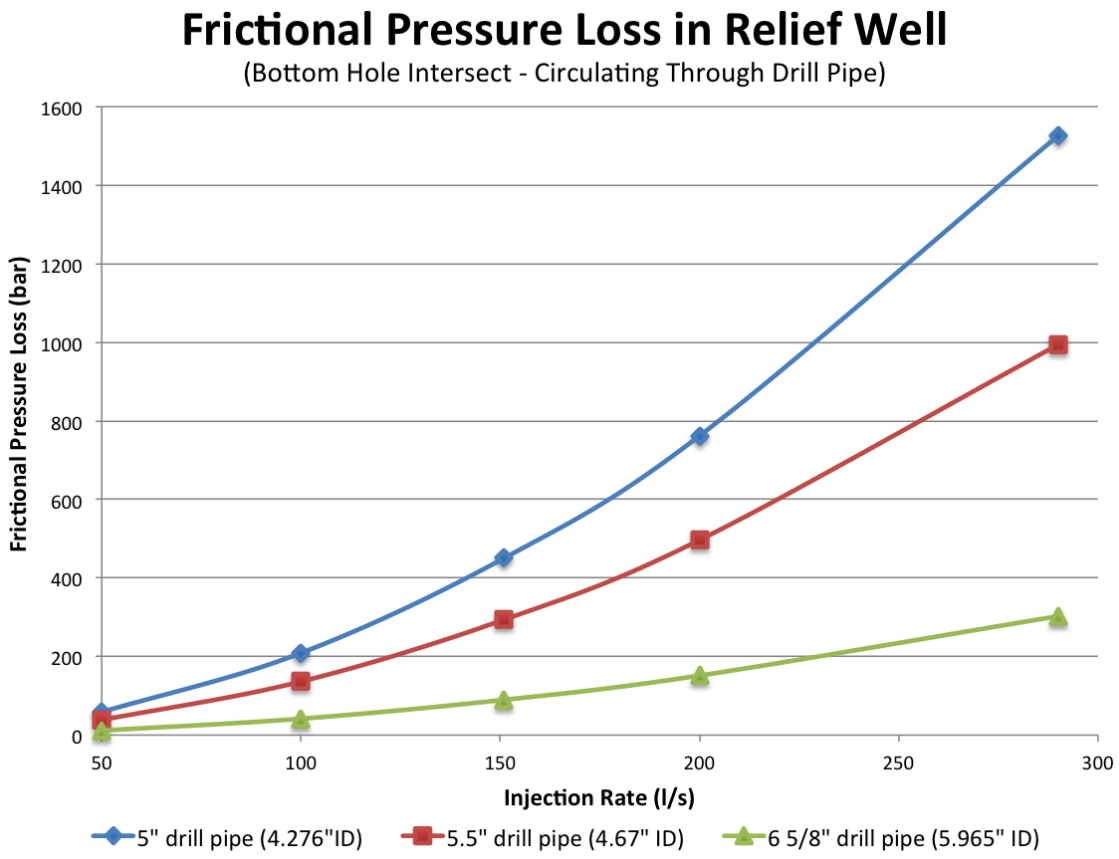

Graph 5.2 - Frictional pressure when circulating down drill string, bottomhole intersect

Circulating at high rates through the drill pipe generates a very high frictional pressure loss. Combined with the high flow rates required to dynamically kill the blowing well, this can become difficult for the kill rig to handle. Using drill pipes with a larger diameter dramatically reduces the frictional pressure drop, however the relief well dimensions might limit the size of the drill pipe.

For the given relief well path described in chapter 4.1, the measured length of the well is 2545 and 3423 meters, for casing shoe- and bottomhole intersection, respectively. This means that bottomhole intersection requires a 35% longer well path. The circulating temperature in the bottom section of the relief well is higher, causing a lower flowing viscosity. Because of this, the frictional pressure loss is between 29 and 32% higher for bottomhole intersection.

Circulating Down Annulus

If the flow area in the annulus is larger, it might be beneficial to circulate the kill fluid down the annulus instead. When utilizing this method, the mud can be circulated down the kill line, riser or both. This is dependent on the well integrity equipment, and the dynamic kill strategy. Graph 5.3 shows the frictional pressure loss through the kill line, while graph 5.4 and 5.5 shows the pressure loss in the annulus, for casing shoe- and bottomhole intersect, respectively. Dimensions were based on numbers suggested by Warriner & Cassity (1988). A graph showing frictional loss in the riser is not included. Because of the large dimensions of the drilling riser, the pressure loss becomes negligible.

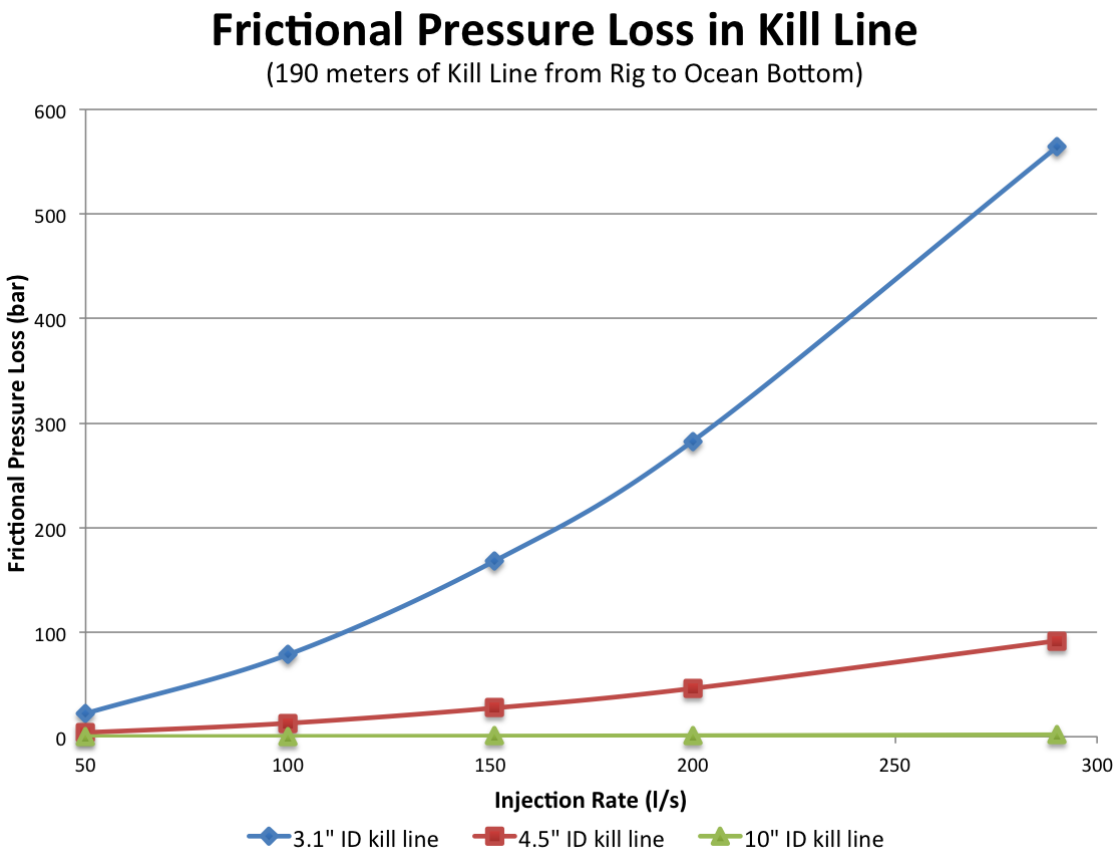

Graph 5.3 – Kill line pressure loss

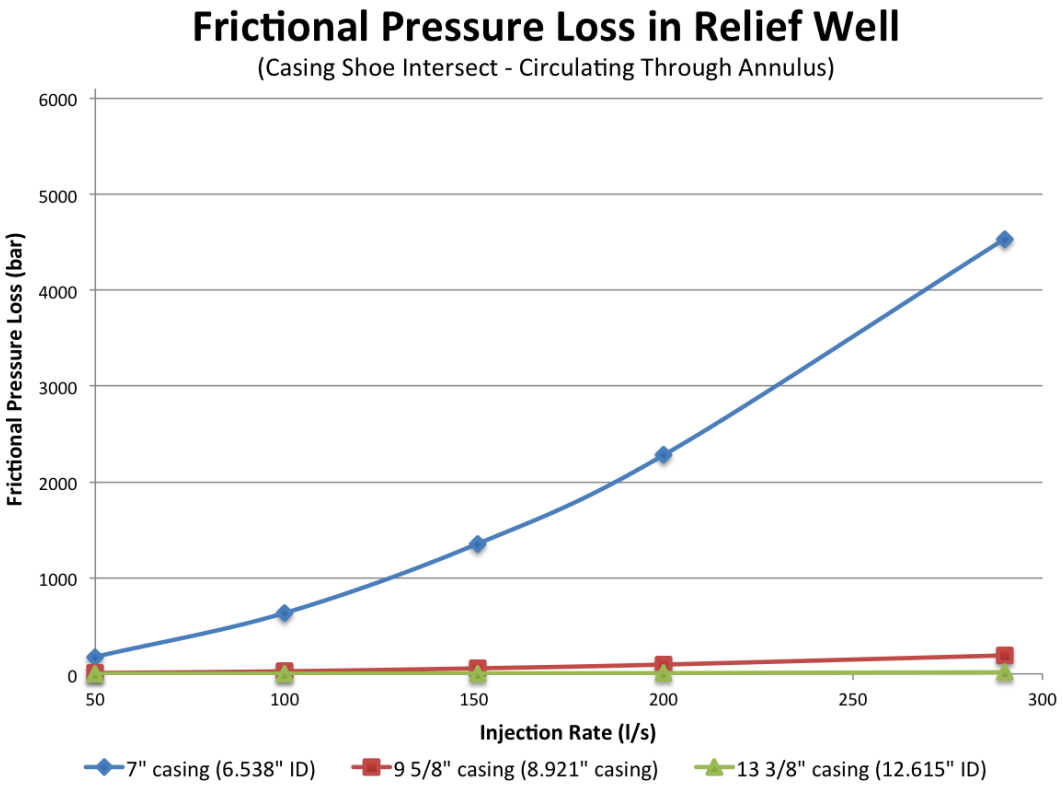

Graph 5.4 – Annular friction loss, casing shoe intersect

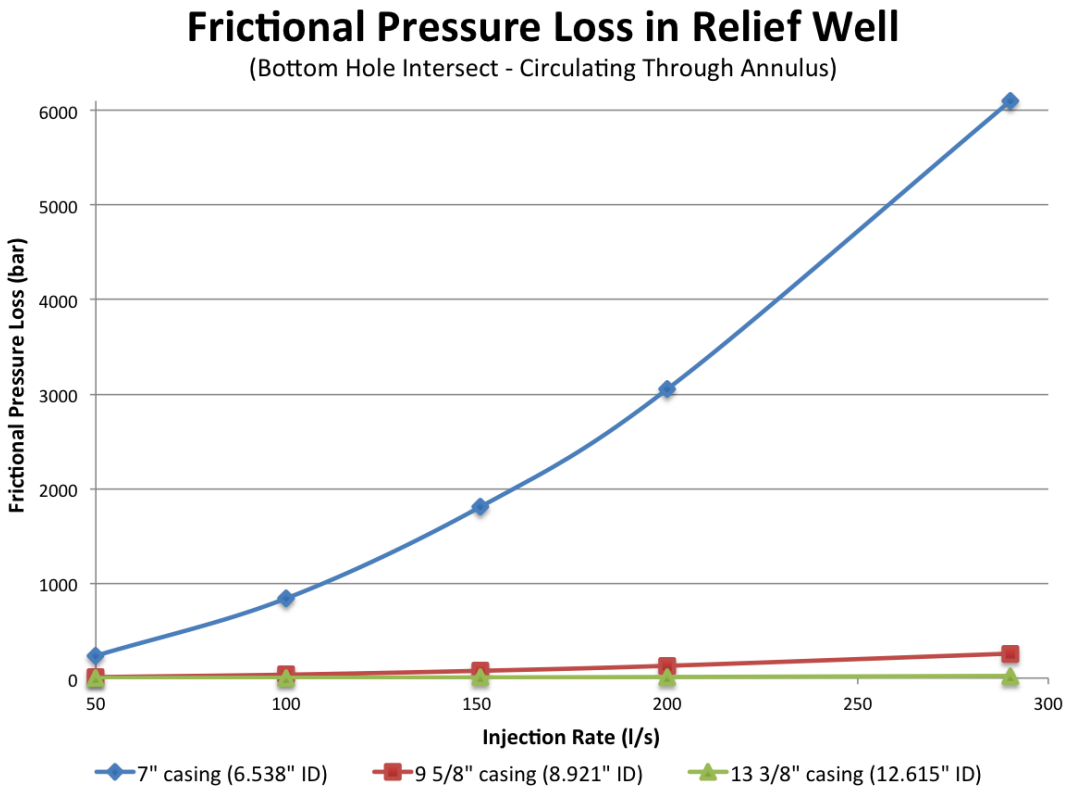

Graph 5.5 - Annular friction loss, bottomhole intersection

When trying to circulate high rates through the narrow flow area of a 7-inch casing, occupied by a 5-inch drill pipe, the frictional pressure loss becomes incredibly high. The frictional pressure loss is greatly reduced if a 9 ⅝-inch casing is used. For the dynamic kill rate of the bottom intersection case, the frictional pressure loss is 77.2 bar. For the dynamic kill rate required when intersecting at the casing shoe, the frictional pressure loss is 192.5 bar. Further, if the casing has an outer diameter of 13 ⅜-inch, the frictional pressure loss for the given dynamic killing rates is 6.9 and 17 bar, for bottomhole- and casing shoe intersection, respectively.

Realistic Wellbore Dimensions – Adaptive Solutions

When drilling the relief well, a casing should be set a couple of meters before the planned intersection point. This is to ensure the structural integrity of the relief well (Leraand et. al 1992). This last casing will probably not be extended all the way up to the surface, but hung off in the last set casing shoe, and cemented in place as a liner. When the 2/4-15S relief well was drilled, a 9 ⅝-inch casing was set at 4267 meters depth, and a 7-inch liner set at 4672 meters (Leraand et. al 1992).

To limit the flow velocity in the relief well, injection can be performed through both drill string and kill line simultaneously. The individual volumetric flow rates that should be circulated through the different flow lines should be investigated, to find the minimum frictional pressure loss. This however, is very dependent on the dimensions and roughness of the different flow paths.

When considering the diameter of the tool joints on the drill pipe, it will be difficult to use standard 5-inch drill pipe inside the 7-inch liner. Standard API NC50 tool joints have an outer diameter of 6⅜-, 6½- or 6⅝-inches. Because of this, a tapered drill string where 4.5-inch diameter, NC46 tool joints, drill pipe is used for the bottom section, should be used. This drill pipe has an inside diameter of 3.958-inch (RSA, 2013)

Case 1 – Standard Kill Line Dimensions and Tapered Drill String

Graph 5.6 and 5.7 shows the frictional pressure throughout the relief well, when circulating through drill string and kill line and annulus, for casing shoe intersection and bottomhole intersection, respectively. A kill line inside diameter of 3.1 inches is used (Warriner & Cassity, 1988). The water depth is 150 meters, air gap is 40 meters, and the 9 ⅝-inch casing is set from ocean bottom to 300 meters before intersection point. The last 300 meters consists of a 7-inch liner. The inside diameter of the casing is 8.921-inch, and 6.538-inch for the liner.

The frictional pressure loss is plotted against the fraction of the dynamic killing rate that is injected through the drill pipe. For casing shoe intersection, the dynamic killing rate is

290 l/s. For a fraction of 0.5, this means that 145 l/s is injected through the drill string, and 145 l/s is injected through the kill line.

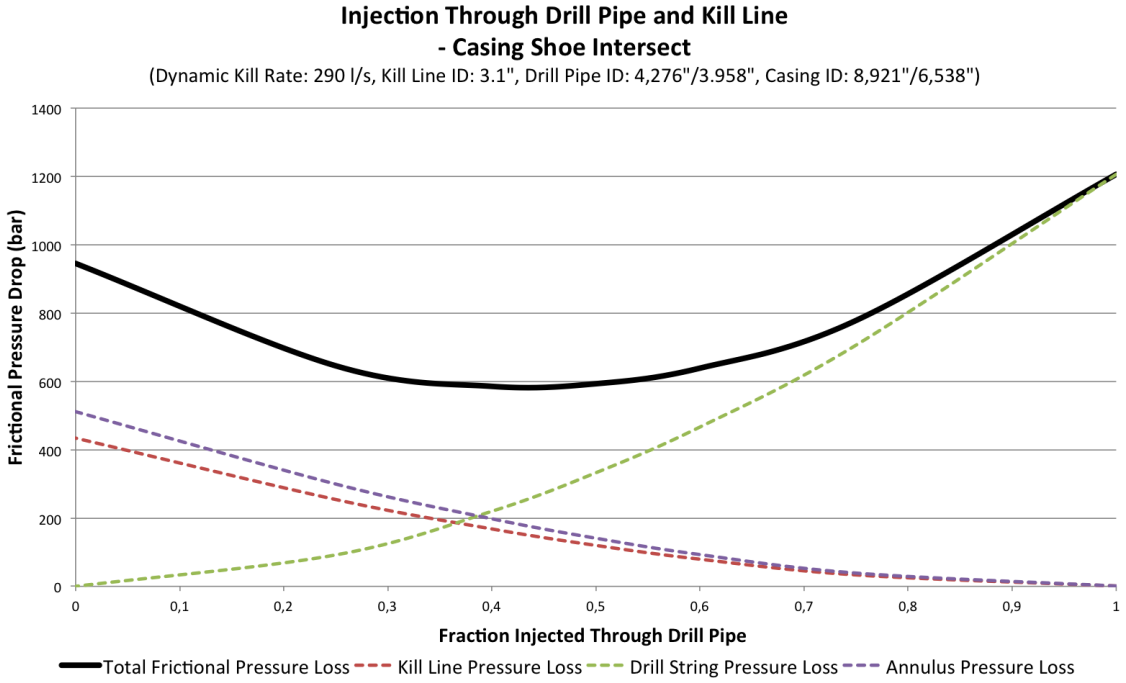

Graph 5.6 – Combined injection, standard kill line dimensions, casing shoe intersect

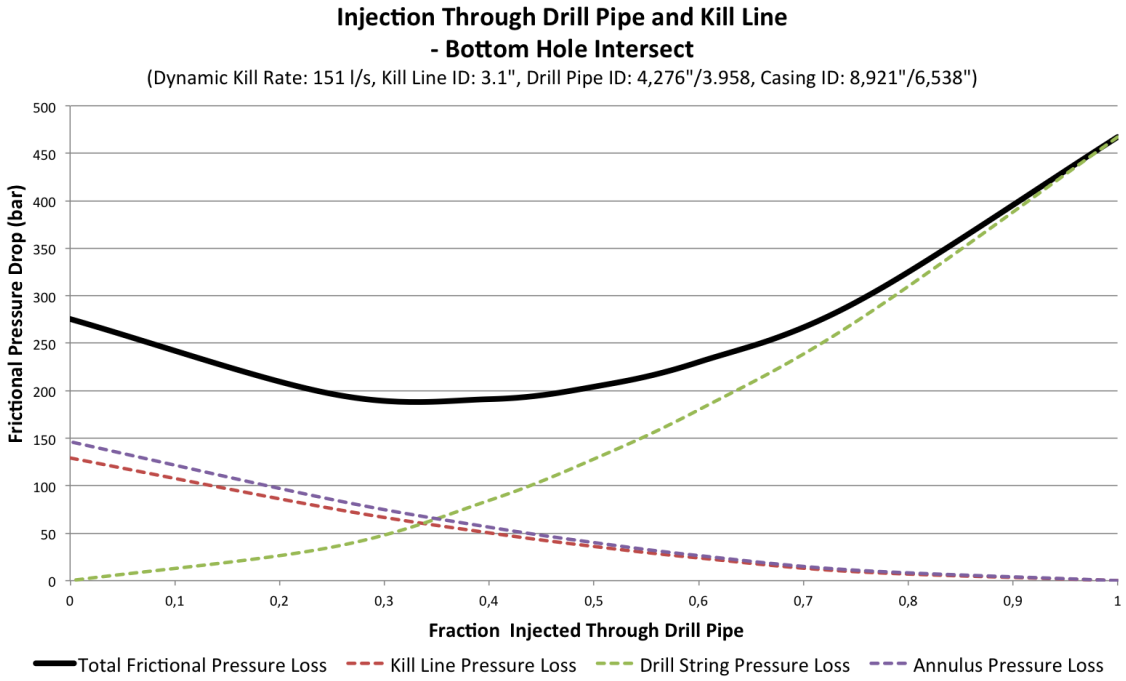

Graph 5.7 – Combined injection, standard kill line dimensions, bottomhole intersection

For casing shoe intersection, the frictional pressure loss is minimized when 43% of the dynamic kill rate is injected through the drill string, and 57% down the kill line and annulus. By utilizing the combined injection method, the friction pressure is drastically reduced, compared to injection through annulus or drill string alone. The total frictional pressure loss becomes 585 bar.

For bottomhole intersection, the length of drill string is longer, and because of this it is favorable to inject a larger fraction of the total dynamic kill rate through the kill line and annulus. The frictional pressure loss is minimized when 68% of the injection fluid is circulated down the kill line, and 32% is circulated down the drill string. The total frictional pressure loss becomes 190 bar.

Case 2 – Larger Dimension Kill and Choke Line

Even when circulating down both drill pipe and kill line, the frictional pressure loss is very large. The biggest frictional pressure loss is experienced in the kill line, and inside the 7" liner. If these could be reduced, circulating through drill string and annulus could yield far lower frictional pressure losses. Warriner & Cassity (1988) investigated the dynamic killing of high-rate offshore blowouts, and emphasized the necessity of replacing conventional kill- and choke lines with large diameter steel hoses or an injection riser. Further, Christman (1999) suggested that circulation could be performed down both choke and kill lines, this would effectively cut the volumetric flow in half, greatly reducing the frictional pressure loss.

Graph 5.8 and 5.9 shows the frictional pressure loss when circulation is performed through the annulus and drill string. The annular preventer in the BOP is closed, and the kill fluid is circulated from the rig through the drill string, choke line and kill line. The inside diameter of the kill and choke lines is set to be 5 inches.

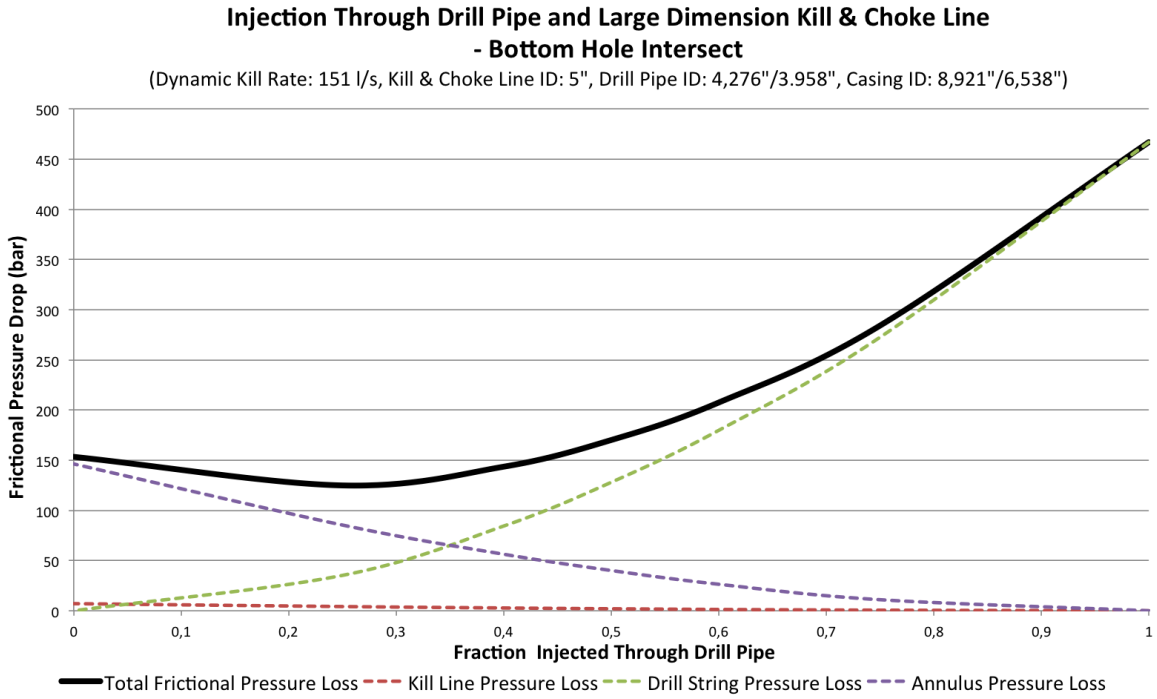

Graph 5.8 – Combined injection, large dimension kill/choke line, bottomhole intersection

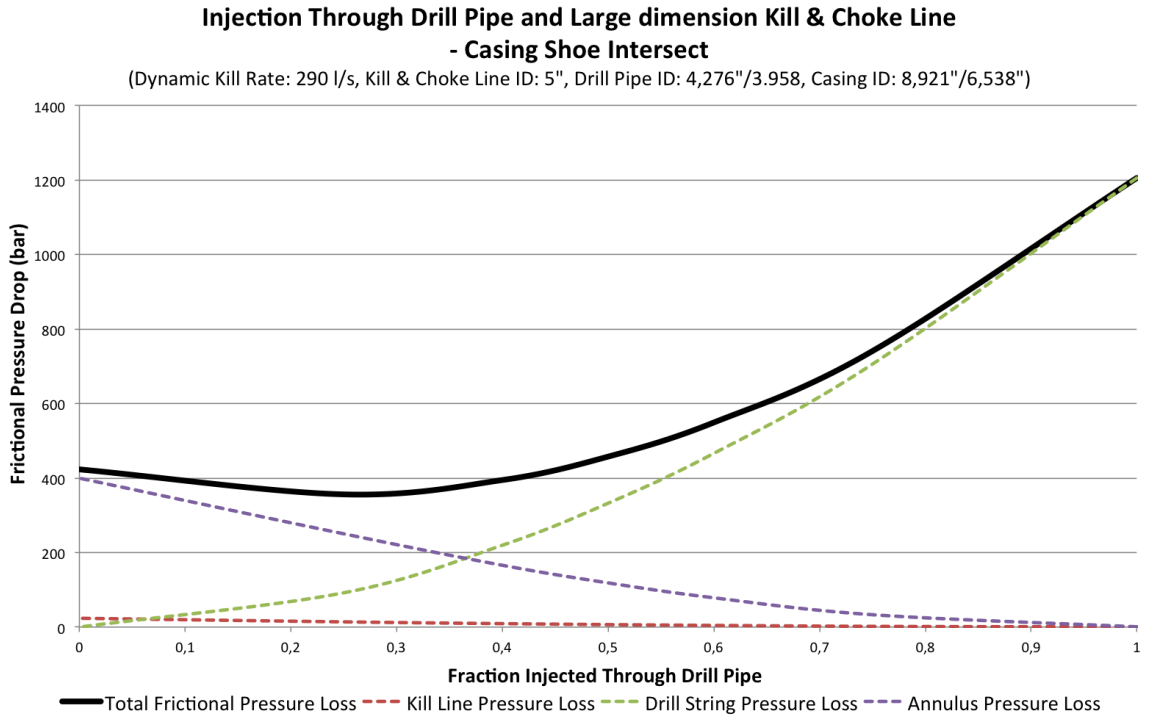

Graph 5.9 – Combined injection, large dimension kill/choke line, casing shoe intersect

For bottom intersection the minimum frictional pressure is obtained through an injection rate where approximately 28% of the dynamic kill rate is injected through the drill string, and 72% through the kill and choke lines. The friction pressure drop then becomes 125 bar. For casing shoe intersection the higher rates makes the frictional pressure losses almost three times higher. The minimum frictional pressure is obtained when 28% of the dynamic kill rate is injected through the drill string. The total frictional pressure loss is 355 bar.

If the frictional pressure loss in the 7" liner becomes a problem, an option could be to pull the drill string up into the bottom of the 9 ⅝-inch casing, to increase the flow area in the 7-inch liner. Graph 5.10 and 5.11 shows how this would affect the frictional pressure loss in both bottom- and casing shoe intersection.

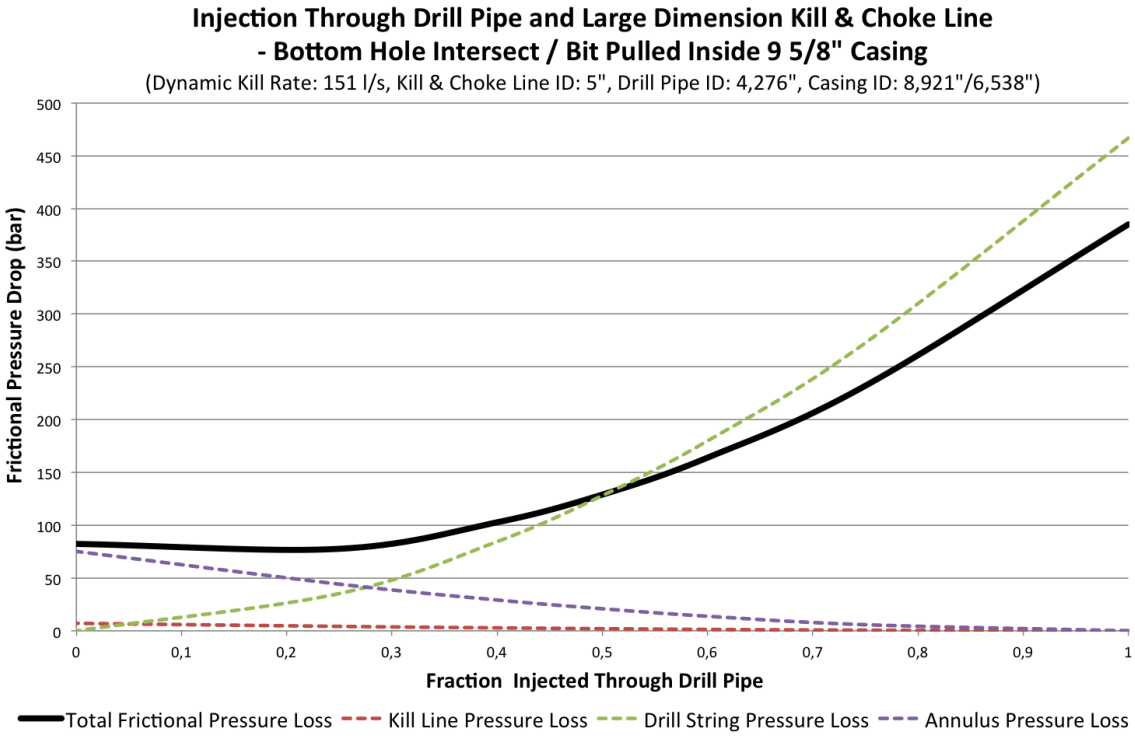

Graph 5.10 – Adaptive solution, bottomhole intersection

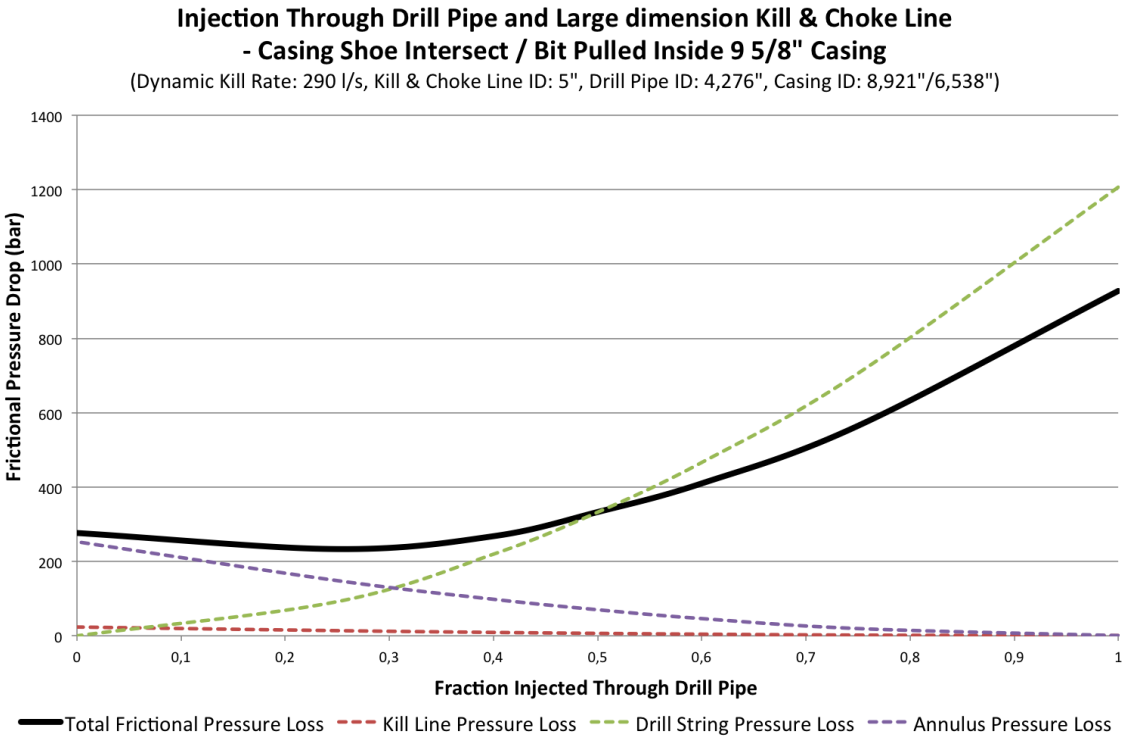

Graph 5.11 – Adaptive solution, casing shoe intersect

As can be observed, the frictional pressure is reduced greatly by utilizing this technique. However, further studies should be performed to ensure the flow performance beyond the casing shoe, before this technique is considered. For bottomhole intersection the minimum frictional pressure is obtained when 25% of the dynamic kill rate is injected through the drill string and 75% through the choke-, kill line and annulus. The frictional pressure loss is reduced to 78 bar. The same fractions yields the lowest frictional pressure for casing shoe intersection as well, however the total frictional pressure in the relief well is 233 bar, because of the higher flow rate.

Pump Pressure after Dynamic Kill

Once the flow from the reservoir has been suppressed, there will be no pressure differential to push the liquid up towards the surface. Because of this, the rig pumps must be able to circulate the fluids in the blowing well. Simulation described in chapter 4 found a frictional pressure loss of 87.4 bar for a stabilized dynamic kill rate in the blowing well, when the kill point were in the bottom of the well. For casing shoe intersection the friction loss was higher, at 141.4 bar.

5.2 Number of Pumps Needed

Table 5.1 summarizes the pump pressure needed for the dynamic kill operation. Table 5.3 shows the properties of a HT-400 Halliburton Triplex Cementing pump. This particular pump has been used in dynamic killing operations in the past (Leraand et al., 1992).

Kill Point	Case	Relief Well Friction (bar)	Pressure to reach overbalance (bar)	Blowing Well Friction (bar)	Total (bar)
Bottomhole intersection	A	451	79	87	617
	B	359			525
	C	190			356
	D	125			291
	E	78			244
	F	241			407
Casing shoe intersection	A	1156	134	141	1431
	B	1219			1494
	C	585			860
	D	355			630
	E	233			508
	F	781			1056

Table 5.1 – Pump pressure needed for different situations

Table 5.2 describes the different cases.

Case	Description
A	Circulation down drill string
B	Circulation down kill line/annulus
C	Combined circulation down kill line and drill string
D	Combined circulation down large dimension 5-inch ID kill and choke lines, and drill string
E	Combined circulation down 5-inch ID kill and choke lines and drill string, in addition to pulling drill string inside 9 ⅝-inch casing shoe
F	Circulation down large dimension 5-inch ID kill and choke lines/annulus

Table 5.2 – Description of cases

HT-400 Cementing Pump					
Plunger Diameter (Inches)	6	5	4.5	4	3.375
Maximum Pressure (bar)	431 (6250 psi)	651 (9000 psi)	772 (11200 psi)	965 (14000 psi)	1379 (20000 psi)
Maximum Rate (l/s)	51,10 (810 GPM)	35,33 (560 GPM)	28,64 (454 GPM)	22,71 (360 GPM)	16.09 (255 GPM)
Maximum HP Input	800	800	800	800	800

Table 5.3 - HT-400 Specifications (Halliburton, 2013)

The dynamic kill rate and pressure requirement dictates the number of pumps that must be run in parallel during the killing operation. A certain redundancy should be planned for when choosing the number of pumps, to account for mechanical failure or contingencies during operation. During the 2/4-15S relief well planning, this redundancy was set to 45%, and this will be used in this work as well (Leraand et al., 1992).

Table 5.4 summarizes the pump power requirements and total number of pumps needed for all circulation methods. Even though the HT-400 pump has a maximum flow- and pressure rating, the power input cannot exceed 800 hp. For comparison, the Treasure Saga rig that were going to kill the 2/4-14 Saga Petroleum well dynamically, were outfitted with 16 HT-400 pumps, for a total power rating of 8600 hp (Leraand et al., 1992).

Kill Point (Rate)	Case	Total Pressure (bar)	Power required (hp)	With 45% redundancy (hp)	Actual Number of pumps
Bottomhole intersection (151 l/s)	A	617	12496 (9322 kW)	118119 (13517 kW)	23
	B	525	10633 (7932 kW)	15417 (11501 kW)	20
	C	356	7210 (5832 kW)	10454 (7799 kW)	14
	D	291	5894 (4925 kW)	8547 (6375 kW)	11
	E	244	4942 (3686 kW)	7166 (5345 kW)	9
	F	407	8243 (6149 kW)	11952 (8916 kW)	15
Casing shoe intersection (290 l/s)	A	1431	55660 (41523 kW)	80707 (60208 kW)	N/A
	B	1494	58111 (43351 kW)	84261 (62858 kW)	N/A
	C	860	33451 (26898 kW)	48503 (36184 kW)	61
	D	630	24505 (21617 kW)	35532 (26507 kW)	45
	E	508	19759 (14740 kW)	28651 (21374 kW)	36
	F	1056	41074 (30641 kW)	59558 (44430 kW)	75

Table 5.4 – Number of HT-400 cement pumps needed for different situations

For bottomhole intersection, and circulating down the drill string only, a minimum of 15.6 pumps must be used. When accounting for required redundancy, the number of pumps rises to 23 pumps. However, by using combined injection, increasing the kill- and choke line dimensions, and pulling the drill string inside the 9 ⅝-inch casing shoe, the total number of HT-800 pumps required was reduced to nine.

For casing shoe intersection the requirements of the pumps will be much higher, both in regards to flow rates and pressure ratings. When the entire flow rate is circulated down the drill string, total pump pressure is 1431 bar. This is too high for the HT-400 pump, and most other well integrity equipment to handle, and an additional relief well might

have to be drilled. When the combined injection strategy described in subchapter 5.1.3 is used, the required pump pressure is reduced to 508 bar. This translates to a total of 36 HT-400 cement pumps.

Utilizing Mud Circulation System Available on Kill Rig

If the mud circulation system can handle the surface pressure during the dynamic killing operation, they can be utilized in combination with the cement pumps. This will reduce the amount of cement pumps needed, and hence reduce the requirements on the kill rig.

Typical mud pumps used on floating drilling rigs can be the National P-series, Continental Emsco FD- and F-series or Wirth TPK-series. These have a horsepower input rating of between 500 and 2200 (NOV, 2013; Wirth Erkelenz, 2006).

The Transocean Spitsbergen 6th generation semi-submersible has four Wirth TPK 7 Triplex 2200hp mud pumps, each with an operating pressure of 517 bar and maximum discharge flow of 55.8 l/s, for a total discharge flow rate of 223 l/s. (Deepwater, 2013; Wirth Erkelenz, 2006).

For bottomhole intersection, calculations show that a high capacity rig can dynamically kill the well using the mud circulating system, as long as the rig is fitted with large dimension kill and choke lines, and a combined injection strategy is performed. If circulation takes place through large dimension kill and choke lines and annulus only, the rig must use approximately four 800hp cement pumps in addition to the mud circulation system.

For casing shoe intersection the surface pressure becomes too high for all cases but one. Only when large dimension kill and choke lines are used, together with pulling the string inside the 9 ⅝-inch casing shoe, does the surface pressure become low enough to utilize the mud circulation system during the dynamic killing operation. In this case, approximately 25×800hp pumps must be used in addition to the mud circulation system. Depending on the deck capacity of the rig, casing shoe intersection most likely means that an additional pumping vessels needs to be mobilized, or even a second rig.

5.3 Discussion

Since the friction pressure loss is dependent on the square of the mixture velocity, naturally the increased flow rate required when intersecting the casing shoe increases the frictional pressure loss greatly. The calculations also emphasize the necessity for specialized injection solutions. Large diameter choke and kill line should be used in conjunction with drill pipe injection to minimize the frictional pressure loss throughout the relief well. It is important that all components in the circulation system can handle the high pressures during the dynamic killing operation.

Casing Dimensions

In these calculations it is assumed that the casing dimensions of the relief well is equal for both casing shoe- and bottomhole intersection. Since the relief well that intersects at the bottom of the blowing well is drilled to a deeper final depth, this is not necessarily true. If an additional casing string is necessary to reach the bottomhole of the blowing well, the dimensions of the two relief wells will be different. Since the bottom intersecting relief well will have tubular of a smaller diameter, the difference in frictional pressure loss will be smaller than calculated in this chapter. This is dependent on the pore pressure and fracture gradient of the specific formations, and will be dependent on the specific situation.

Casing Thickness

It is important that the casing strings used in the relief well has a sufficient burst pressure rating to support the high wellbore pressures during the killing operation. When performing the pump calculations, standard casing inside diameters were used. If a stronger casing is needed, the inside diameter might be smaller. This will cause the pump calculations to change.

Increased Casing Dimensions

Further, the relief well can be planned with increased dimensions, if the calculated frictional pressure loss becomes too large. The pump pressure will be dependent on the particular situation. The calculations in this chapter are true for the base case well. The main purpose is to show how the frictional pressure loss is increased for a higher flow rate, and how this affects the pump requirements on the kill rig.

Pressure Loss over Bit and Intersection Point

In the calculations where circulation was performed down the drill string, it was assumed that the pressure loss over the bit was negligible. During drilling, a high pressure loss is wanted over the bit to aid the drilling process. During dynamic killing frictional pressure loss should be minimized, and circulation down the drill sting would not be performed if there were a significant frictional pressure loss over the bit.

It is also assumed that the relief well intersects the blowing wellbore directly, so that there is no reduction in flow area as the injected water flows into the target wellbore. If hydraulic fracturing has been performed to achieve communication, some frictional pressure loss should be assumed.

6. Main Discussion

6.1 Results

The results from chapter 4 and 5 demonstrated the large benefits a deeper kill point has on both static- and dynamic killing operations. For the given well, the dynamic kill rate was reduced by 48%, the maximum casing shoe pressure during dynamic killing was reduced by 21%, the static kill fluid density was reduced by 24%, the static casing shoe pressure was reduced by 23%, and the pump power requirements was reduced by between 83 and 75%, depending on injection strategy.

Calculations indicate that the reduced pump power requirements when intersecting the bottom of the blowing well might enable dynamic killing using a standard high-capacity drilling rig. Whereas a casing shoe intersection will require mobilization of several additional cement pumps, extra pumping vessels, or even a second rig.

During dynamic killing from the casing shoe, the surface pressure approached the maximum discharge pressure of heavy-duty cement pumps. If the available surface equipment cannot handle the pressure during the killing operation, several relief wells might have to be drilled to reduce the injection rate of each individual well.

When dynamic killing is performed from the casing shoe, the pressure in the openhole section beneath the kill point will increase. If the openhole section consists of weak formation, this might lead to severe fracturing, and potentially result in further well control issues. If dynamic killing is performed from the bottom of the well, the pressure drop in the openhole section is increased, and hence the openhole wellbore pressure is reduced. This will prevent fracturing of weak formations.

In addition, restrictions might be set on the dimensions of a planned well, because it becomes difficult, or impossible, to kill for large diameter holes. If a bottom killing technique is available, the frictional pressure drop in the relief well is increased. Accordingly, a larger diameter hole can be used while still being able to kill the well dynamically.

Further, critical aspects with regards to SSWD will be discussed, and compared to conventional techniques.

6.2 Time from Relief Well Initiation to Static Kill

Considering the emissions from the blowout, operators will seek a method that can stop the flow as quickly as possible. Hence, the method chosen to intersect the blowing wellbore should be the method that offers the fastest termination of the blowout, and has the highest success factor. For SSWD to be beneficial, it is important that a relief well drilled to intersect the bottom of the blowing well does not take an excessively longer time to drill, than a conventional relief well intersecting a shallower casing shoe.

Drilling Time

When SSWD is utilized to facilitate a deeper kill point, the relief well will naturally be longer. In addition to this, it will span over a greater vertical depth, and potentially cross a larger amount of problem zones. Generally, drilling time increases exponentially with drilling depth, and this makes the total depth of the relief well especially critical (Noerager et al., 1987).

Considering the base case properties described in chapter 4, the relief well intersecting at 3190m TVD will have a measured length of 3424 meters, when water depth and air gap is accounted for. The relief well intersecting the casing shoe at 2190m TVD will have a measured length of 2554 meters. Hence, the total measured length of the well is increased by 34%, and the total drilling distance is increased by 36%. However, Thorogood (1987) investigated drilling times for deviated wells in the North Sea, and found that increased inclination generally increased the drilling time as well. Considering an equal horizontal displacement from the blowing wellbore, the relief well that intersects the casing shoe will have a larger inclination in the deviated section. Because of this, it is difficult to conclude that the drilling time will be longer for a bottomhole intersection.

Performing Positioning surveys

Compared to traditional techniques, SSWD use a very different approach to both borehole positioning, and relative distance between the two wells. SSWD requires seismic receiver arrays and source generators to be positioned on or above the seabed (Johansen & Sangesland, 2013). This means that extra equipment and vessels must be mobilized to lay down receivers, and perform the surveys. This might cause the initial preparations to take a longer time than when using conventional techniques.

Subchapter 2.6 described the uncertainty related to borehole positioning surveys. Inclination increases the uncertainty of both gyro- and magnetic surveying tools. Calculations using the Wolff and de Wardt (1981) systematic error model showed that the increased inclination when performing casing shoe intersection increased the

uncertainty of positioning surveys with 41 and 42%, for magnetic- and gyroscopic surveying tools, respectively.

Magnetic survey tools are often integrated into the BHA, and can perform a survey during a pipe connection, when the drill string is at rest. Once the results have been obtained, the results can be transmitted to the surface using mud telemetry (Samuel & Lui, 2001). This means that not a lot of time is lost when performing positioning surveys. However, the increased inclination can cause the uncertainty of magnetic survey results to become so large that the relief well cannot be drilled close enough to the blowing well to use ranging tools. If this is the case, a gyro survey must be performed. Gyro tools integrated into the BHA do exist, but generally a trip must be performed in conjunction with a gyro survey (Bashaar et al., 2010).

If the surface while drilling method works as anticipated, it can be used as a standalone survey method (Johansen & Sangesland, 2013). Surveys can be performed as the bit propagates into the earth, independent of the drilling operation. This will cause the well to be drilled faster. To verify the results, conventional positioning surveys can be performed. The reduced inclination associated with bottomhole intersection will cause surveys performed with conventional tools to be more accurate, and gyro surveys might be redundant.

Intersection

The process of intersecting the blowing wellbore is especially time consuming. Once the relative distance between the two wells is close enough to start the ranging survey, the entire drill string is pulled out of the hole, and replaced with a specialized ranging string. This is performed at fixed drilling intervals to secure a direct intersection.

During the process of intersecting the blowing Macondo well, an electromagnetic ranging survey was performed every 30 to 60 feet, as the bit closed in on the target. It took 24 hours to pull out the entire drill string, 12 hours to perform the ranging survey, and another 24 hours to run the drill string into the hole again. Therefore, the last 300 feet were drilled at a speed of 30 feet every 2.5 days (Marshall, 2011).

The 2/4-14 Saga well were intersected using electromagnetic ranging tools as well. Because of the high accuracy needed, the relief well was drilled past the blowing casing, so that triangulation could be performed. The casing was crossed at a depth of 3829 meters, the well dropped off to vertical, and was drilled parallel to the blowing wellbore, before it was intersected at a depth of 4705 meters. A 13 ⅜-inch casing were set at a depth of 2500 meters, on the 23rd of April 1988. Drilling continued to the first ranging point at a depth of 3559 meters. Five ranging surveys were performed as the well was drilled past the blowing casing. The well dropped off to vertical, and a 9 ⅝-

inch casing were set at 4248m on the 16th of June. The relief well drilling was put on hold for 119 days, as top kill were attempted. However, attempts to kill the blowing well using top kill techniques failed, and the relief well was considered the primary killing method as of the 28th of November. The 2/4-14 well was intersected and killed in the middle of December 1988.

The relief well generally intersects the blowing well at a very low angle. This makes the two wells move in on each other at a slower pace, and adjustments can be made if the relief well is steered off course. If the relief well approaches the blowing well at a higher angle and miss, pulling back, applying a whipstock and drilling a sidetrack might be the only solution (Adams & Kuhlman, 1994). The complex trajectory associated with magnetic ranging tools will cause the drilling time to increase, as more time is used to steer the well, the wellpath becomes longer, and a trip might be needed to change the motor assembly.

SSWD may eliminate the need for a triangulation bypass. Depending on how the method performs in practice, the low intersection angle can be evaluated as well. This will make the intersection process faster and more effective.

Mobilizing Equipment

A specialized rig must be used in the killing operation. If additional pump capacity is required, the kill rig can be equipped with additional cement pumps. The number of pumps that can be fitted on the kill rig is dependent on the deck capacity. If the deck capacity is limiting, additional pumping vessels, or an additional kill rig can be used. If the surface pressure surpasses the rating of pumps and well control equipment, increased relief well dimensions, or even drilling of a second relief well, must be considered.

A bottomhole intersection offers reduced dynamic kill rates, and in most cases reduced surface pressures. This is beneficial because it reduces the requirements on the kill rig. This means that less time can be used to mobilize equipment, and the relief well can be initiated as soon as possible.

Time Analysis

An approximation of the drilling time from spud to intersection of the blowing well for both cases was prepared to give an overview of the total time required to drill the relief well. This is presented in the depth versus time graph shown in graph 6.1. It is based on the paper written by Noerager et al. (1987).

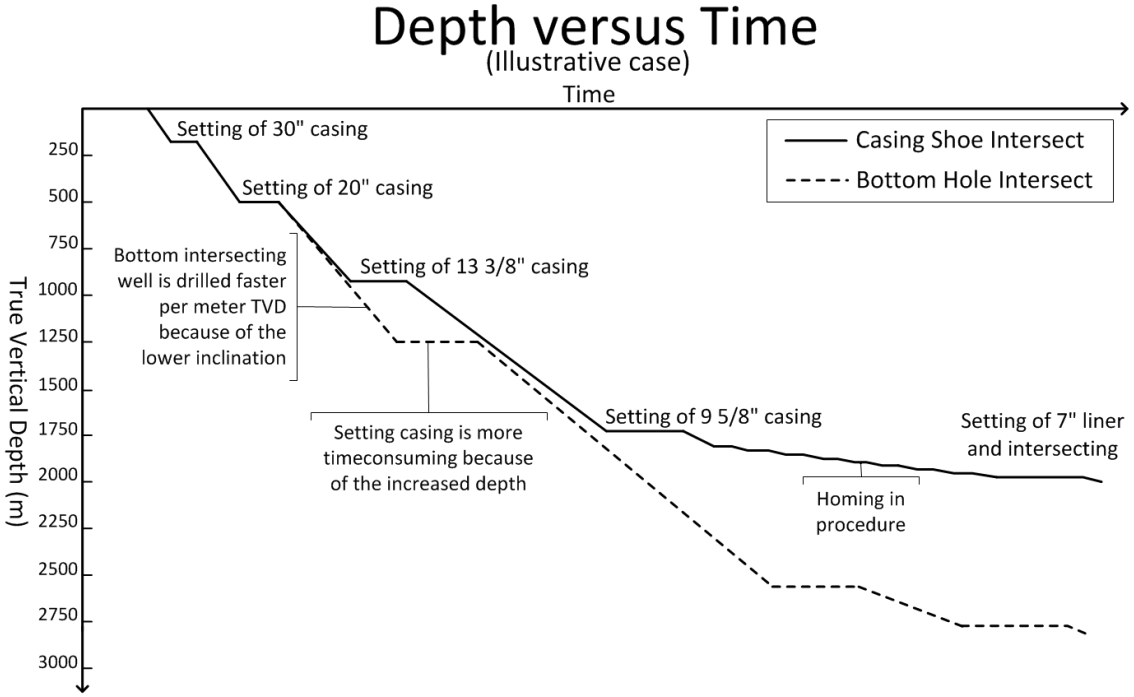

Graph 6.1 – Depth versus Time for both intersection points

It is difficult to estimate the drilling time of the different cases presented in this work. The relief well operation can be divided into three phases. These are the mobilization phase, the drilling phase, and the homing-in and intersection phase.

The time required to mobilize equipment will depend on the situation. A bottom intersection generally requires less pumping capacity, and this might shorten the mobilization phase. However, SSWD also needs specialized seismic equipment to be placed around the wellheads, this can be performed as the well is spudded, or before drilling starts. The second phase is the drilling down to the first ranging point. This phase will be longer for a bottomhole intersection, since the well must be drilled to a deeper point.

The homing-in and intersection phase should take much longer time when using conventional methods to home in on the steel casing. In recent years an electromagnetic

ranging tool that can be integrated into the BHA has been developed, this might shorten the time needed to home in on the steel casing in the blowing well. SSWD can be performed as the bit moves in on the target well, and there is no need to pull the string out of the hole or perform an triangulation bypass, this will increase the effectively of the intersection process.

6.3 Accuracy of Ranging Methods

If a well bypass and triangulation is performed, the uncertainty of a good electromagnetic ranging tool is 10% (Leraand et al., 1992). As long as ranging surveys are performed at short drilling intervals, and the relief well moves in on the target at a slow pace, this is sufficient to secure direct intersection. If hydraulic communication is not obtained, fracturing or acid squeezes can be performed. The last resort will be to pull back, start a sidetrack and perform the homing-in process over again.

If SSWD works as anticipated, it offers accurate and continuous positioning of the well path during drilling. Simulation yielded promising results. However, SSWD is only in the early stages of development, and has not been tested in practice. Because of this, it is difficult to say for certain that it offers the high precision required to facilitate direct intersection at great depths.

If the relative position between the two wells can be established with an uncertainty within a few meters, acid squeezes and hydraulic fracturing can be utilized to attempt to achieve hydraulic communication. However, it will be very risky to drill down to the bottomhole section of the blowing well without being certain that direct intersection can be achieved. Because of this the precision of the survey technique is critical for its success.

If the uncertainty is larger, conventional ranging tools cannot be utilized, because there is no steel present in the hole. It could be possible to locate the fluid flow in the blowing well by utilizing some tool with a high precision acoustic sensor. If this is not possible, SSWD can be used to locate the two wells relative to downhole formations and structures. This might be used to calculate the relative distance between the two wells.

SSWD might offer a fast, reliable and accurate way of performing wellbore-positioning surveys as the bit propagates down into the earth. There are some challenges related to the uncertainty of conventional survey tools. If SSWD could guide the relief well close enough to the target casing to start ranging surveys using magnetic tools, this would also offer benefits to the relief well drilling operation.

6.4 Further Work

Since SSWD is still in the early phases of development, a lot of work still remains before it can be considered an alternative to conventional techniques. Further work should be performed to investigate if the technique can offer the high accuracy required to facilitate a direct intersection.

Work can be performed to make the MATLAB model able to simulate a broader range of situations. First of all, work should be performed to make it possible to change both the trajectory and depths of the blowing well, as well as any reservoir fluid composition. Further, the changes in fluid heat capacity and flowing temperature along the wellpath could be investigated to find the benefits of implementing this into the model.

In addition to this, simulations could be performed in available blowout- and dynamic killing simulation programs, to compare with the results presented in this work.

7. Conclusion

- It is anticipated that Surface Seismic While Drilling (SSWD) can facilitate a direct intersection of a blowing wellbore, regardless of the presence of steel. This means that a blowing well can be intersected at the bottom of the well, as compared to at the casing shoe, when utilizing magnetic ranging methods.

- Simulations performed on a given well showed that a bottom intersection offered several advantages to the killing process. The dynamic kill rate was reduced by 48%, the casing shoe pressure during a dynamic killing operation was reduced by 21%, and the pump power requirements on the kill rig was reduced by 75 to 83%, depending on injection strategy.

- A higher column of kill mud can be displaced into the well once it is dynamically killed, when the blowing well is intersected at the bottom. Simulations showed that the static kill mud density was reduced by 24%, and the casing shoe pressure during static kill was reduced by 23%. When intersecting at the casing shoe, bullheading can be performed to push kill mud into the openhole section of the well. This would lower the density of the required static kill mud, but would also subject the openhole formations to even higher pressure.

- The reduced casing shoe pressure can be critical if the openhole section consists of weak formations. The increased pressures during circulation from the casing shoe could possibly lead to fracturing of weak formations, lost circulation and well integrity issues.

- The reduced dynamic kill rate associated with bottomhole intersection dramatically reduced the pump pressure and rate requirements on the kill rig. Depending on injection strategy, calculations showed that the blowing well could potentially be dynamically killed with a high capacity drilling rig utilizing the mud circulation system alone, or in combination with the cement pumps. This will reduce the time associated with mobilizing equipment, and the overall cost of the operation.

- During casing shoe intersection, the rate and surface pressure were much higher. For the lowest obtainable frictional pressure loss throughout the relief well, 25×800-hp cement pumps would have to be mobilized to supplement the mud circulation system. For other injection strategies, the surface pressure exceeded the maximum output pressure of the mud circulation system, and the operation would have to be performed

exclusively with heavy-duty cement pumps. This means that a large number of pumps and pumping vessels, or even a second rig, would have to be mobilized.

- The surface pressure during dynamic killing from the casing shoe approached the maximum discharge pressure of heavy-duty cement pumps and well control equipment. If available surface equipment cannot handle the high pressures during the killing operation, an additional relief well might have to be drilled to reduce the flow rate in each individual well.

- Bottom intersection requires a longer well, and hence the drilling time will increase. This can be critical during a blowout situation. However, there are extended non-productive time and trajectory requirements associated with conventional relief well drilling. SSWD can be performed continuously as the bit approaches the target well. This can reduce non-productive time and assist in a faster intersection.

- SSWD must offer the high precision required to directly intersect the blowing well. At the bottom of the well there will not be any steel present, and conventional techniques cannot be used as a contingency.

Bibliography

Adams, N. and Kuhlman, L. 1994. *Kicks and Blowout Control*, 2. edition. Tulsa, Oklahoma: PennWell Publishing Company.

Adams, N.J. and Kuhlman, L.G. 1991. Shallow Gas Blowout Kill Operations. Paper SPE 21455 presented at the Middle East Oil Show, Bahrain, 16-19 November. http://dx.doi.org/10.2118/21455-MS.

Add Energy. 2013. The movie «Dynamic kill through relief well. http://www.addenergy.no/well-control-blowout-support/the-movie-dynamic-kill-through-relief-well-article1246-518.html (accessed 20 May 2013).

Andersen, L.B. n.d. Blowout. *The Workplace* **2** (8): 789-793

Baldwin, W. 1984. Locating the relative trajectory of a relief well drilled to kill a blowing well. http://www.google.com/patents/US4480701 (accessed 26 May 2013).

Bashaar, A.A. Hasan, F.A, Stewart, J. Abhijeet, S. Smith, G. 2010. Use of Gyro-MWD Technology Offshore: A Step Change in Drilling Performance in Saudi Aramco. Paper SPE 136499 presented at the Abu Dhabi International Petroleum Exhibition and Conference, Abu Dhabi, UAE, 1-4 November. http://dx.doi.org/ 10.2118/136499-MS.

Beggs, D.H. and Brill, J.P. 1973. A Study of Two-Phase Flow in Inclined Pipes. *Journal of Petroleum Technology*, **25** (5): 607-617. SPE-4007-PA. http://dx.doi.org/ 10.2118/4007-PA.

Bourgoyne Jr, A.T. Millheim, K.K. Chenevert, M.E. Young Jr. F.S. 1986. *Applied Drilling Engineering*, Vol. 2. Richardson, Texas: Textbook Series, SPE.

Brinkman (1952) The Viscosity of Concentrated Suspensions and Solutions, *Journal of Chemical Physics*, **20** (4): 571. http://dx.doi.org/10.1063/1.1700493.

Ceratechinc. 2013. Thermal Resistance Technology Overview. http://www.ceratechinc.com/Products/FIREROK/ThermalResistance (accessed 10 April 2013).

Chen, N.H. 1979. An Explicit Equation for Friction Factor in Pipe. *Ind. Eng. Chem. Fundamen.*, **18** (3): 296-297. http://dx.doi.org/10.1021/i160071a019.

Christman, S.A. 1999. Deepwater Well Control: Circulate With Both C&K Lines? Paper SPE 52762 presented at the SPE/IADC Drilling Conference, Amsterdam, Netherlands, 9-11 March. http://dx.doi.org/10.2118/52762-MS.

CNN. 2010. Oil Estimate raised to 35,000 – 60,000 barrels a day. http://edition.cnn.com/2010/US/06/15/oil.spill.disaster/index.html?hpt=T1&iref=BN1 (accessed 14 May 2013).

C-Therm. 2012. Thermal Conductivity of Sandstone. http://www.ctherm.com/blog/thermal_conductivity_of_sandstone/ (accessed 10 April 2013).

Deepwater. 2013. Transocean Spitsbergen. http://www.deepwater.com/fw/main/Transocean-Spitsbergen-477C17.html?LayoutID=17 (accessed 6 June 2013).

de Lange, J.I. and Darling, T.J. 1990. Improved Detectability of Blowing Wells. *SPE Drilling Engineering* **5** (1): 34-38, SPE-17255-PA. http://dx.doi.org/10.2118/17255-PA.

Dobrnjac, M. 2012. DETERMINATION OF FRICTION COEFFICIENT IN TRANSITION FLOW REGION FOR WATERWORKS AND PIPELINES CALCULATION. http://annals.fih.upt.ro/pdf-full/2012/ANNALS-2012-3-21.pdf (downloaded 4 June 2013).

Falcone, G., Hewitt, G., F., Alimonti, G. 2009. *Multiphase Flow Metering*. Amsterdam, Netherland: Elsevier B.V Publishing.

Fekete Associates Inc. 2012. Average Reservoir Pressure (p or pR). http://www.fekete.com/SAN/TheoryAndEquations/WellTestTheoryEquations/Average_Reservoir_Pressure.htm (accessed 1 June 2013).

Flores-Avila, F.S. Smith, J.R. Bourgoyne Jr., A.T. 2003. New Dynamic Kill Procedure for Off-Bottom Blowout Wells Considering Counter-Current Flow of Kill Fluid. Paper SPE 85292 presented at the SPE/IADC Middle East Drilling Technology Conference and Exhibition, Abu Dhabi, United Arab Emirates, 20-22 October. http://dx.doi.org/10.2118/85292-MS.

Ghanbari, A. Farshad, F.F. Rieke, H.H. 2011. Newly developed friction factor correlation for pipe flow assurance. *Journal of Chemical Engineering and Material Science*, **2**(6): 83-86.

Grace, R.D. 2003. *Blowout and Well Control Handbook*. USA: Gulf Professional Publishing, Elsevier Science.

Grepinet, M. and Flak, L. 2005. Part 7-Shallow Gas Blowouts. http://www.jwco.com/technical-litterature/p07.htm. (downloaded 14 February 2013).

Gudmundsson, J.S. 2009. Prosessering av Petroleum. TPG 4135 Compendium, NTNU, Trondheim, Norway (unpublished). http://www.ipt.ntnu.no/~jsg/undervisning/prosessering/kompendium/KompendiumApril2009.pdf (downloaded 22 May 2013).

Guo, B. and Liu, G. 2011. Applied Drilling Circulation Systems: Hydraulics, Calculations and Models. Houston, Texas, Gulf Publishing Company.

Hall, A.R.W. 2011. THREE-PHASE, GAS-LIQUID-LIQUID FLOWS. http://www.thermopedia.com/content/270/?tid=110&sn=24 (downloaded 22 May 2013).

Hall, K.R. and Yarborogh, L. 1973. A New Equation of State for Z-factor Calculations. *The Oil and Gas Journal*, June 18: 82-92.

Halliburton. 2012. API Casing Chart. http://www.halliburton.com/public/sdbs/sdbs_contents/Data_Sheets/H03038.pdf (downloaded 22 May 2013).

Halliburton. 2006. HT-400 Pump. The Industry Standard. http://www.halliburton.com/public/cem/contents/data_sheets/web/h/h04798.pdf (downloaded 9 June 2013).

Hasan, A.R. Kabir, C.S. Lin, D. 2000. Modeling Wellbore Dynamics During Oil Well Blowout. SPE paper 64644 presented at the International Oil and Gas Conference and Exhibition in China, Beijing, China, 7-10 November. http://dx.doi.org/10.2118/64644-MS

Hide, I. 1994. Saga under høytrykk. In *Norsk Oljemuseums årbok 1994*. Chap. 2, 25-46. Stavanger, Norway: Norsk Oljemuseum.

Holand, P. 1997. OFFSHORE BLOWOUTS: Causes and Control. Comprehensive risk analysis data from the SINTEF Offshore Blowout Database. Houston, Texas: Gulf Publishing Company.

Holmes, C.S. Swift, S.C. 1970. Calculation of Circulating Mud Temperatures. *Journal of Petroleum Technology* **22** (6): 670-674. SPE-2318-PA. http://dx.doi.org/ 10.2118/2318-PA.

Johansen S.E. and Sangesland, S. 2013. Method for measurement of wellbore trajectory in relief well drilling

JWCO. 2009a. John Wright Company. Relief Well Plan for a Cratered Well. http://www.jwco.com/relief_well_plan_cratered_well.htm (downloaded 2 June 2013).

JWCO. 2009b. John Wright Company. Example Horizontal View Electromagnetic Triangulation Bypass. http://www.jwco.com/images/rw_example_2/example_bypass.gif (downloaded 2 June 2013).

Kouba, G.E. MacDougall, G.R. Schumacher, B.W. 1993. Advancements in Dynamic Kill Calculations for Blowout Wells. *SPE Drilling & Completion* **8** (3): 189-194. SPE-22559-PA. http://dx.doi.org/10.2118/22559-PA

Leraand, F. Wright, J.W. Zachary, M.B. Thompson, B.G. 1992. Relief-Well Planning and Drilling for a North Sea Underground Blowout. *Journal of Petroleum Technology* **44**(3): 266-273. SPE-20420-PA. http://dx.doi.org/10.2118/20420-PA.

Marshall, L. 2011. Plugging Macondo: Drilling the Relief Well. http://minesmagazine.com/1745/ (downloaded 2 June 2013).

Nickens, H.V. 1985. A Dynamic Computer Model of a Kicking Well: Part II-Model Predictions and Conclusions. Paper SPE 14184 presented at the SPE Annual Technical Conference and Exhibition, Las Vegas, Nevada, 22-26 November. http://dx.doi.org/ 10.2118/14184-MS

Noerager, J.A. White, J.P. Floetra, A. Dawson, R. 1987. Drilling Time Predictions From Statistical Analysis. SPE paper 16164 presented at the SPE/IADC Drilling Conference, New Orleans, Louisiana, 15-18 March. http://dx.doi.org/10.2118/16164-MS

NORSOK Standard D-010. 2004. *Well Integrity in Drilling and Well Operations*, third edition. Lysaker, Norway: Standards Norway. http://www.standard.no/PageFiles/1315/D-010r3.pdf (downloaded 18 October 2012).

NOV. 2013. Drilling Fluid Equipment – Mud Pumps. http://www.nov.com/Drilling/Drilling_Fluid_Equipment/Mud_Pumps/12-P-160_Triplex_Mud_Pump.aspx (accessed 22. May 2013).

Ohirhian, P.O. and Abu, I.N. 2008. A New Correlation for the Viscosity of Natural Gas. Paper SPE 106391 available from SPE, Richardson, Texas.

Oudeman, P. Baaijens, M.N. Avest, D.t. 1993. Modelling Blowout Control by Means of Downhole Kill Fluid Injection. Paper SPE 26732 presented at Offshore Europe, Aberdeen, United Kingdom, 7-10 September. http://dx.doi.org/10.2118/26732-MS.

Pedersen, K., S. Fredenslund, A. Thomassen, P. 1989. Properties of Oils and Natural Gases. University of Michigan: Golf Publishing Company.

Pipeflow. 2013. Pipe Roughness. http://www.pipeflow.com/pipe-pressure-drop-calculations/pipe-roughness (accessed 10 May 2013).

Regjeringen. 1986. Ukontrollert utblåsing på boreplattformen West Vanguard 6 oktober 1985. http://www.regjeringen.no/upload/kilde/odn/tmp/2002/0034/ddd/pdfv/154614-nou1986-16.pdf (downloaded 3 June 2013).

Romero, D.J. Valko, P.P. Economides, M.J. 2002. The Optimization Of The Productivity Index And The Fracture Geometry Of A Stimulated Well With Fracture Face And Choke Skins. *SPE Production & Facilities*. **18** (1): 57-64. http://dx.doi.org/ 10.2118/81908-PA

Roy, R.S. Nini, C.J. Sonnemann, R. Gillis, B.T. 2009. Driller's Method vs Wait and Weight Method: One offers distinct well control advantages. http://www.drillingcontractor.org/driller's-method-vs-wait-and-weight-method-one-offers-distinct-well-control-advantages-1444 (downloaded 15 February 2013).

RSA. 2013. Drill Pipe/Tool Joint Combination API Grade Drill Pipe. www.regencysteelasia.com/pdf/pdf52.pdf (downloaded 27 May 2013).

Samuel, R. and Liu, X. 2009. Advanced Drilling Engineering: Principles and Designs. USA: Gulf Publishing Company.

Sangesland, S. 2011. Drilling and completion of subsea wells – An Overview. Trondheim, NTNU.

Sangesland, S. 2008. Drilling and completion of subsea wells. NTNU. (unpublished).

Schlumberger, 2013. Oilfield Glossary. http://www.glossary.oilfield.slb.com/en/Terms.aspx?LookIn=term%20name&filter=workover (accessed 20 February 2013).

Schmelzer, J.W.P. Zanotto, E.D. Fokin, V.M. 2005. Pressure depencdence of viscosity. *Journal of Chemical Physics*. **122** (7). http://dx.doi.org/10.1063/1.1851510.

Skalle, P. 2012a. *Pressure Control During Oil Well Drilling*, 3. edition. Ventus Publishing ApS. http://bookboon.com/en/pressure-control-during-oil-well-drilling-ebook (downloaded 14 December 2012).

Skalle, Pål. 2012b. *Drilling Fluid Engineering*, 3. edition. Ventus Publishing ApS. http://bookboon.com/en/drilling-fluid-engineering-ebook (downloaded 14 December 2012).

Skalle, P. and Podio, A.L. 1998. Trends extracted from 800 Gulf Coast blowouts during 1960-1996. Paper SPE 39354 presented at the IADC/SPE Drilling Conference, Dallas, Texas, 3-6 March. http://dx.doi.org/10.2118/39354-MS

Smith, J.P. and Clancy, J. 2010. UNDERSTANDING AGA REPORT NO. 10, SPEED OF SOUND IN NATURAL GAS AND OTHER RELATED HYDROCARBON GASES. http://www.asgmt.com/default/papers/asgmt2010/docs/W1_W2_4.pdf (downloaded 1 June 2013).

Sætren, T.G. 2007. Offshore Blow-out Accidents – An Analysis of Causes of Vulnerability Exposing Technological Systems to Accidents. https://www.duo.uio.no/bitstream/handle/10852/17849/master_saetren.pdf?sequence=1 (accessed 3 June 2013).

Tarr, B.A. and Flak, L. 2006. Part 6 – Underground blowouts. http://www.jwco.com/technical-litterature/p06.htm (downloaded 20 February 2013).

Thome, J.R. 2007. Engineering Data Book III. Wolverine Tube, Inc. http://www.wlv.com/products/databook/db3/data/db3ch12.pdf (accessed 20 April 2013).

Thorogood, J.L. 1987. A MATHEMATICAL MODEL FOR ANALYSING DRILLING PERFORMANCE AND ESTIMATING WELL TIMES. SPE paper 16524 presented at Offshore Europe, Aberdeen, United Kingdom, 8-11 September. http://dx.doi.org/ 10.2118/16524-MS

USGS. 2013. Water Density. http://ga.water.usgs.gov/edu/density.html (downloaded 1 June 2013).

Vector Magnetics. 2011. Wellspot at Bit (WSAB). http://www.vectormagnetics.com/oil-gas/services/wellspot-bit-wsab (accessed 30 May 2013).

Veeningen, D.M. 2013. System and method for steering a relief well. http://www.google.com/patents/US20130118809?dq=relief+well+intersect&hl=en&sa=X&ei=SVOiUeu8EMmg4gTBzoGQDQ&ved=0CDoQ6AEwAA (accessed 26 May 2013).

Warriner, R.A. and Cassity, T.G. 1988. Relief-Well Requirements To Kill a High-Rate Gas Blowout From a Deepwater Reservoir (includes associated paper 19889). *Journal of Petroleum Technology* **40**(12): 1602-1608. SPE-16131-PA. http://dx.doi.org/10.2118/16131-PA.

Weisstein, E.W. 2007. Thermodynamics, Heat Capacity, Specific Heat. http://scienceworld.wolfram.com/physics/SpecificHeat.html (accessed 22 April 2013).

Whitson, C.H and Brulé, M.R. 2000. *Phase Behavior*. SPE Monograph, volume 20, Henry L Doherty Series, Richardson, Texas.

Williamson, H.S. 1999. Accuracy Prediction for Directional MWD. *SPE Drilling & Completion*. **15** (4): 221-233. http://dx.doi.org/10.2118/67616-PA

Wirth Erkelenz. 2006. Performance Chart – Aker Wirth HP Mud Pump TPK 2200. http://wirth-erkelenz.de/fileadmin/resources/pdf/Oil_and_Gas/Pumps_Performance_Charts/TPK-2200-7500PSI.pdf (downloaded 7 June 2013).

Wolff, C.J.M and de Wardt, J.P. Borehole Position Uncertainty – Analysis of Measuring Methods and Derivation of Systematic Error Model. *Journal of Petroleum Technology*. **33**(12): 2338-2350. http://dx.doi.org/10.2118/9223-PA.

Wright, J., W., Flak, L. 2006. Part 11-Relief wells. http://www.jwco.com/technical-litterature/p11.htm (downloaded 27 February 2013).

Appendix A

MATLAB Program

```
%-------------------------------------------------------------------------%
%----------------------BLOWOUT SIMULATOR----------------------------------%
%-------------------------------------------------------------------------%

%-------------------------------------------------------------------------%
%Written by:  Kristoffer Evensen, Spring 2013                             %
%Description: This MATLAB probram will calculate the stabilized          %
%             blowout rate for the given well parameters                  %
%             (specified in input the section)                            %
%             In addition to this, the program can simulate how           %
%             the influx rate will change if dynamic kill fluid is        %
%             injected into the well at different depths                  %
%Purpose:     The program were prepared to simulate the benefits of       %
%             intersecting the blowing well at a deeper point than        %
%             currently possible with existing technology.                %
%             The program can calculate both the difference               %
%             in pumping rates, pressure and static kill fluid            %
%             required.                                                   %
%-------------------------------------------------------------------------%


%-------------------------------------------------------------------------%
%----------------------- First Order Input Variables ---------------------&
%-------------------------------------------------------------------------%

%Dimensions            Description:                Unit:
TD=3000;               %Terminal depth of well     (meters)
CSD=2000;              %Casing shoe depth          (meters)
Pd=5;                  %Pipe diameter              (inch)
OHD=8.5;               %Openhole diameter         (inch)
CID=9.063;             %Casing inside diameter     (inch)

%Properties
RT=100;                %Reservoir temperature      (Celsius)
FFD=461;               %formation fluid density
                       %@ in-situ conditions       (kg/m3)
RP=400;                %Reservoir pressure         (bar)
WD=1000;               %fresh water density        (kg/m3)
SP=15;                 %Wellhead pressure          (bar)
SWD=25;                %Dissolved salt             (kg/m3)
ST=4;                  %Wellhead temperature       (Celsius)

%Wellbore roughness
Cr=0.1;                %Casing absolute roughness  (mm)
Fr=1;                  %Formation absolute roughness(mm)

%Intersection Point
```

```
ID=3000;                %Interception depth          (meter)

%Injection Rate
RR=0;                   %relief well in-situ rate    (l/s)

%-------------------------------------------------------------------%
%------------------- Second Order Input Variables ------------------&
%-------------------------------------------------------------------%

%                    Description:                                  Unit:
HCRF=2500;           %Heat Capacity Of Reservoir Fluid          (J/kg-C)
HCI=4300;            %Heat Capacity Of Injection Water          (J/kg-C)
U=0.6;               %Thermal conductivity of cased section       (W/mK)
U2=2.37;             %Thermal conductivity of openhole section  (W/mk)
hr=0.001;            %heat transfer across pipe            (btu/hrsqftF)
Mi=45.43;            %Initial molar mass of reservoir fluid  (kg/k-mol)
InvPoint=0.5;        %Inversion Point of immiscible liquids      (ratio)
R=0.1;               %Initial blowout rate (to be adjusted)      (l/s)

%-------------------------------------------------------------------%
%---------------------- Initial Calculations ----------------------&
%-------------------------------------------------------------------%

A=zeros(TD,16);      %Answer matrix
                     %(depth(m), depth(ft), wellbore pressure (bar),
                     %flow diameter (m), frictional pressure drop (bar)
                     %hydrostatic pressure drop (bar), flow velocity
                     %(m/s), roughness (mm), liquid density (kg/m3)
                     %mixture density (kg/m3), flow regime
                     %gas density (kg/m3), two phase friction factor,
                     %no-slip friction factor)

PF=Pd/12;            %Pipe diameter in feet
G=(RT-ST)/TD;        %Geothermal gradient (C/m)
GF=G*1.8/3.28084;    %Geothermal gradient (F/ft)
TDF=TD*3.28084;      %Well depth (ft)
CDF=CSD*3.28084;     %Casing shoe depth (ft)

%-------------------------------------------------------------------%
%------------------------ Temperature profile ----------------------&
%-------------------------------------------------------------------%

Constraint=500;
ST2=ST*(9/5)+3;
CT2=ST2+GF*CDF;
mri=(980+SWD)*RR;
mrr=(461.2)*R;

while Constraint>(SP)

if ID==3000
IT=(1.89688*10^-9*RR^4-2.87808*10^-6*RR^3+0.001710826*RR^2-
0.514208719*RR+100.8124059);
else
IT=(4.11744*10^-9*RR^4-4.7389*10^-6*RR^3+0.002088315*RR^2-
0.452446577*RR+67.92743941);
end
```

```
if ID==3000
RT3=IT*(mri/(mrr+mri))+RT*(mrr/(mri+mrr));
else
RT3=RT;
end

RT2=RT3*(9/5)+32;

FFD2=(R/(R+RR))*FFD+(RR/(R+RR))*995;

m=(((R+RR)*FFD2/1000)/0.4536)*60*60; %lb/hr mass flow
U4=U*0.578/(CID/12); %Actual thermal conductivity btu/F sq ft hr cased
interval
U3=U2*0.578/(OHD/12); %Openhole

if ID==3000
   Cp=(HCRF*(mrr/(mrr+mri))+HCI*(mri/(mrr+mri)))*0.000238846;
%Specific heat capacity of mud, assumed constant
   Cp2=(HCRF*(mrr/(mrr+mri))+HCI*(mri/(mrr+mri)))*0.000238846;

else
   Cp2=HCRF*0.000238846;
   Cp=(HCRF*(mrr/(mrr+mri))+HCI*(mri/(mrr+mri)))*0.000238846;
end

TA1=m*Cp2/(2*pi*PF*hr);
TB1=(OHD/(2*12))*U3/((Pd/(2*12))*hr);
TC11=(TB1/(2*TA1))*(1+(1+(4/TB1))^0.5);
TC21=(TB1/(2*TA1))*(1-(1+(4/TB1))^0.5);
TC31=1+(TB1/2)*(1+(1+(4/TB1))^0.5);
TC41=1+(TB1/2)*(1-(1+(4/TB1))^0.5);
GA1=GF*TA1;
EC1H1=exp(TC11*(TDF-CDF));
EC2H1=exp(TC21*(TDF-CDF));
K21=(GA1-(RT2-CT2+GA1)*EC1H1*(1-TC31))/(EC2H1*(1-TC41)-EC1H1*(1-
TC31));
K11=RT2-K21-CT2+GA1;

TA2=m*Cp/(2*pi*PF*hr);
TB2=(CID/(2*12))*U4/((Pd/(2*12))*hr);
TC12=(TB2/(2*TA2))*(1+(1+(4/TB2))^0.5);
TC22=(TB2/(2*TA2))*(1-(1+(4/TB2))^0.5);
TC32=1+(TB2/2)*(1+(1+(4/TB2))^0.5);
TC42=1+(TB2/2)*(1-(1+(4/TB2))^0.5);
GA2=GF*TA2;
EC1H2=exp(TC12*TDF);
EC2H2=exp(TC22*TDF);
K22=(GA2-(RT2-ST2+GA2)*EC1H2*(1-TC32))/(EC2H2*(1-TC42)-EC1H2*(1-
TC32));
K12=RT2-K22-ST2+GA2;
testz=K11*TC31*exp(TC11*0)+K21*TC41*exp(TC21*(0))+GF*((0))+CT2;
testy=K12*TC32*exp(TC12*ID*3.28084)+K22*TC42*exp(TC22*ID*3.38084)+GF*I
D*3.28084+ST2;
diff=testz-testy;

%--------------------------------------------------------------------%
```

```
%-------------------- Pressure Calculations ----------------------&
%-----------------------------------------------------------------%

%---------------------- Flowing Fractions -------------------------&

for i=1:3000
    id=3001-i;

    if id<CSD
        A(id,5)=CID*(2.54/100);
        A(id,9)=Cr;
    else
        A(id,5)=OHD*(2.54/100);
        A(id,9)=Fr;
    end

    ift=id*3.28084;
    A(id,1)=id;
    A(id,2)=ift;

    if ID==3000
        mixc=0;
    else

mixc1=((IT*1.8)+32)*(mri/(mri+mrr))+(K12*TC32*exp(TC12*ID*3.28084)+K22
*TC42*exp(TC22*ID*3.28084)+GF*ID*3.28084+ST2+diff)*(mrr/(mrr+mri));

mixc2=K12*TC32*exp(TC12*ID*3.28084)+K22*TC42*exp(TC22*ID*3.28084)+GF*I
D*3.28084+ST2+diff;
        mixc=mixc2-mixc1;
    end

    if id>=CSD
    AF=K11*TC31*exp(TC11*(ift-(ID*3.28084)))+K21*TC41*exp(TC21*(ift-
(ID*3.28084)))+GF*(ift-(ID*3.28084))+CT2;
    A(id,3)=(AF-32)*(5/9);
    else
    AF=K12*TC32*exp(TC12*ift)+K22*TC42*exp(TC22*ift)+GF*ift+ST2+diff-
mixc;
    A(id,3)=(AF-32)*(5/9);
    end

    G(id,1)=(AF-32)*(5/9);
end

for i=1:300
    id=i*10;
    Gtemp(i,1)=G(id,1);
end

A(3000,4)=RP;

%---------------------- Flowing Fractions -------------------------&

for i=0:2998

    depth=3000-i;
```

```
    p=A(depth,4);

    if p>290
        OV2=1;
    else
        OV2=4.53264*10^-12*p^5-3.0606*10^-9*p^4+7.8059*10^-7*p^3-
8.98995*10^-5*p^2+0.006172453*p+0.074089141;
    end

%---------------------------- Molar Mass -----------------------------&
    if p>290
        OM=45.43510681;
        GM=0;
    else
        OM=-7.07369*10^-10*p^5+5.96024*10^-7*p^4-
0.000190337*p^3+0.029068761*p^2-2.429140018*p+181.9311708;
        GM=1.89868*10^-12*p^6-1.80307*10^-9*p^5+6.67172*10^-7*p^4-
0.000120939*p^3+0.011206502*p^2-0.497904762*p+32.49449801;
    end

%------------------------ Fluid properties -------------------------&

%Pseudo reduced properties from Standings correlation,
%Z-factor from Hall & Yarborogh

    T=A(depth,3)+273.15; %Temperature Kelvin
    P=A(depth,4); %Pressure Bar
    Pp=P*14.5037738; %Pressure Psia
    Tc=A(depth,3); %Temperature Celcius
    Tr=T*1.8;
    rough=A(depth,9);

    if P<290
       SG=GM/28.97;
    if SG<0.75
        Tpc=(168+325*SG-12.5*SG^2)*0.555555556;
        Ppc=(667+15*SG-37.5*SG^2)*(10^5/14.5);
    elseif SG>=0.75
        Tpc=(187+330*SG-71.5*SG^2)*0.555555556;
        Ppc=(706+51.7*SG-1.11*SG^2)*(10^5/14.5);
    end
    Tpr=T/Tpc;
    Ppr=P*10^5/Ppc;

    %Hall-Yarborogh

    t=1/Tpr;
    a=0.06125*t*exp(-1.2*(1-t)^2);
    y=0.01;                                %random value, changed through
iteration
    ytest=1;

    %iteration to solve the Hall-Yarborogh equation
    %is performed by the Newton Raphso method.

    while ytest>10^-5 %constrain can be increased to increase
effectivity
```

```
        fy=-a*Ppr+(y+y^2+y^3-y^4)/(1-y)^3-(14.76*t-
9.76*t^2+4.58*t^3)*y^2+(90.7*t-242.2*t^2+42.4*t^3)*y^(2.18+2.82*t);
        dfy=(1+4*y+4*y^2-4*y^3+y^4)/(1-y)^4-(29.52*t-
19.52*t^2+9.16*t^3)*y+(2.18+2.82*t)*(90.7*t-
242.2*t^2+42.4*t^3)*y^(1.18+2.82*t);
        y0=y;
        y=y-(fy/dfy);
        ytest=(y-y0)^2;
    end
        z=a*Ppr/y;
    else
         z=1;
    end

%--------------------------- Densities -----------------------------&

    GD=(z*P*10^5*GM)/(8.3144621*T*1000); %kg/m3
    GDa=GD*0.0624279606; %lb/ft3

    if p>290
        OD=0.330750716*p+345.4400112;
        viscoil=4.47062*10^-5*p+0.06627409;
        ODi=0.330750716*RP+345.4400112;
        ST=2.790286092;
    else
        OD=6.50336*10^-12*p^6-6.98355*10^-9*p^5+2.8333*10^-6*p^4-
0.000543422*p^3+0.051180284*p^2-3.103346739*p+707.0146945;
        viscoil=-0.129609989*log(p)+0.833227262;
        ODi=0.330750716*RP+345.4400112;
        ST=-1.02387*10^-10*p^5+8.46729*10^-8*p^4-2.62993*10^-
5*p^3+0.003854784*p^2-0.301653023*p+18.49224691;
    end

%--------------------------- Molar Flow -----------------------------%

    Q=(R/1000)*ODi/(87.4/1000);

    if depth>ID
         WD=0.033746509*p+(980.4005001+SWD);
         viscwater=1.36027*10^-8*p+0.463103407;
         WDi=0.033746509*A(ID,4)+(980.4005001+SWD);
         Qw=0;

    else
         WD=0.033746509*p+(980.4005001+SWD);
         viscwater=1.36027*10^-8*p+0.463103407;
         WDi=0.033746509*A(ID,4)+(980.4005001+SWD);
         Qw=(RR/1000)*WDi/(18.02/1000);
    end

    OF=Q*OV2;
    OG=Q*(1-OV2);
    OW=Qw;
    MA=OM*OV2+GM*(1-OV2);

%--------------------- Volumetric flow -----------------------------%
```

```
    if GD==0
       GVF=0;
    else
        GVF=OG*GM/(1000*GD); %cubic metre per second
    end

    OVF=OF*(OM/1000)/OD; %cubic metre per second
    WVF=OW*(18.02/1000)/WD;
    MVF=GVF+OVF+WVF;
    LVF=WVF+OVF;
    LV=LVF/MVF;

%----------------------- Flow Velocity ------------------------------%

    D=A(depth,5);
    Area=pi*(D/2)^2;
    V=(OVF+GVF+WVF)/Area;
    A(depth,8)=V;

 %-------------------------- Viscosity -------------------------------
%

    ratio=(WVF/LVF);

    if ratio <= InvPoint
       viscliquid=viscoil*(1/(1-ratio)^2.5);
    else
       viscliquid=viscwater*(1/ratio^2.5);
    end

    if p<290

       Rg=(0.001031*Pp*Tr)/(Pp-(0.061*Tr));
       Bg=(0.0283*z*Tr)/Pp;
       xg=Rg/(100*Bg);
       viscgas=1.6*(0.0109388-0.0088234*xg-0.0075720*xg^2)/(1.0-
1.3633077*xg+0.0461989*xg^2);
       %In situ gas viscosity (cp)
    else
        viscgas=0;
    end

    mixturevisc=viscliquid*LVF/MVF+viscgas*GVF/MVF;

%-------------- Pressure Loss - Beggs and Brill ---------------------%

    gft=32.2;
    D=A(depth, 5)*3.28084;
    um=MVF*35.3147;
    ul=LVF*35.3147;
    Cl=ul/um;
    Nfr=um^2/(gft*D);
    L1=316*Cl^0.302;
    L2=0.0009252*Cl^-2.4684;
    L3=0.10*Cl^-1.4516;
    L4=0.5*Cl^-6.738;
    ulum=ul-um;
```

```
Vsl=(LVF/Area)*3.28084; %Superficial liquuid velocity
liquiddensity=(WVF/LVF)*WD+(OVF/LVF)*OD;
liquiddensitya=liquiddensity*0.0624279606;
Nvl=1.938*Vsl*(liquiddensitya/(gft*ST));
beta=0;
Elhor=1;
eD=A(depth,9)/(1000*A(depth,5));

if ulum==0

   Flowregime='fluid only';
   A(depth, 13)=0;
   beta=0;
   Elhor=1;

else

if Cl<0.01 && Nfr<L1
    Flowregime='Segregated';
    A(depth, 13)=1;
    Elhor=(0.98*Cl^0.4846)/(Nfr^0.0868);
    beta=(1-Cl)*log((0.011*Nvl^3.539)/(Cl^3.768*Nfr^1.614));

     if beta<0
        beta=0;
    end

elseif Cl>=0.01 && Nfr<L2
    Flowregime='Segregated';
    A(depth, 13)=1;
    Elhor=(0.98*Cl^0.4846)/(Nfr^0.0868);
    beta=(1-Cl)*log((0.011*Nvl^3.539)/(Cl^3.768*Nfr^1.614));

     if beta<0
        beta=0;
    end

elseif Cl>0.01 && Nfr>L2 && Nfr<=L3

    Flowregime='Transition';
    A(depth, 13)=2;
    Elhorseg=(0.98*Cl^0.4846)/(Nfr^0.0868);
    Elhorint=(0.845*Cl^0.5351)/(Nfr^0.0173);
    A9=(L3-Nfr)/(L3-L2);
    B9=1-A9;
    Elhor=A9*Elhorseg+B9*Elhorint;
    beta=(1-Cl)*log((2.96*Cl^0.305*Nfr^0.0978)/(Nvl^0.4473));

    if beta<0
        beta=0;
    end

elseif Cl>=0.01 && Cl<0.4 && Nfr>L3 && Nfr<=L1

    Flowregime='Intermittent';
    A(depth, 13)=3;
    Elhor=(0.845*Cl^0.5351)/(Nfr^0.0173);
```

```
        beta=(1-Cl)*log((2.96*Cl^0.305*Nfr^0.0978)/(Nvl^0.4473));

         if beta<0
            beta=0;
        end

    elseif Cl>=0.4 && Nfr>L3 && Nfr<=L4

        Flowregime='Intermittent';
        A(depth, 13)=3;
        Elhor=(0.845*Cl^0.5351)/(Nfr^0.0173);
        beta=(1-Cl)*log((2.96*Cl^0.305*Nfr^0.0978)/(Nvl^0.4473));

         if beta<0
            beta=0;
        end

    elseif Cl<0.4 && Nfr>=L1

        Flowregime='Distrubuted';
        A(depth, 13)=4;
        Elhor=(1.065*Cl^0.5824)/(Nfr^0.0609);
        beta=0;

    elseif Cl>=0.4 && Nfr>L4

        Flowregime='Distrubuted';
        A(depth, 13)=4;
        Elhor=(1.065*Cl^0.5824)/(Nfr^0.0609);
        beta=0;

    end
    end

      Winc=90; %Wellbore inc.
      B12=1+beta*(sin(1.8*Winc)-(1/3)*(sin(1.8*Winc))^3);
      El=Elhor*B12;

      if El>1  %Limitation according to Beggs and Brill
         El=1;
      end

      if El<Cl
         El=Cl;
      end

      mixdenns=liquiddensitya*Cl+GDa*(1-Cl); %lb/ft3
      mixdenns1=liquiddensity*Cl+GD*(1-Cl); %kg/m3
      mixden=liquiddensity*El+GD*(1-El); %kg/m3
      mixden2=mixden*0.0624279606; %lb/ft3

%-------------------- Hydrostatic Pressure Loss --------------------%

      dPhyd2=((mixden2)/144); %psi/ft
      dPhyd22=((mixden2)/144)*0.226205948; %bar/m
      dPhyd2test=(mixdenns/144);
      dPhyd22test=dPhyd2test*0.226205948;
```

```
%------------------ Determining friction factor --------------------%
      y=(Cl/El^2);
      if y>1 && y<1.2
         S=log(2.2*y-1.2);
      else
         S=log(y)/(-0.0523+3.18*log(y)-
0.872*(log(y))^2+0.01853*(log(y))^4);
      end

      ReNS=1488*mixdenns*V*3.28084*D/mixturevisc;

      if ReNS>4000
          Flow='Turbulent';
          fns=1/(-2*log10((eD/3.7065)-
((5.0452/ReNS)*log10(((eD^1.1098)/2.8257)+(7.149/ReNS)^0.8981))))^2;
      elseif ReNS<2300
          Flow='Laminar';
          fdns=64/ReNS;
          fns=fdns/4;
      else
          Flow='Transient';
          fns=1/(-2*log10((eD/3.7065)-
((5.0452/ReNS)*log10(((eD^1.1098)/2.8257)+(7.149/ReNS)^0.8981))))^2;
      end

%------------------- Adjusting for liquid holdup -------------------%

      ftp=fns*exp(S);
      fdtp=ftp*4;

%--------------------- Frictional Pressure Drop --------------------%

      dPfrictest=(2*fns*((V*3.28084)^2)*mixdenns)/(144*32.174*D);
      dPfrictestbar=dPfrictest*0.22620594;
      dPfric=(2*ftp*((V*3.28084)^2)*mixdenns)/(144*32.174*D); %psi/ft
      dPfric2=dPfric*0.22620594; %bar/m
      dPfric3=fdtp*((mixdenns*16.018463*V^2)/(2*D/3.28084))*10^-5;
%bar/m
      Nextpressure=P-dPfric3-dPhyd22;

      if Nextpressure<SP
         Nextpressure=SP;
      end

      A(depth-1,4)=Nextpressure;
      A(depth, 6)=dPfric2;
      A(depth, 7)=dPhyd22;
      A(depth, 8)=V;
      A(depth, 9)=GD;
      A(depth, 11)=mixden;
      A(depth, 12)=liquiddensity;
      A(depth, 15)=ftp;
      A(depth, 16)=fns;

end
Constraint=A(1,4);
```

```
if Constraint>(SP+40)
    %RR=RR+10
    R=R+10
elseif Constraint<=(SP+50) && Constraint>(SP+15)
    %RR=RR+1
    R=R+1
elseif Constraint<=(SP+15) && Constraint>(SP+1)
    %RR=RR+0.1
    R=R+0.1
else
    %RR=RR+0.01
    R=R+0.01
end
end
    Fricsum=0;
    Hydsum=0;
for i=1:3000
    id=3001-i;
    Fricsum=Fricsum+A(id,6);
    Hydsum=Hydsum+A(id,7);
end


Fricsum
Hydsum
Totsum=Fricsum+Hydsum
```

Appendix B

Case Study: 2/4-14 Blow Out

This chapter describes the process of drilling the 2/4-15S relief well used to kill the 2/4-14 Saga blowout in the Ekofisk area. On the 11th of January 1989, the 2/4-14 well was drilled into an unexpected high-pressure zone at 4733 meters true vertical depth, and started to flow. The annular preventer were activated to seal off the wellbore, but the drilling crew failed to establish circulation. It was decided to cement the BHA at 4700 meter TVD, and plan for a backoff and sidetrack (Leraand et al., 1992).

During this operation, it was observed that the drill string had gotten plugged with cement, and a coiled tubing operation was initiated to clear the obstruction. On the 20th of January, during the coiled tubing operation, the well suddenly started to flow again. It became necessary to cut the pipe and coil tubing, using the shear ram. At this point, a pressure buildup of 700 bar was recorded at the wellhead (Hide, 1994). Bullheading through the kill line were attempted to regain control, but the high pressure caused the flex hose to burst below the slip joint. This caused the well to release fluids to the sea over a short period, before the fail-safe valves were shut and the blowout contained. At this point it was decided to move the rig off location (Leraand et al., 1992).

A plan to kill the well was established. A custom stack and high-pressure riser were going to be used together with a snubbing unit to try to fish out the severed drill pipe and coiled tubing, before efforts could be made to restore circulation. Simultaneously with the top kill operation, a relief well was planned. It was decided that one relief well was adequate, since efforts were made to kill the well using vertical intervention as well (Leraand et al., 1992).

A 9 ⅝-inch casing had been set at 4437 meters TVD in the 2/4-14 well, and the bit had been pulled up and cemented at 4700 meters TVD. It was decided that the relief well would intersect the 2/4-14 well just below the 8 ½-inh bit, and that electromagnetic tools would be used to home in on the steel present in the blowing well (Leraand et al., 1992). Once the relief well had attained communication with the blowing well, the blowout would be killed dynamically by injecting large volumes of seawater. Once the flow from the reservoir had seized, kill mud could be injected to kill the well statically (Leraand et al., 1992).

The 2/4-15S well was spudded with an approximate horizontal displacement compared to the blowing well of 1250 meters (Hide, 1994). A 30-inch conductor was set at 216m TVD, drilling continued vertically, and a 20-inch surface casing was set at 900m TVD. The kickoff point was located at 915 meters TVD, and a target inclination of 30° was obtained through a buildup rate of 1.5°/30m (Leraand et al., 1992).

A 13 ⅜-inch casing was set at 2500 meters TVD, and a gyro survey was performed. This survey would yield the position of the 2/4-15S well with an uncertainty of 3 meters. Because of the higher accuracy of the gyro, compared to MWD surveys performed continuously during drilling, the bottomhole position was shifted 4.5 meters to the east. Drilling continued to 3360m TVD, where the well would drop back to vertical at a rate of 1°/30 m (Leraand et al., 1992).

Homing in procedure

As the relief well closes inn on the blowing wellbore, the relative position between the relief well and steel tubular in the blowing well was measured using electromagnetic ranging tools. Instead of measuring the direct distance between the two wells, a triangulation method was used. This would increase the accuracy, however it required that the well path of the relief well would cross the casing of the blowing well. An error in the position of the blowing well of 1 meter were considered acceptable. The triangulation method reduced the uncertainty down to 10%, and because of this the relief well would have to cross the blowing casing at a distance of maximum 10 meters (Leraand et al., 1992).

At the crossing point, the position of the casing in the blowing well was established through MWD surveys, with an absolute uncertainty of 8 meters. The first ranging point was located at 3559 meters TVD, and measurements positioned the blowing well in the predicted location. As the relief well crossed the blowing well, several ranging surveys were performed. At 3829 meters TVD the casing were crossed with a relative distance of 6.3 meters at 93.5° azimuth, the uncertainty were 0.7 meters (Leraand et al., 1992).

Drilling continued, and the well reached vertical at 4100 meters TVD. At this point the two wells were parallel and around 20 meters apart. A 9 ⅝-inch casing were set at 4249 meters TVD. The section that crossed the casing at 3829 meters TVD was used to calibrate the ranging equipment. The vertical section continued down to 4557 meters TVD. At this point a downhole motor was used to slowly start to move in on the blowing well. This section were especially challenging because of a number of thin weak zones made premature communication possible (Leraand et al., 1992).

Electromagnetic- and gyro surveys were performed as the relief well moved in on the target. At 4673 meters TVD the 7-inch liner were cemented into place, and drilling

continued with a 5 ⅞-inch bit. Surveys revealed a distance of 7.1 meters between the wells. Studies showed that the optimum kill point was at 4705m TVD, and consisted of an impermeable claystone. This would minimize losses during the killing operation. Fluid breakthrough would likely occur if the two wellbores were within a relative proximity of 1 meter, because of the large pressure drawdown, and enlargement of the blowing borehole.

Killing Procedure

Drilling would proceed towards the kill point, located at 4705 meters TVD. At this depth the distance between the wells would be 0.5 meters, and the killing operation could be initiated. However, the positioning uncertainty made it possible to achieve premature communication after drilling past 4700 meters TVD. If communication were not obtained when the bit were at the kill point, the bottomhole pressure would be increased to below the liner shoe test pressure to try to obtain communication through hydraulic fracturing. If this were not successful, drilling would continue down to a more permeable sandstone at 4711 meters TVD. If no communication were obtained at this point, acid squeeze were going to be performed. A sidetrack was considered the last resort contingency plan (Leraand et al., 1992).

When the bit reached the kill point, total losses were experienced, and the drill string fell 1 meter. Pressure response indicated full communication. The bit was pulled into the 7-inch liner, and the annulus filled with 1950 kg/m3 mud. Initially 1600 l/min were lost to the blowing well, however this rate reduced to 500 l/min after 3 hours. Production logging tools were indicating that the mud was filling the 2/4-14 well. The low flow rate was caused by a choking effect of the broken bottomhole assembly, still present in the blowing well. These results lead to the decision to abandon the dynamic killing operation, and start pumping down the 2250 kg/m3 kill mud right away. Initially 1000 l/min were injected, and after a total of 160m^3 injected, it slowed down to 150 liter/min. This low injection rate was obtained for well over 24 hours to circulate out trapped hydrocarbons. Once bottomhole pressure had been increased to above reservoir pressure, pills were circulated down into the blowing well to form a barite plug. After a number of test secured that the well were statically killed, two cement plugs were set and the well temporarily abandoned (Leraand et al., 1992).

Appendix C

Case Study: West Vanguard Shallow Gas Blowout

The West Vanguard semi-submersible was drilling an exploration well in block 6407/6 on the Haltenbanken area, offshore Norway (Regjeringen, 1986). On the 5th of October 1985, the rig had cemented the 30-inch conductor in place at a depth of 318 meters. Shallow gas hazards had been evaluated, and it was decided to drill a 12 ½-inch pilot hole following the 30-inch section. A drilling riser, wellhead and diverter system was installed, but the section was drilled without a BOP. During this operation, a drilling break and high gas readings in the return mud were observed. Drilling was stopped, and the well was circulated several times to prevent gas cut mud (Andersen, n.d.).

Drilling was continued to a depth of 516 meters. At this point the well had been drilled into an unknown gas pocket. The drill string was pulled up to connect a new pipe. At this point a large return flow consisting of a mixture of mud, gas and sand were experienced. The underbalance at the point of inflow might have been caused by swab when pulling the pipe, gas cut mud, or an underestimation of the pore pressure. The return flow escalated fast, and full circulation was initiated to try to regain overbalance. The diverter system was engaged to divert the flow, however the high flow rate and large amount of debris eroded the system and gas was released to the rig deck. The gas was ignited, killing one crewmember and almost completely destroying the rig (Andersen, n.d.).

The blowout continued in full force for six days before the flow gradually started to be reduced. It is typical for shallow gas blowouts to stop because the zone is depleted, or because the well is bridged naturally. The rig towed away from the site after the blowout had seized, and were delivered to a repair site (Sætren, 2007).